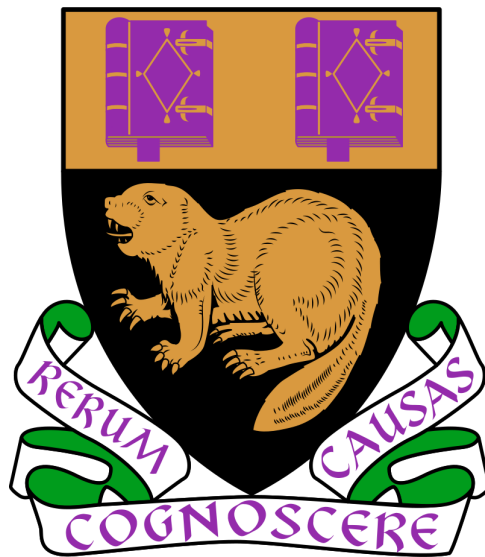


Fire sales and policy interventions in financial networks

Raymond Ka-Kay Pang



A thesis presented for the degree of
Doctor of Philosophy

Department of Mathematics
The London School of Economics and Political Science

London, April 2023

Declaration

I certify that the thesis I have presented for examination for the MPhil/PhD degree of the London School of Economics and Political Science is solely my own work other than where I have clearly indicated that it is the work of others (in which case the the extent of any work carried out jointly by me and any other person is clearly identified in it).

The copyright of this thesis rests with the author. Quotation from it is permitted, provided that full acknowledgement is made. In accordance with the Regulations, I have deposited an electronic copy of it in LSE Theses Online held by the British Library of Political and Economic Science and have granted permission for my thesis to be made available for public reference. Otherwise, this thesis may not be reproduced without my prior written consent.

I warrant that this authorisation does not, to the best of my belief, infringe the rights of any third party.

I declare that the thesis contains 65584 words.

Statement of co-authored work

Chapters 2, 3 and 4 are joint works with my PhD supervisor Luitgard Anna Maria Veraart. In particular, Chapter 2 is based on Pang and Veraart (2023).

Chapter 5 is based on Bardoscia and Pang (2023) and is jointly authored with Marco Bardoscia. This work was partly conducted as a PhD intern and academic visitor at the Bank of England.

Chapter 6 is based on Pang et al. (2021) and is jointly authored with Oscar M. Granados, Harsh Chhajjer and Erika Fille T. Legara.

Abstract

In this thesis, we model the impact of fire sales and the mitigation of systemic losses from policy interventions using tools from the theory of financial networks and complex systems. A fire sales event occurs when banks sell a large quantity of assets at discounted prices. There is a mark-to-market adjustment on assets sold, leading to a depreciation in the asset value and fuelling further fire sales. This channel of systemic risk can be a large contributor to losses, as observed in systemic events like the Great Financial Crisis. The impact of these events spurred a range of policy interventions to enhance financial stability. We use network models to analyse fire sales and policy interventions in interconnected systems.

Our first main result shows that under a partial information setting, policy interventions for mitigating fire sales losses using matrix reconstruction methods outperform policy interventions that do not account for institutions overlapping portfolios. We focus on optimising policy interventions when only the partial information is known, and how this compares with the fully observed data. Using matrix reconstruction methods, we find policy interventions under partial information can be similar to policy interventions under fully observed data. The similarity in performance under partial information highly depends on the chosen matrix reconstruction method.

The second main result is developing a new reverse stress test approach for a multi-stage fire sales event. Under this new approach, we find losses under these derived scenarios are larger than benchmark scenarios used in other stress tests. A reverse stress testing approach is taken, as the scenario reflects the largest losses of banks from the input data and given fire sales mechanism. We find the losses from these derived scenarios are large and have not been observed in previous studies.

Our third main result develops a clearing model for banks that post collateral as part of their financial obligations, where we account for two distinctive channels of fire sales. In this clearing situation, we consider the counterparty losses between banks, fire sales losses from assets used as collateral and fire sales losses from externally held assets. In this new collateral model, the inclusion of external asset holdings towards fire sales losses in a clearing situation can result in larger losses, compared to banks holding no external assets. We find the total losses depend on the overlap between both fire sale channels, and the network topology of the interbank network.

Acknowledgments

I first and foremost would like to thank my PhD supervisor Professor Luitgard Veraart. She has introduced me to this very interesting area of systemic risk and financial networks, which I have enjoyed working on during the PhD. She has been a fantastic supervisor with her kindness, patience and mentorship throughout the PhD. I feel very lucky to have her as a supervisor.

I want to thank my family and close friends for their support during the PhD. There have been many challenges throughout the PhD and I am grateful for their love during those difficult times.

I want to thank Marco Bardoscia as my PhD intern supervisor at the Bank of England and collaborator. I appreciate all the time and advice he has given me throughout our joint project. I have enjoyed working with him very much.

I would like to thank my collaborators Oscar M. Granados, Harsh Chhajer, and Erika Fille T. Legara as part of the COVID-19 workshop resulting in the joint work in this thesis. I felt I highly developed throughout this project and feel proud of how we were able to effectively work online together.

I am grateful to LSE for their financial support from the LSE PhD studentship and professional guidance throughout the PhD. I am particularly grateful to the Department of Mathematics at LSE, where I was part of a friendly community. Within the department, I would like to thank the LSE administration team for their support and help. I am thankful to the LSE Financial Mathematics group for the reading groups, seminars, and workshops which they have organised.

I want to thank the community of LSE PhD students in the maths department throughout my time as a PhD student. I am very grateful to be part of a highly intellectual and socially vibrant group. In particular, I have enjoyed being with the LSE PhD Financial Mathematics group and all the seminars and dinners we had throughout the years. Not being part of this group will be one of the things I will dearly miss.

Contents

Declaration	1
Abstract	2
Acknowledgments	3
1 Introduction	7
2 Assessing and mitigating fire sales risk under partial information	17
2.1 Introduction	17
2.1.1 Related literature	19
2.2 Fire sales in financial networks	21
2.2.1 The financial market	21
2.2.2 The stress test and fire sale mechanism	22
2.2.3 Measuring fire sales risk	23
2.2.4 Observability and choice of model parameters	24
2.3 Fire sale risk under partial information	25
2.3.1 Dependence of fire sales risks on the asset holding matrix	25
2.3.2 Reconstructing matrices	29
2.3.3 Data	31
2.3.4 Empirical results	32
2.3.5 Sensitivity analysis and robustness checks	40
2.4 The effect of policy intervention	42
2.4.1 Leverage caps	43
2.4.2 Capital injections	44
2.4.3 Empirical results on policy interventions	47
2.5 Conclusion	53
3 Reverse stress testing for fire sales risk	55
3.1 Introduction	55
3.1.1 Related literature	57
3.2 Fire sales mechanism	59

3.3	Reverse stress test formulation	61
3.3.1	Frank-Wolfe algorithm	63
3.3.2	Fractional Knapsack Problem	65
3.4	Reverse stress test results	67
3.4.1	Systemicness and Vulnerability	73
3.4.2	Sensitivity	74
3.5	Conclusion	78
4	Collateralized networks with two channels of fire sales	79
4.1	Introduction	79
4.1.1	Related literature	82
4.2	Multi asset model	83
4.2.1	First round of clearing	85
4.2.2	Second round of clearing	88
4.2.3	Systemic risk metrics	91
4.3	Fixed point ordering	92
4.4	Network simulations	95
4.4.1	Small example network	95
4.4.2	Large random network	102
4.5	Conclusion	111
5	Ring-fencing banks in financial networks	112
5.1	Introduction	112
5.2	Institutional details	116
5.3	Ring-fencing one bank	118
5.4	Ring-fencing banks in a financial network	121
5.4.1	Naive equity and external leverage	122
5.4.2	Valuation framework	125
5.4.3	Results on RFBs	129
5.4.4	Results on nRFBs and banking groups	131
5.5	Conclusion	137
6	An analysis of network filtering methods to sovereign bond yields during COVID-19	139
6.1	Introduction	139
6.2	Materials and methods	142
6.2.1	Network filtering methods	143
6.2.2	Sovereign bond data	145
6.3	Network measures	147
6.3.1	Network length	148

6.3.2	Network centrality	150
6.4	COVID-19 networks	151
6.4.1	Network plots	151
6.4.2	Exponential Random Graph Model for COVID-19 networks . . .	153
6.5	Conclusion	156
7	Conclusion and Discussion	157
8	Appendix	178
8.A	Chapter 2: Background information on matrix reconstruction methods .	178
8.A.1	Optimisation-based reconstruction methods	178
8.A.2	Sampling-based reconstruction methods	181
8.B	Chapter 2: Additional empirical results and sensitivity analysis	185
8.B.1	Observed and reconstructed asset holding matrices	185
8.B.2	Computing the maximum and minimum aggregate vulnerability for given row and column sums	188
8.B.3	Additional sensitivity analysis	190
8.C	Chapter 3: Target leverage condition	194
8.D	Chapter 3: Multi-period fire sales measures	197
8.E	Chapter 4: Collateral clearing model: Existence of and convergence to the greatest solution	200
8.F	Chapter 5: Valuation framework: Existence of and convergence to the greatest solution	206
8.G	Proofs	207
8.G.1	Chapter 2 proofs	207
8.G.2	Chapter 4 proofs	209
8.G.3	Chapter 5 proofs	220

Chapter 1

Introduction

Systemic risk is the risk which poses a severe threat to the functionality of a financial system. In a systemic event, the losses from a small group of banks can cascade to other banks, resulting in widespread defaults and substantial losses. These losses are important as they are not solely contained within the financial system, but also have negative implications for the real economy. Because of the damaging effects arising from a systemic event, modelling, assessing and mitigating losses is important for maintaining financial stability.

Multiple channels can contribute to the total losses banks are exposed to. The main channel of losses we focus on is from a fire sale. A fire sale occurs when a large quantity of assets are sold at a discounted value. The assets sold cause a price impact and a decrease in the value of common assets held by other banks. These affected banks may react and sell a proportion of their asset holdings, further depreciating the value of assets sold. The losses compound from each round of fire sales and lead to large bank losses. A fire sale represents an indirect loss for banks, where losses in one bank can result in losses for another bank, even if these two banks do not have a direct relation.

A fire sale may arise for different reasons. In one setting, the bank may be required to sell a proportion of its asset holdings to meet a given target leverage. The target leverage increases the volume of assets sold and the price impact decreases the value of commonly denoted assets e.g., Greenwood et al. (2015), Cont and Schaanning (2017) and Duarte and Eisenbach (2021).

Another reason for the bank to sell a proportion of its assets holding is that these assets are required to meet its outstanding obligations with other banks. The work by Cifuentes et al. (2005) and Feinstein and El-Masri (2017) integrates the fire sales effect on the bank's illiquid asset holdings with the clearing mechanism on the interbank network by Eisenberg and Noe (2001).

We use methods in the theory of financial networks and complex systems to model the losses from a systemic event. We can create a framework using financial networks that account for a range of risks e.g., solvency, liquidity and operational risks. Using financial

networks, we can capture the interconnectedness between banks, and how losses are propagated throughout the system. Also, the non-linear dynamics arising from the higher-order effects of the contagion mechanism are accounted for, which can form a large proportion of the bank's total losses.

Our approach to evaluating losses lies in the area of stress testing. These stress tests are scenario-driven risk management tools, where we assume an initial scenario representing a shock to assets and simulate the spread of losses. Using stress tests, we can incorporate the feedback and cascade of losses that banks are exposed to through a financial network. We contribute to modelling fire sales and how these results can be used to inform policy intervention in this thesis. We consider the individual impact of fire sales and the implications of this channel of systemic risk when banks have interbank assets and liabilities. Secondly, we focus on how financial networks can be used to design policy interventions. Using financial networks helps in modelling the consequences of different policy interventions, and creating regulatory frameworks which increase the resilience of the financial system to future shocks.

Our first main result shows policy interventions for fire sales under partial information can lead to a similar performance in the reduction of losses as using the fully observed data. While there have been several studies that analyse the connection between partial information and fire sales losses, there are no studies to our knowledge which empirically analyse the effect of policy interventions informed by partial information for fire sales. We believe this is an important research direction, as it confirms if these methods which use partial information (which may not be necessarily financially motivated) are valid for informing how policies and regulations can mitigate fire sales losses. These results are in Chapter 2 of the thesis.

We explore policy interventions under partial information because of the potential constraints to obtaining the fully observed data. In several jurisdictions, the financial data is not available or is aggregated such that the individual positions of the bank are not known i.e., we use the European Banking Authority (EBA) data, where the full information is known, but from the Federal Reserve, only the partial information is publicly known. In our case, the fully observed information for fire sales is represented by an asset holdings matrix, where the partial information is represented by the row and column sums of the matrix. While partial information can be used for some risk management measures, we cannot infer the financial network nor the complexity of the contagion purely from the partial information. We, therefore, use matrix reconstruction methods, where the partial information is used to construct an asset holdings matrix to analyse fire sales.

We specifically focus on matrix reconstruction methods by Upper and Worms (2004) (Entropy method), Anand et al. (2015) (Minimum Density method), Squartini et al. (2017) (Statistical Physics method) and Gandy and Veraart (2017) (Bayesian method).

These methods use the partial information to form an asset holdings matrix, where this matrix is consistent with the partial information. We consider these methods in their suitability for evaluating fire sales and how close fire sales losses are to those based on the fully observed data.

We use the fire sales measures to quantify fire sales losses by Greenwood et al. (2015). These measures assume banks sell assets to maintain fixed target leverage, where selling these assets has a fire sales impact. We use these measures because they incorporate the key features of fire sales contagion e.g., the overlap in bank portfolios and the associated price impact when assets are sold.

We focus on two types of policy interventions: capital injections and leverage caps. Applied in any form, these policies will always decrease the magnitude of fire sales. This is because these policies decrease banks' target leverages, which from the fire sales mechanism decreases the total assets which banks need to sell. We consider how to optimise these policies using matrix reconstruction methods under partial information, and how this compares if the fully observed data was used.

We compare the performance of policy interventions under different matrix reconstruction methods for fire sales losses to policy interventions informed by the fully observed data. We find the reduction in fire sales losses from policy interventions under partial information is close to the results under the fully observed data. The results from policy interventions under partial information were closest for sample-based matrix reconstruction methods (methods in which multiple reconstructed matrices are generated). This shows considering methods, where a larger number of reconstructed matrices are included, can decrease fire sales losses from policy interventions.

While there are suitable matrix reconstruction methods which can be used for policy interventions, there are other matrix reconstruction methods that perform poorly. In some cases, not using matrix reconstruction methods and adopting a “naive” approach (one that does not use a reconstruction method) can result in a policy intervention that is closer to the size of the intervention under the fully observed data. One type of naive capital injection policy could assign an equal quantity of capital to all banks, where this allocation of capital does not depend on the assumed partial information. Compared with this naive approach, there may be a matrix reconstruction method which is further away from the individual fire sales losses of banks under the fully observed data.

The optional use of matrix reconstruction methods for policy interventions is one of the key differences in both assessing and mitigating fire sales losses. In assessing fire losses, matrix reconstruction methods are always used, because the contagion dynamics of fire sales cannot be considered without reconstructing the matrix. In comparison, policy interventions can be conducted without any knowledge of the financial network. Therefore, using a matrix reconstruction method is not enough to mitigate fire sales losses, additionally, the performance of the method for the given policy intervention should be

accounted for.

The closest papers to this work are by Di Gangi et al. (2018), Squartini et al. (2017) and Ramadiah et al. (2020). In Di Gangi et al. (2018), they also analyse fire sales under partial information, where they use variations of the maximum entropy method for the matrix reconstruction. In Squartini et al. (2017), they introduce the Statistical Physics method and conduct a first-round analysis of fire sales. Our work is different from these two papers because we explore the area of policy interventions in our fire sales analysis. We also introduce the matrix reconstruction method by Gandy and Veraart (2017) to analyse fire sales, which contrasts with the physics-motivated approaches used by Di Gangi et al. (2018) and Squartini et al. (2017). The work by Ramadiah et al. (2020) does explore policy interventions under partial information, but these policy interventions only compare the change of matrices under partial information e.g., bank mergers and splits. This is different to our work, as we consider policy interventions which are informed by partial information on the fully observed data. All our results on policy interventions capture the real effects of fire sales, as we assess the reduction in losses only on the fully observed data.

Our second main contribution is to develop a reverse stress testing framework to derive scenarios which reflect the largest losses banks are exposed to. Rather than simulating losses based on a given scenario, the losses are assumed and a scenario is derived which is consistent with those assumed losses. Each scenario derived from this approach accounts for the input data and assumed fire sales mechanism. We believe these scenarios are informative in identifying shocks to assets that have not been observed. These results are in Chapter 3 of the thesis.

The motivation for a reverse stress test is to derive scenarios that do not rely on previous assumptions about other datasets or historic events (there may be other motivations in choosing a stress testing scenario). While other datasets can be informative in how current stress tests are conducted, they might be biased by the policymaker choosing the scenario. Therefore, a reverse stress test is useful in identifying extreme losses, which is relevant given the potential nature of fire sales.

Our reverse stress test method is for the fire sales mechanism by Greenwood et al. (2015), as in Chapter 2. This reverse stress testing approach accounts for multiple rounds of deleveraging that may occur in fire sales.

For the initial round of fire sales, we find assets shocked are concentrated in banks with high target leverages. The focus on leverage comes from the fire sales mechanism, where banks with higher target leverages sell a larger proportion of assets, leading to higher price impacts and further asset sales. These leverage-driven scenarios account for the systematic way in which banks liquidate their assets, under the fire sales mechanism. Reverse stress tests in other studies do not show these scenarios, as they are not target leverage-driven in their approach.

We find that for scenarios derived from a reverse stress test, the total fire sales losses are larger than other benchmark stress tests and higher in the number of banks which suffer large losses. This is because scenarios from a reverse stress test are focused on banks with high target leverages, which is reflected in the target leverage approach of asset shocks. While the reverse stress tests are formulated to account for the largest total bank losses, the number of banks with severe losses is an additional consequence of this approach.

We conduct a sensitivity analysis for how scenarios derived from a reverse stress test change when different bounds on the magnitude of shocks are assumed. We find that derived scenarios under different bounded shocks result in a similar level of losses. The difference between reverse stress testing scenarios under different bounds is reflected in the number of assets that are initially shocked in the fire sales scenario. Our results show losses from scenarios, with small-magnitude shocks across a high number of assets are similar to losses from scenarios, with high-magnitude shocks across a small number of assets.

The papers closest to this work are by Baes and Schaanning (2023) and Grigat and Caccioli (2017). The work by Baes and Schaanning (2023) considers a reverse stress testing approach using the fire sales mechanism by Cont and Schaanning (2017). They account for assets sold which depend not on a specific target leverage, but a prescribed target leverage region for which the bank sells its assets. From the reverse stress test, they generate multiple scenarios and evaluate this collection of scenarios using clustering algorithms. In our work, we assume banks sell assets to a fixed target leverage, and therefore, we can optimise the shock under this systematic behaviour. The work by Grigat and Caccioli (2017) is similar to our reverse stress testing approach, where an optimisation problem is formulated and a constraint of the total losses is given. However, this work is on counterparty losses under the DebtRank measure by Battiston et al. (2012c), compared with our work in the channel of fire sales. We also only assume the initial losses are known from a fire sale (as in Baes and Schaanning (2023)), compared with assuming the total fire sales losses. Therefore, we reduce the margin of error in estimating fire sales losses while factoring in losses based on future rounds of fire sales.

Our third main result is developing a collateral-based model with the inclusion of two channels of fire sales. Under this collateral-based model, we find losses are amplified when there is a high overlap between assets externally held by banks and assets used as collateral. Furthermore, the size of losses from the overlap in these assets can be larger than if the bank held no illiquid external asset holdings. These additional losses come from the inclusion of two channels of fire sales, in addition to the interbank network. We account for these channels in a new collateral-based clearing model, where losses are simulated using random network models. These results are in Chapter 4 of the thesis.

We provide a brief description of the role of externally held assets and assets used as

collateral in a clearing situation. A clearing event can occur because the bank is unable to meet its obligations in full. As a result, the bank sells a proportion of its external asset holdings to meet its remaining obligations. If the bank is unable to fully cover its obligations by selling all its external asset holdings, the assets used as collateral are then seized by the associated counterparty and sold. There is a mark-to-market adjustment on illiquid assets sold, leading to a price impact and a decrease in the asset price. The depreciation in the asset value from fire sales can lead to further rounds of fire sales, where a larger quantity of assets are sold. The inability of banks to meet their obligations and the decrease in the price of illiquid assets sold can increase the shortfall of bank payments and increase bank defaults. While only two of the following aspects have been incorporated into a systemic risk model: fire sales on the bank's external asset holdings, fire sales for assets used as collateral and counterparty losses between banks with interbank assets and liabilities, there has been no previous model which considers all three.

We build on the collateral-based clearing model as proposed by Ghamami et al. (2022), in which banks with obligations also post assets as collateral. The model by Ghamami et al. (2022) assumes banks only hold liquid assets in their external asset holdings, and therefore, this model only accounts for one channel of fire sales, represented by illiquid assets used as collateral. We include a portfolio of assets where banks can hold multiple illiquid and liquid assets in a clearing event, as considered by Feinstein and El-Masri (2017). Assets used as collateral are not accounted for by Feinstein and El-Masri (2017), and neither are the illiquid external assets by Ghamami et al. (2022). Leaving out one of these fire sales channels can lead to underestimating losses. Therefore, incorporating both aspects into a single clearing model results in a new clearing model with two channels of fire sales.

We consider a combination of different external asset holdings, and how this interacts with assets used as collateral. We assume the case where assets used as collateral are liquid as in Ghamami et al. (2022) and the case where illiquid assets are used. With the fire sales channel from collateral assets, we consider a variation of external asset holdings portfolios representing different levels of commonality with the overlap of assets used for collateral. We examine how the incorporation of assets under two channels of fire sales can amplify or dampen systemic losses in a clearing event.

Our results show a high overlap with collateral assets and externally held assets can result in losses larger than if the bank held no external illiquid assets. These larger losses depend on how liquid banks' external assets and assets used as collateral are. If assets are highly illiquid, then losses can be larger than if banks held no external asset holdings. We find the increase in losses with additional external asset holdings only comes from the fact that there is some level of commonality with assets used as collateral. If the groups of assets used for collateral and the bank's external asset holdings were independent of each other, then holding external assets will always reduce losses under a clearing event.

This is because the independence between these groups of assets means there is no direct feedback between both channels of fire sales. Losses can still be transmitted through the interbank network, but this would be lower than losses in the same financial network where banks held no external assets.

We examine how the change in network topology affects losses under the collateral model. Our results show an increase in network density decreases the shortfall of bank payments and decreases the total number of bank defaults. Even when there is a high commonality between external asset holdings and assets used as collateral, banks with no external asset holdings in general result in larger bank losses. In the presence of two channels of fire sales, a change in the network topology can reduce bank losses.

The collateral-based models by Chang (2019) and Chang and Chuan (2023) are closest to the new collateral-based model in this work. In Chang (2019), they introduce a clearing mechanism and consider the rehypothecation of assets used as collateral. The work by Chang and Chuan (2023) builds on the work from Chang (2019) and studies network topologies and resilience of banks under the clearing process, in a similar way to the work by Acemoglu et al. (2015) i.e., specific network structures such as ring networks and complete networks. The work by Chang and Chuan (2023) also accounts for the fire sales impact on illiquid assets. Our work is different to these models as we extend the model from Ghamami et al. (2022), which deals with collateral payments using two defined rounds of clearing. We analyse these two rounds in our extended model and determine cases where the number of defaults either increases or decreases, depending on various network parameters.

We highlight another result in this thesis in the areas of policy interventions and financial networks. We build a framework evaluating the policy of ring-fencing, which is a separation of a bank's balance sheet into two separate entities: a ring-fenced bank (RFB) and a non-ring-fenced bank (nRFB). The RFB holds external assets which are independent of the interbank network. The nRFB holds all remaining assets and is still part of the interbank network. To our knowledge, this work is the first to define the operations of ring-fencing for banks in a financial network.

Our results show ring-fencing can increase or decrease the total re-evaluated equity of the RFB and nRFB, compared with the bank before ring-fencing. Secondly, accounting for the financial network, the change in equity after re-evaluation can affect the nRFB and banks which do not ring-fence. These results are in Chapter 5 of the thesis.

We mainly focus on ring-fencing that was implemented in the UK for some of the largest retail banks in 2019. The regulatory motivation of ring-fencing is to separate assets associated with the real economy i.e., domestic deposits and retail assets from the riskier assets the bank holds. These safer assets would be allocated to an RFB, where all other assets would remain with the nRFB. As we assume only external assets would be allocated

to the RFB, the losses incurred with the nRFB from other banks in the interbank network do not spill over to assets associated with the RFB. While this does partially protect the assets of the RFB (only partially because the RFB could still be exposed to other market shocks), it has been argued this makes the nRFB riskier. Hence, the wider financial system could suffer large losses from the ring-fencing policy, at the expense of protecting a smaller subset of assets associated with the real economy.

We find ring-fencing can increase or decrease the total equity, compared with the total equity before ring-fencing. The total equity of the system can change from ring-fencing because the valuation model we consider is based on leverage. Using leverage, ring-fencing can either increase or decrease the leverage component of the RFB and nRFB. The changes in leverage are then reflected in each bank under the valuation model, which can then impact the equity of other banks under re-evaluation.

The valuation model is based on leverage to account for the asset adjustment that occurs before a bank defaults. If we considered the valuation of ring-fencing based only on equity, then ring-fencing would always decrease the equity of the financial system. This is because in all cases, we are taking away a proportion of equity to the RFB, which could be considered as a shock to the financial network. This type of modelling may be suitable in a clearing event, but in this case, we are not assuming banks default from ring-fencing. Therefore, the change in equity is considered relative to the bank's asset holdings, where a decrease in equity from ring-fencing can either increase or decrease the leverage of the RFB and nRFB.

We use a general valuation framework to capture the changes from ring-fencing in a financial network. We use the network valuation model by Barucca et al. (2020), which can account for a variety of clearing and valuation models i.e., clearing models introduced by Eisenberg and Noe (2001) and Rogers and Veraart (2013). As we do not consider ring-fencing to be a systemic event, and model changes in equity before banks default, we use valuation frameworks similar to the work by Bardoscia et al. (2019). The valuation models by Bardoscia et al. (2019) are motivated by the credit risk literature and account for the valuation of assets before a bank has defaulted.

While ring-fencing in financial networks has not been explored, there has been significant empirical work on ring-fencing. The work by Erten et al. (2022) focuses on the access to funding for RFBs and nRFBs, and finds the costs to access funding for RFBs are lower than nRFBs. This can be explained as part of our framework, where the individual riskiness of banks is associated with their leverage. If ring-fencing is performed such that the leverage of the RFB is smaller than the bank before ring-fencing, then the RFB is safer, and therefore, the RFB incurs a lower cost for funding. The work by Caprio et al. (2007) and Laeven and Levine (2007) finds countries which impose ring-fencing lead to lower valuations on the bank's assets. In our model, the decrease in the valuation of the nRFB's assets comes from ring-fencing where the RFB is safer.

Our work on ring-fencing uses a valuation framework, accounting for the topology of the network. The work by Allen and Gale (2000), Gai and Kapadia (2010) and Battiston et al. (2012a) show how different structures impact bank losses under the valuation and clearing frameworks. While we discuss the impact of the network on ring-fencing, the type of ring-fencing conducted means there is no change in the financial network. The only change from ring-fencing is the quantity of external assets and liabilities banks hold. There are similarities in ring-fencing to other structural policy changes in financial networks in works by Rogers and Veraart (2013) on bank mergers and Veraart (2022) on portfolio compression. The underlying message in Rogers and Veraart (2013) and Veraart (2022), along with our work on ring-fencing is that while the policy is intended to increase financial stability, depending on the network, this could increase bank losses.

The last result we highlight is the application of financial networks as an illustrative tool to understand trends between assets. During the COVID-19 period, we found a high positive average correlation between sovereign bond yields compared with the average correlation in the last decade. When using network filtering methods, we see the increase in positive correlation reflected in different subsets of sovereign bonds. We believe this is a significant result because it demonstrates the peak financial and economic impacts of COVID-19 from sovereign bonds. These results are in Chapter 6 of the thesis.

The application of financial networks to understanding asset trends is focused on the COVID-19 period. This period had a significant impact on a range of financial markets, which had not experienced a health crisis in recent years e.g., Europe and the USA. The scale of COVID-19 caused governments to react in drastic ways, and these actions were reflected in the financial markets. We consider the trends of sovereign bond yields because it is an indicator of the economic state of the associated country. Using the data on this asset, we can observe the local changes between countries with large economies i.e., we focus on 17 European sovereign bonds.

We use network filtering methods in the area of Econophysics to understand trends in sovereign bond yields. A network is formed from network filtering methods by selecting a subset of correlations from a correlations matrix. The number of correlations selected is determined by the desired topological properties of the filtered network. By considering a subset of correlations under a network filtering method, we can analyse different relationships between assets under an associated network structure.

As there are multiple ways to form a filtered network, we consider methods by Kruskal (1956) (Minimum Spanning Tree), Qian et al. (2010) (Maximal Spanning Tree), Onnela et al. (2003b) (Asset Graph) and Tumminello et al. (2005) (Triangulated Maximal Filtering Graph). We selected these methods because we can analyse the correlations matrix in a given time window, which is of interest when focusing on the period of COVID-19. An array of methods are used because, in several papers, only the Minimum Spanning Tree

method is used. We argue the Minimum Spanning Tree misses key network features, particularly in the event of COVID-19, where these missing network features are included in other approaches. We believe we are one of the first studies to consider network filtering methods to analyse the financial markets during COVID-19.

While there is a distinctive peak in the period of COVID-19 for the magnitude of average correlations, the trends in network centrality are similar to previous years. More specifically, the centrality of nodes in networks reflecting more negative correlations is more volatile compared with networks reflecting more positive correlations. As we focus on European sovereign bonds, we see the level of stability from positive correlations associated with assets which adopt the Euro, compared with networks of negative correlations which are associated with assets that are non-Euro denominated. These trends are no different during the COVID-19 period where there is a greater observation of these groups. We argue a level of fragmentation during COVID-19 between sovereign bonds that have not been observed since the 2008 Great Financial Crisis or 2012 Euro Debt Crisis e.g., groups of similar countries between GIIPS (Greece, Ireland, Italy, Portugal and Spain) and ABFN (Austria, Belgium, Finland and the Netherlands).

Different network filtering methods are used for DAX30 stocks by Birch et al. (2016). A combination of both network filtering methods and entropy measures have been used for the S&P500 by Kukreti et al. (2020). A comparison of network filtering methods where associated network centrality measures are applied for the US equity data is considered by Aste et al. (2010). Our study differs from these papers in a comparison of filtering methods because we evaluate both positive and negative correlations. We, therefore, examine a large selection of correlations, which we believe is relevant given the impact of COVID-19.

There has been a wide application of Econophysics approaches to study trends in the financial markets. Laloux et al. (2000) and Junior and Franca (2012) have used random matrix methods to study the distribution of eigenvalues of a financial correlations matrix. Information theory to assess the uncertainty of financial markets using entropy has been used by Huang et al. (2012) and Darbellay and Wuertz (2000). Community analysis has been used by Vodenska et al. (2016) to identify groups between assets, where this technique is useful when including a large number of assets. The advantage of using network filtering methods compared to other approaches is the output of a network, allowing a visual representation of a subset of correlations between nodes.

Chapter 2

Assessing and mitigating fire sales risk under partial information

2.1 Introduction

Fire sales pose a key threat to financial stability since they can significantly amplify initial losses. They are one of the main channels of systemic risk. During the 2007-2008 Global Financial Crisis (GFC) amplification mechanisms played a major role. It was estimated that \$ 300 bn of subprime mortgage-related losses were turned into over \$ 2.5 trillion of potential write-downs in the global banking sector within a year (Brazier, 2017). Therefore it is a key concern for financial regulators to identify any potential channels of systemic risk and find tools and mechanisms to mitigate their impact. In this chapter, we will focus on fire sales.

While significant progress on modelling fire sales has been made, the models proposed usually assume that the asset holdings of the financial institutions are observable, see e.g., Shleifer and Vishny (2010); Cont and Wagalath (2013); Greenwood et al. (2015); Cont and Schaanning (2017, 2019). In practice, however, often only partial information about the asset holdings is available. Usually, regulators have only detailed information on the banks that they regulate and not beyond.

In this chapter, we show how one can both assess and mitigate fire sales risk under partial information. We consider a matrix X , where each element X_{nk} represents the amount of asset k that bank n holds (in EUR). We are interested in situations in which these individual positions are not observable but the corresponding column and row sums of X representing the total market capitalisation of asset k and the total assets of bank n are observable. To conduct stress testing under partial information, we use matrix reconstruction methods by (Upper and Worms, 2004; Anand et al., 2015; Cimini et al., 2015; Gandy and Veraart, 2017, 2019) to reconstruct the asset holding matrix X from the observed row and column sums.

This chapter makes two main contributions: First, it conducts a horse race between different network reconstruction methods and compares their performance in quantifying fire sales risk in financial stress tests under partial information. Second, we show that there are clear benefits of using suitable network reconstruction techniques not just for quantifying fire sales risk but also for mitigating it. In particular, we show that policy interventions based on suitable network reconstruction methods can significantly outperform ad hoc policy interventions that do not account for the interconnectedness of financial institutions. We identify which network reconstruction methods are best suited to use for policy interventions to mitigate fire sales risk. To the best of our knowledge, our analysis is the first that considers the mitigation of fire sales risk under partial information.

We consider the modelling framework and risk measures developed by Greenwood et al. (2015) to assess fire sales risk. Their key assumption is that banks aim to maintain their target leverage, i.e., the ratio of debt to equity.¹ Empirical evidence for this behaviour has been provided by Adrian and Shin (2010). We conduct a stress testing exercise using empirical data from the European Banking Authority (EBA) that they used in their 2011 and 2016 EBA stress tests. The EBA has collected full information on the asset holdings of the banks that participated in these stress tests. This allows us to compare results under partial information to results under full information.

We find that all matrix reconstruction methods considered are able to reproduce the general trend, namely, that fire sales risk was lower in 2016 than in 2011. We show how the performance of the different network reconstruction methods applied to quantifying fire sales risk depends on the stress scenarios. Overall, we find that reconstruction methods attempting to approximate the distribution of the underlying network such as Cimini et al. (2015); Gandy and Veraart (2017, 2019) are better suited to assess fire sales risk from partial information than optimisation-based network reconstruction methods such as the ones by Upper and Worms (2004); Anand et al. (2015).

Next, we consider several policy interventions to reduce fire sales risk. In particular, we are interested in evaluating whether it is possible to conduct policy interventions at an early stage of a fire sales cascade to mitigate losses. At such an early stage, it is unlikely that full information on the underlying asset holdings is available. We therefore again conduct two types of analyses: First, we assume that full information on the underlying asset holding network is available and use this full information to decide on

¹To see the effect of leverage targeting, consider a bank with a stylised balance sheet whose asset side consists of securities and whose liabilities side consists of debt and equity. So, if market stress leads to a decrease in the value of securities, i.e., the assets, then on the liabilities side of the balance sheet the value of the equity decreases, and hence the leverage increases. To move back to the target leverage a bank can now sell assets to pay off some of its debt. Hence, a decrease in asset values can trigger (fire) sales. If large quantities of assets are liquidated, this creates a price impact, i.e., their prices decrease. This forces other institutions to re-evaluate their portfolios, which might lead to further rounds of deleveraging and price impacts.

policy interventions. Second, we base all policy intervention decisions on asset holding networks that were reconstructed from partial information and we compare the outcome of the system to the outcome under full information. We compare ad hoc strategies that do not use network reconstruction to strategies that use network reconstruction to decide on policy interventions. We find that there are clear benefits of using network reconstruction over ad hoc methods. In particular, we find that the Bayesian approach to network reconstruction by Gandy and Veraart (2017, 2019) is particularly successful when used for policy interventions to mitigate fire sales risk.

Another contribution of our analysis is to show theoretically how the fire sales risk measures introduced by Greenwood et al. (2015) depend on the individual entries of the asset holdings matrix and how much they only depend on the aggregate information, i.e., the row and column sums of the asset holding matrix. We provide theoretical results that show that for some stress scenarios, only very limited information on the underlying asset holdings matrix is required to either assess the related fire sales risk or to make a meaningful intervention to mitigate these risks. In particular, we show that determining the initial spread of losses via connected portfolios requires far less information than determining who is eventually negatively affected by fire sales. This explains why policies aimed at mitigating the initial round of fire-sales losses can still be successfully applied under partial information.

We emphasise that these theoretical results are not only for the matrix reconstruction methods used in this study, but are applicable to a wide range of matrix reconstruction methods. Furthermore, they provide an analytical framework to study the sensitivities of the fire sales measures, with respect to various model parameters.

The structure of this chapter is as follows. In Section 2.2, we describe the modelling framework by Greenwood et al. (2015) for quantifying fire sales. In Section 2.3, we provide theoretical results on how the fire sales measure depended on the asset holding matrices. Furthermore, we provide some background on the network reconstruction methods used. In addition, we describe the stress testing data by the European Banking Authority (EBA) that we use in our empirical analysis. We compare the performance of different matrix reconstruction methods in replicating fire sales measures by Greenwood et al. (2015) for the EBA data. In Section 2.4, we present our results on the performance of policy interventions based on both full and partial information. Finally, Section 2.5 concludes.

2.1.1 Related literature

Our analysis is based on the framework for quantifying fire sales risk by Greenwood et al. (2015). In contrast to Greenwood et al. (2015) who assume full knowledge of the asset holdings, we assume that only partial information of the asset holdings is available.

Hence, we conduct a two-step analysis. In the first step, we reconstruct the network of asset holdings from partial information. In a second step, we apply the measures by Greenwood et al. (2015) to the reconstructed networks and compare the results to those obtained under full information.

We will consider a range of reconstruction methods to obtain an estimate of the asset holding matrix based on partial information. The goal of all these methods is to reconstruct the individual entries of the matrix from given row and column sums. We will consider the network reconstruction methods proposed by Upper and Worms (2004), Anand et al. (2015), Cimini et al. (2015), and Gandy and Veraart (2017, 2019) in our analysis and compare their performance. We provide more details on them in Appendix 8.A.

Several papers have compared the performance of different matrix reconstruction methods. Gandy and Veraart (2019) have compared the Bayesian method by Gandy and Veraart (2017) (and some extensions) to the approaches by Cimini et al. (2015) and Upper and Worms (2004) using network data of Credit Default Swaps exposures where the reference entity was a UK institution. They found that the Bayesian method outperformed alternative reconstruction methods using a wide range of matrix comparison measures. Anand et al. (2018) compares a wide range of methods (not including the Bayesian approach by Gandy and Veraart (2017, 2019)) by applying them to data from 25 different markets from 13 jurisdictions. They find that it depends on the characteristics of the networks which method works best for its reconstruction. Among the probabilistic methods, they found that the method by Cimini et al. (2015) worked best. Lebacher et al. (2019) compare several network reconstruction methods including, e.g., entropy, Bayesian and gravity (a regularised entropy method with a penalising factor) type reconstruction methods using SWIFT data. Their paper finds that the performance of the reconstruction methods is dependent on the type of network being reconstructed, arriving at a similar conclusion as in Anand et al. (2018).

The papers Di Gangi et al. (2018), Squartini et al. (2017) and Ramadiah et al. (2020) conduct a similar analysis as we do - in the sense that they apply network reconstruction methods for assessing fire sales. Di Gangi et al. (2018) focuses on variations of the maximum entropy method for the network reconstruction and uses the Greenwood et al. (2015) measures to quantify fire sales risk using data from the USA. Squartini et al. (2017) apply the model by Cimini et al. (2015) to reconstruct bipartite networks of asset holdings. They use data on security holdings by the European Central Bank and use the fire sales measure by Greenwood et al. (2015) to consider a relative systemicness index in evaluating the reconstructed matrices. Ramadiah et al. (2020) evaluate a range of reconstruction methods with systemic risk indicators for fire sales risk. They use data from bank-firm interactions in Japan and analyse the effect of aggregation on the performance of reconstructed matrices.

This work deviates from the existing literature by first analysing the Bayesian reconstruction methods by Gandy and Veraart (2017, 2019) in the context of fire sales risk and by comparing them to other approaches. But second and most importantly, we also analyse the effect of different policy interventions under both full and partial information.

So far policy interventions have only been studied under full information. Shleifer and Vishny (2010) considers the effect of credit easing on fire sales risk in comparison with other policies. Capponi and Larsson (2015) builds on the systemic measures from Greenwood et al. (2015) and Duarte and Eisenbach (2021) propose a liquidation strategy to reduce the systemic risk of the network. Greenwood et al. (2015) consider a wide selection of policy interventions to mitigate fire sales risk. But all these papers have not considered such interventions in only partially observed financial networks which is what we do here.

2.2 Fire sales in financial networks

We now describe the modelling framework for stress testing and assessing fire sales risk by Greenwood et al. (2015).

2.2.1 The financial market

The financial market consists of $N \in \mathbb{N}$ banks and $K \in \mathbb{N}$ assets, the set of banks is denoted by $\mathcal{N} = \{1, \dots, N\}$ and the set of assets is denoted by $\mathcal{S} = \{1, \dots, K\}$. The main model considers two periods with time indices $t = 1, 2$.²

We denote by $X = (X_{nk})_{n \in \mathcal{N}, k \in \mathcal{S}} \in [0, \infty)^{N \times K}$ the asset holdings matrix at time $t = 1$, where X_{nk} represents the amount of asset $k \in \{1, \dots, K\}$ that bank $n \in \{1, \dots, N\}$ holds in million EUR. Furthermore, we consider the row and column sums of X given by

$$\alpha_{n1} = \sum_{k=1}^K X_{nk} \quad \forall n \in \mathcal{N}, \quad c_k = \sum_{n=1}^N X_{nk} \quad \forall k \in \mathcal{S}, \quad (2.1)$$

and refer to α_{n1} as the total assets of bank n at time $t = 1$ and to c_k as the total capitalisation of asset k . (Strictly speaking, c_k is the total capitalisation of asset k among the nodes \mathcal{N} , but since we do not consider other financial institutions beyond those in \mathcal{N} we will not make this distinction.)

We also define the matrix of portfolio weights denoted by $M = (m_{nk})_{n \in \mathcal{N}, k \in \mathcal{S}} \in \mathbb{R}^{N \times K}$, where $m_{nk} = X_{nk}/\alpha_{n1}$ i.e., m_{nk} describes the weight of asset k within the total asset portfolio of bank n . In particular, for all $n \in \mathcal{N}$, $\sum_{k=1}^K m_{nk} = 1$.

²Extension to more than two periods have been discussed in Greenwood et al. (2015) as well, but we will not consider these extensions here. Multiple rounds of deleveraging have also been considered in Cont and Schaanning (2017) and Huang et al. (2013). To account for higher order effects, fire sales have also been modelled directly as fixed point problems, see e.g., Cifuentes et al. (2005) and Amini et al. (2016).

Assets	Liabilities
assets α_{nt}	debt d_{nt}
	equity e_{nt}

 Table 2.1: Balance sheet of bank $n \in \mathcal{N}$ at time t .

We consider a stylised balance sheet, see Table 2.1, in which for each bank $n \in \mathcal{N}$ its time t debt is denoted by d_{nt} and its time t equity is denoted by e_{nt} . Then, its total assets at time t are given by $\alpha_{nt} = e_{nt} + d_{nt}$ and the time t leverage of bank n is given by

$$b_{nt} = \frac{d_{nt}}{e_{nt}} = \frac{\alpha_{nt} - e_{nt}}{e_{nt}}. \quad (2.2)$$

2.2.2 The stress test and fire sale mechanism

As part of a stress testing exercise, Greenwood et al. (2015) assume that at time $t = 1$ there is a negative shock to (some of the) assets. We denote by $F_1 = (f_{11}, \dots, f_{K1})^\top$, with $f_{k1} \leq 0$ for all $k \in \mathcal{S}$, the shock vector which is a vector of non-positive net asset returns. The unlevered return on the portfolios of the N banks, denoted by $R_1 = (R_{11}, \dots, R_{N1})^\top \in \mathbb{R}^N$, is then given by $R_1 = MF_1$. In particular, $R_{n1} = \sum_{k=1}^K m_{nk} f_{k1}$ for all $n \in \mathcal{N}$.

Greenwood et al. (2015) assume that, in response to such a negative shock, banks will sell assets to return to their target (original) leverage b_{n1} .³

Furthermore, they assume that banks sell assets proportionally to their existing holdings determined by the matrix of portfolio weights M .⁴ In addition, they assume that the sale of assets will have a linear price impact, modelled by K parameters $l_1, \dots, l_K \in [0, \infty)$. In particular, the parameter $-l_k \leq 0$ models the negative shock to asset $k \in \mathcal{S}$ per million EUR of asset k sold.⁵ In particular, the fire sale in one specific asset does not affect prices in any other assets. This price impact represents a second shock to the market which could in principle lead to further deleveraging, but we do not consider later rounds of deleveraging in this chapter.

³For a bank directly affected by the shock it holds that $\alpha_{n1}R_{n1} < 0$. Hence, its leverage increases from $b_{n1} = d_{n1}/e_{n1}$ to $d_{n1}/(e_{n1} + \alpha_{n1}R_{n1})$. It therefore sells $y_{n1} = -\alpha_{n1}b_{n1}R_{n1} > 0$ assets, if it has enough assets still available, i.e., if $-\alpha_{n1}b_{n1}R_{n1} < \alpha_{n1}(1 + R_{n1})$. It then pays back parts of its debt leading to a new leverage of $(d_{n1} - y_{n1})/(e_{n1} + \alpha_{n1}R_{n1}) = b_{n1}$, which is indeed the original (target) leverage. (Since a bank can never sell more assets than it has, to be precise one would need to set $y_{n1} = (\min\{-\alpha_{n1}b_{n1}R_{n1}, \alpha_{n1}(1 + R_{n1})\})^+$. In our case studies, this cap was never reached, therefore we ignore it in the following to keep the notation simpler.

⁴This means, that bank n sells $-m_{nk}y_{n1} \geq 0$ of asset k (in million EUR). In our empirical analysis, all nodes had enough assets left to sell according to this rule.

⁵The total amount of asset k sold is $\phi_{k1} = -\sum_{n=1}^N m_{nk}\alpha_{n1}b_{n1}R_{n1}$ and the resulting time 2 shock to asset k is then $f_{2k} = -l_k\phi_{k1}$.

2.2.3 Measuring fire sales risk

We now define the measures for quantifying fire sales risk proposed by Greenwood et al. (2015) using slightly different notations in some places.

The **aggregate vulnerability**, denoted by \mathcal{AV} , is the total banks' equity lost due to deleveraging following an initial shock F_1 divided by the total equity in the system before the shock. Mathematically it is defined as

$$\mathcal{AV} = \sum_{n=1}^N \mathcal{SYS}(n), \quad (2.3)$$

where $\mathcal{SYS}(n) \in [0, \infty)$ denotes the systemicness of bank $n \in \mathcal{N}$. Hence, the *systemicness* of a bank quantifies the effect that an individual bank $n \in \mathcal{N}$ has on the aggregate vulnerability.

For each bank $n \in \mathcal{N}$, the **systemicness** $\mathcal{SYS}(n) \in [0, \infty)$ measures the contributed relative equity loss from an individual bank n (relative to the total equity of banks in the network). The systemicness of a bank $n \in \mathcal{N}$ is defined as

$$\mathcal{SYS}(n) = \gamma_{n1} \frac{\alpha_{n1}}{\sum_{\nu=1}^N e_{\nu 1}} b_{n1} (-R_{n1}), \quad (2.4)$$

$$\gamma_{n1} = \sum_{k=1}^K \left(\sum_{p=1}^N \alpha_{p1} m_{pk} \right) l_k m_{nk} = \sum_{k=1}^K c_k l_k m_{nk}. \quad (2.5)$$

From this representation, one can see that systemicness is a product of four factors which all have an economic interpretation. In particular, as discussed in Greenwood et al. (2015), the systemicness of a bank is larger if: γ_{n1} , referred to as ‘‘connectedness’’ in Greenwood et al. (2015), is larger meaning that it is more connected in the sense that it holds assets with a large market capitalisation c_k , or whose sale has a large price impact l_k ; the size measured by $\frac{\alpha_{n1}}{\sum_{\nu=1}^N e_{\nu 1}}$ is larger since banks with larger total assets will liquidate more assets in a fire sale; the leverage b_{n1} is larger since the leverage amplifies the volume of assets sold in order to maintain the target leverage; $(-R_{n1})$ is larger, i.e., it is hit by a larger shock.

The **direct vulnerability** of bank $n \in \mathcal{N}$, denoted by $\mathcal{DV}(n) \in [0, \infty)$, is the fraction of its equity lost directly due to the initial shock F_1 . It is given by

$$\mathcal{DV}(n) = \frac{\alpha_{n1} (-R_{n1})}{e_{n1}}. \quad (2.6)$$

The **indirect vulnerability** for a bank $n \in \mathcal{N}$, denoted by $\mathcal{IV}(n) \in [0, \infty)$, measures the fraction of its equity that is lost due to the deleveraging of the banks. It is defined as follows

$$\mathcal{IV}(n) = \frac{\alpha_{n1}}{e_{n1}} \sum_{k=1}^K \left[l_k m_{nk} \left((-1) \sum_{j=1}^N m_{jk} \alpha_{j1} b_{j1} R_{j1} \right) \right]. \quad (2.7)$$

The intuition behind the formula (2.7) is as follows. The first factor α_{n1}/e_{n1} measures the effect of the leverage of a bank. Higher leverage will result in higher indirect vulnerability. The second term of interest is $l_k m_{nk}$ and as shown in Greenwood et al. (2015) it can be interpreted as an illiquidity-weighted exposure measure to asset k . Finally, the total volume of asset k sold is $-\sum_{j=1}^N m_{jk} \alpha_{j1} b_{j1} R_{j1} \geq 0$. Hence, nodes that hold a large amount of illiquid assets that are sold in large quantities have a high indirect vulnerability.

Although the systeminess and the indirect vulnerability share common factors, a bank n may have a high $\mathcal{IV}(n)$ and a low $\mathcal{SYS}(n)$ or vice versa, as noted in Greenwood et al. (2015).

2.2.4 Observability and choice of model parameters

The financial market is characterised by a matrix of asset holdings X and the equity of the institutions e_{n1} , $n \in \mathcal{N}$. The equities e_{n1} are in principle observable from balance sheet data. The asset holding matrix is not necessarily fully observable.

Definition 2.2.1 (Full and partial information). *We refer to a stress test as being under full information if the asset holding matrix X is fully observed, i.e., if for all $n \in \mathcal{N}, k \in \mathcal{S}$, the individual entries X_{nk} are known.*

We refer to a stress test as being under partial information if only the row and column sums of the asset holding matrix X given in (2.1) are known, but for all $n \in \mathcal{N}, k \in \mathcal{S}$, the individual entries X_{nk} are unknown.

In both situations, we assume that the equity e_{n1} is known for all $n \in \mathcal{N}$.

In practice, detailed information on individual asset holdings X_{nk} is often not available, in particular when one considers financial institutions operating in different jurisdictions. The row and column sums of the asset holding matrix are more widely available (from balance sheet and market data).

To conduct the stress testing exercise we will need to specify the shocks f_{k1} , $k \in K$ and the price impact parameters l_k , $k \in \mathcal{S}$. We will consider different choices for the shocks f_k , $k \in \mathcal{S}$.

Definition 2.2.2 (\tilde{K} -asset shock and all asset shock). *We refer to a situation in which only $0 < \tilde{K} \leq K$ assets are shocked as a \tilde{K} -asset shock. We denote the indices of shocked assets by $\mathcal{I}^{\tilde{K}} \subseteq \mathcal{S}$. Then, $|\mathcal{I}^{\tilde{K}}| = \tilde{K}$. Furthermore, $f_i < 0$ for all $i \in \mathcal{I}^{\tilde{K}}$ and $f_i = 0$ for all $i \in \mathcal{S} \setminus \mathcal{I}^{\tilde{K}}$.*

If all assets are shocked equally, i.e., $f_1 = \dots = f_K = f < 0$, we will refer to such a shock as an all asset shock.

Note that according to our definition, every all asset shock is a K -asset shock, but not every K -asset shock is an all asset shock since an all asset shock has the additional feature that all assets are shocked equally.

We will distinguish between two different parametric choices for the price impact parameters l_k .

Definition 2.2.3 (Constant and capitalisation-dependent price impact). *We will refer to a price impact given by $l_1 = \dots = l_K = l \in [0, \infty)$, as a constant price impact.*

We will refer to a price impact given by $l_k = \frac{\rho}{c_k} \quad \forall k \in \mathcal{S}$, where $\rho > 0$ and $c_k > 0$ is the capitalisation of asset k defined in (2.1), as the capitalisation-dependent price impact. If, $c_k = 0$, we set $l_k = 0$.

A constant price impact was assumed in the empirical analysis in Greenwood et al. (2015). Since it has been argued that a constant price impact can overestimate the losses for liquid assets and underestimate the losses for illiquid assets (Cont and Schaanning, 2017, p. 19), we additionally consider a capitalisation-dependent price impact which assumes that the sale of assets with larger market capitalisation leads to a smaller price impact. This implicitly assumes that assets with a larger market capitalisation are more liquid and therefore cause a smaller price impact when sold.⁶ One could adjust the definition of a capitalisation-dependent price impact if one wanted to allow for the existence of external investors in the model.⁷

2.3 Assessing fire sales risk under full and partial information

Next, we conduct stress testing to analyse fire sales risk under both full and partial information.

2.3.1 Dependence of fire sales risks on the asset holding matrix

We start by presenting our theoretical results on the dependence of the systemicness, the aggregate vulnerability, and the direct vulnerability on the asset holding matrix X . We

⁶In our empirical analysis we will set $\rho = -\log(0.1)$. This parametric assumption is inspired by models such as Cifuentes et al. (2005), which use an exponential function to describe the inverse demand function that maps the quantities being sold to a price. In our case, we do not consider the quantities being sold, but the total market capitalisation and therefore our definition is slightly different from the classical characterisation in terms of an inverse demand function. One could also consider other inverse demand functions in this setting, see e.g., Bichuch and Feinstein (2022).

⁷These external investors would hold (some of) the assets but would not engage in the leverage targeting/fire sales mechanisms. The total market capitalisation of an asset k would then consist of $c_k + c_k^{(e)}$, where c_k is the market capitalisation of asset k among the nodes in \mathcal{N} and $c_k^{(e)}$ is the market capitalisation of asset k held by external investors. Then a capitalisation-dependent price impact could be defined as $l_k^e = \frac{\rho}{c_k + c_k^{(e)}}$ for a fixed $\rho > 0$. We will not consider this generalisation in the following.

assume that the row and column sums of X , given in Definition 2.1, are known and we determine how much these three risk measures (\mathcal{AV} , $\mathcal{SYS}(n)$ and $\mathcal{DV}(n)$) depend on the individual entries of X (beyond the information contained in the row and column sums). We show that there are several situations in which some of these risk measures do not depend on the individual entries of the asset holdings matrix X at all but only on its row and column sums.

Proposition 2.3.1. *Let $X \in [0, \infty)^{N \times K}$ be an asset holdings matrix. Suppose that its row and column sums $\alpha_{n1}, n \in \mathcal{N}$ and $c_k, k \in \mathcal{S}$, defined in (2.1), are known.*

1. *for each $n \in \mathcal{N}$, the systemicness $\mathcal{SYS}(n)$ can depend on the individual entries of X only via γ_{n1} and R_{n1} ;*
2. *the aggregate vulnerability \mathcal{AV} can depend on the individual entries of X only via γ_{n1} and R_{n1} , where $n \in \mathcal{N}$;*
3. *the direct vulnerability $\mathcal{DV}_1(n)$ of an institution n can depend on the individual entries of X only via R_{n1} ;*
4. *For a constant price impact, γ_{n1} can depend on the individual entries of X only via its n th row; for a capitalisation dependent price impact, γ_{n1} does not depend on X .*
5. *R_{n1} can depend on the individual entries of X only via its n th row; furthermore,*
 - (a) *for an all asset shock, R_{n1} and hence $\mathcal{DV}(n)$ do not depend on the individual entries of X .*
 - (b) *for a \tilde{K} -asset shock, R_{n1} and hence $\mathcal{DV}(n)$ only depend on the columns with indices in $\mathcal{I}^{\tilde{K}}$ within the n th row, but not on the full n th row of X .*

Corollary 2.3.2. *In addition to the assumptions of Proposition 2.3.1, let the price impact be capitalisation-dependent and let $n \in \mathcal{N}$. Then,*

1. *for an all asset shock, the systemicness $\mathcal{SYS}(n)$, the direct vulnerability $\mathcal{DV}(n)$ and the aggregate vulnerability \mathcal{AV} do not depend on the individual entries of X .*
2. *for a \tilde{K} -asset shock, both the systemicness $\mathcal{SYS}(n)$ and the direct vulnerability $\mathcal{DV}(n)$ only depend on the columns with indices in $\mathcal{I}^{\tilde{K}}$ of the n th row, but not on the full n th row of X . Furthermore, the aggregate vulnerability \mathcal{AV} only depends on X via its columns with indices in $\mathcal{I}^{\tilde{K}}$.*

The proofs of Proposition 2.3.1 and Corollary 2.3.2 are in Appendix 8.G. Note that the indirect vulnerability often depends on the individual entries of X . In the following, we will focus our analysis on situations in which the risk measures do indeed depend on (parts of) the underlying matrix X and assess the effect of using different matrix reconstruction methods to estimate the individual entries of the matrix X .

Remark 2.3.3 (Notation). To make it clear which matrix is used to compute the corresponding risk measures, we will sometimes write $\mathcal{SYS}^X(n)$, \mathcal{AV}^X , $\mathcal{DV}^X(n)$, $\mathcal{IV}^X(n)$ to show explicitly that these risk measures are computed based on the matrix X . In our analysis we will later allow the matrix X to be random, i.e., each element of X is a random variable, in which case then the corresponding systemic risk measures also become random variables.

We will also later use the notation $\gamma_{n1} = \gamma_{n1}(X)$ and $R_{n1} = R_{n1}(X)$, where $n \in \mathcal{N}$, to indicate that both γ_{n1} and R_{n1} can depend on X .

We have seen that the asset holding matrix X enters the different risk measures only via R_{n1} and γ_{n1} , where $n \in \mathcal{N}$. It plays a different role in these two quantities.

In R_{n1} , the asset holding matrix directly influences the magnitude of the original shock. In particular, the loss of bank n 's equity after the initial shock is given by

$$\alpha_{n1}R_{n1} = \alpha_{n1} \sum_{k=1}^K m_{nk}f_{k1} = \alpha_{n1} \sum_{k=1}^K \frac{X_{nk}}{\alpha_{n1}} f_{k1} = \sum_{k=1}^K X_{nk}f_{k1} \leq 0. \quad (2.8)$$

For an all asset shock, equation (2.8) simplifies further to $\alpha_{n1}R_{n1} = f \sum_{k=1}^K X_{nk} = f\alpha_{n1}$. Hence, for an all asset shock, one only needs to know the row sum α_{n1} rather than the individual entries of X to determine the magnitude of the shock.

In γ_{n1} , the asset holding matrix enters through the rule of how assets are sold following a stress. Greenwood et al. (2015) assume that stressed banks sell assets according to the proportion of their original portfolio positions, i.e., if bank n sells a total of y_{n1} assets (in EUR), it sells $m_{nk}y_{n1} = \frac{X_{nk}}{\alpha_{n1}}y_{n1}$ of asset k (in EUR).

One can generalise the selling rule by assuming that banks no longer sell according to the matrix m but according to a matrix $\mu \in [0, 1]^{N \times K}$, where $\sum_{k=1}^K \mu_{nk} = 1$ for all $n \in \mathcal{N}$.⁸ Then, for a general selling rule characterised by the matrix μ we use

$$\gamma_{n1}^{(\mu)} = \sum_{k=1}^K c_k l_k \mu_{nk},$$

rather than $\gamma_{n1} = \sum_{k=1}^K c_k l_k \frac{X_{nk}}{\alpha_{n1}}$ in the formulae for the different fire sale risk measures. Such a formulation allows us to capture situations in which the actual selling rule that banks use under stress is unknown, which would often be the case in practice.

⁸The general selling rule does not exclude short-selling. If one wanted to exclude short-selling for the general selling rule one would need to require that $\mu_{nk}y_{n1} \leq X_{nk}(1 + f_{k1})$, where the left-hand side is the total amount of asset k sold by bank n , and the right-hand side is the amount of asset k that bank n has after the shock. This implies the following additional condition on μ , namely

$$\mu_{nk} \leq \frac{X_{nk}(1 + f_{k1})}{y_{n1}} \quad \forall k \in \mathcal{S}, \quad (2.9)$$

for all $n \in \mathcal{N}$ with $y_{n1} > 0$. (We set $\mu_{nk} = 0$ for all $n \in \mathcal{N}$ with $y_{n1} = 0$ and $\forall k \in \mathcal{S}$.)

We can then compute bounds on the influence of the selling rule by considering for each $n \in \mathcal{N}$

$$\begin{aligned} & \max_{\mu \in [0,1]^{N \times K}} \gamma_{n1}^{(\mu)} \\ & \text{subject to } \sum_{k=1}^K \mu_{nk} = 1. \end{aligned} \quad (2.10)$$

or the corresponding minimisation problem. These linear optimisation problems can be solved analytically. The maximum of the objective function is $\max_{k \in \mathcal{S}} \{c_k l_k\}$ which is attained by setting $\mu_{nk} = 1$ at the index k where the maximum $\max_{k \in \mathcal{S}} \{c_k l_k\}$ is attained and $\mu_{nk} = 0$ for all remaining indices k . In particular, the optimal solution does not depend on n . The corresponding result in which max is replaced by min holds for the minimum. The optimal strategy corresponding to the maximisation problem selects the asset with the highest capitalisation-weighted price impact.⁹

These results hold for general price impact parameters l_1, \dots, l_K . For a capitalisation-dependent price impact, however, the connectedness simplifies to

$$\gamma_{n1}^{(\mu)} = \sum_{k=1}^K c_k l_k \mu_{nk} = \sum_{k=1}^K c_k \frac{\rho}{c_k} \mu_{nk} = \rho$$

and hence it does not depend on the selling rule μ .

Furthermore, we find that if $\gamma_{n1}^{(\mu)} = \tilde{\gamma}$ for all $n \in \mathcal{N}$, i.e., if all banks n have the same connectedness, then the network effect arising from $\gamma_{n1}^{(\mu)}$ only becomes a scaling factor in the aggregate vulnerability, in particular,

$$\mathcal{AV} = \sum_{n=1}^N \gamma_{n1} \frac{\alpha_{n1}}{\sum_{\nu=1}^N e_{\nu 1}} b_{n1} (-R_{n1}) = \frac{-\tilde{\gamma}}{\sum_{\nu=1}^N e_{\nu 1}} \sum_{n=1}^N b_{n1} \sum_{k=1}^K X_{nk} f_{k1}. \quad (2.11)$$

This situation arises, as discussed for a capitalisation-dependent price impact. It also arises for all selling strategies μ that are not bank specific, i.e., for which $\mu_{nk} = \tilde{\mu}_k$ for all $n \in \mathcal{N}$ and for $\tilde{\mu}_1, \dots, \tilde{\mu}_K \in [0, 1]$ with $\sum_{k=1}^K \tilde{\mu}_k = 1$.¹⁰

These considerations show that in order to have a more involved interaction between the two network effects $\gamma_{n1}^{(\mu)}$ and R_{n1} , one needs to consider shocks that are not an all asset shock, selling strategies that vary between banks (as e.g., the strategy considered in Greenwood et al. (2015)) and a price impact that is not capitalisation-dependent.

In the following, we will therefore focus on the selling strategy assumed by Greenwood

⁹The solution to the optimisation problem (2.10) and the corresponding minimisation problem are useful as upper and lower bounds on the potential influence of the selling rule. It is possible, that banks do not hold the amount of assets that need to be sold according to these optimal strategies. To exclude short-selling one would need to include the additional condition (2.9) in the optimisation problems.

¹⁰An example of such a selling strategy would be to sell according to equal proportions $\mu_{nk} = 1/K$ for all $n \in \mathcal{N}$ and for all $k \in \mathcal{S}$.

et al. (2015), where $\mu = m$ and we will not consider other strategies any further. To analyse the different effects of R_{n1} and γ_{n1} , we will include an all asset shock in our analysis, to isolate the effect of γ_{n1} for fixed (meaning that they do not depend on the individual entries of the asset holding matrix) R_{n1} . Similarly, we will also include a capitalisation-dependent price impact to isolate the effect of R_{n1} for fixed γ_{n1} . Furthermore, we will consider shocks that affect only some assets and use a constant-price impact to study the interaction between γ_{n1} and R_{n1} .

2.3.2 Reconstructing matrices

We consider five existing methods for reconstructing the asset holding matrix X from the given row and column sums. We briefly summarise them below. More details can be found in Appendix 8.A.

We consider two optimisation-based methods: the Entropy method by Upper and Worms (2004) and the minimum density method by Anand et al. (2015) (MinDen). The optimisation-based matrix reconstruction methods consist of a suitably chosen objective function that is optimised over the set of matrices that satisfies the given constraints on the row and column sums. The result of the reconstruction problem is one matrix that satisfies the constraints. Other possible characteristics that this matrix might have depend on the chosen objective function. For the Entropy method, the resulting matrix is usually complete, i.e., all entries are non-zero as long as all the row and column sums are non-zero. This means that the banks then have a fully diversified portfolio since they hold positions in each asset. For the MinDen method, the resulting matrix is usually very sparse, i.e., most of the entries are equal to zero. This means that the banks have more diverse positions.¹¹ For the Entropy method, the matrix that solves the corresponding optimisation problem is available analytically. Therefore, it is possible to characterise all fire sales measures, i.e., the direct and indirect vulnerability, the systemicness, and the aggregate vulnerability, derived from the reconstructed matrix using the Entropy method analytically. We provide the corresponding formulae in Appendix 8.A, Proposition 8.A.1. We also consider three probabilistic methods: the statistical physics method by Cimini et al. (2015) (StatPhys) (and extended to bipartite networks by Squartini et al. (2017)) and the Bayesian approach by Gandy and Veraart (2017), where we assume two different priors within the Bayesian framework, an Erdős-Rényi-type prior (BayeER) and an empirical fitness type prior (BayeEF) as in Gandy and Veraart (2019). All probabilistic models assume that the matrix of asset holdings is random, i.e., all its elements are random variables. They provide methodologies to generate samples from the distribution of this random asset holding matrix. Therefore, the result of a network reconstruction

¹¹For further discussion and results on the relationship between fire sales risk and diversification versus diversity in asset portfolios we refer to Capponi and Weber (2022) and Detering et al. (2022).

method using any of the probabilistic methods is a sample of matrices and not just one matrix. All three probabilistic models are calibrated to match the (true) density of the network. For all three probabilistic methods, our analysis uses a sample size of 10,000.¹² The StatPhys method is related to the Entropy method and it is possible to compute the expectation of the fire sale measures applied to the random matrix that is used in the StatPhys method analytically. We provided the details in Appendix 8.A.2. We will now illustrate how the choice of the reconstruction methods affects the risk measures to assess fire sales risk. First, we consider a toy example.

True X	Entropy	MinDen		True X	Entropy	MinDen	
$\begin{pmatrix} 2 & 2 & 0 \\ 2 & 0 & 2 \\ 0 & 2 & 2 \end{pmatrix}$	$\begin{pmatrix} \frac{4}{3} & \frac{4}{3} & \frac{4}{3} \\ \frac{4}{3} & \frac{4}{3} & \frac{4}{3} \\ \frac{4}{3} & \frac{4}{3} & \frac{4}{3} \end{pmatrix}$	$\begin{pmatrix} 4 & 0 & 0 \\ 0 & 4 & 0 \\ 0 & 0 & 4 \end{pmatrix}$		$\mathcal{SVS}(1)$	1.2%	0.8%	
				$\mathcal{SVS}(2)$	1.2%	0.8%	
				$\mathcal{SVS}(3)$	0.0%	0.8%	
				\mathcal{AV}	2.4%	2.4%	
	True X	Entropy	MinDen		True X	Entropy	MinDen
$\mathcal{DV}(1)$	30.0%	20.0%	60.0%	$\mathcal{IV}(1)$	2.7%	2.4%	7.2%
$\mathcal{DV}(2)$	30.0%	20.0%	0.0%	$\mathcal{IV}(2)$	2.7%	2.4%	0.0%
$\mathcal{DV}(3)$	0.0%	20.0%	0.0%	$\mathcal{IV}(3)$	1.8%	2.4%	0.0%

Table 2.2: The three matrices on the left in the first row represent the true asset holding matrix X and the two reconstructed matrices using the Entropy and MinDen methods, respectively. The table on the right in the first row shows the systemicness $\mathcal{SVS}(n)$ and \mathcal{AV} , and the tables in the second row show the direct vulnerability $\mathcal{DV}(n)$ and the indirect vulnerability $\mathcal{IV}(n)$ for each bank n corresponding to the shock F_1 , specified in Example 2.3.4, and applied to the true and the two reconstructed matrices.

Example 2.3.4 (Toy example: Assessing fire sale losses on reconstructed matrices). We consider the asset holdings matrix $X \in [0, \infty)^{3 \times 3}$ reported in Table 2.2, and two reconstructions of X from its row and column sums using the Entropy method and the MinDen method, respectively. According to the true matrix X each institution holds two assets and each asset is held by two institutions. The Entropy method distributes the weights evenly across the different cells of the matrix resulting in a complete network, meaning all institutions hold all assets, whereas the MinDen method finds the sparsest possible solution in which each institution only holds one asset and this asset is not held by anyone else.

The total assets are $\alpha_{n1} = 4$ for all $n \in \{1, 2, 3\}$. We assume that all three banks have the same equity, namely $e_{n1} = 1$ which results in a leverage of $b_{n1} = 3$ for all $n \in \{1, 2, 3\}$.

¹²For the Bayesian approach (in which the distribution of interest is approximated using a Gibbs sampler) we choose thinning and burn-in parameters as 10% of the total number of samples as in Gandy and Veraart (2017). We use the R-package *systemicrisk* available at <https://CRAN.R-project.org/package=systemicrisk> that implements the methods by Gandy and Veraart (2017, 2019).

We consider a constant price impact of $l_k = 10^{-2}$ for all assets $k \in \{1, 2, 3\}$. We consider a 1-asset shock given by $F_1 = (-0.15, 0, 0)^\top$ which only affects the first asset directly.

We report the \mathcal{AV} , $\mathcal{SYS}(n)$, $\mathcal{DV}(n)$ and $\mathcal{IV}(n)$ for the true and the two reconstructed matrices for all three institutions $n \in \{1, 2, 3\}$ in Table 2.2. We find that under this 1-asset shock, the systemicness, the direct and the indirect vulnerability can change significantly with respect to the network that is used as input.

In particular, we find that the Entropy method underestimates the systemicness, the direct vulnerability, and the indirect vulnerability of banks 1 and 2 (which have the highest systemicness and direct and indirect vulnerability in this example), and overestimates the systemicness, the direct and indirect vulnerability of bank 3 (which is the lowest among all banks in this example).

The MinDen method only attributes a positive systemicness, and direct and indirect vulnerability to bank 1 (and significantly overestimates the true values), and otherwise provides estimates of zero for all three measures for banks 2 and 3.

For the aggregate vulnerability, however, we see that it is correctly estimated by both the Entropy and the MinDen method in this example.

2.3.3 Data

In our empirical analysis, we consider data¹³ collected by the European Banking Authority (EBA)¹⁴ for their stress tests of EU banks in 2011 and 2016. The data consists of balance sheets of some of the largest banks in the EU. The data include $N = 90$ banks in 2011 and $N = 51$ banks in 2016 covering the EU countries (which includes the UK in these years).

We aggregate the asset classes such that all asset classes are consistent across both years. There are $K = 36$ asset classes which include corporate, retail, 30 EEA sovereign loans, US, Japan, Latin America, and other sovereign loans (an aggregated class of remaining sovereign loans). Hence the asset holding matrix is a 90×36 matrix in 2011 and a 51×36 matrix in 2016. All other assets which are not recorded in both years are not included in the asset holdings matrix.¹⁵ We assume that all assets are marketable and can be liquidated, i.e., we apply the framework by Greenwood et al. (2015) directly to the full asset holding matrix as in the empirical case study provided in Greenwood et al. (2015).¹⁶

¹³The data are publicly available from <https://eba.europa.eu/risk-analysis-and-data/eu-wide-stress-testing/2011> and <https://eba.europa.eu/risk-analysis-and-data/eu-wide-stress-testing/2016>.

¹⁴The EBA is an independent EU authority whose objective is to maintain financial stability in the EU. It has been established to develop consistent prudential regulation and supervision of the EU's banking sector. Together with the European Systemic Risk Board (ESRB), the EBA conducts stress testing of the EU banking sector to assess its resilience to adverse shocks.

¹⁵This is done for consistency purposes so that we can apply the same initial shock to both datasets.

¹⁶In practice, only a part of a bank's assets can be liquidated, see e.g., Cont and Schaanning (2017) for discussion and more details on this. It would be possible to restrict the modelling framework so that only a subset of the available assets are marketable. Related work that considers both marketable and

Table 2.3 provides some descriptive statistics for the EBA data used in our empirical analysis. We see that the network densities (defined as $\frac{1}{NK} \sum_{n=1}^N \sum_{k=1}^K \mathbb{I}_{\{X_{nk}^{\text{year}} > 0\}}$, where X^{year} represents either the observed assets holding matrix in 2011 or in 2016) is almost the same in both years (0.44 in 2011 and 0.48 in 2016). With almost half of the entries being positive in the asset holding matrix, we expect that there is indeed scope for serious contagion effects if fire sales are triggered.

The leverage values that we report in this table corresponds to $b_{n1} = d_{n1}/e_{n1}$, where the equity e_{n1} was set to be equal to the common equity Tier 1 capital reported for each bank $n \in \mathcal{N}$ and the debt d_{n1} was set to be equal to $\alpha_{n1} - e_{n1}$. We see that leverages were generally significantly higher in 2011 than in 2016. In the empirical analysis we will cap the leverage at 30 as in Greenwood et al. (2015), this means that we set

$b_{n1} = \min\{30, \text{observed leverage of bank } n \text{ at time } 1\}$ to avoid having to deal with a small number of banks which have very high leverages (such as, e.g., maximum leverage of 540.68 in 2011).

Table 2.3 also shows the range of banks' total assets α_{n1} , $n \in \mathcal{N}$, with the lowest total assets at 329 million EUR in 2011, compared with the largest bank at 1.39tn EUR in 2016. The assets which form the largest total capitalisation in both networks are corporate and retail, comprising 82% of the total assets in 2011 and 80% in 2016. The highest sovereign loans in 2011 are German (2.89%), other sovereign (1.98%), and Italian (1.93%) compared with French (2.68%), German (2.64%), and US (2.13%) sovereign assets in 2016. Asset classes with a large capitalisation which are held by a large number of banks are German, French, Spanish, UK, and Italian sovereign assets.

Year	Number of banks	Network density	Leverage			Total assets (EUR)		
			Min	Mean	Max	Min (bn)	Mean (tn)	Max (tn)
2011	90	0.44	3.56	33.60	540.68	0.33	0.19	1.21
2016	51	0.48	7.48	19.68	43.15	2.93	0.28	1.39

Table 2.3: Summary statistics for the EBA data.

We provide heatmaps and further discussions on the structure of the empirically observed asset holding matrix and the performance of its reconstruction using different methods for the 2016 EBA data in Appendix 8.B.1.

2.3.4 Empirical results

Next, we consider the fire sales risk measures for the EBA data for three different stress scenarios and compare the results obtained by using the fully observed matrix of asset holdings to the results derived based on reconstructed asset holding matrices.

non-marketable assets includes Braouezec and Wagalath (2019), Feinstein (2020), Banerjee and Feinstein (2021).

The three stress scenarios are as follows:

GIIPS shock: This is a 5-asset shock. We consider a 5% shock to the sovereign loans of Greece, Italy, Ireland, Portugal and Spain (GIIPS), which were countries highly impacted by the 2008 financial crisis. This shock has also been considered in Greenwood et al. (2015). Mathematically, this corresponds to setting $f_k = -0.05$ for each index $k \in \mathcal{S}$ that corresponds to a GIIPS asset and setting $f_k = 0$ for all remaining $k \in \mathcal{S}$ in the initial shock vector.

Bad Brexit shock: This is a 1-asset shock. We consider an economic shock of 10% to UK sovereign loans as a possible scenario for negative consequences arising from Brexit. Mathematically this is captured by setting $f_k = -0.1$ for the index $k \in \mathcal{S}$ that corresponds to the UK asset class and setting $f_k = 0$ for all remaining $|K| - 1$ assets.

All asset shock: We consider a 0.1% shock to all assets. This corresponds to setting $f_k = -0.001$ for all $k \in \mathcal{S}$ in the initial shock vector. This type of shock is widespread and affects all assets in the same way.

For the optimisation-based reconstruction methods, i.e., for MinDen and Entropy, we can apply the different fire sales measures directly to the reconstructed matrix returned by these methods since we only evaluate one matrix. As mentioned before, for the Entropy method we have analytical expressions for all fire sale measures, see Proposition 8.A.1 in Appendix 8.A. Since, there are three bank specific measures, namely the systemicness $\mathcal{SYS}(n)$, the direct vulnerability $\mathcal{DV}(n)$, and the indirect vulnerability $\mathcal{IV}(n)$, we consider the average of these measures across all institutions. For example, instead of N measures for the direct vulnerability of the individual institutions, we report the average direct vulnerability over all institutions given by $\frac{1}{N} \sum_{n=1}^N \mathcal{DV}(n)$. Table 2.4 reports the results and $\mathcal{DV}11$ then corresponds to the average direct vulnerability across the N banks in 2011 and $\mathcal{DV}16$ represents the average direct vulnerability in 2016. The same notation is used for the indirect vulnerability. Since the aggregate vulnerability is a measure for the whole system we can report it directly. Note that the aggregate vulnerability is equal to N times the average systemicness and therefore we do not report the average systemicness.¹⁷

¹⁷We also considered other measures for bank specific quantities. We investigated the L_1 -error between the fire sales measures of reconstructed matrices and the true matrix, e.g., for systemicness we consider $\sum_{n=1}^N |\mathcal{SYS}^{\text{True}}(n) - \mathcal{SYS}^X(n)|$ for the Entropy and the MinDen method, and for the sampling methods, we average the L_1 -error across all samples, i.e., we consider $\frac{1}{d} \sum_{\nu=1}^d \sum_{n=1}^N |\mathcal{SYS}^{\text{True}}(n) - \mathcal{SYS}^{X^{(\nu)}}(n)|$. For the three different bank-specific fire sale measures we find a larger deviation for systemicness and indirect vulnerability compared to the direct vulnerability. Generally, the MinDen reconstruction methods results in the largest L_1 error due to the sparsity of the reconstructed matrix and the concentration of asset losses from a few banks. Entropy and StatPhys have the greatest similarity, and the performance of the Bayesian approach depends on the measures considered. Overall, the results are similar to those reported in Table 2.4.

For the probabilistic reconstruction measures, i.e., for StatPhys, BayeER, and BayeEF, we obtain a sample of networks denoted by $X^{(1)}, \dots, X^{(d)}$, i.e., the sample size is $d = 10,000$. For each reconstructed network $X^{(\nu)}$, we compute the direct vulnerability of each bank and consider the mean direct vulnerability of all banks for this given network $X^{(\nu)}$. We then average this mean direct vulnerability over the full sample. More precisely, in the two rows corresponding to $\mathcal{DV}11$, we show the following two numbers (sample mean of the average direct vulnerability and corresponding standard deviation in *italic*):

$$\begin{aligned}\bar{\mu}_d^{DV} &= \mu_d \left(\frac{1}{N} \sum_{n=1}^N \mathcal{DV}11^{X^{(\nu)}}(n) \right) = \frac{1}{d} \sum_{\nu=1}^d \left(\frac{1}{N} \sum_{n=1}^N \mathcal{DV}11^{X^{(\nu)}}(n) \right), \\ \sigma_d \left(\frac{1}{N} \sum_{n=1}^N \mathcal{DV}11^{X^{(\nu)}}(n) \right) &= \sqrt{\frac{1}{d-1} \sum_{\nu=1}^d \left(\frac{1}{N} \sum_{n=1}^N \mathcal{DV}11^{X^{(\nu)}}(n) - \bar{\mu}_d^{DV} \right)^2}\end{aligned}$$

for the probabilistic methods using the 2011 data. The same methodology is applied to the reporting of indirect vulnerability. The aggregate vulnerability in the table corresponds to the average aggregate vulnerability computed over the d elements of the sample, i.e.,

$$\begin{aligned}\bar{\mu}_d^{AV} &= \mu_d \left(\mathcal{AV}11^{X^{(\nu)}} \right) = \frac{1}{d} \sum_{\nu=1}^d \mathcal{AV}11^{X^{(\nu)}}, \\ \sigma_d \left(\mathcal{AV}11^{X^{(\nu)}} \right) &= \sqrt{\frac{1}{d-1} \sum_{\nu=1}^d \left(\mathcal{AV}11^{X^{(\nu)}} - \bar{\mu}_d^{AV} \right)^2},\end{aligned}$$

where again the second quantity is the corresponding standard deviation.

For the StatPhys method, we have derived analytical expressions for the expected fire sale measures in Appendix 8.A.2. In the following, we report the Monte Carlo estimates such as $\bar{\mu}_d^{AV}$ of these expectations which are very close to the analytical results.

Table 2.4 reports the averaged fire sale risk measures. Values highlighted in bold indicate the best-performing reconstruction method per row and per price impact. The direct vulnerabilities are reported only for the capitalisation-dependent price impact since they coincide with those for the constant price impact, see Definition 2.6. For the all asset shock, several risk measures do not depend on the individual entries of X (see Corollary 2.3.2) which we indicate by writing *true* in the corresponding entry in the table to highlight, that this value is identical to the value in the column *True*.

We first consider the fire sales measures based on the fully observed matrix (the columns named *True* in Table 2.4). We observe that all but one fire sales measure corresponding to the 2011 data are consistently higher than the corresponding measures for the 2016 data. This means that overall the fire sales risk has decreased from 2011 to 2016. This observation holds true under both constant and capitalisation-dependent price impact. The only exception, where we observe an increase from 2011 to 2016, is the aggregate

vulnerability under a constant price impact for the Bad Brexit shock. A high contributing factor for the general tendency for the fire sales risk measures to decrease from 2011 to 2016 is the difference between the leverages and the target leverages (which is observed leverage capped at 30) which both decrease substantially from 2011 to 2016. In 2011, several banks held low equity levels compared with 2016 which resulted in high leverages in 2011. The average leverage of banks also decreased from 2011 to 2016, because of the banks included in each dataset. The higher leverage in 2011 was largely driven by a small number of banks, which were not all part of the 2016 data. For example, Greek banks were not part of the 2016 data but included a bank with the second-highest leverage. Therefore, the change in capital requirements and the types of banks included in the EBA stress tests contributed to a decreased leverage.

Furthermore, we consider the effect of the two different choices for the price impact on the fire-sales measures under complete information. First, note that the direct vulnerability $\mathcal{DV}(n)$ does not depend on the price impact, i.e., it does not depend on the parameters l_1, \dots, l_K , and hence the direct vulnerabilities corresponding to different price impacts coincide. In contrast, the other fire-sales measures do depend on the price impact. In the 2011 data, we find that the constant price impact results in higher risks associated with fire sales than the capitalisation-dependent price impact, but for the 2016 data this is not necessarily the case. Overall, the key features of the stress tests remain consistent for both choices of price impact, namely that risks from fire sales in 2016 were smaller than in 2011.

Next, we consider the fire sales measures obtained by using five different matrix reconstruction methods. The entry shown in bold represents the best-performing method for this particular row indicating the fire sales measure and a given price impact. Overall, we see there is no clear winner in the sense that one of the methods would consistently outperform all other methods across all fire sales measures and for different types of shocks and price impacts.

	Capitalisation-dependent Price Impact ($l_k = \rho/c_k \forall k$)						Constant Price Impact ($l_k = 5 \times 10^{-13} \forall k$)					
	True	MinDen	Entropy	StatPhys	BayeER	BayeEF	True	MinDen	Entropy	StatPhys	BayeER	BayeEF
GIIPS (%)												
$\mathcal{DV}11$	15.58	3.23	7.81	7.81	20.21	17.68	same results as for capitalisation-dependent price impact					
	-	-	-	(0.53)	(3.06)	(3.07)						
$\mathcal{TV}11$	460.79	296.96	416.80	417.58	612.49	544.98	506.76	304.77	523.63	523.68	274.71	325.00
	-	-	-	(10.67)	(38.58)	(30.92)	-	-	-	(13.36)	(16.91)	(18.00)
$\mathcal{AV}11$	291.70	238.77	288.49	288.96	292.38	294.24	357.49	178.63	362.43	362.43	275.36	293.40
	-	-	-	(6.15)	(5.26)	(5.12)	-	-	-	(7.41)	(11.41)	(10.23)
$\mathcal{DV}16$	5.64	5.33	4.42	4.42	8.24	7.57	same results as for capitalisation-dependent price impact					
	-	-	-	(0.18)	(0.78)	(0.82)						
$\mathcal{TV}16$	187.19	254.15	214.86	215.22	240.26	228.39	151.35	51.69	221.46	221.47	139.97	153.33
	-	-	-	(5.87)	(10.34)	(8.73)	-	-	-	(5.90)	(7.91)	(7.99)
$\mathcal{AV}16$	189.29	244.47	220.83	221.20	209.70	210.34	174.81	52.08	227.62	227.63	179.05	186.32
	-	-	-	(5.79)	(5.08)	(5.05)	-	-	-	(5.75)	(9.37)	(8.69)
Bad Brexit (%)												
$\mathcal{DV}11$	1.47	0.85	3.01	3.01	8.39	6.46	same results as for capitalisation-dependent price impact					
	-	-	-	(0.47)	(2.55)	(2.43)						
$\mathcal{TV}11$	120.19	140.82	160.85	161.21	240.11	207.43	155.05	183.76	202.08	202.17	103.70	126.37
	-	-	-	(7.25)	(23.28)	(17.30)	-	-	-	(9.13)	(8.82)	(9.63)
$\mathcal{AV}11$	90.23	144.07	111.34	111.55	112.09	113.62	109.02	135.01	139.87	139.92	104.02	114.58
	-	-	-	(4.74)	(4.03)	(3.87)	-	-	-	(5.92)	(8.02)	(7.40)
$\mathcal{DV}16$	1.59	1.92	2.87	2.87	5.50	4.82	same results as for capitalisation-dependent price impact					
	-	-	-	(0.21)	(0.90)	(0.90)						
$\mathcal{TV}16$	130.07	126.60	139.24	139.53	156.38	147.43	136.35	105.51	143.53	143.59	90.33	99.77
	-	-	-	(5.92)	(10.07)	(08.30)	-	-	-	(6.08)	(7.25)	(7.46)
$\mathcal{AV}16$	149.58	152.24	143.11	143.41	135.77	136.34	159.82	106.67	147.51	147.58	115.61	121.39
	-	-	-	(6.00)	(5.24)	(5.31)	-	-	-	(6.14)	(9.27)	(8.87)
All Asset (%)												
$\mathcal{DV}11$	3.46	true	true	3.46	true	true	same results as for capitalisation-dependent price impact					
	-	-	-	(0.05)	-	-						
$\mathcal{TV}11$	185.51	185.95	184.72	185.07	185.60	185.89	228.63	255.63	232.07	232.38	153.11	172.48
	-	-	-	(3.24)	(0.68)	(0.60)	-	-	-	(4.32)	(7.81)	(7.99)
$\mathcal{AV}11$	127.86	true	true	128.07	true	true	160.87	161.00	160.63	160.82	160.24	159.99
	-	-	-	(1.32)	-	-	-	-	-	(1.68)	(0.30)	(0.30)
$\mathcal{DV}16$	2.07	true	true	2.07	true	true	same results as for capitalisation-dependent price impact					
	-	-	-	(0.02)	-	-						
$\mathcal{TV}16$	100.62	99.58	100.47	100.64	99.33	99.66	92.06	103.63	103.56	103.66	82.60	87.37
	-	-	-	(1.45)	(0.23)	(0.20)	-	-	-	(1.54)	(1.45)	(1.69)
$\mathcal{AV}16$	103.26	true	true	103.43	true	true	106.59	105.72	106.43	106.55	107.69	107.59
	-	-	-	(1.28)	-	-	-	-	-	(1.34)	(0.25)	(0.25)
Bold	-	6	2	2	3	1	-	0	3	4	2	3

Table 2.4: The table presents average fire sales risk measures (averaged over the banks and additionally averaged over the samples) for the 2011 and 2016 EBA data for three different shock scenarios for the true and reconstructed matrices. All numbers are given in percent.

So, we will look more specifically at the different fire sales measures. To get an overview, we compare the performance of three model classes: the MinDen, Entropy & StatPhys, BayeER & BayeEF. We provide more details in Appendix 8.A.2 on how the Entropy and the StatPhys are indeed related. It is no coincidence that the estimates derived from using the Entropy or the StatPhys methods are very similar. We start with the aggregate vulnerability since this is the only measure that provides a holistic view of the whole network. We find that the Entropy, StatPhys, BayeER, and BayeEF methods provide estimates for the aggregate vulnerability that is often rather close to the true value. Indeed, out of the 10 cases (corresponding to 4 cases for the capitalisation-dependent price impact and 6 cases for the constant price impact) for which we compute an aggregate vulnerability the Entropy & StatPhys method is the best-performing method in 5 cases and the BayeER & BayeEF are the best-performing methods in the remaining 5 cases. The MinDen performs best in only one scenario for estimating aggregate vulnerability. In most cases, it overestimates or underestimates the aggregate vulnerability.

For the bank specific measures that we have just averaged over all banks in the network, i.e., direct and indirect vulnerability we find the following. For the indirect vulnerability, we have 12 different cases (3 stress scenarios \times 2 price impacts \times 2 years). The MinDen performed best in 3 cases, the Entropy & StatPhys method performed best in 5 cases and the BayeER & BayeEF performed best in 4 cases. For the direct vulnerability, we observed 4 cases (2 stress scenarios \times 2 years; note that the price impact does not affect the direct vulnerability). The MinDen performed best in 3 cases and BayeER & BayeEF performed best in 1 case.¹⁸

Hence, to summarise, the best method for estimating the direct vulnerability across all types of shocks considered here is the MinDen, for the indirect vulnerability the performance of the three classes of methods are very similar, and for estimating the aggregate vulnerability the best methods are the Entropy & StatPhys method and the BayeER & BayeEF.

When distinguished by the type of shock, we find that the Entropy, StatPhys, BayeER, and BayeEF methods tend to be the preferred methods for the GIIPS shock (which affects 5 columns of the asset holding matrix), whereas the MinDen method seems to be the preferred method for the Bad Brexit shock which only affects one column of the asset holding matrix. For the All Asset shock, we know from Corollary 2.3.2 that under a capitalisation-dependent price impact $\mathcal{SYS}(n)$, \mathcal{AV} , $\mathcal{DV}(n)$ do not depend on the individual entries of X . Hence, if one was interested in such a situation, there is no need to reconstruct the network. If we ignore this result and compute the corresponding risk measures from the reconstructed networks, then we indeed recover the true values exactly (indicated by *true* in the entry in the table) for all methods except for the StatPhys

¹⁸The fact that the direct vulnerabilities for the Entropy and the StatPhys methods coincide in expectation, is not a coincidence, but it follows from the theoretical results derived in Appendix 8.A.2.

method. The matrices reconstructed using the StatPhys method do not individually satisfy the constraints on the row and column sums but only in expectation and therefore they do not reproduce the true value when plugged into the general formula for the risk measures that have not been simplified in line with the results of Corollary 2.3.2. To indicate this effect, we have reported the values computed from the matrices returned by the StatPhys method in the table. As discussed this is no contradiction to Corollary 2.3.2.

Finally, we investigate what the best and worst aggregate vulnerabilities are that are consistent with the given row and column sums of the asset holding matrix. Hence, we consider an additional (optimisation-based) network reconstruction method that maximises (or minimises) the aggregate vulnerability over all (non-negative) matrices that satisfy the row and column constraints. We provide more details on this in Appendix 8.B.2. Table 2.5 shows the results.

We find that in general there is quite a large difference between the minimum and the maximum aggregate vulnerabilities. Furthermore, the true aggregate vulnerability, i.e., the aggregate vulnerability derived from the true network, is quite centred between the minimum and the maximum aggregate vulnerability. Given this wide range of possible aggregate vulnerabilities, the aggregate vulnerabilities obtained from the different reconstruction methods are remarkably close to the true aggregate vulnerabilities.

Furthermore, we find that the difference between the minimum and maximum aggregate vulnerabilities is generally larger for a constant price impact compared to a capitalisation-dependent price impact. This is in line with our theoretical results (Proposition 2.3.1 and Corollary 2.3.2). Also in line with these theoretical results, is the fact that the GIIPS shock scenario in which 5 assets are shocked, has a larger difference between the minimum and maximum aggregate vulnerability than the Bad Brexit shock in which only one asset is shocked.

As discussed before, for an all asset shock and a capitalisation-dependent price impact, the aggregate vulnerability only depends on the asset holding matrix via its row and column sums and therefore the minimum and maximum aggregate vulnerabilities coincide with the true aggregate vulnerability. For an all asset shock with constant price impact, the individual entries of the asset holding matrix do matter, but we find the range of aggregate vulnerabilities to be rather small.

	Capitalisation-dependent ($l_k = \rho/c_k \forall k$)			Constant ($l_k = 5 \times 10^{-13} \forall k$)		
GIIPS (%)						
	True	Min	Max	True	Min	Max
$\mathcal{AV}11$	291.70	172.18	373.30	357.49	6.26	494.91
$\mathcal{AV}16$	189.29	131.88	294.12	174.81	4.95	311.53
Bad Brexit (%)						
	True	Min	Max	True	Min	Max
$\mathcal{AV}11$	90.23	49.16	144.07	109.02	1.00	216.65
$\mathcal{AV}16$	149.58	60.08	195.02	159.82	1.59	220.78
All Asset (%)						
	True	Min	Max	True	Min	Max
$\mathcal{AV}11$	127.86	true	true	160.87	150.19	171.73
$\mathcal{AV}16$	103.26	true	true	106.59	99.93	113.69

Table 2.5: True aggregate vulnerability and minimum and maximum of aggregate vulnerabilities derived from asset holding matrices that satisfy the given row and column sums. Two different price impacts and three shock scenarios are considered.

2.3.5 Sensitivity analysis and robustness checks

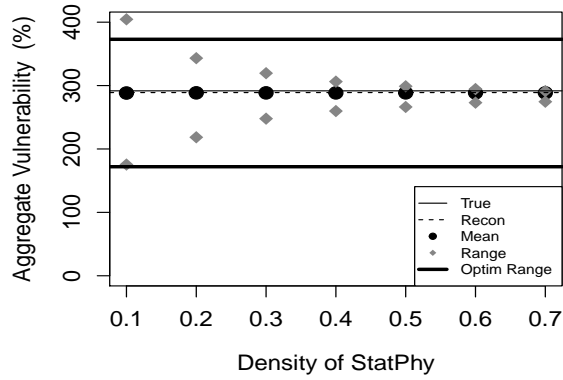
We have seen so far that the sampling-based reconstruction methods (StatPhys, BayeER and BayeEF) provide superior results for several measures of fire sale risk. One might think that this result is purely driven by the fact that these sampling-based methods can be (and in Table 2.4 have been) calibrated to the true density of the network which was not the case for the MinDen and the Entropy method. In the following, we show that this result remains robust even if the underlying assumption on the network density is changed.

Figure 2.1 shows how the aggregate vulnerability computed using the StatPhys, BayeER and BayeEF network reconstruction methods depends on the choice of the target density of the network. It shows the aggregate vulnerabilities as a function of the network density for three sampling-based reconstruction methods (StatPhys (top), BayeER (middle), BayeEF (bottom)). The aggregate vulnerabilities are computed as the mean over a sample of 10,000 reconstructed networks. Additionally, we show the range (labelled “Range”) of the aggregate vulnerabilities from this sample and the minimum and maximum (labelled “Optim Range”) of aggregate vulnerabilities obtained by minimising or maximising the aggregate vulnerability over all asset holding matrices consistent with the row and column sums. The horizontal line (labelled “True”) shows the aggregate vulnerability computed based on the true network, and the dashed horizontal line (labelled “Recon”) shows the reconstructed aggregate vulnerability using the true density for the reconstruction.

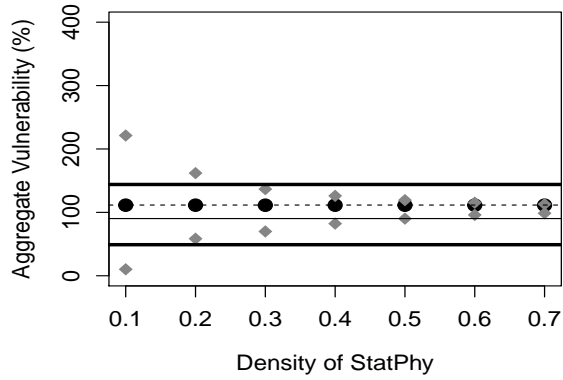
We find that even if the networks are reconstructed using a target density that does not coincide with the true density of the network, the aggregate vulnerabilities remain close to the true aggregate vulnerabilities.

We find that the range of the aggregate vulnerabilities computed using the StatPhys method exceeds the range of aggregate vulnerabilities derived by solving the optimisation problem that maximises or minimises the aggregate vulnerability for small densities. This is not a mistake, but a consequence of the StatPhys method not satisfying the row and column constraints exactly, but only in expectation.

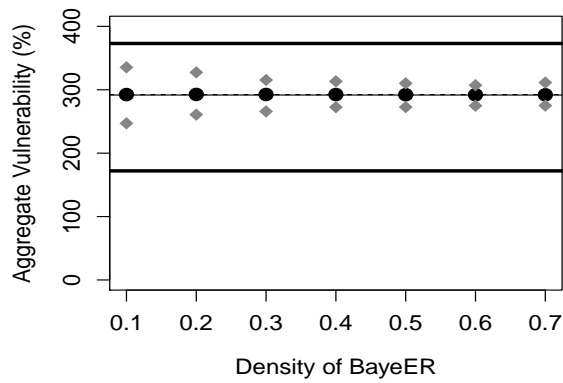
We provide more empirical results (for a constant price impact) and further discussions on the sensitivity of the results with respect to additional information (such as the density of the network) in Appendix 8.B.3. We also discuss there how additional information can be included in the MinDen and Entropy method.



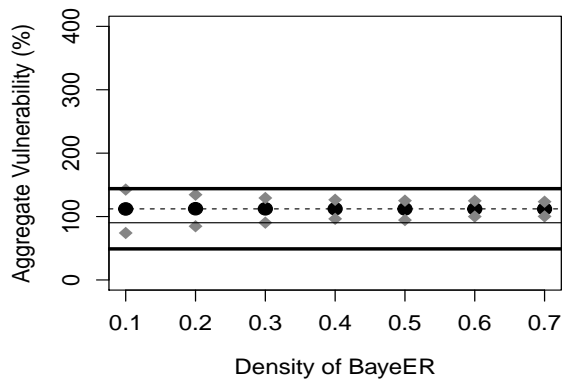
(a) StatPhys under GIIPS 2011.



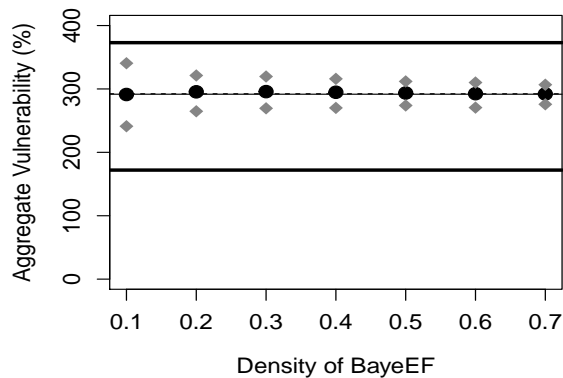
(b) StatPhys under Bad Brexit 2011.



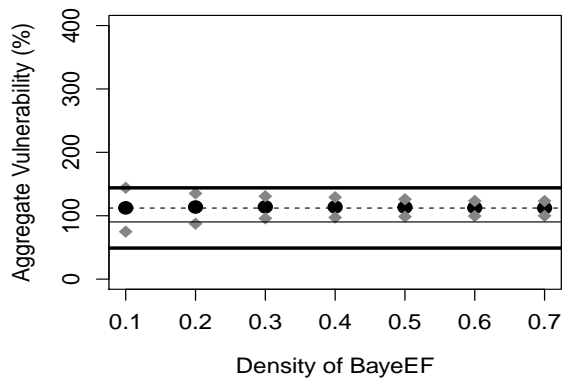
(c) BayeER under GIIPS 2011.



(d) BayeER under Bad Brexit 2011.



(e) BayeEF under GIIPS 2011.



(f) BayeEF under Bad Brexit 2011.

Figure 2.1: Aggregate vulnerabilities as a function of the network density for three sampling-based reconstruction methods (StatPhys (top), BayeER (middle), BayeEF (bottom)). The results are for the 2011 data and a capitalisation-dependent price impact.

Furthermore, we conduct a robustness check with respect to the main inputs into the network reconstruction: the row and column sums of the asset holding matrix. To do this we add a noise term to the row and column sums and reconstruct the networks based on the perturbed row and column sums. We find that the reconstructed direct, indirect, and aggregate vulnerabilities remain reasonably close to the true quantities in most cases even for noisy observation. The MinDen method seems to be the most sensitive with respect to the parameter inputs compared to the other reconstruction methods. Hence, the Entropy method and the sampling-based methods seem to be more robust in our case studies and one might therefore use those rather than the MinDen method if there is uncertainty about the input parameters. We report the detailed empirical results in Appendix 8.B.3 (see specifically Table 8.1).

Finally, we analyse the sensitivity of our results with respect to the selling rule μ for a constant price impact.¹⁹ As discussed before, for a capitalisation-dependent price impact the selling rule does not matter. We solve the maximisation problem (2.10) and the corresponding minimisation problem that determines upper and lower bounds on γ_{n1} . Figure 2.2 reports the results for the 2011 and 2016 data. It shows boxplots (and violin plots, i.e., the corresponding densities) of $\gamma_{11}, \dots, \gamma_{N1}$ corresponding to the proportional selling rule by Greenwood et al. (2015) together with the upper and lower bound from the optimisation problem and the constant $\gamma^{\text{Entropy}} = \gamma_{n1}(X^{\text{Entropy}})$ (see Proposition 8.A.1) derived from using the Entropy reconstruction method. We see that the γ_{n1} , $n \in \mathcal{N}$ that correspond to the proportional selling rule by Greenwood et al. (2015) are rather similar for most of the banks and overall rather close to the upper bound. Only for 2016, we find a small number of banks whose parameters γ_{n1} are close to the lower bound. We also find that the estimate $\gamma^{\text{Entropy}} = \gamma_{n1}(X^{\text{Entropy}})$, $n \in \mathcal{N}$ that is obtained from using the Entropy reconstruction method (indicated by the dotted line in Figure 2.2) is close to the median of the true γ_{n1} , $n \in \mathcal{N}$. Furthermore, we show in Appendix 8.A.2 that the expected connectivity using the StatPhys method coincides with the connectivity derived using the Entropy method, formally $\gamma^{\text{Entropy}} = \mathbb{E}[\gamma_{n1}(X^{\text{StatPhys}})]$ for all $n \in \mathcal{N}$.

2.4 Assessing the effect of policy interventions under full and partial information

We now investigate how fire sales risk can be mitigated through policy interventions. In contrast to Greenwood et al. (2015), we investigate how well fire sales risk can be mitigated if a policymaker decides on an intervention without the full knowledge of the asset holding network. We focus on two types of interventions: leverage caps and capital

¹⁹In the fire sale literature, a wide range of liquidation strategies has been considered. Some are exogenous and some are the result of an optimisation problem, see e.g., Caballero and Simsek (2013), Feinstein (2017), Braouezec and Wagalath (2019), Banerjee and Feinstein (2021).



Figure 2.2: The box and violin plots of $(\gamma_{n1})_{n \in \mathcal{N}}$ are based on the full information and a constant price impact. There are three horizontal lines: The solid line is at $\max_{\mu \in [0,1]^{N \times K}, \sum_{k=1}^K \mu_{nk}=1} \gamma_{n1}^{(\mu)}$ (which is the same for all n), the dashed line is at $\min_{\mu \in [0,1]^{N \times K}, \sum_{k=1}^K \mu_{nk}=1} \gamma_{n1}^{(\mu)}$ (which again is the same for all n), and the dotted line is at $\gamma^{\text{Entropy}} = \gamma_{n1}(X^{\text{Entropy}})$.

injections.

2.4.1 Leverage caps

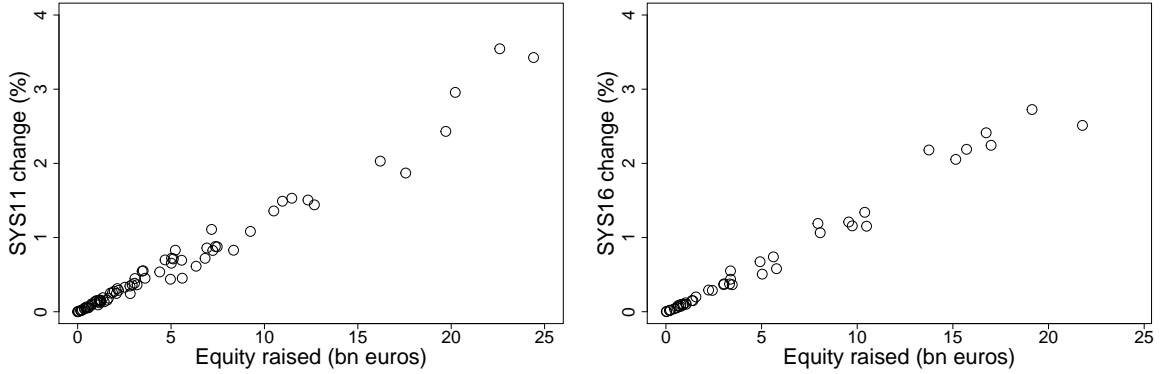
Greenwood et al. (2015) have analysed a range of policy interventions to mitigate the effects of fire sales. In particular, for a GIIPS shock, they consider the effect of debt renationalisation, an introduction of Eurobonds, ring-fencing risky assets, merging exposed banks with unexposed ones and leverage caps. They find that “capping leverage is the only policy that delivers a sizeable reduction in \mathcal{AV} [aggregate vulnerability]”, (Greenwood et al., 2015, p. 481). We will therefore focus on a leverage cap first.

The leverage cap policy in Greenwood et al. (2015) can be defined as follows.

Definition 2.4.1 (Policy intervention: Leverage cap). *For each bank $n \in \mathcal{N}$ with leverage d_{n1}/e_{n1} , the leverage cap policy sets the target leverage to $b_{n1} = \min \left\{ B, \frac{d_{n1}}{e_{n1}} \right\}$ for a constant $B > 0$. It is assumed that all banks $n \in \mathcal{N}$ for which $d_{n1}/e_{n1} > B$, are able to raise equity to reach the new lower leverage of B without changing the size of their balance sheet.*

In our empirical analysis, we set the leverage cap to be $B = 15$. Recall that all banks in the sample had leverage of at most 30 (after an initial cap had been applied).

A reduction in target leverage automatically reduces the need to fire-sell assets as shown in Greenwood et al. (2015) and hence such a strategy reduces the aggregate vulnerability.



(a) Changes in $\mathcal{SYS}(n)$ for $n \in \mathcal{N}$ in 2011. (b) Changes in $\mathcal{SYS}(n)$ for $n \in \mathcal{N}$ in 2016.

Figure 2.3: The scatter plots represent the changes in the \mathcal{SYS} between capping target leverage at 30 and at 15, relative to the total amount of equity raised for 2011 (left) and 2016 (right). The displayed points are for banks whose target leverage is higher than the leverage cap of 15.

The potential problem with such a strategy is that banks might need to raise a significant amount of equity to satisfy a leverage cap that significantly reduces fire sales risk, “The cost of the policy is large [...], and the action is drastic”, (Greenwood et al., 2015, p. 481). To illustrate the cost of this strategy, we present Figure 2.3. For each bank n , it shows the change in the $\mathcal{SYS}(n)$ between a target leverage at 30 and at 15, relative to the raised equity for each individual bank. In this example, we consider the capitalisation-dependent price impact ($\rho = -\log(0.1)$) and an all asset shock ($f_k = f = -0.001, \forall k \in \mathcal{S}$), see Section 2.3.4. We observe a linear relationship between the change in $\mathcal{SYS}(n)$ values and the equity raised. For both plots (i.e., for both years 2011 and 2016), there is a cluster of banks where a smaller increase in equity results in small decreases in the contributed equity loss. The effect of a leverage cap only becomes distinctive between banks when larger equity values are considered, in this case past 10bn EUR. We also see that in 2011, a larger amount of equity needs to be raised by some banks to reach the same target leverage compared to 2016.

Overall, we find that banks would need to raise 357.2 billion EUR in 2011 and 233.85 billion EUR in 2016 to satisfy a leverage cap of 15.

Remark 2.4.2 (Leverage cap under partial information). The leverage cap policy does not depend on the asset holding matrix X . Therefore, implementing a leverage cap is equally successful with or without full information on the asset holding matrix.

2.4.2 Capital injections

Since reducing fire sales externalities via leverage caps is expensive, Greenwood et al. (2015) considered optimal equity injection as an alternative and the most cost-effective

way to reduce aggregate vulnerability. The assumption is that a regulator has a fixed amount of cash $I > 0$ that can be distributed among the N banks. We first define a capital injection policy.

Definition 2.4.3 (Policy intervention: Capital injection). *Let $0 < I \leq \sum_{n=1}^N d_{n1}$ be the total amount of cash that a regulator is willing to invest in banks' equity at time 1. Then, a capital injection policy is characterised by a vector $\underline{i} = (i_1, \dots, i_N)^\top$, where $0 \leq i_n \leq d_{n1} \forall n \in \mathcal{N}$ and $\sum_{n=1}^N i_n = I$. Each bank n uses its capital injection i_n to repay parts of its debt, leading to a new leverage after the capital injection of*

$$b_{n1}^* = \frac{d_{n1} - i_n}{e_{n1} + i_n}. \quad (2.12)$$

We assume that capital injections would occur in time period $t = 1$. One could extend the analysis to multiple rounds of deleveraging and multiple rounds of capital injections. Now, the goal is to find an optimal capital injection policy, i.e., an optimal choice of $\underline{i} = (i_1, \dots, i_N)^\top$. Greenwood et al. (2015) considered the objective to minimise the systemicness of each bank under a GIIPS shock subject to some budget constraints. We consider the aggregate vulnerability as the objective function, which is just the sum of the systemicness of each bank. This allows us to consider the key system-wide measure developed in Greenwood et al. (2015) not just for measuring fire sale risk but also for mitigating it. We define an optimal capital injection as follows.

Definition 2.4.4 (Policy intervention: Optimal capital injection). *Let $0 < I \leq \sum_{n=1}^N d_{n1}$. Let $\mathcal{AVI} : [0, d_{11}] \times \dots \times [0, d_{N1}] \rightarrow [0, \infty)$ be given by*

$$\mathcal{AVI}(\underline{i}; X) = \sum_{n=1}^N \gamma_{n1}(X)(-R_{n1}(X)) \frac{\alpha_{n1}}{\sum_{\nu=1}^N e_{\nu 1}} \frac{d_{n1} - i_n}{e_{n1} + i_n},$$

where X denotes the asset holding matrix. Consider the optimisation problem

$$\begin{aligned} & \min_{\underline{i}=(i_{11}, \dots, i_{N1})^\top} \mathcal{AVI}(\underline{i}; X), \\ & \text{subject to} \\ & 0 \leq i_n \leq d_{n1} \quad \forall n \in \mathcal{N}, \\ & \sum_{n=1}^N i_n = I. \end{aligned} \quad (2.13)$$

We refer to a solution $\underline{i}^{Opt}(X) = (i_1^{Opt}(X), \dots, i_N^{Opt}(X))^\top$ of (2.13) as an optimal capital injection policy.

Greenwood et al. (2015) find that the optimal capital injections are strongly positively correlated with systemicness, i.e., the optimal i_n^{Opt} are positively correlated with $\mathcal{SYS}(n)$.

We therefore also consider a simplified capital injection strategy, in which the injected capital is chosen to be proportional to the systemicness.

Definition 2.4.5 (Policy intervention: Proportional capital injection). *Let X be an asset holding matrix. We refer to a capital injection $\underline{i}^{Prop} = (i_1^{Prop}(X), \dots, i_N^{Prop}(X))^\top$, where*

$$i_n^{Prop}(X) = I \frac{\mathcal{SYS}(n)(X)}{\mathcal{AV}(X)} \quad (2.14)$$

for all $n \in \mathcal{N}$ as a proportional capital injection policy.

As a benchmark strategy for capital injections, we consider a “naive” strategy, that allocates capital relative to the total asset holdings of banks. This strategy is independent of the network topology.

Definition 2.4.6 (Policy intervention: Naive capital injection). *We refer to a capital injection $\underline{i}^{Naive} = (i_1^{Naive}, \dots, i_N^{Naive})^\top$, where*

$$i_n^{Naive} = I \frac{\alpha_{n1}}{\sum_{\nu=1}^N \alpha_{\nu 1}} \quad (2.15)$$

for all $n \in \mathcal{N}$ as a naive capital injection policy.

Remark 2.4.7 (Choice of total capital I). For our empirical analysis, we assume that the total allocation of capital I is set to 10% of the total equity of the banks, i.e., $I = 0.1 \sum_{n=1}^N e_{n1}$. This means that in 2011 we have $I = 70.55$ billion EUR and in 2016 $I = 68.21$ billion EUR.

Finally, to be able to compare capital injections to leverage caps, we consider a capital injection strategy that injects capital such that all institutions have leverage of at most $\tilde{B} > 0$. We define it formally as follows.

Definition 2.4.8 (Policy intervention: Leverage cap capital injection). *We refer to the capital injection $\underline{i}^{lev} = (i_1^{lev}, \dots, i_N^{lev})^\top$, where*

$$i_n^{lev} = \max \left\{ \frac{\alpha_{n1}}{1 + \tilde{B}} - e_{n1}, 0 \right\} \quad (2.16)$$

as the leverage cap capital injection policy with leverage cap $\tilde{B} > 0$.

Indeed, for an $n \in \mathcal{N}$ it holds that

$$i_n^{lev} = \frac{\alpha_{n1}}{1 + \tilde{B}} - e_{n1} > 0 \Leftrightarrow \frac{\alpha_{n1}}{1 + \tilde{B}} > e_{n1} \Leftrightarrow b_{n1} = \frac{\alpha_{n1} - e_{n1}}{e_{n1}} > \tilde{B}.$$

Hence, the leverage cap capital injection policy injects capital in exactly those institutions that exceed the leverage cap \tilde{B} . Furthermore, for all $n \in \mathcal{N}$ with $b_{n1} > \tilde{B}$, it follows

directly from the definition of i_n^{lev} that $\frac{d_{n1} - i_n^{\text{lev}}}{e_{n1} + i_n^{\text{lev}}} = \tilde{B}$, i.e., those institutions that previously exceeded the leverage cap get a capital injection to reach the leverage of \tilde{B} .

Remark 2.4.9 (Choice of leverage cap \tilde{B} in leverage cap capital injection). In our empirical analysis, we determine the leverage cap \tilde{B} , by solving

$$\sum_{n=1}^N i_n^{\text{lev}} = \sum_{n=1}^N \max \left\{ \frac{\alpha_{n1}}{1 + \tilde{B}} - e_{n1}, 0 \right\} = I$$

for \tilde{B} for a given total capital of I that is chosen as in Remark 2.4.7. Then, the total amount of capital used in the leverage cap capital injection strategies coincides with the total capital used in the other capital injection strategies. This allows us to compare these strategies directly.

We find that injecting a total amount of $I = 70.55$ billion EUR in 2011 corresponds to a leverage cap of $\tilde{B} = 26.77$ for the leverage cap capital injection method in 2011; injecting a total amount of $I = 68.21$ billion EUR in 2016 corresponds to a leverage cap of 21.68 in 2016.

Remark 2.4.10 (Capital injection under partial information). By construction, the naive capital injection policy and the leverage cap capital injection strategy do not depend on the individual entries of the asset holding matrix X . The optimal capital injection policy and the proportional capital injection policy, however, will usually depend on the individual entries of the asset holding matrix X .

2.4.3 Empirical results on policy interventions

We will now analyse how well leverage caps and the different capital injection strategies work in the 2011 and 2016 data, under both full and partial information. To do so, we compute the relative reduction in aggregate vulnerability between the network without intervention and the network with intervention. We analyse these policies for a GIIPS shock of 5% that we have already considered in the previous section.

Empirical results - leverage cap

First, we consider the intervention of capping the leverage. As already discussed, the leverage cap intervention is independent of the underlying network. Hence, the relative reduction in aggregate vulnerability between the network without a leverage cap and the network with a leverage cap relative to the network without a leverage cap is given by

$$\Delta \mathcal{AV}^{\text{Leverage cap}} = \frac{\mathcal{AV} - \mathcal{AV}^{\text{Leverage cap}}}{\mathcal{AV}}$$

under both full and partial information. Here, $\mathcal{AV}^{\text{Leverage cap}}$ refers to the aggregate vulnerability that is obtained by setting the target leverage to $b_{n1} = \min\{B, \frac{d_{n1}}{e_{n1}}\}$, where we consider two choices of B : $B = 15$ and $B = \tilde{B}$, where $\tilde{B} = 26.77$ in 2011 and $\tilde{B} = 21.68$ in 2016. The choices of \tilde{B} correspond to the leverage caps derived in Remark 2.4.9, i.e., the amount of equity that needs to be raised to achieve this cap, corresponds to the total amount of capital used in the capital injection strategies. In this sense, the costs of the leverage cap strategy with the target leverage of $b_{n1} = \min\{\tilde{B}, \frac{d_{n1}}{e_{n1}}\}$ coincides with the cost of the capital injection policies.

Table 2.6 reports the results. When capping the leverage at 15, we see that the leverage cap in 2011 yields a much larger relative reduction in aggregate vulnerability compared to 2016. This is not surprising, since the leverages and the target leverages were generally higher in 2011 than in 2016 and therefore capping the leverage at 15 (from 30) has a much larger effect in 2011 than in 2016.

Capping the leverage at \tilde{B} , which in both years is significantly larger than 15, yields smaller relative decreases in aggregate vulnerability than capping at 15, which was to be expected. Of course, less equity needs to be raised to reach a higher cap at \tilde{B} than reaching the lower cap of 15, but then one does not obtain the same benefit from it.

More interesting is the comparison between capping the leverage at \tilde{B} and the capital injection strategies, since these strategies have comparable costs. We find that in both years, even the naive capital injection strategy outperforms the leverage cap strategy at a cap of \tilde{B} . More sophisticated capital injection strategies do generally outperform the leverage cap strategy at a cap of \tilde{B} by a larger amount (even if they are used with a network reconstruction method rather than under full information).

Empirical results - capital injection

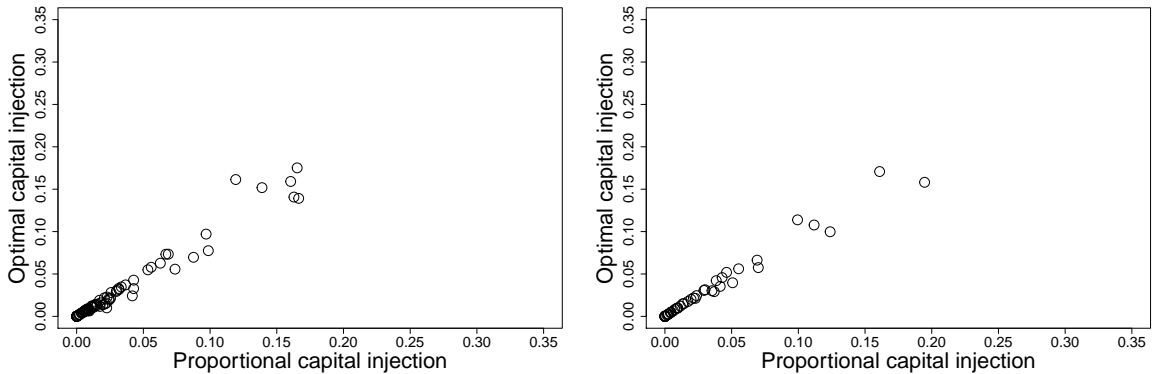
Second, we consider intervention via capital injection. We set the total capital I that is injected in the network to be equal to 10% of the total equity in the given network. We consider different capital injection strategies \underline{i} and compute the relative reduction in aggregate vulnerability in the true financial network corresponding to such a capital injection strategy. In particular, for a given capital injection strategy \underline{i} the corresponding relative reduction in aggregate vulnerability is given by

$$\Delta\mathcal{AV}^{\text{Injection}}(\underline{i}) = \frac{\mathcal{AVI}(\underline{0}; X^{\text{true}}) - \mathcal{AVI}(\underline{i}; X^{\text{true}})}{\mathcal{AVI}(\underline{0}; X^{\text{true}})}, \quad (2.17)$$

where $\underline{0}$ is the N -dimensional zero vector, and therefore $\mathcal{AVI}(\underline{0}; X^{\text{true}})$ represents the aggregate vulnerability in the fully observed financial network with zero capital injection. Again, Table 2.6 shows the results. We first look at the results under full information, i.e., the columns labelled *True*, meaning that the strategy $\underline{i} = \underline{i}(X^{\text{true}})$ is computed based

		Capitalisation-Dependent Price Impact ($-\log(0.1)/c_k \forall k$)					Constant Price Impact ($5 \times 10^{-13} \forall k$)						
		True	MinDen	Entropy	StatPhys	BayeER	BayeEF	True	MinDen	Entropy	StatPhys	BayeER	BayeEF
GIIPS (%)													
2011	Naive capital injection	7.29	-	-	-	-	-	7.43	-	-	-	-	-
-	Proportional capital injection	16.11	3.52	7.47	7.28	8.99	9.88	15.94	3.66	7.64	7.82	8.55	8.31
-	Proportional capital injection (Average)	-	-	-	7.47	9.48	9.32	-	-	-	7.63	8.77	8.71
-	Optimal capital injection	19.81	2.95	10.56	7.54	8.44	9.95	19.51	3.09	10.52	7.93	9.16	9.56
-	Optimal capital injection (Average)	-	-	-	10.31	11.98	11.80	-	-	-	10.38	11.27	11.44
-	Leverage Cap ($B = 26.77$)	3.53	-	-	-	-	-	3.41	-	-	-	-	-
-	Leverage Cap ($B = 15$)	36.51	-	-	-	-	-	36.44	-	-	-	-	-
2016	Naive capital injection	8.97	-	-	-	-	-	9.06	-	-	-	-	-
-	Proportional capital injection	23.67	3.10	8.33	8.35	10.60	7.98	22.53	3.82	8.47	8.46	10.41	6.85
-	Proportional capital injection (Average)	-	-	-	8.34	10.17	10.16	-	-	-	8.47	9.57	9.50
-	Optimal capital injection	27.03	3.42	5.57	8.17	10.47	10.66	25.66	3.96	5.65	8.46	8.53	8.30
-	Optimal capital injection (Average)	-	-	-	5.99	9.46	9.56	-	-	-	6.07	8.69	8.61
-	Leverage Cap ($B = 21.68$)	2.96	-	-	-	-	-	2.79	-	-	-	-	-
-	Leverage Cap ($B = 15$)	18.39	-	-	-	-	-	19.07	-	-	-	-	-

Table 2.6: Relative decrease (in percent) in aggregate vulnerability for the EBA 2011 and 2016 data for different policies (capital injections and leverage caps) and for two different price impacts (capitalisation-dependent and constant). Values in bold indicate which network reconstruction method performed best when used for a given capital injection strategy. Values in a box represent the best capital injection method in a given year and for a given price impact. Entries labelled “-” indicate that these values coincide with the value reported in the column labelled *True*.



(a) *SYS* under capital injections for 2011 data. (b) *SYS* under capital injections for 2016 data.

Figure 2.4: The plot of the optimal capital injection strategy against the proportional capital injection strategy under full information for a 5% GIIPS shock and a capitalisation-dependent price impact.

on the fully observed asset holding matrix X . They show the relative reduction in aggregate vulnerability when the capital injection \hat{z} was computed from the fully observed asset holding matrix X^{true} . The optimal capital injection policy performs best throughout which it should do. What is interesting, is that the proportional capital injection strategy still performs only slightly worse than the optimal injection strategy. This implies that injecting capital proportional to the systemicness of the nodes seems to be a good approximation to the optimal strategy derived from solving (2.13). This is further

confirmed by Figure 2.4 which shows a scatter plot of the optimal capital injection strategy under full information plotted against the proportional capital injection policy under full information. We see that these two strategies are indeed very similar.

The naive capital injection strategy performs worst throughout with a relative reduction of aggregate vulnerability of around 7% in 2011 and 9% in 2016, respectively, which is significantly lower than e.g., the 19% and 25-27% reductions achieved by using the optimal capital injection policy. Hence, we see that there is a clear benefit of using an optimal strategy (or an approximation of the optimal strategy) in the case of full information.

Next, we consider the potential benefits of the different capital injection strategies if the vector \underline{i} representing the capital injections is determined under partial information by using matrix reconstruction. Any type of capital injection improves aggregate vulnerability. Therefore, even under partial information, capital injections will still reduce the overall aggregate vulnerability. It is not clear, however, how much reduction in aggregate vulnerability can be achieved and this is what we investigate here.

Since the naive capital injection policy is independent of the network, the relative reduction in aggregate vulnerability under full and partial information is the same. Hence, we only consider the optimal and the proportional capital injection strategy under partial information.

For the optimisation-based matrix reconstruction methods MinDen and Entropy, determining the capital injections based on partial information means that we compute $\underline{i}^{\text{Opt}}(\hat{X})$, $\underline{i}^{\text{Prop}}(\hat{X})$, where \hat{X} is the reconstructed matrix that is either derived using the MinDen or the Entropy method. Both optimisation-based reconstruction methods only return one matrix, therefore the corresponding strategies are well defined.²⁰ Then, we consider the relative reduction in aggregate vulnerabilities $\Delta\mathcal{AV}^{\text{Injection}}(\underline{i}^{\text{Opt}}(\hat{X}))$ and $\Delta\mathcal{AV}^{\text{Injection}}(\underline{i}^{\text{Prop}}(\hat{X}))$ as given in (2.17).

Since the sample-based reconstruction methods StatPhys, BayeER, and BayeEF return not just one reconstructed network but a sample of reconstructed networks, there are different ways how we can compute the proportional and optimal capital injection strategy under partial information. We will consider two approaches: the first approach will just average the strategies derived from the different reconstructed networks. The second approach will choose a strategy associated with the tail of the distribution of aggregate vulnerabilities.

Consider a sample of asset holding matrices $X^{(1)}, \dots, X^{(d)}$ and denote by X^{true} the true asset holding matrix. One possible approach is to compute the proportional or optimal

²⁰Since the reconstructed matrix obtained from the Entropy method is available in closed form, we can also express $\underline{i}^{\text{Prop}}(X^{\text{Entropy}})$ analytically. In particular, we show in Corollary 8.A.3 that

$$\underline{i}_n^{\text{Prop}}(X^{\text{Entropy}}) = I \frac{\mathcal{SY}\mathcal{S}^{X^{\text{Entropy}}}(n)}{\mathcal{AV}^{X^{\text{Entropy}}}} = I \frac{\alpha_{n1} b_{n1}}{\sum_{\nu=1}^N \alpha_{\nu 1} b_{\nu 1}}.$$

injection strategy on every network $X^{(\nu)}$ of the sample, i.e., determine $\underline{i}^{\text{Prop}}(X^{(\nu)})$ and $\underline{i}^{\text{Opt}}(X^{(\nu)})$ and then consider the sample averages of these strategies given by

$$\underline{i}^{\text{Prop, average}} = \frac{1}{d} \sum_{\nu=1}^d \underline{i}^{\text{Prop}}(X^{(\nu)}), \quad \underline{i}^{\text{Opt, average}} = \frac{1}{d} \sum_{\nu=1}^d \underline{i}^{\text{Opt}}(X^{(\nu)}).$$

We will refer to these strategies as proportional capital injection (average) and optimal capital injection (average) in Table 2.6.

In addition to these average strategies, we are also interested in the tails of the distribution of aggregate vulnerabilities under capital injection. For the proportional capital injection strategy we determine the injection strategy that corresponds to the 95% percentile of the empirical distribution function of the sample of aggregate vulnerabilities under proportional capital injection, i.e., we determine the index $\tilde{\nu} \in \{1, \dots, N\}$ such that

$$\mathcal{AVI}(\underline{i}^{\text{Prop}}(X^{(\tilde{\nu})}); X^{(\tilde{\nu})}) = \inf \left\{ x \in \mathbb{R} \mid \frac{1}{d} \sum_{\nu=1}^d \mathbb{I}_{\{\mathcal{AVI}(\underline{i}^{\text{Prop}}(X^{(\nu)}); X^{(\nu)}) \leq x\}} \geq 0.95 \right\}$$

and we denote this index by $\nu^{(0.95)}$.²¹ Hence, this corresponds to one of the highest aggregate vulnerabilities observed in the sample in which proportional capital injection was used. We then compute the relative reduction in aggregate vulnerability that corresponds to the strategy $\underline{i}^{\text{Prop}}(X^{(\nu^{(0.95)})})$ and report this in Table 2.6 (in the row *Proportional capital injection*).

For the optimal capital injection policy we consider the optimisation problem which aims to find the capital injection strategy that minimises the 0.95-Percentile of the empirical cumulative distribution function of the aggregate vulnerabilities derived from the d sample networks with capital injection. Formally, we consider

$$\begin{aligned} \min_{\underline{i}} \quad & \inf \left\{ x \in \mathbb{R} \mid \frac{1}{d} \sum_{\nu=1}^d \mathbb{I}_{\{\mathcal{AVI}(\underline{i}; X^{(\nu)}) \leq x\}} \geq 0.95 \right\}, \\ \text{subject to} \quad & \\ & 0 \leq i_n \leq d_{n1} \quad \forall n \in \mathcal{N}, \\ & \sum_{n=1}^N i_n = I. \end{aligned} \tag{2.18}$$

We then consider the strategy that is a solution to (2.18) and report the corresponding relative reduction in aggregate vulnerability in Table 2.6.

When considering the performance of the proportional and optimal capital injection policies under partial information in Table 2.6 we see that the reduction in relative aggregate

²¹If there is more than one index $\tilde{\nu}$ satisfying the equation we select one suitable index randomly.

vulnerability is significantly lower under partial information than under full information for all types of reconstruction methods. Furthermore, we see that under partial information, sometimes the proportional capital injection policy performs better than the optimal capital injection strategy. For example, for the 2016 data and a constant price impact, the proportional capital injection strategy based on the Entropy method gives a relative reduction of the aggregate vulnerability of 8.47%, compared to a relative reduction of 5.65% achieved by the optimal capital injection strategy. The reason for this is that the optimal capital injection is optimal for the reconstructed asset holding matrix X^{Entropy} and not necessarily optimal for the true matrix X^{true} . When evaluating the performance of the different strategies, however, we use the true matrix X^{true} to compute the relative reduction of aggregate vulnerability (2.17). Under full information, the optimal capital injection strategy cannot perform worse than the proportional capital injection strategy. Still, we overall find that in our four test cases (2 years and 2 price impacts), the best-performing capital injection strategy (indicated by a box in Table 2.6) is an optimal capital injection strategy in three cases²² and a proportional capital injection strategy in only one case²³.

Among the different reconstruction methods, the MinDen method performs worst in both years and for both choices of price impact. Capital injection strategies that rely on the MinDen method only reduce the relative aggregate vulnerability by around 3%. This level of reduction is therefore much lower than the reduction of around 7-9% that can be achieved with the naive capital injection strategy that does not even attempt to reconstruct the underlying network.

The other network reconstruction methods, i.e., Entropy, StatPhys, BayeER, and BayeEF perform generally better when used to decide on capital injections. Out of these four methods, the Bayesian methods seem to perform best overall. For the four test cases (2 years and 2 price impacts), the best capital injection strategy (indicated by a box in Table 2.6) is always one that uses a Bayesian network reconstruction. For the 2011 data, the best capital injection strategy is the optimal capital injection (average) using the BayeER method under the capitalisation-dependent price impact and the BayeEF method under the constant price impact. They reduce the aggregate vulnerability by 11.98% and 11.44% respectively, which is better than the naive strategy which achieves a relative reduction between 7.24 - 7.43%.

For the 2016 data, the optimal capital injection method using the BayeER method is best under the capitalisation-dependent price impact assumption (10.66% relative reduction in aggregate vulnerability compared to 8.97% achieved by the naive capital injection strategy). For the constant price impact assumption, the proportional capital injection strategy using the BayeER method performs best (achieving a relative reduction in ag-

²²for both price impacts in 2011 and for the capitalisation-dependent price impact in 2016

²³for a constant price impact in 2016

gregate vulnerability of 10.41% compared to 9.06% achieved by the naive strategy).

When fixing the type of capital injection strategy (proportional capital injection, proportional capital injection (average), optimal capital injection, optimal capital injection (average)), and then checking which network reconstruction method performs best in a given year and for a given price impact, then we find that out of the 16 cases, the BayeER performs best in 10 cases, BayeEF performs best in 4 cases and the Entropy method performs best in 2 cases. The StatPhys is never the best-performing method in our examples but still performs reasonably well.

Overall the best-performing capital injection methods using network reconstruction methods reduce the relative aggregate vulnerability in the range between 10 - 11% and are therefore better than the naive capital injection strategy which achieves a reduction between 7 - 9%. In particular, in each of the two years and for both types of price impact we see that all capital injection strategies that use the BayeER network reconstruction always outperform the naive capital injection strategy and the BayeER is the only network reconstruction method considered here for which this is the case.

Hence, we see that using suitable network reconstruction methods to decide on risk mitigation mechanisms in financial networks is indeed beneficial and can achieve better outcomes than using naive intervention strategies.

2.5 Conclusion

We have investigated how well fire sales risk can be measured and mitigated under partial information. We used the fire sales measures (systemicness, aggregate vulnerability, direct vulnerability and indirect vulnerability) developed by Greenwood et al. (2015) and analysed their dependence on the asset holdings matrix. We then investigated how well these four different measures quantifying risk associated with fire sales can be estimated when the individual entries of the underlying asset holdings matrix are not observable but its row and column sums are. We considered two empirical asset holding matrices, available in the data published by the EBA for their 2011 and 2016 stress tests, and assumed that they were not fully observable. We estimated the asset holding matrix using five different network reconstruction methods available in the literature and found that in general these fire sales measures could be estimated reasonably accurately for a range of shock scenarios.

We then analysed how well risk from fire sales can be mitigated if policy interventions are based on partial information and network reconstruction techniques are used to decide on policies. We considered two policies that were highly effective in the analysis under full information in Greenwood et al. (2015), namely leverage caps and capital injections. Leverage caps are generally independent of the underlying network and therefore do not require network reconstruction techniques to implement them. In 2011 leverage caps

lead to better outcomes than capital injections, but in 2016 when banks' leverages were generally lower, intervention via capital injections lead to better outcomes than leverage caps. Therefore, in the more recent data, capital injections appear more beneficial.

Capital injections can be done using ad hoc methods that do not rely on the asset holding matrix or can be done in a more targeted approach that would account for characteristics of the asset holding matrix. We considered a naive capital injection strategy in which capital is injected in proportion to the size of a bank (measured in terms of the total assets on its balance sheet); no information on the individual entries of the asset holding matrix is needed for this approach. We compare this to capital injection strategies that inject capital in proportion to the systemicness of an institution or in an optimal way (with the objective of reducing the aggregate vulnerability) and these methods then rely on the (reconstructed) asset holding matrix.

We find that it is possible to achieve a significant relative reduction in aggregate vulnerability even under partial information. While the naive capital injection strategy, which does not require network reconstruction, achieves relative reductions in aggregate vulnerability in the range of 7 - 9% in our study, the best-performing capital injection strategies that rely on network reconstruction methods achieved a relative reduction of aggregate vulnerability between 10 - 11%. We found that the Bayesian method (Gandy and Veraart, 2017, 2019) for network reconstruction was the best overall method when used for deciding on capital injections. In particular, we found that any capital injection strategy that we considered that was based on the Bayesian network reconstruction method with an Erdős-Rényi-type prior, always outperformed the naive capital injection strategy.

Hence, we see that network reconstruction techniques are not just useful for measuring risk, but also for managing it. As we have already discussed, the intervention strategies considered here can never do any harm (in the sense that using them cannot increase the aggregate vulnerability of the network). So it was clear that even using them in a non-optimal way can bring potential benefits. What is interesting, however, is to see how much better some of them perform in comparison to naive strategies that do not attempt to reconstruct the underlying network.

Chapter 3

Reverse stress testing for fire sales risk

3.1 Introduction

Stress tests are used to evaluate banks' losses under explanatory scenarios, to which banks may be exposed. These scenarios show if the financial system can continue performing its daily financial operations even if banks suffer significant losses. In one type of stress test, a forward approach is conducted where the scenario is chosen and the losses are simulated under this scenario. The formulation of the scenario can come from a range of different motivations e.g., historical or economic motivations. In all cases, scenarios used for a forward stress testing approach can reveal the losses of banks under various shocks. The problem with choosing the scenario for the stress test is the scenario is subjective and the losses from this scenario may underestimate the bank's potential losses in future events. Designing stress tests where the largest losses of banks are known is important for evaluating financial stability and systemic risk in the worst-case situations.

We focus on a stress testing approach known as a reverse stress test. In a reverse stress test, we ask "What scenario can cause X amount of losses?". The total losses banks are exposed to are assumed and a scenario is derived which is consistent with such losses. An advantage of a reverse stress test is identifying scenarios not observed in previous financial events. Historically motivated scenarios used in forward stress tests are less likely to reoccur, because of the change in financial regulation since the event took place. A scenario with an economic motivation involves factoring in various indicators, and justifying how these indicators correspond to a specific choice and size of the asset shock. For all motivations of the given scenario, a forward stress test adds a level of bias, where the individual size of asset shocks can vary depending on the regulator or policymaker overseeing the stress test.

The need for reverse stress tests addresses a concern highlighted in a speech from the

deputy governor of financial stability for The Bank of England “*financial stability authorities must focus on what could happen rather than just what is most likely to happen*”¹ (Jon Cunliffe, March 2022). In this respect, a reverse stress test can provide scenarios and losses not previously observed in a systemic event.²

Developing tools for stress testing is important for assessing financial stability. This was highlighted by Anderson (2016), particularly since the Great Financial Crisis. The importance of stress testing was discussed by Daniel Tarullo³, a member of the Federal Reserve Board of Governors from 2004 to 2017 who categorised stress testing as “*the single most important advance in prudential regulation since the crisis*”. Many central banks and monetary institutions employ stress testing approaches with further detail on supervisory stress tests provided by Duffie (2018).

There are different channels of systemic risk which can be modelled using stress testing. We focus on stress tests for fire sales. A fire sales event occurs if assets are sold at a discounted value in large volumes. The selling of assets triggers a mark-to-market adjustment and a price impact for common asset holdings, resulting in further sales. Multiple rounds of fire sales can continue to occur, where losses increase at each round. We specifically consider the fire sales mechanism by Greenwood et al. (2015), where banks sell assets to meet their target leverage. Assuming banks maintain their target leverage increases the quantity of assets sold in a fire sale and fuels further losses to itself and other banks.

We develop an optimisation-based macro-prudential reverse stress testing approach. This optimisation method accounts for the multiple rounds of fire sales and the heterogeneity of the bank balance sheet. This heterogeneity is reflected in the bank balance sheet and the commonality of the bank’s asset holdings with other banks. We assume an initial scenario and optimise the scenario resulting in a reverse stress test scenario, reflecting the largest total losses to banks. We compare the losses from the reverse stress test to other scenarios that could be used in a stress test.

Using the 2016 EBA data, we find the size of shocks allocated to assets under a reverse stress test is sparse. This sparsity is represented by shocks of high magnitude for a few asset holdings, where all other shocks are negligible or small in size. The shocks to assets

¹Recollections of Financial Stability, Oxford union, 2nd March 2022, <https://www.bankofengland.co.uk/speech/2022/march/jon-cunliffe-speech-at-the-oxford-union-current-financial-stability-environment>.

²The Bank of England has published a report for 2021-2022 providing a descriptive analysis of the supervision of CCPs for stress testing *2021-22 CCP Supervisory Stress Test: results report*, <https://www.bankofengland.co.uk/stress-testing/2022/ccp-supervisory-stress-test-results-2021-22>. The recent prevalence of CCPs means few historic scenarios can be drawn to assess bank losses and so a reverse stress test approach is adopted. Other reports have also been commissioned considering a reverse stress test analysis i.e., the European Securities and Market Authority (ESMA) in 2022 *4th ESMA Stress Test Exercise for Central Counterparties*, https://www.esma.europa.eu/sites/default/files/library/esma91-372-2060_4th_esma_ccp_stress_test_report.pdf.

³Stress Testing after Five Years: a speech at the Federal Reserve Third Annual Stress Test Modelling Symposium, Boston, Massachusetts, June 25, 2014.

correspond to asset-holding portfolios of banks with high target leverages. As shocks result in losses to banks with high target leverages, a larger quantity of assets is sold which leads to larger losses to other banks.

Under different constraints on the size of asset shocks, we find losses on the total asset holdings of banks from a scenario under a reverse stress test are not unique. Multiple scenarios with different magnitudes of asset shock size result in the same total losses for banks. As the magnitude of the potential shock size to assets decreases, there is a decrease in the magnitude of losses for banks with large losses and an increase in losses for banks with small losses.

We consider the losses of banks relative to their equity holdings. Under the systemicness and indirect vulnerability fire sales measures by Greenwood et al. (2015), we find a small number of banks contribute to the total equity losses. From scenarios under a reverse stress test, the equity losses which banks contribute to a fire sale highly vary and equity losses incurred by banks in a fire sale are similar on average. These findings provide further insights into the 2016 EBA stress testing data and banks of systemic importance in a fire sales event.

Another contribution in this chapter is the theoretical results on fire sales measures when banks can meet their target leverages, which we provide in the appendix. We state conditions for which all banks can meet their target leverages, across a range of stress-testing scenarios. As a consequence of these conditions, we formulate various inequalities relating to the size of a bank's cumulative returns in connection to its connectivity. These results are important for the implementation of the new reverse stress testing method, but also in the understanding of fire sale measures by Greenwood et al. (2015).

We organise this chapter as follows. In Section 3.2, we introduce the multiple period fire sales measures by Greenwood et al. (2015). We formulate the optimisation problem and introduce the algorithm for the reverse stress tests in Section 3.3. In Section 3.4, we consider reverse stress tests for the 2016 EBA data. We conclude in Section 3.5. We provide further detail on fire sales measures and proofs in the appendix.

3.1.1 Related literature

We consider the contagion mechanism of fire sales, where banks sell assets with consideration to their leverage. The leveraged-focused fire sales build on the evidence by Adrian and Shin (2010) that leverage is a driver of asset mark-to-market changes. The papers by Duarte and Eisenbach (2021), Cont and Schaanning (2017) and Ramadiah et al. (2022) focus on leverage-driven fire sales mechanisms. Other works which consider fire sales but do not leverage targeting include Huang et al. (2013). These papers acknowledge fire sales are a larger contributor to bank losses in a systemic event. As the losses from fire sales can be significant in a systemic event, it is of interest to apply a reverse stress

testing approach.

The area of fire sales is also of interest because of how incorporated it is into other types of financial mechanisms. The work by Capponi et al. (2020) considers swing pricing, which mitigates the operational costs passed to shareholders from first movers. In Cont et al. (2020), they consider multiple sources of funding i.e., repo markets, collateral, and how this is affected by liquidity and solvency risks. The work by Cont et al. (2020) provides an application of their model to reverse stress testing.

We believe the papers by Baes and Schaanning (2023) and Grigat and Caccioli (2017) are the closest to our approach for reverse stress testing. They use an optimisation-based method for reverse stress testing and incorporate the contagion modelling of systemic risk. In Baes and Schaanning (2023), they consider a reverse stress testing approach using the fire sales mechanism presented by Cont and Schaanning (2017). The paper by Grigat and Caccioli (2017) focuses on a reverse stress test for banks under DebtRank. This is a solvency contagion mechanism representing the losses which propagate through a network of banks, with interbank assets and liabilities Battiston et al. (2012c).

Our work differs from Baes and Schaanning (2023), as we do not assume a probabilistic distribution for which the initial scenario is drawn, where the corresponding losses are then aggregated. In our approach, we only assume the initial total losses of banks where the output from the reverse stress testing scenario shows small changes from the initial scenario assumed for the optimisation. We also differ from the reverse stress testing approach by Grigat and Caccioli (2017), as the total losses after the clearing mechanism are assumed for all banks. In this regard, one could categorise our approach as a “partial” reverse stress test, partial in the sense that only the initial total losses of banks are assumed. Assuming only the initial losses reduces the margin in the magnitude of losses while incorporating the dynamics of the fire sale.

Other papers consider approaches where a distribution (a probabilistic approach) or a set of scenarios are derived. The work by Flood and Korenko (2015) uses a grid search approach incorporating a mix of stress testing and reverse stress testing. In Glasserman et al. (2015), they consider a statistical approach using an empirical likelihood estimator of incorporated risk factors. The work by Breuer and Summer (2020) approaches reverse stress testing from extreme value theory and generates a probability distribution of losses using the EBA stress testing data. A set of risk measures is considered by McNeil and Smith (2012), where they derive scenarios resulting in losses equivalent to losses under the VaR measure. Our approach is different from these papers, as we generate one scenario from the reverse stress test. We find our results are still informative for assessing fire sales as we outperform the largest total losses compared with other scenarios used in stress testing.

3.2 Fire sales mechanism

We describe a market setting by Greenwood et al. (2015). The setup is similar to the setup in Chapter 2 but extended to multiple rounds of fire sales where required.

The setup of the bank balance sheet is identical to Chapter 2. We define the number of financial institutions in the system as N with indices in a set $\mathcal{N} = \{1, \dots, N\}$. We assume that the bank can hold K assets with indices in a set $\mathcal{S} = \{1, \dots, K\}$.

We define the asset holdings matrix $X = (X_{nk})_{n \in \mathcal{N}, k \in \mathcal{S}} \in [0, \infty)^{N \times K}$, where each entry X_{nk} represents the asset holdings of bank $n \in \{1, \dots, N\}$ in the asset $k \in \{1, \dots, K\}$ holds in million Euros.

We deviate from Chapter 2 by incorporating multiple rounds of fire sales. The total number of rounds of fire sales is defined as $T \in \mathbb{N}$ where $t \in \{1, \dots, T\}$.

The total assets of the bank are defined as $\alpha_t \in [0, \infty)^N$, where α_{nt} represents the total assets of the bank n at time- t . The total capitalisation is defined as $c_t \in [0, \infty)^K$, where c_{kt} represents the total capitalisation of the asset k at time- t . At $t = 1$, the initial total assets of the bank and asset capitalisation represent the row and column sums of the asset holdings matrix i.e.,

$$\alpha_{n1} = \sum_{k=1}^K X_{nk} \quad \forall n \in \mathcal{N}, \quad c_{k1} = \sum_{n=1}^N X_{nk} \quad \forall k \in \mathcal{S}.$$

We assume the total asset holdings of all banks at $t = 1$ is non-negative i.e., $\alpha_{n1} \geq 0 \quad \forall n \in \mathcal{N}$ and the initial total capitalisation of all assets is positive i.e., $c_{k1} > 0 \quad \forall k \in \mathcal{S}$. The total asset holdings of the bank can be represented by the sum of its debt and equity. We refer to $d_t \in [0, \infty)^N$ and $e_t \in [0, \infty)^N$ as the debt and equity, where d_{nt} and e_{nt} represents the debt and equity of the bank n at time- t , in particular

$$\alpha_{nt} = d_{nt} + e_{nt} \quad \forall n \in \mathcal{N}. \quad (3.1)$$

The asset holdings at time- t are represented by (3.1). The initial debt and equity are denoted as d_{n1} and e_{n1} .

As part of the fire sales mechanism, we introduce the target leverage of the bank, representing the ratio of the bank's debt relative to its equity. We define $b \in [0, \infty)^N$ as the target leverage, where b_n represents the target leverage of bank n :

$$b_n = \min \left\{ \frac{d_{n1}}{e_{n1}}, b^{\max} \right\} \quad \forall n \in \mathcal{N} \quad (3.2)$$

and $b^{\max} \geq 1$ is the maximum target leverage for any given bank. The maximum target leverage represents a regulatory constraint imposed on the bank. Under the assumptions by Greenwood et al. (2015), the target leverage remains the same in all rounds of fire

sales.

We define the matrix of portfolio weights as $m = (m_{nk})_{n \in \mathcal{N}, k \in \mathcal{S}} \in \mathbb{R}^{N \times K}$, where $m_{nk} = X_{nk}/\alpha_{n1}$ and each entry m_{nk} represents the weight of asset k within the total asset portfolio of bank n . From the definition of the matrix, $\sum_{k=1}^K m_{nk} = 1 \quad \forall n \in \mathcal{N}$.

We assume an initial negative shock of the bank's asset holdings as part of the fire sales. We define the shock as $f_t \in (-\infty, 0]^K$, where f_{kt} represents the shock to asset k at time- t . The initial shock is denoted as f_1 . The initial net returns, which represent the relative shock to the asset holdings of the bank are denoted as $R_t \in (-\infty, 0]^N$, where at time- t :

$$R_{nt} = \sum_{k=1}^K m_{nk} f_{kt} \quad \forall n \in \mathcal{N}.$$

The shock to the bank results in the bank selling a proportion of its asset holdings. This triggers a price impact within the respective asset k . We define the price impact $l \in [0, \infty)^K$, where l_k represents the price impact to asset k . This incorporates the mark-to-market adjustment for assets in a fire sale.

We introduce the fire sales mechanism by Greenwood et al. (2015). The following is assumed about the fire sales:

- Banks sell assets to meet their target leverage where possible.
- Banks proportionally sell their asset holdings.
- Assets sold trigger a price impact on the asset.

These assumptions on the fire sale hold in the first round (as in Chapter 2) and subsequent rounds of fire sales. Incorporating the dynamics of the fire sale, we introduce the total assets of the bank and the shock to assets for multiple rounds of fire sales as follows:

$$\begin{aligned} \alpha_{n(t+1)} &= \alpha_{nt} \left(1 + b_n \sum_{k=1}^K m_{nk} f_{kt} \right)^+, \\ f_{k(t+1)} &= -l_k \sum_{p=1}^N m_{pk} \alpha_{pt} \delta(R_{pt}), \end{aligned} \tag{3.3}$$

$$\text{where } \delta(x_n) = (\min(-b_n x_n, 1 + x_n))^+ \quad \forall n \in \mathcal{N} \quad \text{and} \quad t \geq 1.$$

The time-dependent total assets of the bank and shock to assets in (3.3) incorporates the fire sales feedback effect between banks and assets.

We describe the interaction between the asset shock and the bank's total asset holdings in a fire sale: First, a shock (the initial shock f_1) is applied to the bank's asset holdings decreasing the total asset holdings of banks. The losses in its assets lead to the bank proportionally selling its asset holdings to meet its target leverage. The total sales of the asset trigger a mark-to-market valuation and a price impact which decreases the asset's

value. This creates an indirect shock and results in additional losses for banks. If the bank is unable to sell its asset holdings to maintain its target leverage then the bank sells all its asset holdings. Further rounds of fire sales occur leading to continued losses in the total asset holdings of banks.

The function $\delta : \mathbb{R} \rightarrow \mathbb{R}$ represents the quantity of assets sold (the same as in Chapter 2) and the ability of the bank to meet its target leverage. If its remaining asset holdings are larger than its leveraged net returns, then the bank sells all its remaining assets.

A studied metric in fire sales contagion by Greenwood et al. (2015) is the connectivity component of the bank. This is a measure of losses from a bank to all other banks in the network. The discussion on connectivity for $t = 1$ and the price impact on assets follows in the same way as in Chapter 2. The connectivity is defined as $\gamma_t \in [0, \infty)^N$, where γ_{nt} represents the connectivity of bank n at time- t :

$$\gamma_{nt} = \sum_{k=1}^K l_k m_{nk} \left(\sum_{p=1}^N m_{pk} \alpha_{pt} \right) \quad \forall n \in \mathcal{N} \text{ and } t \geq 1.$$

The connectivity represents a measure of the commonality of the bank's asset holdings with other banks, with the inclusion of the price impact. As the total asset holdings of the bank are non-increasing in each stage of the fire sales, the connectivity is also non-increasing in each stage of fire sales.

The choice of price impact can have different functional forms. In Greenwood et al. (2015), a constant price impact is assumed for all assets i.e., $l = l_1 = \dots = l_k \quad \forall k \in \mathcal{S}$, where $l \geq 0$ represents the magnitude of the constant price impact. We consider a capitalisation-dependent price impact motivated by Cifuentes et al. (2005), as in Chapter 2. The capitalisation-dependent price impact is defined as follows:

$$l_k = \frac{\rho}{c_{k1}} \quad \forall k \in \mathcal{S},$$

where $\rho \geq 0$ and $c_{k1} > 0$. The larger the capitalisation of the asset, the smaller the price impact of selling the asset. Assuming that the price impact is capitalisation-dependent, then the connectivity component ρ is constant. As shown in Chapter 2, under the capitalisation-dependent price impact, then the connectivity of all banks is equal to the connectivity constant i.e., $\gamma_{n1} = \rho \quad \forall n \in \mathcal{N}$.

3.3 Reverse stress test formulation

We introduce the optimisation problem for the reverse stress test. We consider a scenario from the reverse stress test which maximises the total losses of banks from a fire sale. As the number of rounds under the optimisation can differ from the number of simulated

fire sales rounds, we denote the rounds under the optimisation as $Q \leq T$.

We compare scenarios under a reverse stress test to another scenario if the initial losses of both scenarios are bounded by the same value. The constraint on the initial losses removes reverse stress testing scenarios where losses are only larger than another scenario because the size of shocks has been scaled i.e., the losses from a scenario under a reverse stress test are larger than another scenario only because the magnitude of shocks has been multiplied by a value > 1 . With this constraint, a scenario is more severe than another scenario if the total losses from the fire sale are larger and the bound on the total initial losses is the same in both scenarios. We denote the total initial losses assumed in the optimisation problem as $W \geq 0$.

We denote $f^{\min} \in (-\infty, 0]^K$ as a lower bound to the shock on assets, where each f_k^{\min} represents the lower bound shock of the asset k . This constraint on the optimisation problem represents the largest negative initial shock to an asset.

We now formulate the optimisation problem that identifies a scenario (in our case a vector f_1 that minimises the total asset holdings of all banks after Q rounds of fire sales). It is given as follows:

$$\begin{aligned} \min_{f_1 \in (-\infty, 0]^K} : & \sum_{n=1}^N \alpha_{n(Q+1)} \quad \forall Q \geq 1, \\ \text{subject to :} & \\ & -W \leq \sum_{k=1}^K c_{k1} f_{k1}, \\ & -\frac{1}{1+b_n} \leq \sum_{k=1}^K m_{nk} f_{k1} \quad \forall n \in \mathcal{N} \quad \text{and} \quad \rho \leq \frac{1}{1+b_{\max}}, \\ & f_k^{\min} \leq f_{k1} \leq 0 \quad \forall k \in \mathcal{S}. \end{aligned} \tag{3.4}$$

Other objectives could also be considered to measure the severity of the scenario i.e., the objective function for minimising the smallest fluctuation between shocks is considered by Grigat and Caccioli (2017).⁴

The first constraint is on the initial total losses from the scenario under a reverse stress test. The second constraint represents a condition on the initial inputs in which the bank is always able to meet its target leverage. Further details about this condition are provided in Appendix 8. The last constraint is the severity of the shock size to assets. We assume that the shock is non-positive and the lower bound of shocks can vary for different assets.

The constraint space of the scenario is defined under the set of inequalities from the optimisation problem (3.4), which we denote as \mathcal{C} . The inequalities for the initial scenario

⁴An objective function which can be considered as a measure of the fluctuation of the total asset holdings of banks after Q rounds under the fire sales mechanism is $\sum_{t=1}^Q \sum_{n=1}^N (\alpha_{n(t)} - \alpha_{n(t+1)})^2$.

represent a convex and compact space for the fire sales scenario (satisfied under the linearity of the shock under the optimisation constraints) and are feasible for all parameter choices. As the constraint space is compact, convex, non-empty (there always exists a scenario satisfying the constraint space i.e., $\exists \tilde{f}_1$ in which $\tilde{f}_1 \in \mathcal{C}$) and bounded, then the set of optimal solutions to (3.4) is non-empty, convex and compact. From these conditions, provided that the initial input to the optimisation is in \mathcal{C} there is an output from the reverse stress test scenario. Further details for the set of optimal solutions to constrained optimisation problems can be found in Bertsekas et al. (2003). The objective function of the optimisation problem is non-convex, as a result, there may be no unique minimiser to the optimisation problem under the constraints of the optimisation problem.

3.3.1 Frank-Wolfe algorithm

We focus on the approach to solve the optimisation problem (3.4). There is a wide application of constrained optimisation-based approaches to study financial networks and systemic risk. In Pichler et al. (2021), they minimise the Markowitz mean-variance under a QCQP (quadratically constrained quadratic program), in the context of fire sales. They solve the portfolio optimisation problem using different branch and bound methods e.g., KNITRO Byrd et al. (2006) and BARON Sahinidis (1996).

The work by Diem et al. (2020) minimises the losses from solvency contagion on the inter-bank network between banks. A mixed integer linear programming problem is formulated under the DebtRank measure.

We consider the Frank-Wolfe algorithm for the optimisation problem, which accounts for multiple rounds of fire sales. Introduced in the paper by Frank and Wolfe (1956), the Frank-Wolfe method falls under the class of convex-constrained optimisation methods. Stochastic variants of the Frank-Wolfe method incorporating stochastic gradient descent have been developed by Hazan and Luo (2016). Further detail on these types of approaches in the context of machine learning is provided by Lan (2020). Other known constrained optimisation methods include the projection gradient descent Rosen (1961). The difference between the Frank-Wolfe method with the projection gradient descent is that the Frank-Wolfe method is projection-free, where the optimisation stays in the feasible set.

The idea of the Frank-Wolfe algorithm is to transform one non-linear optimisation into multiple linear programming problems. Each linear program is a linear combination of the shocks with associated weights, where weights are dependent on the inputs of the fire sale mechanism. From the optimised scenario, convex combinations of the previous input and optimised scenario are taken, resulting in an updated scenario. The updated scenario is used as input in the next iteration step. Each sublinear optimisation can be considered as a linear approximation to the non-linear problem, represented by the

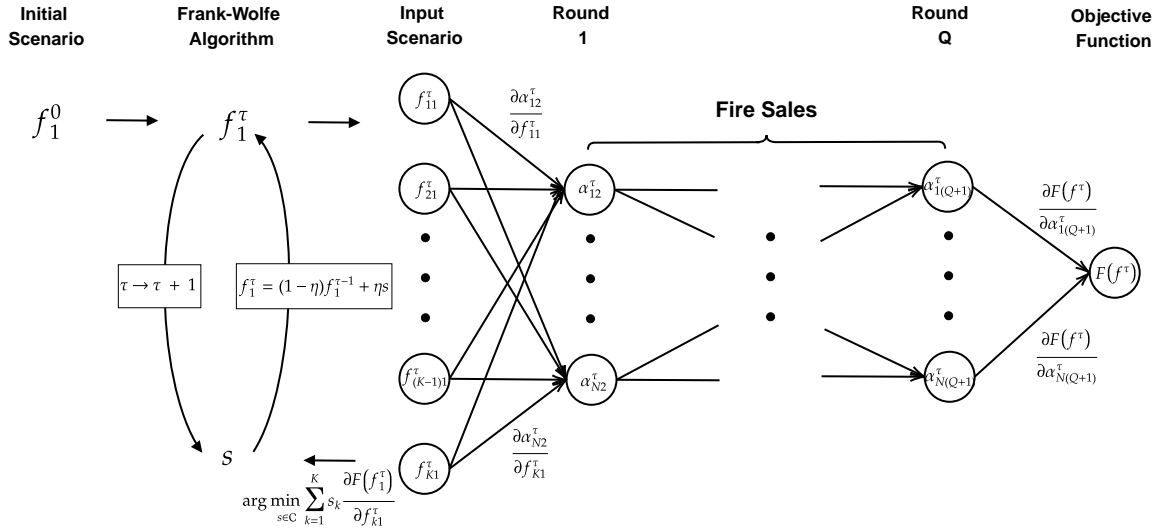


Figure 3.1: The figure represents a combination of the Frank-Wolfe algorithm with the fire sales mechanism. Partial derivatives terms correspond to links between two nodes. The algorithm starts with an initial input and derivative terms under the initial input. These terms are used in the constrained optimisation problem for computing the oracle (a linear minimiser of the optimisation problem). The updated scenario is then formed from a convex combination of the previous input and the oracle. Multiple iterations of the optimisation problem are taken where the last updated scenario represents the reverse stress testing scenario.

first-order expression of a Taylor expansion.

The advantage of the Frank-Wolfe method is the calibration of hyperparameters and computational speed to achieve a solution. For the step size, simple functions (those which only depend on the number of iterations) can be used for the method. The transformation to a linear program is also easier to solve than a nonlinear optimisation problem.

The constraint space is convex and compact. The objective function is differentiable under the target leverage condition. The objective function is non-convex, so the output solution may only be a local optimiser. If the global optimiser is reached, then this is only an approximate solution under the gradient descent type approach. There has been work on using the Frank-Wolfe method for non-convex optimisation problems i.e., network flow optimisation Chari et al. (2015).

Algorithm 1 Frank-Wolfe algorithm (1956)

Let $f_1^0 \in \mathcal{C}$

for $\tau = 0 \dots \mathcal{T}$ **do**

Compute $s = \arg \min_{s \in \mathcal{C}} \sum_{k=1}^K s_k \frac{\partial F(f_1^\tau)}{\partial f_{k1}^\tau}$

Update $f_1^{\tau+1} = (1 - \eta) f_1^\tau + \eta s$ for $\eta(\tau) := \frac{2}{\tau+2}$

end for

We introduce the Frank-Wolfe algorithm. We define the number of iterations (or epochs) as $\mathcal{T} \geq 1$. This represents the total number of updates we consider for the algorithm. The constraint space of the optimisation problem is denoted by \mathcal{C} . The initial input that denotes the initial shock is denoted as f_t^0 , with updated values of the shock as f_t^τ at time- t , where each f_{kt}^τ represents the shock to asset k at time- t , from the initial shock f_1^τ under the iteration τ .

The linear minimisation oracle is defined as s , and the objective function is denoted as $F : \mathbb{R}^K \rightarrow \mathbb{R}$. The step size at each iteration period is defined as $\eta \in [0, 1]$, where $\eta(\tau)$ depends on the iteration τ .

There can be different functions for the choice in step size, provided that the step size is $\eta \leq 1$. The step size chosen is a non-increasing function of the total number of iterations from the Frank-Wolfe method. The objective function is equal to the total asset holdings of all banks after Q rounds of fire sales, under the initial scenario at iteration τ :

$$F(f_1^\tau) = \sum_{n=1}^N \alpha_{n(Q+1)}^\tau \quad \forall n \in \mathcal{N} \text{ and } Q \geq 1,$$

where α_{nt}^τ denotes the total asset holdings of the bank n at time- t , from the initial shock f_1^τ at iteration τ . To use the Frank-Wolfe method, we calculate the derivative terms, which depend on the updated total assets of the bank, shock and previous derivative terms. The gradient terms represent the change of the total assets of the bank w.r.t the initial shock. Calculating the partial derivatives of the total asset holdings of all banks and the shock to assets at time- t :

$$\begin{aligned} \frac{\partial F(f_1^\tau)}{\partial f_{k1}^\tau} &= \sum_{n=1}^N \frac{\partial \alpha_{nt}^\tau}{\partial f_{k1}^\tau} \\ \frac{\partial \alpha_{nt}^\tau}{\partial f_{k1}^\tau} &= \alpha_{n1} \sum_{j=1}^{t-1} \left(\prod_{i \neq j}^{t-1} \left(1 + b_n \sum_{k=1}^K m_{nk} f_{ki}^\tau \right) \right) b_n \sum_{k=1}^K m_{nk} \frac{\partial f_{kj}^\tau}{\partial f_{k1}^\tau} \quad \forall n \in \mathcal{N}, \\ \frac{\partial f_{kt}^\tau}{\partial f_{k1}^\tau} &= l_k \sum_{n=1}^N m_{nk} \left(\frac{\partial \alpha_{n(t-1)}^\tau}{\partial f_{k1}^\tau} b_n \sum_{k=1}^K m_{nk} f_{k(t-1)}^\tau + \alpha_{n(t-1)}^\tau b_n \sum_{k=1}^K m_{nk} \frac{\partial f_{k(t-1)}^\tau}{\partial f_{k1}^\tau} \right) \quad \forall k, \forall t \geq 2. \end{aligned}$$

The partial derivative expressions are used in the linear program optimisation, which updates the output scenario.

3.3.2 Fractional Knapsack Problem

To gain an intuition on the solution arising from the optimisation method, we consider one round of fire sales. We assume there is no lower bound on the magnitude of each shock, simplifying the number of constraints on the optimisation. We define the simplified one-round optimisation as follows:

$$\begin{aligned}
 & \min_{f_1 \in (-\infty, 0]^K} : \sum_{n=1}^N \alpha_{n2}, \\
 & \text{subject to :} \\
 & -W \leq \sum_{k=1}^K c_{k1} f_{k1}, \\
 & -\frac{1}{1+b_n} \leq \sum_{k=1}^K m_{nk} f_{k1} \leq 0 \quad \forall n \in \mathcal{N} \quad \text{and} \quad \rho \leq \frac{1}{1+b^{\max}}.
 \end{aligned}$$

Using the expression of the total assets of the bank after one round of fire sales and the definition of the initial asset capitalisation, then:

$$\begin{aligned}
 & \min_{f_1 \in (-\infty, 0]^K} : \sum_{n=1}^N \alpha_{n1} \left(1 + b_n \sum_{k=1}^K m_{nk} f_{k1} \right), \\
 & \text{subject to :} \\
 & -W \leq \sum_{n=1}^N \alpha_{n1} \left(\sum_{k=1}^K m_{nk} f_{k1} \right), \tag{3.5} \\
 & -\frac{1}{1+b_n} \leq \sum_{k=1}^K m_{nk} f_{k1} \leq 0 \quad \forall n \in \mathcal{N} \quad \text{and} \quad \rho \leq \frac{1}{1+b^{\max}}.
 \end{aligned}$$

In the following, we show that the optimisation problem (3.5) is a fractional knapsack problem. We assume that the connectivity constant is chosen such that it satisfies the inequality on the maximum target leverage. By only considering the component that is dependent on the scenario in the objective, and taking the negative for the inequalities in the constraints, we state a general formulation for a similar corresponding problem.

For $p, w \in \mathbb{R}_{++}^n$ and $W \in \mathbb{R}$ and $\frac{p_1}{w_1} \geq \dots \geq \frac{p_n}{w_n}$ wlog:

$$\begin{aligned}
 & \max_{u_n \in \mathbb{R}^N} : \sum_{n=1}^N p_n u_n, \\
 & \text{subject to :} \\
 & \sum_{n=1}^N w_n u_n \leq W, \\
 & 0 \leq u_n \leq u_n^{\max} \quad \forall n \in \mathcal{N}.
 \end{aligned}$$

For the corresponding one round fire sales optimisation, then $u_n = \sum_{k=1}^K m_{nk} (-f_{k1})$, $p_n = \alpha_{n1} b_n$, $w_n = \alpha_{n1}$ and $u_n^{\max} = \frac{1}{1+b_n} \quad \forall n \in \mathcal{N}$.

The formulation of the optimisation problem is known as the fractional knapsack problem (or continuous knapsack problem). The algorithm was introduced by Dantzig (1957), with further detail on the knapsack approach provided by Korte et al. (2011). A knapsack problem is an optimisation when the objective is maximising the profit value of each variable while respecting the capacity available. We state the general proposition used by Baes and Schaanning (2023) Proposition 7 in the appendix. The proposition is modified to reflect the different upper bounds assumed in the optimisation.

Proposition 3.3.1. *If $\sum_{n=1}^N w_n u_n^{\max} \leq W$, the solution to the fractional knapsack problem is $u^* = u_n^{\max} \quad \forall n$, and if $W \leq 0$, then $u^* = 0$. Otherwise, the solution u^* is $u_1^* = u_1^{\max}, \dots, u_{p-1}^* = u_{p-1}^{\max}, u_p^* = \frac{W - \sum_{n=1}^{p-1} w_n u_n^{\max}}{w_p}, u_{p+1}^* = \dots = u_N^* = 0$ for the only $n \in \{1, \dots, N\}$ for which $\sum_{n=1}^{p-1} w_n u_n^{\max} < W \leq \sum_{n=1}^p w_n u_n^{\max}$.*

Proposition 3.3.1 represents a greedy algorithm for the maximisation of the objective. The value of each u_n is based on the relative metric p_n/w_n , where p_n is part of the objective function with an associated capacity w_n .

In the context of the fire sales, as we assume that initial losses are non-negative, there will always be an associated corresponding shock from the optimisation problem. With u_n representing the net returns of each bank, as the total assets of the bank are in the numerator and denominator of p_n/w_n , the losses are solely allocated to banks depending on their target leverage. The banks with higher target leverages lead to an increase in asset sales and further losses to other banks.

For the scenario itself, the assets shocked will correspond to banks with high target leverages. As the optimisation problem (3.4) constrains the size of the shock and accounts for multiple rounds of fire sales, the scenario from the reverse stress test will not fully represent a fractional knapsack solution.

3.4 Reverse stress test results

We consider the reverse stress testing approach for the 2016 EBA stress testing data. This is the same dataset used in Chapter 2, which consists of 51 banks and 36 different asset holdings. As we only consider assets with positive total capitalisation, we do not include the sovereign loans of Liechtenstein.⁵ We have in total 51 banks with 35 different asset holdings.

We assume that all assets are marketable and can be sold in a fire sales event. We introduce the stress testing scenarios for fire sales as follows:

⁵This asset was included in Chapter 2 because banks in the 2011 EBA dataset did hold sovereign loans in Liechtenstein.

Reverse stress test shock (RVTshock): The scenario of shocks to assets is determined by the reverse stress test under the optimisation problem (3.4) for Q rounds of fire sales.

All asset shock (Allshock): All assets are shocked by an equal value f , where $f = f_{k1} \quad \forall k \in \mathcal{S}$. In our case, the scenario corresponds to a 1% shock ($f = 0.01$) to all assets.

Dual asset shock (Dualshock): We define \mathcal{S}' as the set of shocked assets and $\bar{\mathcal{S}} \in \mathcal{S} \setminus \mathcal{S}'$ as assets not shocked. The assets shocked in \mathcal{S}' where $f = f_{k'1} \quad \forall k' \in \mathcal{S}'$ and $f_{k1} = 0 \quad \forall k \in \bar{\mathcal{S}}$ otherwise. We consider a shock to retail and corporate assets $\mathcal{S}' = \{1, 2\}$ of 1.24% ($f = 0.0124$). These two assets form 80% of the total capitalisation of all asset holdings.

As an additional metric to assess the severity of fire sales, we introduce the notion of a bank being under stress. Banks will always be able to meet their target leverages under the target leverage condition. However, there may be additional regulatory thresholds that the bank does not meet. As part of the 2016 EBA requirements, only banks with €30bn participate in the bank's annual stress testing exercise. We define the notion of a stressed bank as follows.

Definition 3.4.1. *A bank $n \in \mathcal{N}$ is under stress at time- t if the bank's total asset holdings at time- t relative to its initial total asset holdings is below the threshold $\Theta \in (0, 1]$,*

$$\alpha_{nt} < \alpha_{n1}\Theta \quad \forall t \geq 1.$$

If $\Theta = 1$ the bank is stressed before the fire sale. If $\Theta \in (0, 1)$, this represents a state of stress when the total asset holdings of the bank decrease during the fire sale. In this setting, we set the threshold $\Theta = 0.1$, representing that a bank is stressed if the total asset holdings of the bank are below 10% of its initial total asset holdings.

Input	Numerical Value
Initial total losses (W)	$0.01 \sum_{n=1}^N \alpha_{n1}$
Max shock ($-f^{\min}$)	1
Capitalisation-dependent constant (ρ)	10^{-2}
Fire sales maturity (T)	8
Rounds for optimisation (Q)	4
Total number of iterations (\mathcal{T})	200
Max target leverage (b^{\max})	30
Stress threshold (Θ)	0.1

Table 3.1: Input values for the RVTshock and associated measures.

We consider the inputs in Table 3.1 for the reverse stress test and associated measures. We assume a capitalisation-dependent price impact and set the capitalisation-dependent

constant such that it satisfies the upper bound, as in the optimisation problem (3.4). We consider an initial loss equal to 1% of the total assets (equivalent to 146bn euros). In total, we simulate 8 rounds of fire sales and optimise over 4 rounds. The Allshock and Dualshock satisfy the constraints of the optimisation problem for the values in Table 3.1. We show that for different initial inputs of the reverse stress test, there is only a small difference in the updated scenario under perturbed scenarios of both the Allshock and Dualshock. We sample from a perturbed Allshock and Dualshock, in which perturbations follow a normal distribution. We only consider a perturbation of the initial scenario if it satisfies the constraints of the optimisation in (3.3).

We consider D number of samples where $d \in \{1, \dots, D\}$ for each initial scenario. We denote $f_1^{\tau,d}$ as the initial input and shock for sample d , under the iteration τ . The perturbed Allshock for the initial input is $f_{k1}^{0,d} = f_{k1}^0 + \mathcal{N}\left(0, (\sigma^{\text{all}})^2\right) \quad \forall k \in \mathcal{S}$. The perturbed Dualshock $f_{k1}^{0,d} = f_{k1}^0 + \mathcal{N}\left(0, (\sigma^{\text{dual}})^2\right) \quad k \in \{1, 2\}$ and $f_{k1}^{0,d} = f_{k1}^0 \quad \forall k \in \mathcal{S} \setminus \{1, 2\}$. The normal distribution has a mean of 0 and a standard deviation of σ^{all} for the Allshock and σ^{dual} for the Dualshock. The perturbations are only applied to assets which are shocked under each scenario i.e., $f_{k1} > 0$.

As a metric representing the similarity of updated scenarios, we define $\text{Error}(f_1^{\mathcal{T}})$ as the mean range between the smallest and largest shocks from all updated perturbed scenarios, where:

$$\text{Error}(f_1^{\mathcal{T}}) = \frac{1}{K} \sum_{k=1}^K \left(\max_d f_{k1}^{\mathcal{T},d} - \min_d f_{k1}^{\mathcal{T},d} \right).$$

This is a measure of the deviation across all shocks, where the perturbed Allshock and Dualshock are used.

We consider $D = 1000$ for each input scenario, with $\sigma^{\text{all}} = 0.01$ and $\sigma^{\text{dual}} = 0.1$ under the values in Table 3.1. In total, we compute the error for 2,000 different samples, with 1,000 samples for the Allshock and 1,000 for the Dualshock. We find the mean range across the Allshock and Dualshock is around 7×10^{-4} . This shows that the values on average under perturbation have a small difference, and the output from scenarios under the reverse stress test is similar in magnitude. As the difference in the error range of values is small, we aggregate all updated generated scenarios from the reverse stress test $\bar{f}_1^{\mathcal{T}}$, where:

$$\bar{f}_{k1}^{\mathcal{T}} = \frac{1}{D} \sum_{d=1}^D f_{k1}^{\mathcal{T},d} \quad \forall k \in \mathcal{S}.$$

We now present the results of our case study in Figure 3.2. We find a similar Knapsack solution for the RVTshock for the allocation of shocks under the reverse stress test. The scenario consists of large shocks to assets of different capitalisations i.e., the shocks applied to Denmark and Luxembourg sovereign loans have small capitalisations while the UK and the US sovereign loans have large asset capitalisations. Interestingly, retail and

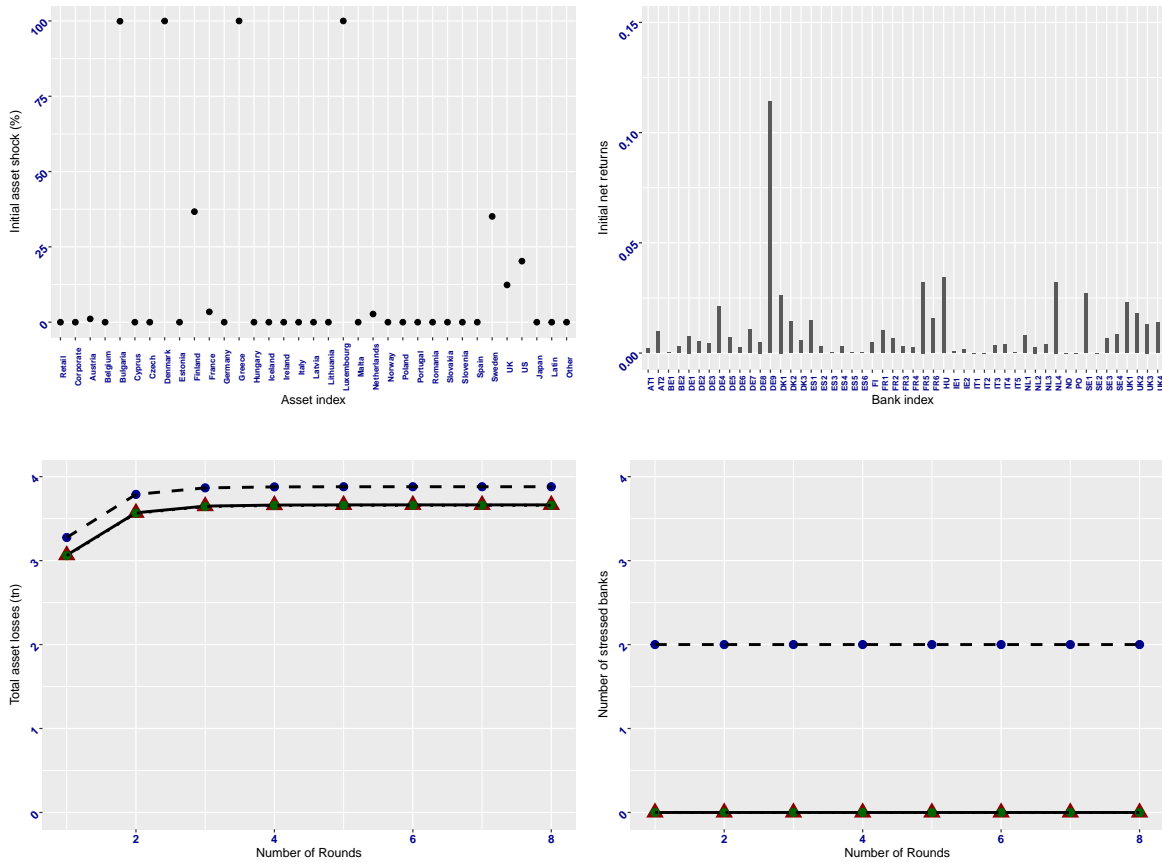


Figure 3.2: For the RVTshock under the parameters in Table 3.1, the plots in the top row represent the initial shock ($-f$) for assets (top left) and the initial net returns ($-R$) for banks (top right). The plots in the row below represent the total losses from the fire sale (bottom left) and the total number of stressed banks (bottom right), across 8 rounds of fire sales. We compare the total losses and number of stressed banks across all three scenarios. The dashed line (blue circle) represents the RVTshock, the solid line (green circle) the Dualshock and the dotted (red triangle) represents the Allshock.

corporate assets are not shocked under the reverse stress testing scenario, even though these assets have the highest total capitalisation and are the most held assets by banks. This could be from the total capacity of sovereign loans, which is smaller than retail and corporate assets. From the optimisation formulation, larger shocks can be applied to sovereign loans, leading to larger losses for banks. Because of the similarity of asset holdings of sovereign loans for corresponding located countries, the assets shocked under the reverse stress test are targeted towards groups of banks with high target leverages i.e., these groups are represented by Greek, Swedish, and UK banks.

The shock to Greek assets is associated with the high target leverages of Greek banks, and UK assets towards UK banks with large total asset holdings and asset holdings in multiple assets. The shock to Nordic sovereign loans is less apparent. From the EBA 2016 stress testing data, the largest Nordic banks have similar portfolios and small capital holdings. This commonality is shown by the shock of Swedish sovereign loans, in which

Danish banks have a large proportion of asset holdings. The overlapping portfolios of Nordic banks with high target leverages are part of the RVTshock, having a larger effect on losses than shocks to other assets e.g., Spain or Italy.

On the initial returns in Figure 3.2, the largest returns are for French and German banks. Even though the sovereign loans of these countries were not shocked, these banks held assets from other countries resulting in larger net returns. The net returns from these banks are higher than the net returns of some UK banks, whose corresponding sovereign loans were shocked under the reverse stress test. The net returns under the reverse stress test for Italian and Spanish banks remain low, even though banks from these countries were highly affected during the Great Financial Crisis. For the magnitude of initial net returns under the reverse stress test, there are banks which have a net return of around 0.1. Compared with the AllShock, this is a $\times 10$ increase in the magnitude of initial net returns to which the bank is exposed.

For the second row of plots in Figure 3.2, we consider the losses of banks across T fire sales periods, for all three scenarios. The results show that considering additional rounds of fire sales does contribute to the total losses of banks. This is the case across all three scenarios, where there is a 27% decrease in the total capitalisation of banks after T periods. After the 4th round of fire sales, the total losses of banks converge and remain unchanged. From the RVTshock, the largest proportion of losses and the total number of stressed banks are concentrated in the first round of fire sales. We find the RVTshock to result in the largest losses, which is 3% higher than other scenarios. Comparing the Allshock and Dualshock (where the lines in Figure 3.2 overlap with each other), the aggregate losses and the number of stressed banks are similar compared with the RVTshock.

Figure 3.3 are plots of the total assets of the bank and the asset capitalisation after T periods of fire sales. We find the largest losses for the total assets of the bank to be concentrated in France and the UK, and relative losses within Germany and the UK. The largest group of losses is from UK banks, followed by French banks. From the total assets of the bank, these groups of banks have the largest total asset holdings, which scales the volume of losses from the given shock. Other prominent banks with large bank losses are Nordic banks (DK1, SE1) and German banks (DE4). Banks from the Netherlands have small losses, but all these banks from the Netherlands are affected by the RVTshock. Losses are overall clustered in specific groups denominated by the country.

For the relative bank losses, we find no singular group of banks with the largest relative losses. This reflects a different picture than the losses on the bank's asset holdings, where the losses were reflected by the country. The relative total asset losses for German, French and Dutch banks are the highest, resulting in $> 90\%$ relative bank losses for two banks from the fire sales. These relative losses are high for banks with high capitalisation, whereas relative losses are small for other banks with a larger presence in the dataset.

The asset capitalisation of corporate and retail have the largest losses in Figure 3.3 be-

cause 80% of the total capitalisation of assets is concentrated in both these assets. Other prominent sovereign asset losses include large economically sized countries i.e., France, Germany, the UK and the US. For the relative losses in the total capitalisation of the asset, the range of the losses between asset groups is similar, with no one asset having a significantly higher relative loss than another asset. This may arise from the proportional selling assumption on asset holdings in the fire sale, where a quantity of each asset is sold from the fire sales.

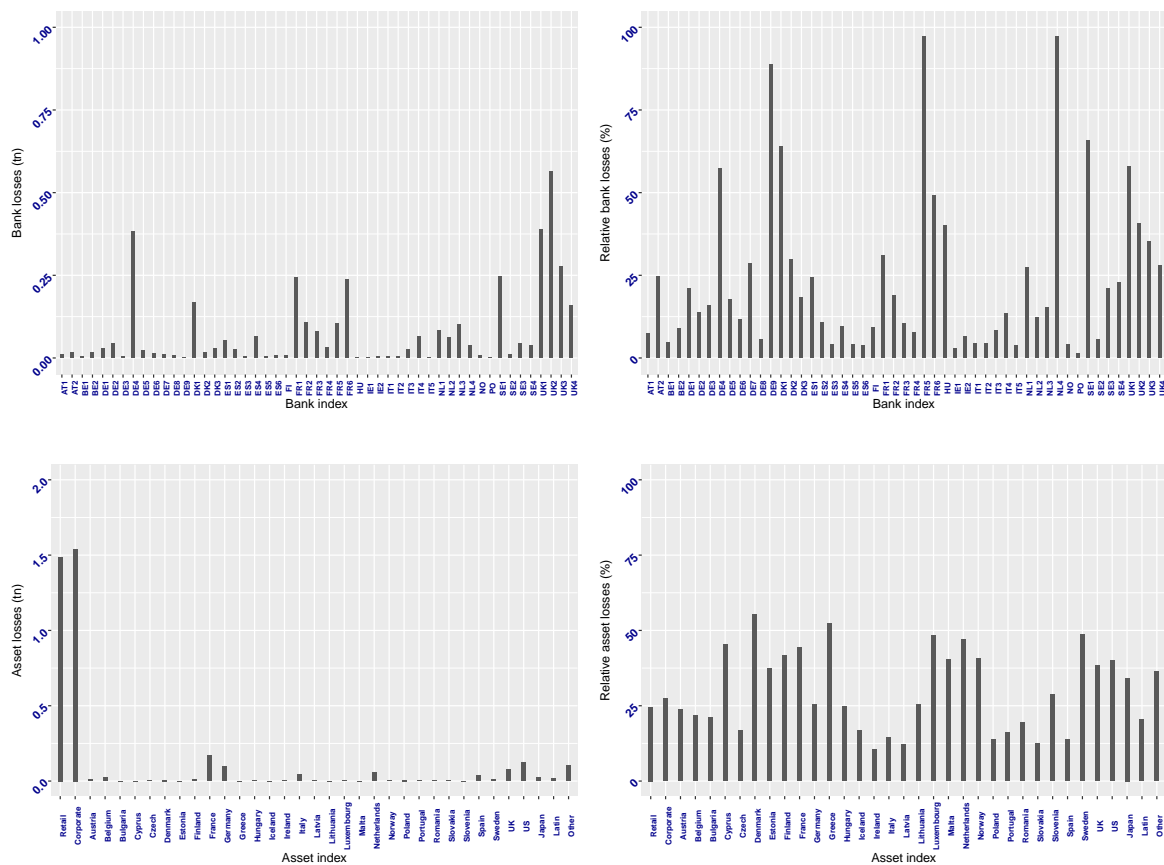


Figure 3.3: For the RVTshock using the parameters in Table 3.1, the plots in the top row represent the bank's losses across all rounds of fire sales (top left) and losses relative to its initial total asset holdings (top right). The plots in the bottom row represent the losses in each asset class (bottom left) and the losses in each asset class relative to its initial capitalisation (bottom right).

3.4.1 Systemicness and Vulnerability

We consider the equity losses from the perspective of systemicness and indirect vulnerability. We use the measures by Greenwood et al. (2015), which are the same measures used in Chapter 2. Compared with Chapter 2, we extend the definition of systemicness for multiple rounds of fire sales. Further details can be found in the Appendix 8.

The systemicness $\mathcal{SYS}_t \in [0, \infty)^N$ is a measure of equity losses, where $\mathcal{SYS}_t(n)$ is the contributed equity losses of bank $n \in \mathcal{N}$ at time- t . The indirect vulnerability $\mathcal{IV}_t \in [0, \infty)^N$ is a measure of equity losses incurred by the bank, where $\mathcal{IV}_t(n)$ is the incurred equity loss of bank $n \in \mathcal{N}$ at time- t . Both these measures reflect different aspects of fire sales losses. We define these measures, assuming banks can meet their target leverages:

$$\mathcal{SYS}_T(n) = \sum_{t=1}^T \gamma_{nt} \frac{\alpha_{nt}}{\sum_{n=1}^N e_{n1}} b_n(-R_{nt}),$$

$$\mathcal{IV}_T(n) = \sum_{t=1}^T \left(\frac{\alpha_{nt}}{e_{n1}} \sum_{k=1}^K m_{nk}(-f_{k(t+1)}) \right) \quad \forall n \in \mathcal{N} \quad T \geq 1.$$

The systemicness comprises of four bank components: connectivity (γ), size ($\frac{\alpha}{\sum e}$), target leverage (b), and net returns ($-R$). The indirect vulnerability is a measure of the net returns from the updated shock and the target leverage component, represented by the total assets of the bank divided by the equity.

As stated by Greenwood et al. (2015), these two measures represent two independent ways of evaluating the losses to and from banks. For example, a bank with a high indirect vulnerability may have a low systemicness, and vice versa. We consider these measures for the RVTshock.

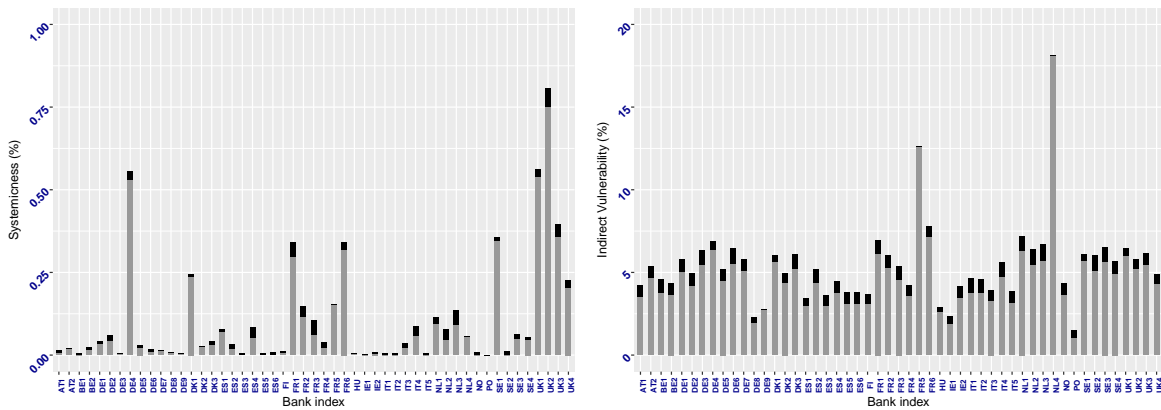


Figure 3.4: For the RVTshock, the plots represent the systemicness (\mathcal{SYS}) and indirect vulnerability (\mathcal{IV}) after all rounds of fire sales. The shaded grey represents the systemicness and indirect vulnerability for the first round and black areas represent losses for all subsequent higher-order rounds.

Figure 3.4 shows contributions from systemicness and indirect vulnerability, where losses are differentiated between the first round and higher-order rounds. We find large differences in equity losses contributed by banks under systemicness i.e., UK banks have a higher systemicness than Italian banks on average. For the indirect vulnerability, there is a similarity in equity losses incurred by banks, where the majority of equity losses are between 0%–10%. For systemicness, banks with the largest equity losses are from France and the UK. There are also individual banks in Germany and the Netherlands with a high systemicness. We find the systemicness of banks is similar to a scaled version of the bank’s losses. The similarity is reflected in the contribution of the first round, where the connectivity is constant and all other terms represent the change in the bank’s total asset holdings in the first round.

For the indirect vulnerability, there are some banks with higher indirect values i.e., banks from the Netherlands but values overall remain consistent. This shows that relative to the equity losses, the RVTshock has a wider effect on all banks. In the plots, we highlight the systemicness and indirect vulnerability between the first round and later stages of the fire sale. For all banks, the largest proportion of losses is concentrated in the first round. As reflected in the total largest losses, there is a larger concentration in the first round of fire sales that is observed on the individual bank level.

3.4.2 Sensitivity

We evaluate the RVTshock for different initial losses and lower bounds on the shock. We assume all other parameters are the same as in Table 3.1 and calculate the scenarios from the reverse stress test. For the change in the total initial losses, we scale the shocks of the Allshock and Dualshock, relative to the change in the initial loss.

For each of the optimisation problems for different initial losses, the scenarios are consistent with the constraints in the optimisation problem. For the sensitivity of the lower bound shock, we compute the scenario from the reverse stress test of different lower bounds and the total losses from the scenario. We only consider the sensitivity of the shock with the reverse stress test approach, as the Allshock and Dualshock cannot be adjusted such that it is consistent with the assumed initial losses.

From Figure 3.5, we find an overall monotonic relation between the initial and total losses from the fire sale. Between all scenarios, the total losses from the RVTshock are higher than the Allshock and Dualshock in all cases. As the initial losses increase, this amplifies the total losses banks are exposed to i.e., 70% total fire sales loss from a scenario from 3% in initial total losses. Even with no bank defaults, banks can suffer large losses on their asset holdings triggering a state of stress.

The increase in losses also results in a higher number of stressed banks under the RVTshock, compared with other scenarios. As the shock to assets under the RVTshock is

sparse and shocks of high magnitude are allocated to few assets, this results in higher losses for a few banks and increases the number of stressed banks. The increase in the number of stressed banks reflects another consequence of scenarios generated from the reverse stress test.

For different lower bounds on the shock scenario, we find small changes in the total losses and the number of stressed banks in Figure 3.5. There is no observable difference in the number of stressed banks under the set threshold. For a smaller subset of possible shocks, the variation in the losses of banks and the number of stressed banks is small. While the aggregate metric remains the same, there are deviations in the level of losses for each bank. This shows multiple reverse stress testing scenarios can cause larger losses to banks than other benchmark stress testing cases.

In Figure 3.6, we plot the initial shock, initial net returns and losses for banks for a lower bound of $f^{\min} = -0.1$ for all assets. The decrease in the magnitude of shock decreases the largest shocks to assets and increases shocks to other asset holdings. This is shown by an increase in shocks to other Nordic countries e.g., Finland and Norway and shocks applied to previously shocked assets of large asset capitalisation. There is also a decrease in the size of net returns with the largest value. The initial net returns of other banks have increased compared with other scenarios. The adjustment in the size of shocks shows for the fire sales losses with this dataset, large shocks to a few assets result in the same total losses as small shocks to several asset holdings.

The losses of the bank from Figure 3.6 also show a change in the allocation of bank losses. The relative asset losses of Spanish and Italian banks have increased, whereas German losses have decreased. While the losses of banks remain similar (because of the large exposure of French and UK banks), there is a change in the relative bank losses. A widespread shock overall increases the relative net returns of other banks.

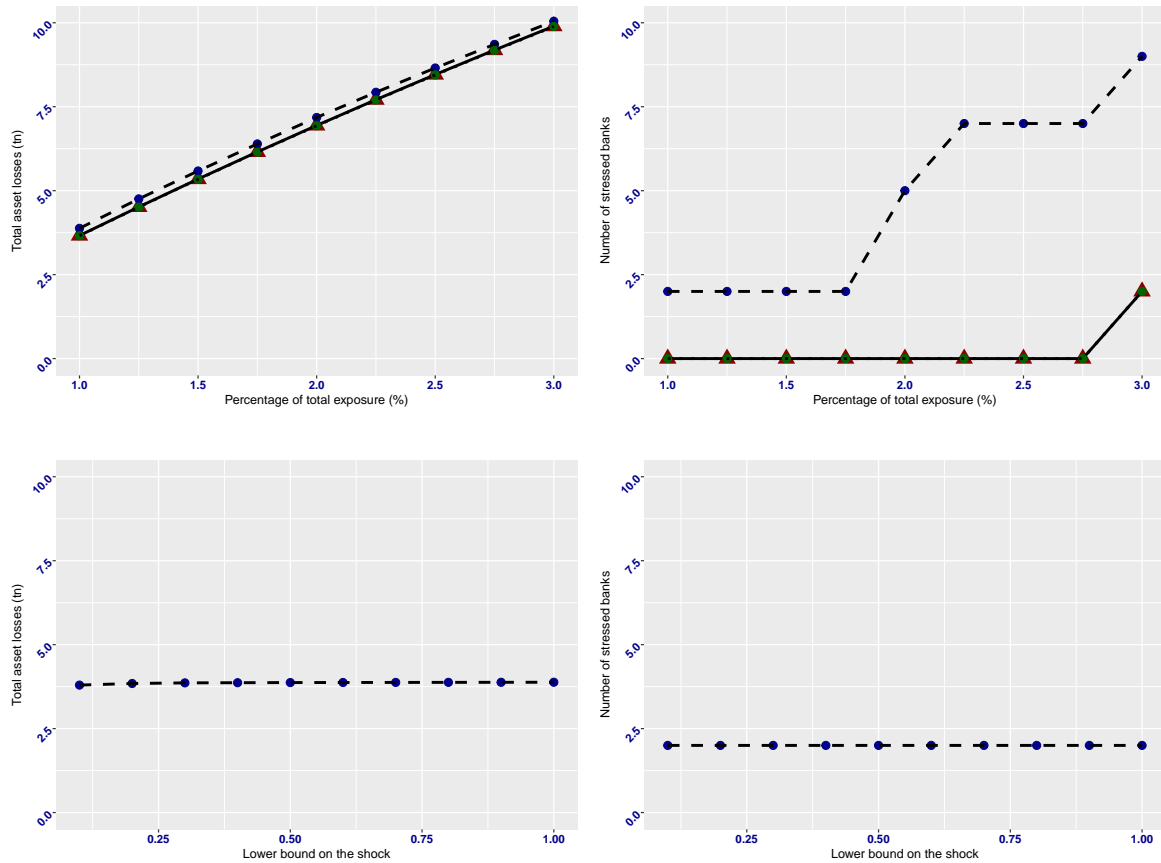


Figure 3.5: The plots in the top row represent the total losses (top left) and number of stressed banks (top right) for different initial losses (W), represented by a percentage of the total asset holdings. The plots in the row below represent the total initial losses assuming the same parameters in Table 3.1, for different lower bound shocks ($-f^{\min}$). The plots (bottom left) represent the total losses and (bottom right) the number of stressed banks. The dashed line (blue circle) represents the RVTshock, the solid line (green circle) the two scenario shocks and the dotted (red triangle) represents the all-asset scenario.

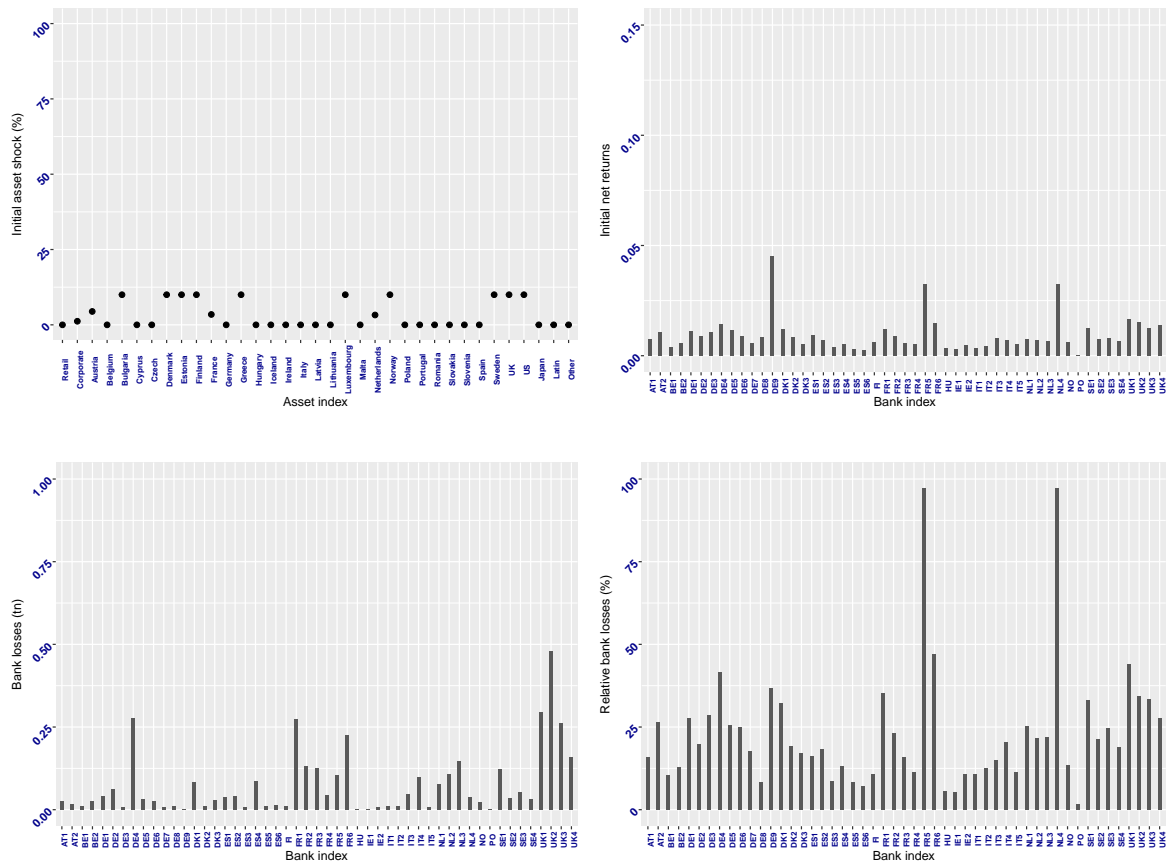


Figure 3.6: For the RVTshock, we consider the parameters in Table 3.1, with a lower bound of $(-f^{\min} = 0.1)$ on the shock to all assets. The plots represent the initial shock to assets (top left), initial returns to banks (top right), the bank's losses across all rounds (bottom left) and the bank's losses relative to its initial total asset holdings (bottom right).

3.5 Conclusion

We introduced an optimisation reverse stress testing approach, accounting for multi-periods of fire sales. We applied the Frank-Wolfe algorithm under the target leverage condition, where we optimise for the initial scenario resulting in the largest losses for a fire sale. We considered an optimisation for only one round of fire sales, which resembled a fractional knapsack problem. In this setup, the net returns were highest for banks with high target leverages, reflecting the leverage targeting mechanism from the fire sales.

From the reverse stress test, the output scenario allocated shocks of high magnitude to few assets, where all other shocks were negligible or small in size. Our results show that the reverse stress test scenario resulted in higher bank losses and a higher number of stressed banks than other stress testing scenarios. We find the largest losses were for banks with larger total asset holdings, where several of these banks were not initially affected by the fire sale. For the equity losses of banks, the results showed that contributed equity losses were overall heterogeneous (highly varying between different banks) and incurred losses were homogeneous (on average similar in size across all banks) from the reverse stress tests. We showed the largest proportion of losses was concentrated in the first round, where these results were similar for different bounds on the shock size.

Chapter 4

Collateralized networks with two channels of fire sales

4.1 Introduction

The Great Financial Crisis (GFC) showed the lack of liquidity available to banks to meet their obligations. The shortfall in the banks' obligations resulted in a run on their liquidity reserves and widespread losses to banks.¹

From the consequences of the GFC, one reform was the introduction of initial margin requirements for banks, with other reforms discussed by Duffie (2018). This reform was one of the recommendations from the Financial Stability Board (2017) and was implemented as a coordinated response by G20 countries. With the introduction of Basel 3, a large volume of OTC derivatives that were non-centrally cleared as well as derivatives cleared through central counterparties (CCPs) were required to post initial margins.

We consider a network of banks with interbank assets and liabilities, where banks post assets as collateral as part of their initial margin requirements. The initial margin requirement is allocating assets to cover a proportion of the bank's obligations to another bank. This is a bilateral relationship where the debtor, the bank borrowing assets has an interbank liability with another bank, represented as the lender. The debtor posts assets used as collateral to the lender, representing an interbank asset for the lender.

Assets used as collateral are only considered if the debtor defaults on its obligations. If the debtor can meet its obligations then the assets as part of its initial margin are not utilised. If the debtor cannot meet its obligations, the bank enters a state of default and

¹The collapse in the collateralized debt market contributed to the scarce supply of liquidity. This was explored by Gorton and Metrick (2012) for the US repo markets during the GFC. There were concerns about the liquidity in the US bond market which was used as collateral for repo transactions. The uncertainty resulted in large haircuts on these assets, where banks were unable to access short-term funding. This fuelled the insolvency of banks in the US, where the losses spilt over to other countries. The run on the repo market and the extent to which it impacted the GFC was studied by Krishnamurthy et al. (2014).

a fraction of the assets that the bank has allocated to cover its obligation would be seized by the lender. The fraction of assets recovered by the lender may affect its ability to meet its obligations to other banks. This can result in a liquidity contagion scenario and a cascade of losses if multiple banks are unable to fully meet their short-term obligations. The effectiveness of assets used as collateral to cover the bank's outstanding obligations may be affected by the effects of a fire sale. In the situation where the debtor defaults, the lender sells assets used as collateral to meet its outstanding obligations. If illiquid assets are used, the assets sold result in a mark-to-market adjustment, decreasing the asset value and other commonly denoted assets used as collateral by banks. This can lead to a larger shortfall in the obligations of other banks, and induce further rounds of sales.²

We build on the collateral model introduced by Ghamami et al. (2022). This model incorporates the interbank network of assets and liabilities, where banks can post collateral to other banks in the network. The market value of assets used as collateral is also affected by a fire sale, representing the mark-to-market adjustment from the quantity of assets sold. The clearing scenario is represented by a two-stage process:

- **Stage 1:** If the bank is in default, the assets used as collateral are seized by the counterparty to meet its outstanding obligations. The counterparty sells these assets which are then used to meet its outstanding obligations to other banks.
- **Stage 2:** After all payments have been settled using designated collateral assets, banks in default can use their remaining collateral from Stage 1 to meet their outstanding obligations.

The key contribution of our work is the integration of an additional channel of fire sales into the collateral model by Ghamami et al. (2022). This additional channel of fire sales arises because we assume banks externally hold illiquid assets i.e., retail or corporate assets. These external assets are not used as part of the bank's collateral requirements but can be sold by the bank to meet its total obligations. Selling these illiquid assets triggers a mark-to-market adjustment and a fire sales impact on the assets sold.

These illiquid asset holdings are not considered in the model by Ghamami et al. (2022), where banks are assumed only to hold liquid assets. Our extension of the model by Ghamami et al. (2022) where banks hold illiquid assets holdings results in two distinct channels of fire sales. The commonality between the assets the bank externally holds and assets used as collateral can lead to a feedback effect between both channels of fire sales, amplifying the losses of banks.

²Considering the impact of fire sales, the volume of assets required for the use of collateral may not be sufficient to meet liquidity demands. As discussed by Cont (2018), the guidelines recommend the initial margin to meet 99% quantile losses under VaR over 10 days. This however does not account for the liquidity sensitivity or the market depth of the asset posted.

We first formulate the new collateral clearing model with the inclusion of external asset holdings, representing the additional channel of fire sales. We show in a clearing event, there exists a state of equilibrium represented by the fixed point, where specifically, we provide further details on how the greatest fixed point can be obtained. The proof of the existence of a fixed point is obtained in a similar way to Ghamami et al. (2022) and Veraart and Aldasoro (2022), where further details can be found in the appendix. This existence result is important as the fixed point is used to determine banks' losses in a clearing event.

We then study how the effects of a fire sale impact the total payments of the bank under a collateral model with two channels of fire sales. We differentiate the ordering of the bank's total payments across both rounds of clearing. We consider how the ability of the bank to meet its total obligations depends on other financial factors i.e., bankruptcy costs, the size of its liquid assets and the price impact on illiquid asset holdings. These financial factors have implications for the shortfall in the bank's obligations and the number of banks unable to meet their outstanding obligations.

Using simulations of networks generated from a random graph model, we show that the additional channel of fire sales increases the bank's outstanding obligations. We find the losses from this additional channel of fire sales to be significant for banks, across both rounds of clearing. The magnitude of losses increases when there is a higher commonality between the bank's external asset holdings and assets used as collateral.

The inclusion of external illiquid asset holdings not only increases losses, but in some cases, these losses are higher compared with networks if banks do not hold any external illiquid assets. This is from the interaction of fire sales between assets sold as collateral and external asset holdings sold. Selling a proportion of external asset holdings triggers a mark-to-market adjustment which decreases the value of common assets used as collateral. The decrease in assets used as collateral increases the shortfall in the bank's obligations, requiring a larger proportion of external illiquid assets to be sold. In some cases, the losses from a fire sale are larger than the losses from the interbank network.

Between the different stages of clearing, we find the second stage for the bank to meet its remaining obligations contributes highly to the bank's total payment when the total losses for all banks are high. The larger bank losses increase the number of banks unable to meet their outstanding obligations in the first round. This increases the number of banks with outstanding obligations, which can mutually settle their remaining obligations with other banks in the second round.

This chapter is structured as follows. In Section 4.2, we introduce the extended collateral model that incorporates two channels of fire sales. We establish ordering relations in Section 4.3 for the payments of banks in the first and second rounds of clearing. In Section 4.4, we illustrate the clearing process under a small network and generate large networks under a random graph model. We conclude our results in Section 4.5. We

provide proofs in the appendix.

4.1.1 Related literature

The collateral model by Ghamami et al. (2022) builds on the clearing mechanism by Eisenberg and Noe (2001). The model by Eisenberg and Noe (2001) establishes a set of payments in which banks fully meet their obligations or make partial payments proportionally. The clearing mechanism assumes banks make payments were possible, the same assumption used by Ghamami et al. (2022). The model by Ghamami et al. (2022) extends the clearing model with the inclusion of collateral assets, where the value of these assets is affected by fire sales. The incorporation of the mark-to-market adjustment from fire sales for assets used as collateral is motivated by Cifuentes et al. (2005). There is further work by Ghamami et al. (2022) exploring different contract termination mechanisms and the bank's implications for meeting its obligations.

Our main contribution is the additional channel of fire sales to the collateral model, where banks hold external illiquid asset holdings. The inclusion of fire sales for external illiquid assets holdings to the clearing mechanism is developed by Feinstein and El-Masri (2017) and Feinstein (2017). They consider the clearing mechanism by Eisenberg and Noe (2001), where banks can additionally hold multiple illiquid asset holdings. They explore different selling rules where banks are required to sell a proportion of their asset holdings i.e., selling assets to meet a leverage target or a waterfall approach to assets sold. The model by Feinstein and El-Masri (2017) does not include assets for the use of collateral and therefore excludes this channel of fire sales. In the setting by Feinstein and El-Masri (2017), Amini et al. (2016) shows under certain conditions that the set of bank payments in a clearing model with multiple illiquid asset holdings is unique. We assume a proportional selling rule under the minimal liquidation condition, where banks only sell the minimum quantity of assets required to meet their outstanding obligations.

We include different channels of losses as this incorporates the compounding effect of losses in a systemic event. The work by Weber and Weske (2017) also considers the clearing mechanism by Eisenberg and Noe (2001) and the following channels of systemic risk: bankruptcy costs by Rogers and Veraart (2013) and Glasserman and Young (2015), fire sales on the bank's external asset holdings by Cifuentes et al. (2005) and the losses from bank's cross-holdings by Elsinger (2011) and Elliott et al. (2014). In Weber and Weske (2017), they investigate the contribution of losses from different channels using simulations of networks generated from random graph models. This chapter follows similarly to this type of analysis, where we generate networks from a random graph model and simulate the clearing mechanism under the collateral model. The model we use is however different, as we consider assets that are used as collateral, which is a channel of systemic risk not included in the model by Weber and Weske (2017).

The use of collateral in a clearing event has been explored for banks and CCPs. The work by Veraart and Aldasoro (2022) considers the collateral model Ghamami et al. (2022), for the cascade of losses between different CCPs. They also build on the work by Ghamami et al. (2022), where they include the losses from bankruptcy costs in a clearing event as considered by Rogers and Veraart (2013). Our work also factors in the losses from bankruptcy costs as by Veraart and Aldasoro (2022), where banks can additionally hold multiple external illiquid assets.

A collateral model that deviates from the mechanism by Ghamami et al. (2022) is the work by Chang (2019). They model the rehypothecation of collateral assets, where banks are unable to seize collateral from banks in default because these collateral assets have been allocated to other banks. The work by Chang and Chuan (2023) does not focus on endogenous effects as by Chang (2019) but on the robustness and resilience of networks in the clearing setting with collateral.³ The work by Bichuch and Feinstein (2019) also accounts for collateral and the fire sales effect in a clearing scenario. The bank strategically borrows collateral depending on its solvency state, resulting in a Nash equilibrium.

4.2 Multi asset model

We consider a financial network of N different financial institutions (referred to as banks) denoted by $\mathcal{N} = \{1, \dots, N\}$. For the first round of clearing (R1), we define the obligations matrix as $\bar{p}^{\text{R1}} \in [0, \infty)^{N \times N}$. Here, \bar{p}_{ij}^{R1} represents the obligations that bank i has to bank j . We denote the total obligations of bank i in the interbank network as \bar{p}_i^{R1} , where:

$$\bar{p}_i^{\text{R1}} = \sum_{j=1}^N \bar{p}_{ij}^{\text{R1}}$$

and $\bar{p}_{ii}^{\text{R1}} = 0 \quad \forall i \in \mathcal{N}$. The diagonal of zeroes represents that banks do not have obligations to themselves.

As part of the assets of the bank balance sheet, the bank holds interbank assets, liquid and illiquid assets. The bank holds assets that it uses as collateral and other liquid or illiquid asset holdings. We denote the assets that the bank does not use as collateral and are not interbank assets as the bank's external asset holdings.

We assume there are K illiquid assets and one liquid asset the bank holds denoted by $\mathcal{S} = \{1, \dots, K, K + 1\}$. The liquid asset that the bank externally holds is denoted as the

³The losses from a clearing event have been studied on how the network topology amplifies or dampens contagion. The work by Acemoglu et al. (2015) studies different network structures i.e., complete or ring networks, and the resilience of such networks depending on the size of the shock. This leads to conclusions as by Gai et al. (2011), Caccioli et al. (2012) and Bardoscia et al. (2017) in which diversification can increase instability because the increased connections amplify losses. This forms part of the analysis of the impact of collateral on the resilience of banks in an interbank network with fire sales risk from the model by Chang and Chuan (2023).

liquidity buffer $b \in [0, \infty)^N$. Assets that would be part of a bank's liquidity buffer would be cash holdings for example.

We consider the bank's external illiquid asset holdings, which is an extension to the model by Ghamami et al. (2022). We define the illiquid asset holdings in terms of the matrix $S \in [0, \infty)^{N \times K}$. Each entry S_{ik} represents the number of shares the bank i holds of the illiquid asset k .

The bank additionally posts collateral to other banks. We define the matrix $\zeta \in [0, \infty)^{N \times N}$ as the collateral matrix, in which ζ_{ij} represents the amount of collateral that the bank i posts to bank j . As in the obligations matrix, the bank does not post collateral to itself i.e., $\zeta_{ii} = 0 \quad \forall i \in \mathcal{N}$.

We distinguish between the types of assets that can be posted as collateral. In Ghamami et al. (2022), they consider only one type of illiquid asset. In our setting, the collateral that each bank posts can be a different kind of asset.⁴

We define the matrix $T \in \{0, 1, \dots, K+1\}^{N \times N}$, where each entry $T_{ij} > 0$ represents the type of asset k that the bank i posts to bank j . If $\zeta_{ij} = 0$, then we set $T_{ij} = 0$. The index denoting the type of asset used as collateral is the same as the illiquid asset holdings of the bank. If $k = 0$, this represents no asset is posted as collateral, $k = K+1$ denotes a liquid asset used as collateral and an entry $k \in \{1, \dots, K\}$ is an illiquid asset used as collateral.

In the first round of clearing, we denote the total assets A_i^{R1} of the bank i as follows:

$$A_i^{R1}(\pi, p) = b_i + \sum_{k=1}^K S_{ik} \pi_k + \sum_{j=1}^N p_{ji},$$

where $\pi \in [0, \infty)^{K+1}$ is the market price of the assets. As a measure of the state of solvency of the bank, we define the equity of the bank in the first round e_i^{R1} as follows:

$$e_i^{R1}(\pi, p) = A_i^{R1}(\pi, p) - \bar{p}_i^{R1}.$$

This represents the difference between the bank's total asset holdings and total obligations. The assets used as collateral are not accounted for in the bank's equity, as these assets are already posted to other banks. Assets used as collateral are only accounted for by their counterparties if the bank is in default.

⁴One could further generalise this assumption by assuming banks post a portfolio of assets as part of their initial margin requirements. However, we focus on only one type of illiquid asset used as collateral which still captures the fire sales dynamics of this channel.

4.2.1 First round of clearing

We consider the fixed point equilibrium of bank payments and the market price of assets in R1. This establishes the set of values in which banks settle their payments to other banks, at the current market price.

We define the payments of banks in R1 as p^{R1} and the market price of collateral and illiquid assets in R1 as π^{R1} . We are interested in the fixed point of the clearing process, representing the position in which all banks have settled their total payments. We assume the fixed point problem in R1 of the function $\Phi^{R1} : [0, 1] \times [0, \bar{p}^{R1}] \rightarrow [0, 1] \times [0, \bar{p}^{R1}]$. We denote $(\hat{\pi}^{R1}, \hat{p}^{R1})$ as a fixed point of the clearing function if:

$$(\hat{\pi}^{R1}, \hat{p}^{R1}) = \Phi^{R1}(\hat{\pi}^{R1}, \hat{p}^{R1}).$$

There may be multiple fixed points that satisfy the fixed point property for the R1 clearing function. We define the first round clearing function as follows:

$$\begin{aligned} \Phi_{1,(k)}^{R1}(\pi, p) &= \exp(-l_k \Delta_k(\pi, p)), \\ \Phi_{2,(ij)}^{R1}(\pi, p) &= \begin{cases} \min \left\{ \bar{p}_{ij}^{R1}, \pi_{T_{ij}} \zeta_{ij} \right. \\ \left. + a_{ij}^{R1}(\pi) \left(\gamma_i^1 \left(b_i + \sum_{k=1}^K S_{ik} \pi_k \right) + \gamma_i^2 \sum_{j=1}^N p_{ji} \right) \right\} & \text{if } i \in \mathcal{D}^{R1}(\pi, p), \\ \bar{p}_{ij}^{R1} & \text{if } i \in \mathcal{N} \setminus \mathcal{D}^{R1}(\pi, p). \end{cases} \end{aligned}$$

The clearing function consists of two parts: the first component $\Phi_{1,(k)}^{R1}$ represents the market price of the asset k . It depends on the total number of shares that the bank sells Δ_k of the asset, and the change in the market price depending on the price impact $l \in [0, \infty)^{K+1}$. A price impact $l_k > 0$ is the associated price impact for an illiquid asset, otherwise $l_k = 0$ for a liquid asset.

The second component $\Phi_{2,(ij)}^{R1}$ represents the payments from bank i to bank j . If the bank is unable to meet its obligations, then the bank is in default. We define \mathcal{D}^{R1} as the set of first-round bank defaults as follows:

$$\mathcal{D}^{R1}(\hat{\pi}, \hat{p}) = \{i \in \mathcal{N} | e_i^{R1}(\hat{\pi}, \hat{p}) < 0\}.$$

The bank is in default if it has negative equity, representing that its asset holdings are smaller than its total obligations. We distinguish defaults which occur initially and defaults from the contagion process. We define the set of defaults \mathcal{F}^{R1} as fundamental

defaults in R1 from the banks obligations and initial market price:

$$\mathcal{F}^{R1} = \mathcal{D}^{R1} (1, \bar{p}^{R1}) = \{i \in \mathcal{N} | e_i^{R1} (1, \bar{p}^{R1}) < 0\}.$$

We consider the set of contagious defaults $\mathcal{D}^{R1} (\hat{\pi}^{R1}, \hat{p}^{R1}) \setminus \mathcal{F}^{R1}$ as defaults that are not fundamental defaults.

As part of the clearing process, if the bank is unable to meet its obligations in full, then the bank allocates its remaining assets to other banks in a proportional way. We define the relative proportional obligations matrix as $a^{R1}(\pi) \in [0, 1]^{N \times N}$, where each entry a_{ij}^{R1} represents the relative proportion of the bank's total obligations from bank i to bank j . As the collateral is only accounted for when the bank is unable to meet its obligations, this is factored in the proportional allocation between banks:

$$a_{ij}^{R1}(\pi) = \frac{\max \{\bar{p}_{ij}^{R1} - \pi_{T_{ij}} \zeta_{ij}, 0\}}{\sum_{l=1}^N \max \{\bar{p}_{il}^{R1} - \pi_{T_{il}} \zeta_{il}, 0\}}.$$

The row sums of the matrix is such that $\sum_{j=1}^N a_{ij}^{R1}(\pi) = 1 \quad \forall i \in \mathcal{N}$. This implies that the bank's total obligations are to all banks within the network. The relative asset holdings matrix also depends on the market price of illiquid assets.

The total shares of assets sold in Δ_k in the asset k are the total shares the bank sells in its external asset holdings and shares of assets used as collateral:

$$\Delta_k(\pi, p) = \sum_{i=1}^N \min \{S_{ik}, \Omega_{ik}(\pi, p)\} + \sum_{i=1}^N \sum_{j=1}^N \Upsilon_{ij}(\pi, p) \mathbf{1}(T_{ij} = k). \quad (4.1)$$

Here, we define $\Omega : [0, 1] \times [0, \bar{p}^{R1}] \rightarrow [0, \infty)$ as a function of the number of shares of illiquid assets sold. The Ω_{ik} represents bank i selling the number of shares in asset k . This is an extension to Ghamami et al. (2022), in which only the assets used as collateral in (4.1) contribute to the price impact of illiquid assets.

We consider the proportion of assets sold by each bank as in Feinstein (2017) and Feinstein and El-Masri (2017). They consider the number of shares that the bank sells to meet its outstanding obligations. They assume that banks will only sell a minimum number of shares, which meet the outstanding obligations of the bank. This is referred to as the minimal liquidation condition. We define the minimal liquidation condition as in Assumption 3.1 by Feinstein (2017).

Definition 4.2.1 (Minimal liquidation condition). *The matrix of the number of shares sold $\Omega(\pi, p)$ satisfies the minimal liquidation condition, if:*

$$\sum_{k=1}^K \min \{S_{ik}, \Omega_{ik}(\pi, p)\} \pi_k = \min \left\{ \sum_{k=1}^K S_{ik} \pi_k, \left(\bar{p}_i^{R1} - b_i - \sum_{j=1}^N p_{ji} \right)^+ \right\}.$$

The economic interpretation is that the terms on the left-hand side represent the sale of shares which the bank holds. This excludes the cases in which the bank can short-sell. The right-hand side represents that banks only sell shares of assets to meet outstanding obligations. If the required payment that the bank needs to make is larger than its asset holdings, then the bank sells all shares of its asset holdings, at the current market price. We consider the matrix of illiquid assets sold under a proportional selling rule, as in Example 3.3 by Feinstein (2017). The bank sells a proportional amount of shares in each of its asset holdings, under the current market price. The matrix of assets sold by banks under proportional selling is defined as follows:

$$\Omega_{ik}(\pi, p) = \frac{S_{ik}}{\sum_{k=1}^K S_{ik}\pi_k} \left(\bar{p}_i^{R1} - b_i - \sum_{j=1}^N p_{ji} \right)^+. \quad (4.2)$$

Here, the bank sells a proportion of each of its asset holdings, that depend on outstanding obligations. The matrix is non-increasing in the market price of assets and bank payments. The smaller the payments and market price of assets, the larger the quantity of assets the bank needs to sell.

Other types of selling functions can also be considered i.e., ordered selling function, where the bank sells assets first which have the lowest price impact for example. We assume the proportional selling matrix as the matrix of illiquid asset holdings sold.

The second type of assets the bank sells is the assets used as collateral defined as $\Upsilon : [0, 1] \times [0, \bar{p}^{R1}] \rightarrow [0, \infty)$, as in Ghamami et al. (2022). The term Υ_{ij} represents the number of shares of collateral that the bank j seizes and sells from bank i . The quantity of collateral sold depends on the collateral posted, and the obligations of the bank at the current market price:

$$\Upsilon_{ij}(\pi, p) = \begin{cases} \min \left\{ \zeta_{ij}, \frac{\bar{p}_{ij}^{R1}}{\pi_{T_{ij}}} \right\} & \text{if } i \in \mathcal{D}^{R1}(\pi, p), \\ 0 & \text{if } i \in \mathcal{N} \setminus \mathcal{D}^{R1}(\pi, p), \end{cases}$$

for $\pi_k > 0 \quad \forall k \in \mathcal{S}$. If the market price is $\pi_k = 0$, then the collateral seized by bank j from i is defined as follows:

$$\Upsilon_{ij}(\pi, p) = \begin{cases} \zeta_{ij} & \text{if } i \in \mathcal{D}^{R1}(\pi, p) \quad \text{and} \quad \bar{p}_{ij}^{R1} > 0, \\ 0 & \text{if } i \in \mathcal{N} \setminus \mathcal{D}^{R1}(\pi, p). \end{cases}$$

If the bank is in default, there may be additional costs that the bank incurs. These costs are accounted for by the decrease in the bank's interbank and external assets. We characterise these costs as bankruptcy costs, similar to the bankruptcy costs under the clearing model by Rogers and Veraart (2013). These bankruptcy costs were also included as part of the collateral model by Veraart and Aldasoro (2022), which builds on the

collateral model introduced by Ghamami et al. (2022).

We define $\gamma^1 \in [0, 1]^N$ as the bankruptcy costs on the bank's external assets and $\gamma^2 \in [0, 1]^N$ as the bankruptcy costs on its interbank assets. Each term γ_i^1 and γ_i^2 represents the external and interbank bankruptcy costs on bank i . We consider these parameters as the operational risk associated with the bank in a clearing event.

The potential existence of multiple fixed points leads to various characterisations of bank payments. We specifically characterise two fixed points of the clearing function in R1. We denote (π_*^{R1}, p_*^{R1}) as the least fixed point and $(\pi^{*,R1}, p^{*,R1})$ as the greatest fixed point, where for all fixed points $(\hat{\pi}^{R1}, \hat{p}^{R1})$ then:

$$(\pi_*^{R1}, p_*^{R1}) \leq (\hat{\pi}^{R1}, \hat{p}^{R1}) \leq (\pi^{*,R1}, p^{*,R1}).$$

The fixed points represent bounds on the payment of banks and the market price of assets. Intuitively, banks with larger payments sell a smaller number of shares of external asset holdings and collateral assets. The decrease in the number of shares of assets sold leads to a higher market price for assets.

We focus on the greatest fixed point, which represents the largest payment of banks and the largest market price of assets. This is considered the best scenario for the bank, as this represents the largest equity holdings of the bank and the highest payments that banks can make under the clearing scenario.

We denote the asset holdings of the bank in R1 under the greatest fixed point as $A^{*,R1} = A^{R1}(\pi^{*,R1}, p^{*,R1})$ and equity $e^{*,R1} = e^{R1}(\pi^{*,R1}, p^{*,R1})$. Unless specified, the results from the fixed points are represented by the greatest fixed point.

Further details and proofs about the existence and convergence to the greatest fixed point can be found in Theorem 8.E.2 in Appendix 8. The proof for the existence of the greatest solution is a generalisation of the existence result by Veraart and Aldasoro (2022), where we consider the inclusion of external illiquid asset holdings.

4.2.2 Second round of clearing

We consider the second round of clearing (R2) where banks redistribute collateral not used in R1. The remaining collateral assets are used to meet outstanding payments the bank has from R1. We denote the outstanding payments of bank in R2 as $\bar{p}^{R2} \in [0, \bar{p}^{R1}]$ where \bar{p}_{ij}^{R2} represents the outstanding obligation which bank i has to bank j :

$$\bar{p}_{ij}^{R2} = \bar{p}_{ij}^{R1} - p_{ij}^{*,R1} \quad \forall i, j \in \mathcal{N}.$$

If the bank can fully meet its obligations in R1 i.e., $p^{R1} = \bar{p}^{R1}$, then it does not take part in the second round of clearing. Only banks that do not fully meet their obligations in R1 participate in R2.

We define the matrix of reallocated collateral as $r(\pi^{*,R1}, p^{*,R1}) \in [0, \infty)^{N \times (K+1)}$, where $r_{ik}(\pi^{*,R1}, p^{*,R1})$ represents the remaining collateral that bank i holds of asset k , under the R1 greatest fixed point:

$$r_{ik}(\pi^{*,R1}, p^{*,R1}) = \begin{cases} \sum_{j=1}^N (\zeta_{ij} - \Upsilon_{ij}(\pi^{*,R1}, p^{*,R1})) \mathbf{1}(T_{ij} = k) & \text{if } i \in \mathcal{D}^{R1}(\pi^{*,R1}, p^{*,R1}), \\ \sum_{j \in \mathcal{D}^{R1}(\pi^{*,R1}, p^{*,R1})} \zeta_{ij} \mathbf{1}(T_{ij} = k) & \text{if } i \in \mathcal{N} \setminus \mathcal{D}^{R1}(\pi^{*,R1}, p^{*,R1}). \end{cases}$$

The assets included are illiquid and liquid, as both types of assets can be used as collateral. The reallocated collateral assets are assets that were not used to cover the bank's outstanding obligations in default in R1. If the bank is not in default in R1, its remaining assets are the total collateral assets that it seized from defaulted banks in R1.

We define the fixed point function for the second round $\Phi^{R2} : [0, \pi^{*,R1}] \times [0, \bar{p}^{R2}] \rightarrow [0, \pi^{*,R1}] \times [0, \bar{p}^{R2}]$. We denote $(\hat{\pi}^{R2}, \hat{p}^{R2})$ as a fixed point of R2 clearing function if:

$$(\hat{\pi}^{R2}, \hat{p}^{R2}) = \Phi^{R2}(\hat{\pi}^{R2}, \hat{p}^{R2}).$$

As in R1 of clearing, there can be multiple values that satisfy the fixed point condition in R2. We define the second round clearing function as follows:

$$\begin{aligned} \Phi_{1,(k)}^{R2}(\pi, p) &= \pi_k^{*,R1} \exp(-l_k \Gamma_k(\pi, p)), \\ \Phi_{2,(ij)}^{R2}(\pi, p) &= \min \left\{ \bar{p}_{ij}^{R2}, a_{ij}^{R2} \left(c_i^{*,R1} + \sum_{k=1}^K r_{ik}(\pi^{*,R1}, p^{*,R1}) \pi_k + \sum_{j=1}^N p_{ji} \right) \right\}, \end{aligned}$$

where

$$c_i^{*,R1} = r_{i(K+1)}(\pi^{*,R1}, p^{*,R1}).$$

For remaining collateral assets which are liquid $c^{*,R1}$, this is not affected by the market-to-market adjustment as $\pi_{K+1} = 1$. This can be considered as the associated liquidity buffer for banks in R2. We distinguish liquid assets used as collateral separately from other illiquid assets.

The relative outstanding obligations matrix in the second round of clearing is denoted as $a^{R2} \in [0, 1]^{N \times N}$, where each entry a_{ij}^{R2} represents the relative outstanding obligations that bank i has to bank j :

$$a_{ij}^{R2} = \frac{\bar{p}_{ij}^{R2}}{\sum_{l=1}^N \bar{p}_{il}^{R2}}.$$

The total outstanding obligations $\sum_{j=1}^N a_{ij}^{R2} = 1 \quad \forall i \in \mathcal{N}$ represents that banks only have outstanding obligations to banks in the network, as in R1.

The clearing mechanism for the second round is the same one introduced by Ghamami et al. (2022). The difference is that the asset holdings and the market price depend on

the values of R1, which incorporates the fire sales effect by Cifuentes et al. (2005). The total number of shares of collateral that banks sell Γ_k in R2 in the asset k is defined as follows:

$$\Gamma_k(\pi, p) = \sum_{i=1}^N \Gamma_{ik}(\pi, p),$$

where

$$\Gamma_{ik}(\pi, p) = \min \left\{ \frac{r_{ik}(\pi^{*,R1}, p^{*,R1})}{\sum_{k=1}^K r_{ik}(\pi^{*,R1}, p^{*,R1}) \pi_k} \left(\sum_{j=1}^N \bar{p}_{ij}^{R2} - c_i^{*,R1} - \sum_{j=1}^N p_{ji} \right)^+, r_{ik}(\pi^{*,R1}, p^{*,R1}) \right\}.$$

Here, the Γ_{ik} term represents the number of shares the bank i sells of the remaining collateral assets in the asset class k . As in R1, the bank first uses its remaining liquid collateral assets and interbank assets before selling its illiquid asset holdings. We denote the equity e_i^{R2} of the bank i in the second round of clearing as follows:

$$e_i^{R2}(\pi, p) = c_i^{*,R1} + \sum_{k=1}^K r_{ik}(\pi^{*,R1}, p^{*,R1}) \pi_k + \sum_{j=1}^N p_{ji} - \bar{p}_i^{R2}.$$

The equity represents the difference in the bank's remaining asset holdings and outstanding obligations in R2. The assets used for collateral are considered in the bank's asset holdings in R2 because these assets are used by the bank to meet its outstanding obligations. We denote \mathcal{D}^{R2} as the set of banks that are unable to meet their total obligations across two rounds of clearing:

$$\mathcal{D}^{R2}(\hat{\pi}^{R2}, \hat{p}^{R2}) = \{i \in \mathcal{N} | e_i^{R2}(\hat{\pi}^{R2}, \hat{p}^{R2}) < 0\}.$$

Even if the bank can meet its remaining obligations in R2, it is still considered to be in default because it was unable to fully meet its obligations in R1.

As in R1, we consider the greatest fixed point of the second clearing round, which we denote as $(\pi^{*,R2}, p^{*,R2})$ where $(\hat{\pi}^{R2}, \hat{p}^{R2}) \leq (\pi^{*,R2}, p^{*,R2})$. Furthermore, we denote the total assets of the bank in R2 under the greatest fixed point $A^{*,R2} = A^{R2}(\pi^{*,R2}, p^{*,R2})$ and equity $e^{*,R2} = e^{R2}(\pi^{*,R2}, p^{*,R2})$.

The existence of the greatest fixed point and the iterative sequence to obtain the greatest fixed point is given by Ghamami et al. (2022). This still holds in our setting for the second round of clearing, in which the bank holds multiple illiquid external assets.

4.2.3 Systemic risk metrics

We introduce measures representing the losses for the first and second rounds of clearing. We define the relative shortfall as a measure of obligations not fulfilled, as by Glasserman and Young (2015).

We define $h \in [0, 1]^N$ as the difference between the bank's total obligations and its total payments under the greatest fixed points, where h_i represents the relative shortfall of bank i , after two rounds of clearing:

$$h_i = \frac{\sum_{j=1}^N \max \left\{ \bar{p}_{ij}^{R1} - p_{ij}^{*,R1} - p_{ij}^{*,R2}, 0 \right\}}{\sum_{i=1}^N \sum_{j=1}^N \bar{p}_{ij}^{R1}}.$$

For the shortfall across all banks, we define the relative total shortfall $H \in [0, 1]$ as the total relative shortfall in the bank's obligations:

$$H = \sum_{i=1}^N h_i.$$

We secondly evaluate the number of defaults and banks with outstanding obligations, across two rounds of clearing. We define the total number of bank defaults in the first round Λ^{R1} , and the total number of banks that do not fulfil outstanding obligations in the second round Λ^{R2} , under the greatest fixed point:

$$\Lambda^{R1} = \sum_{i=1}^N \mathbf{1} \left(e_i^{*,R1} < 0 \right)$$

and

$$\Lambda^{R2} = \sum_{i=1}^N \mathbf{1} \left(e_i^{*,R2} < 0 \right).$$

From the definition of the equity of banks, the number of banks in default is larger than the number of banks that do not fulfil outstanding obligations:

$$\Lambda^{R2} \leq \Lambda^{R1}. \tag{4.3}$$

This is because banks with outstanding obligations in R2 were in default in R1. However, if the bank is in default, then the bank may be able to meet its total obligations in both the first and second rounds.

We consider metrics to differentiate the losses between the first and second rounds of clearing. We define the relative first-round payments $\mathcal{P} \in [0, 1]$ as the total payments of the bank in the first round of clearing relative to the total payments of all banks:

$$\mathcal{P} = \frac{\sum_{i=1}^N p_i^{*,R1}}{\sum_{i=1}^N (p_i^{*,R1} + p_i^{*,R2})}.$$

A larger \mathcal{P} represents banks with a larger proportion of total obligations in R1. As a measure between banks that default and do not meet outstanding obligations, we define $\mathcal{V} \in [0, 1]$ as the relative number of banks with outstanding obligations in the second round:

$$\mathcal{V} = \frac{\Lambda^{R2}}{\Lambda^{R1}}.$$

From the inequality in (4.3), the relative number of banks with outstanding obligations is less than 1. If $\mathcal{V} = 1$, then all banks in default in the first round also have outstanding obligations across two rounds. If $\mathcal{V} = 0$, then all banks in default in the first round can meet outstanding obligations across both rounds of clearing.

4.3 Fixed point ordering

We consider the monotonic property of the fixed point, under different parameterizations of the clearing function. This is to establish the factors that can change the magnitude of the greatest fixed point. The parameters we consider are the liquidity buffer (b), bankruptcy costs (γ^1, γ^2), and the price impact of illiquid asset holdings (l).

We show an ordering of payments and the market price of illiquid assets under the fixed point, in the first round of clearing.

Theorem 4.3.1. *For the first round clearing function $\Phi^{R1,\nu}$ that depends on the following parameters:*

$$(l^\nu, \gamma^{1,\nu}, \gamma^{2,\nu}, b^\nu),$$

where $\nu = \{A, B\}$. If the parameters between two R1 clearing functions are such that:

$$l_k^A \geq l_k^B \quad \forall k \in \mathcal{S}$$

and

$$\left(\gamma_i^{1,A}, \gamma_i^{2,A}, b_i^A \right) \leq \left(\gamma_i^{1,B}, \gamma_i^{2,B}, b_i^B \right) \quad \forall i \in \mathcal{N},$$

then the corresponding greatest fixed point $(\pi^{*,R1,\nu}, p^{*,R1,\nu})$ under the clearing function satisfies:

$$\left(\pi^{*,R1,A}, p^{*,R1,A} \right) \leq \left(\pi^{*,R1,B}, p^{*,R1,B} \right).$$

As the bank increases the price impact, this further decreases the market price of illiquid assets and decreases the magnitude of the fixed points. If there are larger bankruptcy costs and the bank holds a smaller liquidity buffer, this also decreases the fixed payment

of banks and the market price of illiquid assets. For R1, a larger fire sales effect and smaller liquid asset holdings decrease the value of assets and the payments of banks. For the assumption of illiquid assets sold, the matrix of illiquid assets sold satisfies the ordering of R1 clearing function parameters. This ordering only considers the fixed points from R1. Across two rounds of clearing, we consider the total payment of the bank in R1 and R2.

Theorem 4.3.2. *For the first and second round clearing functions $\Phi^{R1,\nu}$ and $\Phi^{R2,\nu}$, we define the clearing process that depends on the following parameters:*

$$(l^\nu, \gamma^{1,\nu}, \gamma^{2,\nu}, b^\nu)$$

where $\nu = \{A, B\}$. For the corresponding greatest fixed point $(\pi^{*,R1,\nu}, p^{*,R1,\nu})$ under the clearing function $\Phi^{R1,\nu}$ and $(\pi^{*,R2,\nu}, p^{*,R2,\nu})$ under $\Phi^{R2,\nu}$. Assuming the collateral posted by all banks is smaller than its obligations, and the absence of interbank bankruptcy costs i.e.,

$$\bar{p}_{ij}^{R1} \geq \zeta_{ij} \quad \forall i, j \in \mathcal{N}$$

and

$$\gamma_i^{2,A} = \gamma_i^{2,B} = 1 \quad \forall i \in \mathcal{N}.$$

If the parameters between two clearing functions are such that

$$l_k^A \geq l_k^B \quad \forall k \in \mathcal{S}$$

and

$$\left(\gamma_i^{1,A}, b_i^A \right) \leq \left(\gamma_i^{1,B}, b_i^B \right) \quad \forall i \in \mathcal{N}$$

then

$$\pi^{*,R2,A} \leq \pi^{*,R2,B}$$

and

$$p^{*,R2,A} + p^{*,R1,A} \leq p^{*,R2,B} + p^{*,R1,B}.$$

For an ordering on the total payments after two rounds of clearing, we assume that the collateral posted is smaller than its obligations. If the assets used as collateral are larger than the corresponding obligation, there can be remaining collateral assets not seized in R1 and used in R2. As the remaining collateral assets in R2 are not subject to bankruptcy costs, the payments of the bank using these remaining collateral assets can be higher across both rounds of clearing. Hence, banks that post collateral assets higher than the obligation can lead to higher payments across both rounds of clearing, even if more banks default in R1.

If interbank bankruptcy costs are present, interbank assets are subject to larger discounts

in R1 compared with R2. Therefore, the interbank assets may be higher in R2 than in R1 and lead to a higher fixed payment of the bank. From these assumptions, the payments of banks are always larger if banks settle their total obligations where possible.

We showed that the first round of payments and total payments across two rounds of clearing have the same ordering. We consider the ordering of the greatest fixed point, for payments that only occur in the second round of clearing.

Proposition 4.3.3. *For the second round clearing function $\Phi^{R2,\nu}$ with $\nu = \{A, B\}$. If the greatest fixed points in the first round of clearing between two different systems $(\pi^{*,R1,\nu}, p^{*,R1,\nu})$ satisfies:*

$$(\pi^{*,R1,A}, p^{*,R1,A}) \leq (\pi^{*,R1,B}, p^{*,R1,B})$$

and the obligations of all banks are larger than the collateral posted i.e.,

$$\bar{p}_{ij}^{R1} \geq \zeta_{ij} \quad \forall i, j \in \mathcal{N}$$

then

$$p^{*,R2,A} \geq p^{*,R2,B}.$$

Only in the second round, the payments in the system A are larger than in B . This comes from the higher bankruptcy costs and a smaller liquidity buffer, in which the bank has a higher magnitude of outstanding obligations, from the first round. From the total payments across two rounds of clearing, the bank still makes smaller payments because of R1, and the total payment is smaller as established in Theorem 4.3.2.

The ordering of bank payments and the market price of assets can be applied to the systemic risk metrics, as in Section 4.2.3. We show that the ordering of the first and second round payments on the market price and bank payments leads to an ordering of systemic risk metrics.

Theorem 4.3.4. *For the first and second round clearing functions $\Phi^{R1,\nu}$ and $\Phi^{R2,\nu}$ where $\nu = \{A, B\}$. If there is an ordering between two systems such that*

$$l_k^A \geq l_k^B \quad \forall k \in \mathcal{S}$$

and

$$\left(\gamma_i^{1,A}, \gamma_i^{2,A}, b_i^A \right) \leq \left(\gamma_i^{1,B}, \gamma_i^{2,B}, b_i^B \right) \quad \forall i \in \mathcal{N}.$$

For $\Lambda^{R1,\nu}, \mathcal{P}^\nu, h^\nu$ and $\Lambda^{R2,\nu}$ representing the systemic risk metrics under the parameters ν , then:

$$\Lambda^{R1,A} \geq \Lambda^{R1,B}.$$

Additionally, if $\bar{p}_{ij}^{R1} \geq \zeta_{ij} \quad \forall i, j \in \mathcal{N}$, then:

$$\mathcal{P}^A \leq \mathcal{P}^B.$$

Furthermore, in the absence of interbank bankruptcy costs $\gamma_i^{2,A} = \gamma_i^{2,B} = 1 \quad \forall i \in \mathcal{N}$. Then,

$$h_i^A \geq h_i^B \quad \forall i \in \mathcal{N},$$

and

$$H^A \geq H^B,$$

and

$$\Lambda^{R2,A} \geq \Lambda^{R2,B}.$$

The change in parameters leads to a change in systemic risk measures. This is amplified by the asset holdings of the bank if they are illiquid. For the relative number of defaults \mathcal{V} , there is no ordering between the different systems under the assumptions of collateral assets posted and the absence of interbank bankruptcy costs. The relative number of defaults can either increase or decrease from the change in the equity of banks in R2.

4.4 Network simulations

We illustrate the interaction of the clearing process with two channels of fire sales risk for different networks. For a small network, we consider several portfolios of the bank's external asset holdings under a clearing event. We analyse the commonality of these assets with collateral posted. We expand this analysis to networks generated under a large random graph model. We analyse the sensitivity of losses under different systemic risk metrics for different parameterisations across both clearing rounds.

4.4.1 Small example network

We consider a network with $N = 4$ banks and $K = 2$ illiquid asset holdings, where assets include a liquidity buffer and two illiquid asset holdings. We assume the absence of bankruptcy costs on the bank's assets i.e., $\gamma_i^1 = \gamma_i^2 = 1 \quad \forall i \in \mathcal{N}$.

We characterise the asset type used as collateral under the matrix T for the small network as follows: if $T_{ij} = \{1, 2\}$, then the bank posts collateral assets $\zeta_{ij} > 0$ in illiquid asset 1 ($k = 1$) or illiquid asset 2 ($k = 2$). If $T_{ij} = 3$, then the bank posts collateral assets $\zeta_{ij} > 0$ that are liquid. We consider two types of assets that banks can post as collateral.

- **Liquid collateral (A1):** The bank only posts collateral assets that are liquid i.e., $T_{ij} = 3 \quad \forall \zeta_{ij} > 0$. The collateral is not subject to any price impact when sold.

- **Illiquid collateral (A2):** The bank only posts collateral assets that are illiquid asset 1 i.e., $T_{ij} = 1 \quad \forall \zeta_{ij} > 0$. This represents illiquid assets used as collateral and subject to a price impact when sold.

$$\bar{p}^{R1} = \begin{pmatrix} 0 & 20 & 0 & 0 \\ 0 & 0 & 20 & 0 \\ 0 & 0 & 0 & 20 \\ 0 & 0 & 0 & 0 \end{pmatrix}, \quad \zeta = \begin{pmatrix} 0 & 5 & 0 & 0 \\ 0 & 0 & 5 & 0 \\ 0 & 0 & 0 & 5 \\ 0 & 0 & 0 & 0 \end{pmatrix}, \quad l = 0.01 \times \begin{pmatrix} 1.8 \\ 2.5 \\ 0 \end{pmatrix}.$$

Table 4.1: The parameters for the network for the bank’s obligations, collateral posted and the price impact of illiquid assets. The price impact is for liquid and illiquid collateral (in total three assets). All other parameters are defined in the different types of collateral assets and network configurations.

We specify the obligations matrix, collateral matrix, and price impact of assets in Table 4.1. All banks have an interbank asset or an obligation with another bank. We consider a higher price impact of illiquid asset 2 than illiquid asset 1, to differentiate the risks from different types of illiquid assets. In total, there are three different types of external assets the bank can hold and assets for collateral the bank can post.

From the interbank network, we define the asset holdings of banks which we denote as the network configuration. We consider a combination of both liquid and illiquid asset holdings, for the external asset holdings of the bank.

- **Configuration 1 (C1):** No bank holds a liquidity buffer or illiquid asset i.e., $b_i = 0$ and $S_{i1} = S_{i2} = 0 \quad \forall i \in \mathcal{N}$. The equity of each bank is the difference between its interbank assets and interbank liabilities.
- **Configuration 2 (C2):** All banks only hold a liquidity buffer $b_i = 10 \quad \forall i \in \mathcal{N}$ and no illiquid assets i.e., $S_{i1} = S_{i2} = 0 \quad \forall i \in \mathcal{N}$. This corresponds to external asset holdings as considered in Ghamami et al. (2022), where the fire sales impact has no impact on the bank’s external asset holdings.
- **Configuration 3 (C3):** All banks do not hold a liquidity buffer $b_i = 0 \quad \forall i \in \mathcal{N}$, and only hold illiquid asset 1 i.e., $S_{i1} = 10$ and $S_{i2} = 0 \quad \forall i \in \mathcal{N}$. This corresponds to the same asset that banks externally hold and use as collateral.
- **Configuration 4 (C4):** All banks do not hold a liquidity buffer $b_i = 0 \quad \forall i \in \mathcal{N}$, and only hold illiquid asset 2 i.e., $S_{i1} = 0$ and $S_{i2} = 10 \quad \forall i \in \mathcal{N}$. The asset holdings of the bank and collateral posted represent two channels of independent fire sales risk.
- **Configuration 5 (C5):** All banks do not hold a liquidity buffer $b_i = 0 \quad \forall i \in \mathcal{N}$ and hold equal quantities of both illiquid assets 1 and 2 i.e., $S_{i1} = S_{i2} = 5 \quad \forall i \in \mathcal{N}$.

The configuration represents a diversification of the external asset holdings with partial commonality with assets used as collateral.

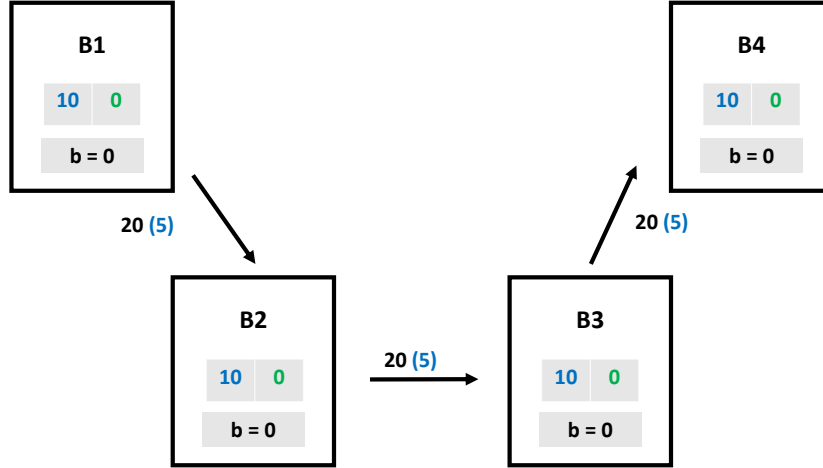


Figure 4.1: The figure represents the network configuration C3 and illiquid collateral A2. Each node represents a bank and its external asset holdings, in two different illiquid assets and a liquidity buffer. The assets used as collateral are represented in brackets, with the associated obligations between banks. The colours represent the type of illiquid asset the bank holds or uses as collateral with illiquid asset 1 = blue (left entry) and illiquid asset 2 = green (right entry).

Each of the configurations represents the asset holdings of the bank and the outcome of the shortfall position. The liquidity of the asset determines the market value of the asset and how it is used to meet the bank's obligations, given changes in further iterations of the clearing process.

In total, we have 10 different network structures that compromise 2 types of collateral posted and 5 network configurations. We calculate the bank's shortfall and the number of defaults for all combinations.

We illustrate the clearing process for the network as in Figure 4.1. From the network structure, we consider the payments for $\{B1, B2, B3\}$, and the corresponding losses. The total assets sold consist of only assets in illiquid asset 1:

$$p^{*,R1} = \begin{pmatrix} 0 & \min \left\{ 20, 15\pi_1^{*,R1} \right\} & 0 & 0 \\ 0 & 0 & \min \left\{ 20, 15\pi_1^{*,R1} + p_{12}^* \right\} & 0 \\ 0 & 0 & 0 & \min \left\{ 20, 15\pi_1^{*,R1} + p_{23}^* \right\} \\ 0 & 0 & 0 & 0 \end{pmatrix}. \quad (4.4)$$

The matrix (4.4) represents the fixed point payments of banks. As both illiquid asset

holdings and collateral are of the same asset, this gives a total value of 15 to all banks. We secondly define the total assets sold under the fixed point Δ^* as follows:

$$\begin{pmatrix} \sum_{i=1}^3 \min \{ S_{ik}, \Omega_{ik}(\pi^{*,R1}, p^{*,R1}) \} \\ 0 \\ 0 \end{pmatrix} + \begin{pmatrix} \Upsilon_{12}(\pi^{*,R1}, p^{*,R1}) + \Upsilon_{23}(\pi^{*,R1}, p^{*,R1}) + \Upsilon_{34}(\pi^{*,R1}, p^{*,R1}) \\ 0 \\ 0 \end{pmatrix}.$$

As banks only hold illiquid asset 1, there is only a price impact in the first entry of the total assets and collateral sold. For the first round of clearing, the initial equity of banks is:

$$e(\pi^0, p^0) = \begin{pmatrix} -10 \\ 10 \\ 10 \\ 30 \end{pmatrix}.$$

As the initial equity of B1 is negative, it is in fundamental default selling all its illiquid assets. As the asset holdings of B1 do not fully cover its total obligations, the collateral asset posted is seized by B2, which the bank uses to cover its obligations. As the collateral is illiquid, B2 selling the asset results in a mark-to-market adjustment and price impact on the asset value. With the illiquid assets sold by B1 and collateral assets sold by B2, the market price on the illiquid asset 1 is updated:

$$\Delta(\pi^0, p^0) = \begin{pmatrix} 15 \\ 0 \\ 0 \end{pmatrix} \implies \pi^1 \approx \begin{pmatrix} 0.76 \\ 1 \\ 1 \end{pmatrix}.$$

Under the current market price and the proportional allocation of the bank's asset holdings, the equity after one iteration in the first round of clearing:

$$e(\pi^1, p^1) \approx \begin{pmatrix} -12.37 \\ 2.63 \\ 7.63 \\ 27.63 \end{pmatrix}.$$

The decrease in the market price of illiquid asset 1 requires B2 to sell a proportion of its external asset holdings to meet its obligations to B3. This results in a second update to the market price of illiquid asset 1 and an update to the fixed point payments from banks,

$$\Delta(\pi^1, p^1) = \begin{pmatrix} 21.5 \\ 0 \\ 0 \end{pmatrix} \implies \pi^2 \approx \begin{pmatrix} 0.68 \\ 1 \\ 1 \end{pmatrix}.$$

The change in the market price leads to the following update on its equity holdings

$$e(\pi^2, p^2) \approx \begin{pmatrix} -13.22 \\ -1.76 \\ 6.78 \\ 26.78 \end{pmatrix}.$$

Under this second iteration, the equity of B1 is lower because of the additional assets sold by B2, which are the same type of asset B1 holds. This further decreases the market value of illiquid asset 1 requiring B2 to sell a larger proportion of its asset holdings. As Bank B2 is in default, it sells all its illiquid asset holdings and the collateral posted to B3 is seized. B3 sells the seized collateral asset to meet its obligations and this further contributes to the decrease in the market value of illiquid asset 1.

Iterative updates continue to occur resulting in all external asset holdings and assets posted as collateral in illiquid asset 1 being sold by banks B1, B2 and B3. As B4 has no obligations, it does not sell any shares of its asset holdings. The resulting fixed point for the market value of assets:

$$\Delta(\pi^*, p^*) = \begin{pmatrix} 45 \\ 0 \\ 0 \end{pmatrix} \implies \pi^* \approx \begin{pmatrix} 0.445 \\ 1 \\ 1 \end{pmatrix}$$

and the equity under the fixed point:

$$e(\pi^*, p^*) \approx \begin{pmatrix} -15.55 \\ -8.88 \\ -2.21 \\ 24.45 \end{pmatrix}.$$

The clearing process leads to three defaults $\{B1, B2, B3\}$, in which one is fundamental default $\{B1\}$ and $\{B2, B3\}$ are contagious defaults. We analyse the losses of banks by considering systemic risk measures. We calculate the relative shortfall of banks in R1. The total obligations between banks in the small network,

$$\sum_{i=1}^N \sum_{j=1}^N \bar{p}_{ij}^{R1} = 60.$$

The relative shortfall for B1 in the first round of clearing:

$$h_1 = \frac{1}{60} \sum_{j=1}^N \max \left\{ \bar{p}_{1j}^{R1} - p_{1j}^{*,R1}, 0 \right\} = \frac{\max \{20 - (0.445 \times 15), 0\}}{60} \approx 0.22. \quad (4.5)$$

The shortfall in B1's total obligations is 22% of the total obligations in R1. For B2, as the bank has interbank assets from B1, this is accounted for in the shortfall

$$h_2 = \frac{1}{60} \sum_{j=1}^N \max \left\{ \bar{p}_{2j}^{R1} - p_{2j}^{*,R1}, 0 \right\} = \frac{\max \{20 - (0.445 \times 30), 0\}}{60} \approx 0.11. \quad (4.6)$$

As B2 has interbank assets from B1, this increases its interbank assets and decreases outstanding payments. This subsequently decreases the relative shortfall of B2 (4.6) compared with B1 (4.5). For the relative shortfall of bank B3,

$$h_3 = \frac{1}{60} \sum_{j=1}^N \max \left\{ \bar{p}_{3j}^{R1} - p_{3j}^{*,R1}, 0 \right\} = \frac{\max \{20 - (0.445 \times 45), 0\}}{60} = 0. \quad (4.7)$$

The collateral seized and the interbank assets coming from B1 and B2 result in no shortfall for B3 (4.7). As B4 has no obligations to any bank than $h_4 = 0$. From the shortfall of B3, although the bank is still in default, the bank was able to meet its obligations. This is because the bank was able to seize collateral from B2, which defaulted on its obligations to B3.

We consider the changes that occur in the second round of clearing. At this stage, banks that have outstanding obligations participate in the clearing process. We define the matrix of outstanding obligations and reallocated assets in Table 4.2.

$$\bar{p}^{R2} = \begin{pmatrix} 0 & 13.33 & 0 & 0 \\ 0 & 0 & 6.65 & 0 \\ 0 & 0 & 0 & 0 \\ 0 & 0 & 0 & 0 \end{pmatrix}, \quad r(\pi^{*,R1}, p^{*,R1}) = \begin{pmatrix} 0 & 0 & 0 \\ 0 & 0 & 0 \\ 0 & 0 & 0 \\ 0 & 0 & 0 \end{pmatrix}.$$

Table 4.2: The parameters represent the bank's outstanding obligations and the reallocated collateral of banks in R1.

From the assumptions of posted collateral, there is no reallocated collateral for banks that are in default. The clearing process in the second round is that of Eisenberg and Noe (2001). The result leads to no change in the shortfall or banks meeting outstanding obligations. This is because B1 is unable to meet its outstanding obligations, as it has no interbank assets or external asset holdings. This leads to B2 also having outstanding obligations because there are no interbank assets from B1. Hence, the relative shortfall across two rounds of clearing is the same as the shortfall in the first round.

The small network illustrates both clearing rounds. In R1, there is feedback from the

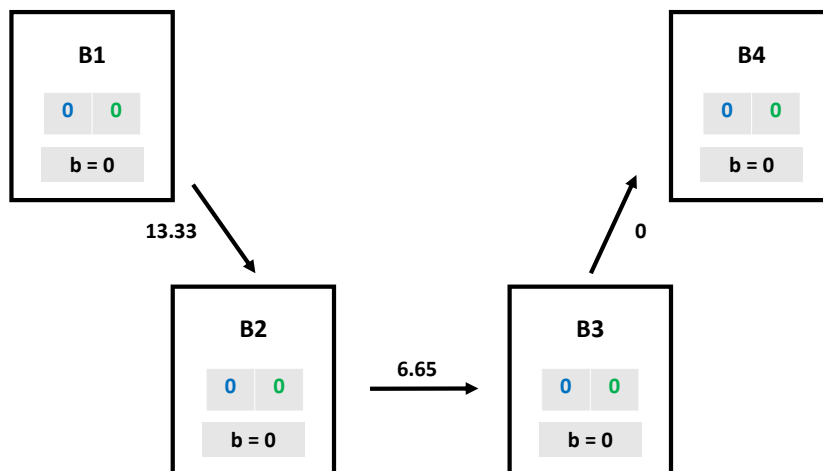


Figure 4.2: The figure represents the network configuration C3 and illiquid collateral A2, in the second round of clearing. Each node represents a bank and its external asset holdings, in two different illiquid assets and a liquidity buffer. The assets used as collateral are represented in brackets, with the associated obligations between banks. The colours represent the type of illiquid asset the bank holds or uses as collateral with illiquid asset 1 = blue (left entry) and illiquid asset 2 = green (right entry).

fire sales effect that contributes to illiquid assets and collateral losses. Because of these updates, the fire sales losses result in a contagious default for B3. As no bank can meet its outstanding obligations, there is no change in the relative shortfall of banks.

We illustrate the relative shortfall and the number of defaults in Table 4.3, for different network configurations and collateral assets posted. Our result shows that the asset holdings of the bank do influence the shortfall and number of defaults. We find the largest losses correspond to C3 when the collateral assets are the same asset as the external asset holdings. Although the associated price impact is smaller for illiquid asset 1, the combined price impact when banks sell this asset leads to further decreases in the market price. This is higher than the bank's asset holdings, in which it holds an illiquid asset with a higher price impact factor. By assuming the collateral is liquid, there is a smaller price impact from collateral and values in A1 compared with A2. The smallest losses for banks that hold illiquid assets are in C5, under a diversified portfolio. This shows a situation where diversifying assets with different price impacts does reduce losses to the bank.

For an amplified price impact, we find the losses also increase for all banks. The increase in the price impact results in larger losses when the collateral is illiquid ($\times 4$ higher in the total shortfall compared with $\times 2$ when collateral is illiquid). From the increase in the price impact, there is a higher number of defaults for all configurations that hold illiquid assets. Comparing C1 and C4 metrics, there is a small decrease in losses under C4 compared to banks holding no illiquid assets. This shows with the increased fire sales effect, the effectiveness of collateral decreases to reduce losses to banks. We consider the

Measure	Asset holdings of network				
	C1	C2	C3	C4	C5
A1 collateral					
Shortfall (l)	$(0.25, 0.17, 0.08, 0)^T$	$(0.08, 0, 0, 0)^T$	$(0.13, 0, 0, 0)^T$	$(0.15, 0, 0, 0)^T$	$(0.11, 0, 0, 0)^T$
$(l \times 4)$	$(0.25, 0.17, 0.08, 0)^T$	$(0.08, 0, 0, 0)^T$	$(0.23, 0.13, 0.03, 0)^T$	$(0.24, 0.15, 0.06, 0)^T$	$(0.20, 0.07, 0, 0)^T$
Defaults (\mathcal{D})	$(1, 1, 1, 0)^T$	$(1, 0, 0, 0)^T$	$(1, 1, 0, 0)^T$	$(1, 1, 0, 0)^T$	$(1, 0, 0, 0)^T$
$(l \times 4)$	$(1, 1, 1, 0)^T$	$(1, 0, 0, 0)^T$	$(1, 1, 1, 0)^T$	$(1, 1, 1, 0)^T$	$(1, 1, 0, 0)^T$
A2 collateral					
Shortfall (l)	$(0.27, 0.21, 0.14, 0)^T$	$(0.09, 0, 0, 0)^T$	$(0.22, 0.11, 0, 0)^T$	$(0.16, 0, 0, 0)^T$	$(0.15, 0, 0, 0)^T$
$(l \times 4)$	$(0.31, 0.28, 0.25, 0)^T$	$(0.11, 0, 0, 0)^T$	$(0.32, 0.31, 0.30, 0)^T$	$(0.30, 0.26, 0.22, 0)^T$	$(0.30, 0.26, 0.22, 0)^T$
Defaults (\mathcal{D})	$(1, 1, 1, 0)^T$	$(1, 0, 0, 0)^T$	$(1, 1, 1, 0)^T$	$(1, 1, 0, 0)^T$	$(1, 1, 0, 0)^T$
$(l \times 4)$	$(1, 1, 1, 0)^T$	$(1, 0, 0, 0)^T$	$(1, 1, 1, 0)^T$	$(1, 1, 1, 0)^T$	$(1, 1, 1, 0)^T$

Table 4.3: The table represents the shortfall and defaults of banks for different configurations. The rows in grey represent the shortfall and number of defaults when the price impact is amplified $l \times 4$. For bank defaults, an entry of 1 represents a bank defaulting in the first round of clearing with 0 representing no default.

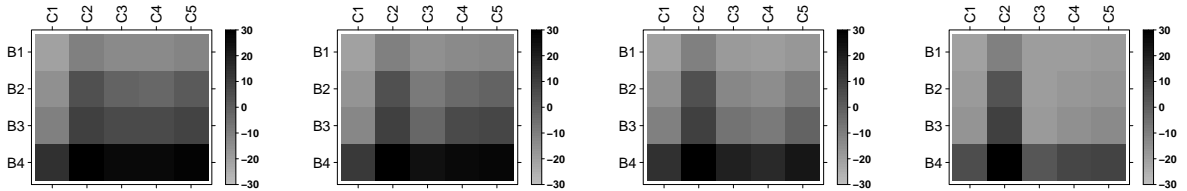


Figure 4.3: The plots represent the equity of banks under the greatest fixed point, for different configurations and price impact factors: A1 with price impact l (left), A2 with price impact l (middle left), A1 with price impact $l \times 4$ (middle right) and A2 with price impact $l \times 4$ (right).

equity losses of banks for different configurations and collateral posted under heat plots in Figure 4.3. The smallest equity values are under C1, in which the bank holds no illiquid assets or capital buffer. For other configurations, the equity losses as in the shortfall and number of defaults are higher when collateral is illiquid, and the price impact is high. The smallest changes to the equity are for B4, in which the bank has no obligations and C2 when banks only hold a liquidity buffer. Even though the banks have no shortfall and are not in default, the equity of banks does change depending on the price impact and its asset holdings.

4.4.2 Large random network

We generate a sample of random networks for the banks' obligations. We bilaterally net obligations and assign collateral assets on the netted obligations. We consider the clearing scenario from banks with outstanding obligations, that are generated from the random network.

We define the $N \times N$ random matrices for banks obligations $\tilde{p}^{ER, \tau}$, where τ represents a sample of the total number of generated matrices $D \in \mathbb{N}$. We denote the matrices

by ER to represent the assumption of an Erdős-Rényi graph, in which the probability a link forms between two banks is equal. We define $\lambda \in [0, 1]$ as the probability that a link forms between two banks. Each entry of the obligations matrix is generated from a discrete Bernoulli distribution:

$$\begin{aligned}\mathbb{P}\left(\tilde{p}_{ij}^{ER,\tau} = \frac{W^{(1)}}{\lambda N(N-1)}\right) &= \lambda, \\ \mathbb{P}\left(\tilde{p}_{ij}^{ER,\tau} = 0\right) &= 1 - \lambda \quad \forall i \neq j, \\ \mathbb{P}\left(\tilde{p}_{ii}^{ER,\tau} = 0\right) &= 1 \quad \forall i \in \mathcal{N},\end{aligned}$$

and $W^{(1)} \in [0, \infty)$ denotes the total obligations of all banks. As there are no links on the diagonal, we account for this in the weight distribution, in which $N(N-1)$ links can only be present.

We bilaterally net obligations in the generated matrices. We define the bilaterally netted matrices $\bar{p}^{ER,\tau}$, where each entry $\bar{p}_{ij}^{ER,\tau}$ represents the bilaterally netted obligations between banks i and j :

$$\bar{p}_{ij}^{ER,\tau} = \max\left\{\tilde{p}_{ij}^{ER,\tau} - \tilde{p}_{ji}^{ER,\tau}, 0\right\} \quad \forall i, j \in \mathcal{N}.$$

As the links are bilaterally netted and the weights assigned to each link are equal if $\lambda = 1$ the netted matrix has no links. The collateral is assigned to banks from the netted obligations between banks

$$m_{ij}^{ER,\tau} = \frac{C}{W^{(1)}} \bar{p}_{ij}^{ER,\tau} \quad \forall i, j \in \mathcal{N}$$

and $C \in [0, \infty)$ denotes the total collateral posted. For a network with $N = 20$ nodes, we define the total link weights $W^{(1)} = 60$ and $C = 15$. This represents the same total obligations and collateral as in Section 4.4.1. We consider $D = 1000$ for the total number of generated random networks.

We assume banks have a liquidity buffer and two illiquid asset holdings for different collateral and network configurations, as in Section 4.4.1. The total shares of liquid and illiquid assets for each bank are adjusted by the total number of banks in the network i.e., for each configuration (except for Configuration 1 where banks hold no external asset holdings). The total shares of external assets which the bank has for each configuration are equal to:

$$b_i + \sum_{k=1}^K S_{ik} = \frac{W^{(2)}}{N} \quad \forall i \in \mathcal{N},$$

where $W^{(2)} \in [0, \infty)$ represents the total quantity of shares of external assets for all

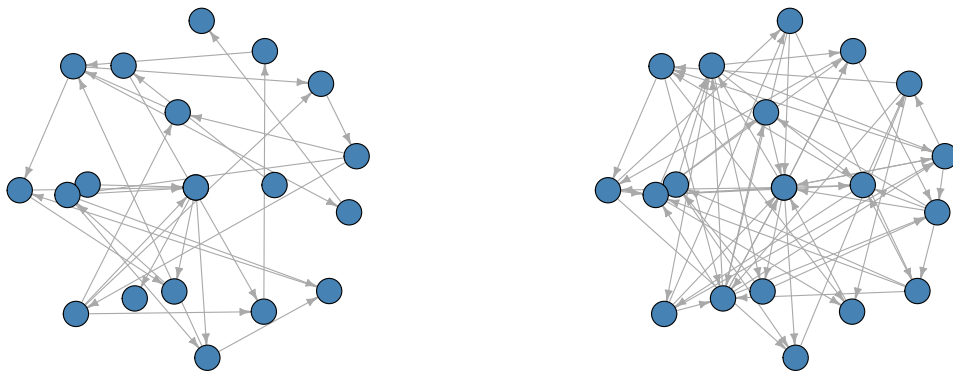


Figure 4.4: The plot represents one network from the sample of bilaterally netted random graphs for a density of $\lambda = 0.1$ (left) and $\lambda = 0.3$ (right).

banks. We assume $W^{(2)} = 40$ as the total number of shares of external assets for all banks. The total number of shares determines the number of shares allocated to each asset for different configurations of asset holdings.

We evaluate the change in the systemic risk metrics, for different price impact factors. We assume no bankruptcy costs for external and interbank assets $\gamma_i^1 = \gamma_i^2 = 1 \quad \forall i \in \mathcal{N}$. We denote the change in the price impact $l(\beta)$ under different exponents $\beta \in \mathbb{R}$ as follows:

$$l(\beta) = l_0 \times 2^{(\beta-5)},$$

and l_0 represents the initial price impact. The change in the price impact $l(\beta)$ depends on the exponent β , relative to the constant factor. Under the chosen constant, if $\beta < 5$, there is a decrease in the price impact, if $\beta > 5$ the price impact increases and for $\beta = 5$ there is no change in the price impact.⁵

We assume that l_0 values are the same as in the small network in Section 4.4.1, and consider different values of β in the clearing process.

We define the systemic metrics for a sample of networks. We define the average total relative shortfall and number of defaults for a sample of D networks as follows:

$$\bar{H} = \frac{1}{D} \sum_{\tau=1}^D \sum_{i=1}^N h_i^\tau,$$

and

$$h_i^\tau = \frac{\sum_{j=1}^N \max \left\{ \bar{p}_{ij}^{R1,\tau} - p_{ij}^{*,R1,\tau} - p_{ij}^{*,R2,\tau}, 0 \right\}}{\sum_{i=1}^N \sum_{j=1}^N \bar{p}_{ij}^{R1,\tau}}.$$

The $p^{*,R1,\tau}$ and $p^{*,R2,\tau}$ represent the greatest fixed point payments in R1 and R2 from the

⁵The factor of 5 was chosen because of the values from networks generated under the random graph model. Other values can be considered for the change in price impact.

randomly generated obligations matrix $\bar{p}^{R1,\tau} = \bar{p}^{ER,\tau}$, of sample τ . Across all samples, we define the average total number of banks that are in the default $\bar{\Lambda}^{R1}$ and the average total number of banks with outstanding obligations $\bar{\Lambda}^{R2}$ as follows:

$$\bar{\Lambda}^\iota = \frac{1}{D} \sum_{\tau=1}^D \Lambda^{\iota,\tau},$$

where

$$\Lambda^{\iota,\tau} = \sum_{i=1}^N \mathbf{1}(e_i^{*,\iota,\tau} < 0) \quad \iota \in \{R1, R2\}.$$

The term $e^{*,\iota,\tau}$ represents the equity of the bank under the greatest fixed point in the round ι , for sample τ . We define the average relative proportion of payments in the first round compared with total payments as:

$$\bar{\mathcal{P}} = \frac{1}{D} \sum_{\tau=1}^D \mathcal{P}^\tau,$$

where

$$\mathcal{P}^\tau = \frac{\sum_{i=1}^N p_i^{*,R1,\tau}}{\sum_{i=1}^N (p_i^{*,R1,\tau} + p_i^{*,R2,\tau})}.$$

We define the average proportion of banks with outstanding payments compared with the total number of bank defaults as follows:

$$\bar{\mathcal{V}} = \frac{1}{d} \sum_{\tau=1}^d \mathcal{V}^\tau,$$

where

$$\mathcal{V}^\tau = \frac{\Lambda^{R2,\tau}}{\Lambda^{R1,\tau}}.$$

Provided that payments satisfy the conditions on the parameters and assets posted as collateral in Theorem 4.3.4, then the ordering of systemic risk measures for the average across all sample networks still holds.

Obligations and Defaults: In Figure 4.5, we find the configuration of the network does impact the shortfall and banks with outstanding obligations. For $\beta < 5$, there are small differences between the asset losses of different configurations, with C1 representing the largest losses to banks. As $\beta > 5$, there is a higher mark-to-market adjustment and larger losses for configurations with a higher commonality of C3 and C5. Furthermore, the total shortfall and outstanding obligations exceed those of C1, in which the bank holds no external assets. This shows the combined fire sales effect can result in higher losses for banks with illiquid assets than those without.

The smallest loss is for C2 when the bank holds only a liquid buffer. This is not affected by the price impact and hence results in smaller losses compared to other configurations. The losses of banks are still affected by the change in price impact, because of the illiquid assets used as collateral.

Initially, C4 losses are smaller than C5, when the collateral and illiquid assets are of the same type with a small price impact. As the price exponent increases, the commonality leads to larger losses compared with the diversification represented in C5. The magnitude of the price impact determines how susceptible different configurations are to the effects of the fire sale.

The shortfall and number of banks with outstanding obligations are smaller in C5 than in C1. This is because two different types of assets are used for external asset holdings and posted collateral assets. The decrease in external asset holdings from the fire sales does not decrease the market price of assets used as collateral. This means the losses of banks are lower holding external assets which are different to the assets used as collateral, even if these assets are subject to the fire sales effect. Hence, holding external assets under this configuration always decreases the losses of banks compared to holding no quantity of external asset holdings.

Relative Obligations and Defaults: From the relative contribution of different rounds, we find the shortfall is largely concentrated in the first round. The changes in the relative contribution are for configurations in which the bank holds external assets, where the overall values in C1 remain similar. As banks in default do not have collateral to reallocate in the second round, this reduces the total payments banks make in R2.

The R2 does affect the total payments of banks only when the price impact exponent is high. This comes from an increase in bank defaults from the first round and leads to networks in which banks can multilateral meet outstanding obligations. This increases the payments in R2 and hence reduces the total contribution of payments in R1. We only find a contribution of R2 for configurations resulting in the largest losses, which are in C3 and C5.

We find a large proportion of banks that default do not meet outstanding obligations in R2. For $\beta = 5$, this results in the smallest value of $\bar{\mathcal{V}}$, in which the largest proportion of banks can meet outstanding obligations in R2. This may be from the magnitude of the price impact, which is small enough such that there are banks with outstanding obligations, but not large enough to substantially decrease the market price of assets used for collateral. The trajectory of losses is not monotonic, so we cannot characterise the ordering of this metric as with other systemic metrics from Theorem 4.3.4. We find C4 has the smallest number of relative banks with outstanding obligations, and these values correspond to the trajectory of banks with outstanding obligations.

Network density: We consider an increase in the network density of $\lambda = 0.3$. We generate a sample of networks from an Erdős-Rényi random graph model and bilaterally net obligations.

We find the total shortfall and the total number of banks with outstanding obligations are smaller under a higher network density. As the density of the network increases, this decreases the associated weight of each formed link between bank payments and collateral. This decreases the variation in the difference between interbank assets and obligations, and results in a smaller number of banks in fundamental default, and subsequently a smaller number of contagious defaults.

Under this network, C1 mostly has the largest losses across all other types of configurations, in which the bank holds external assets. In this regard, holding illiquid assets even with a high commonality with collateral posted does reduce the shortfall number of banks with outstanding obligations.

For different price impact exponents, the relative number of banks that cannot meet total obligations across both rounds is $< 30\%$. This represents a significant decrease in bank losses compared to networks generated under the random graph model with a network density of $\lambda = 0.1$. For different configurations of asset holdings, the plots in Figure 4.6 show C5 asset holdings have the largest losses, for a high price impact exponent. As the losses are smaller under a higher network density, there are smaller differences between the different configurations. This shows the diversification of the bank's obligations can decrease the shortfall and number of banks with outstanding obligations.

Bankruptcy costs: We include bankruptcy costs for banks in the first round of clearing. We consider external and interbank bankruptcy costs for different network densities. As C1 holds no external assets, there is no change in its relative first-round contribution under external bankruptcy costs.

From Figure 4.7, we find that interbank bankruptcy costs largely decrease the relative total payments of the first round, compared with external bankruptcy costs. As there is a decrease in total first-round payments, this increases the bank's outstanding obligations in R2. A larger proportion of banks can meet outstanding obligations from R2 compared with R1. We find the largest impact of bankruptcy costs is for C3 and C5 configurations. The network density has an impact on the proportion of first-round total payments. When external bankruptcy costs are present, the first round proportion is smaller for $\lambda = 0.3$. This is different in the presence of interbank bankruptcy costs, which show a larger proportion of first-round payments in R1 for $\lambda = 0.3$. This shows that while a higher network density reduces the dependence on the second round for external bankruptcy costs, it also amplifies the dependence on interbank bankruptcy costs. This provides further considerations in assessing the resilience of a network of higher density when additional financial factors are included in the clearing process.

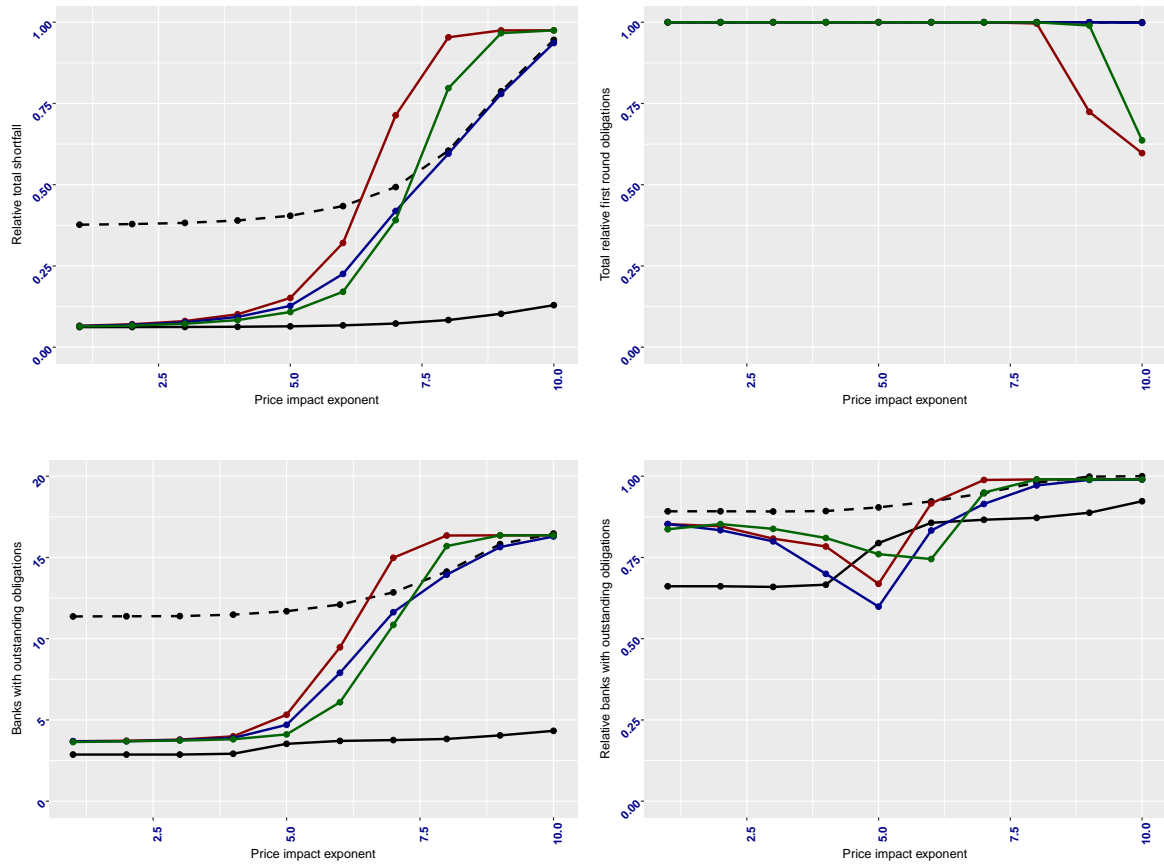


Figure 4.5: The plots represent the following metrics: Relative total shortfall \bar{H} (top left), relative total obligations from the first round $\bar{\mathcal{P}}$ (top right), the total number of banks with outstanding obligations $\Lambda^{\bar{R}2}$ (bottom left) and the relative total number of banks with outstanding obligations $\bar{\mathcal{V}}$ (bottom right) for $\lambda = 0.1$. The dashed line represents C1 and the colours represent different configurations with external asset holdings: black = C2, red = C3, blue = C4 and green = C5.

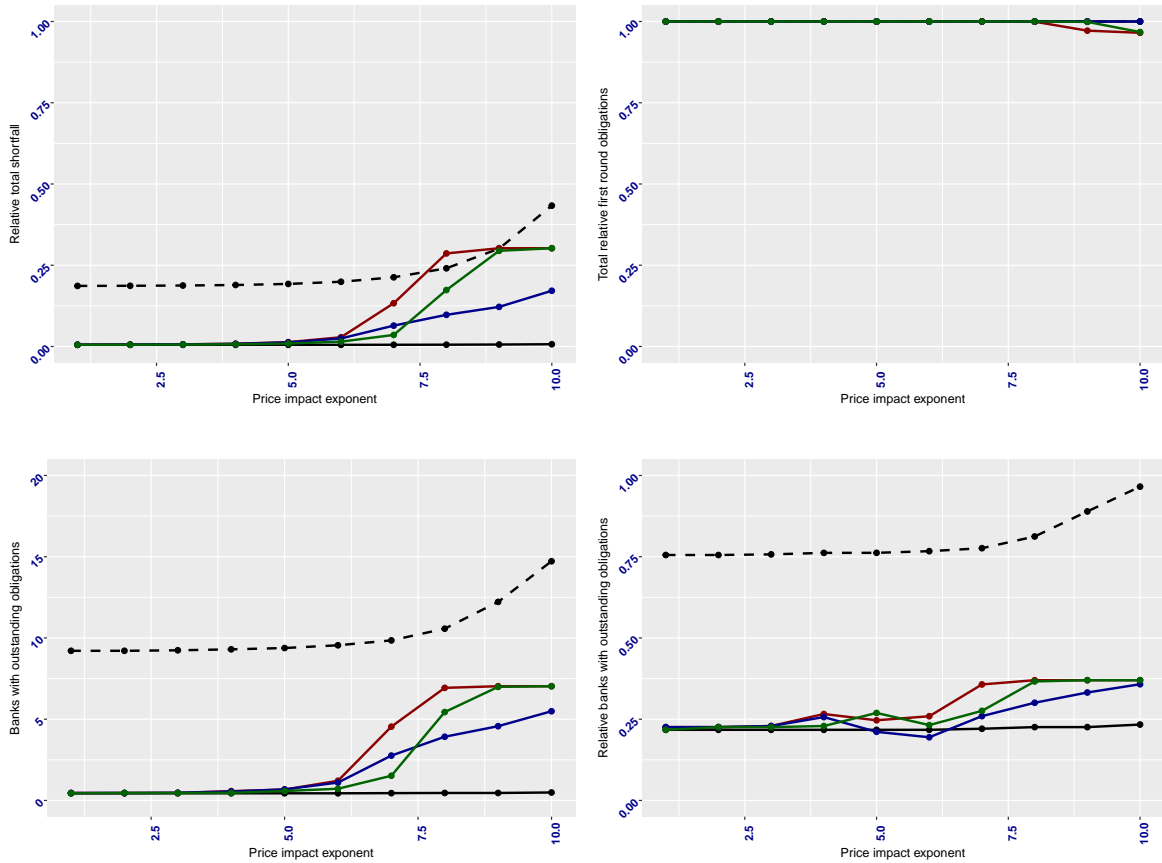


Figure 4.6: The plots represent the following metrics: Relative total shortfall \bar{H} (top left), relative total obligations from the first round $\bar{\mathcal{P}}$ (top right), the total number of banks with outstanding obligations $\Lambda^{\bar{R}2}$ (bottom left) and the relative total number of banks with outstanding obligations $\bar{\mathcal{V}}$ (bottom right) for $\lambda = 0.3$. The dashed line represents C1 and the colours represent different configurations with external asset holdings: black = C2, red = C3, blue = C4 and green = C5.

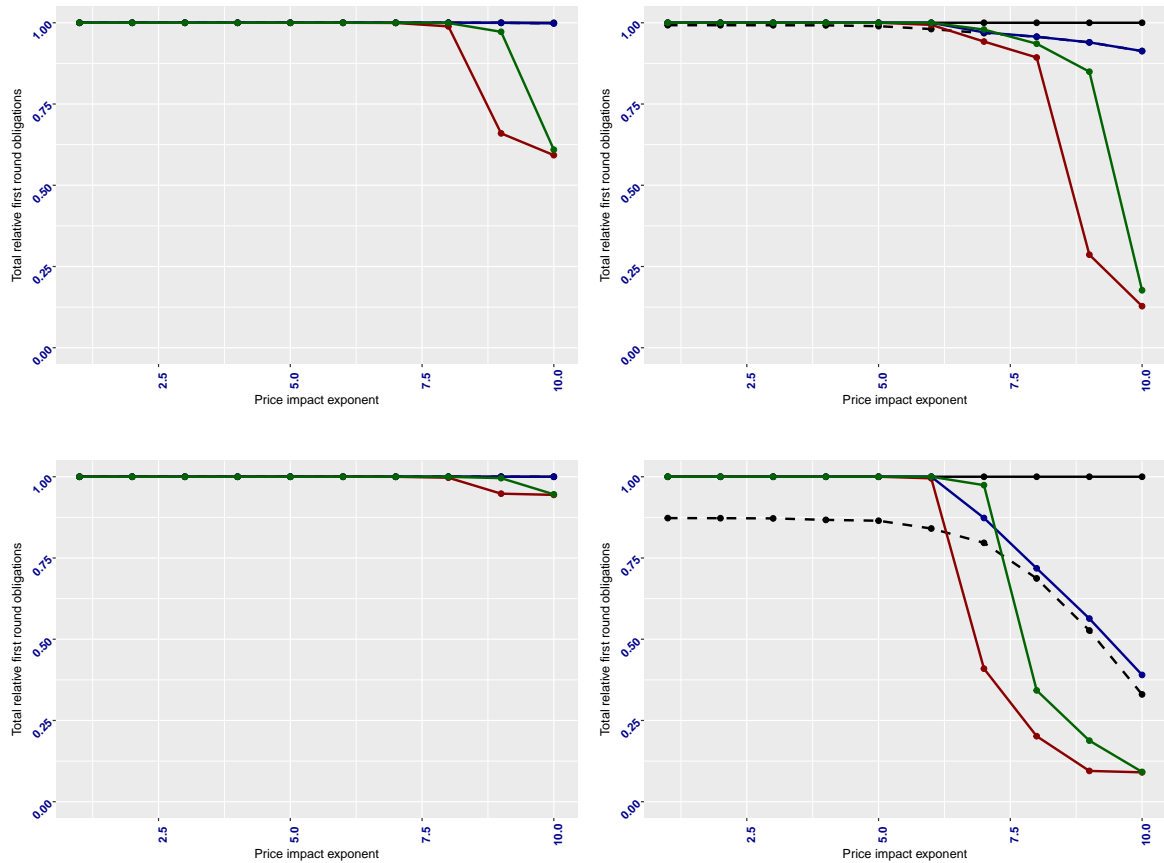


Figure 4.7: The plots represent the total relative first round payment $\bar{\mathcal{P}}$ with external bankruptcy costs $\gamma_i^1 = 0.1 \quad \forall i \in \mathcal{N}$ (left) and interbank bankruptcy costs $\gamma_i^2 = 0.1 \quad \forall i \in \mathcal{N}$ (right) for $\lambda = 0.1$ (top) and $\lambda = 0.3$ (bottom). The dashed line represents C1 and the colours represent different configurations with external asset holdings: black = C2, red = C3, blue = C4 and green = C5.

4.5 Conclusion

We extend the collateral model by Ghamami et al. (2022) and accounted for an additional channel of fire sales, incorporating two channels of fire sales. We established the fixed point of the clearing process and studied the changes for both clearing rounds. We were able to establish an ordering between the payments under different systems, and how this was reflected in the systemic risk metrics.

From the small network example, we illustrated that banks' losses are sensitive to the price impact. This was particularly the case when assets used as collateral were illiquid and banks held the same type of asset. This shows the compounding effect of fire sales, even if the illiquid asset used has a smaller price impact than other illiquid assets.

We extended our analysis to networks generated from a random graph model and distinguished losses between different clearing rounds. Our results showed configurations of banks' asset holdings with a high commonality between external asset holdings and assets used as collateral resulted in larger losses, compared with networks in which the bank held no external assets. This was evident for a high price impact and networks with a small density. Increasing the density and diversifying the obligations of banks in the network reduces the initial loss of banks, and decreases the fire sales impact on the bank's asset holdings.

From analysing the different stages of clearing, we find the importance of R2 when losses are large. If bankruptcy costs are present, the total payments from R2 in some cases contributed to $< 80\%$ of the total payments from banks. From the generated random networks and when the bank's losses are large, the R2 represents a significant contribution for banks to meet outstanding obligations in both clearing rounds.

Chapter 5

Ring-fencing banks in financial networks

5.1 Introduction

After the Global Financial Crisis, several reforms have been put in place worldwide to limit the propagation of shocks between financial institutions and between those and the real economy. Ring-fencing refers to separating retail services provided by banks, such as taking deposits from households and small businesses, from investment and international banking. According to the Independent Commission on Banking (ICB), which recommended its introduction, ring-fencing would (ICB, 2011): protect the provision of core financial services to retail customers — deposit-taking, making and receiving payments — from shocks that might impact riskier activities; make it easier to resolve banks without taxpayer support; reduce excessive risk-taking driven by the expectation of government guarantees. For example, ICB argues that (ICB, 2011) for the Royal Bank of Scotland:

The ring-fence would have isolated its EEA banking operations from its global markets activities where most of its losses arose. Together with more loss-absorbent debt, this would have given the authorities credible alternative options to injecting £45bn of taxpayer funds into the group — e.g. isolating the ring-fenced bank for sale or temporary public ownership and an orderly wind-down of the rest of the group at no public cost.

Ring-fencing has been introduced in the UK legislation with the Financial Services (Banking Reform) Act 2013 and it came into effect at the beginning of 2019, affecting banks with more than £25 billion in retail deposits.¹

We propose a theoretical model to analyse the implications of ring-fencing for systemic risk. In particular, we focus on one channel through which shocks can spread across

¹A full list of banking groups that have implemented ring-fencing is available in Bank of England (2022).

banks: solvency contagion. When one bank’s assets are hit by an exogenous shock, other banks re-evaluate the assets corresponding to their investment in that bank because they expect to recover a smaller proportion of their investment. As a consequence, the value of *their own* assets diminishes, triggering a second round of re-evaluations. Banks continue to adjust their asset valuations in subsequent rounds until the equilibrium valuation is reached (Bardoscia et al., 2019; Barucca et al., 2020). As a result, shocks propagate from one bank to another when their creditworthiness changes, even in the absence of defaults. This channel was especially active during the Global Financial Crisis. In fact, according to the Basel Committee on Banking Supervision, “roughly two-thirds of losses attributed to counterparty credit risk were due to CVA losses² and only about one-third were due to actual defaults” (BIS, 2011).

We treat the implementation of ring-fencing as an exogenous shock. In fact, ring-fencing requires some banking groups to split their activities between ring-fenced bodies (RFBs) and non-ring-fenced bodies (nRFBs). In our model, this means that the groups that implement ring-fencing allocate some of their assets and liabilities to their RFB and the remainder to their nRFB. Consistently with the spirit of the reform, RFBs can only hold *external* assets, corresponding for example to mortgages and corporate credit, and *external* liabilities, corresponding to deposits. In addition to those, nRFBs can also hold *interbank* assets, corresponding to investments in other banks, and interbank liabilities, corresponding to funding from other banks.³ In reality, the allocations of assets and liabilities are partly determined by law and regulations and partly by banks’ individual choices. In fact, while some activities must sit within RFBs and some other activities are “prohibited” and must sit within nRFBs, there are activities that banking groups can assign either to their RFB or to their nRFB, such as lending to large corporates. Within the context of our model, such allocation of assets and liabilities impacts the creditworthiness of RFBs and nRFBs in two ways. First, RFBs are insulated from counterparty credit risk because they do not hold interbank assets. Instead, nRFBs hold interbank assets and are exposed to counterparty credit risk, like banks before ring-fencing. Second, if external assets are allocated to RFBs and nRFBs in different proportions, also their leverage might change. We stress that these effects are mechanical, in the sense that they occur when assets and liabilities are allocated to RFBs and nRFBs, and *no further action is taken* to change either the size or the composition of the balance sheet of RFBs and nRFBs.

We now summarise our main results. First, we find conditions on the allocation of assets and liabilities that lead to a safer RFB, i.e. that make its probability of default smaller

²Credit Valuation Adjustment (CVA) losses originate from incorporating counterparty credit risk into asset valuations.

³As a consequence, RFBs cannot invest or receive funding from any nRFB, including the nRFB within their own group. Therefore, as in Farhi and Tirole (2021), any RFB is not exposed to the nRFB belonging to the same group.

than to its group prior to ring-fencing. When the net interbank lending of a bank is zero, this happens when a larger proportion of assets than liabilities is allocated to its RFB, so that its leverage decreases with respect to the external leverage of its group prior to ring-fencing. However, when a bank is a net lender (borrower) in the interbank market, in order to decrease the external leverage of its RFB and therefore make it safer, it needs to allocate proportionally more (fewer) assets or fewer (more) liabilities to their RFB compared to the case in which their net interbank lending is zero.

Second, we find conditions that lead to a less safe nRFB with respect to its group prior to ring-fencing. Since nRFBs can hold interbank assets of other nRFBs, their creditworthiness depends on the creditworthiness of other nRFBs. Indeed, a nRFB becomes less safe than its group prior to ring-fencing when *both that group and all the groups to which that group is directly or indirectly exposed* implement ring-fencing so that the leverage of their RFBs is sufficiently below the external leverage of their groups prior to ring-fencing. As a consequence, while those RFBs have a smaller probability of default with respect to their groups prior to ring-fencing, the corresponding nRFBs have larger external leverage than their groups prior to ring-fencing, and therefore also a larger probability of default. Third, we compare the equity of the group after the introduction of ring-fencing (i.e. the equity of the RFB plus the equity of the nRFB) with the equity of the group prior to ring-fencing. Interestingly, we find that the equity of the group after the introduction of ring-fencing does not depend on whether that group actually implements ring-fencing (and how), but only on whether the groups to which that group is directly or indirectly exposed implement ring-fencing (and how). We find that when *all the groups to which that group is directly or indirectly* exposed bring the leverage of their RFBs sufficiently below the external leverage of their groups prior to ring-fencing, then the equity of that group is smaller after the implementation of ring-fencing. Intuitively, when sufficiently more assets are allocated to a RFB to lower its external leverage, making it safer, fewer assets are allocated to the corresponding nRFB, thereby increasing its external leverage and making it less safe. However, a riskier nRFB has downstream effects on the other nRFBs exposed to it. The lost equity corresponds precisely to the loss in the value of interbank assets held by the nRFB that is exposed to these other riskier nRFBs. We stress that this result does not apply to a group if, for example, one of the groups to which that group is directly or indirectly exposed implements ring-fencing by increasing the external leverage of its RFB, or by not decreasing it sufficiently. In this case, the equity of that group would not necessarily be smaller after the implementation of ring-fencing.

Finally, we point out that the equity lost by one banking group after the implementation of ring-fencing is not gained by other banking groups. Indeed, if *all* groups implement ring-fencing so that their RFBs have a leverage sufficiently smaller than the external leverage of their groups prior to ring-fencing, then the aggregate equity of the banking system will be smaller after the implementation of ring-fencing.

Our model is necessarily stylised and therefore subject to some limitations. First, after the assets and liabilities of banking groups are allocated to RFBs and nRFBs, no further action is taken on the size or composition of their balance sheets. However, banking groups can react to the outcome of this allocation — either directly, or by responding to regulation — in several ways. One possibility is to deleverage the nRFB. Another possibility is to narrow the scope for solvency contagion, for example by reducing the exposure of the nRFB to other banks by converting some of its interbank assets into external assets, which corresponds to divesting from other banks and investing in the real economy. The alternative is to reallocate some external assets from the RFB to the nRFB. This reduces the external leverage of the nRFB, but it also increases the external leverage of the RFB, and therefore its probability of default. Second, while we make the simplifying assumption that RFBs cannot hold interbank assets, in reality, they could still be exposed to other RFBs. Those exposures could, everything else equal, lower their creditworthiness. Third, we assume that the intrinsic riskiness of external assets held by RFBs and nRFB is safe. In reality, by holding intrinsically safer assets, RFBs could be made safer when their leverages are larger than the external leverages of their groups prior to ring-fencing.

Empirical research on ring-fencing in the UK focused on a few key aspects. Erten et al. (2022) find that RFBs face lower funding costs than prior to the implementation of the reform, whereas nRFBs funding costs do not change significantly. To the extent that probabilities of default can be taken as a proxy for funding costs, our model can accommodate that outcome. This could happen, for example, if a RFB had a smaller external leverage than the group prior to ring-fencing, *and* if banks to which the nRFB is exposed had also reduced their external leverage. This could occur either mechanically, as a result of the external assets and liabilities allocated to those nRFBs, or because those nRFBs decided to deleverage after the implementation of ring-fencing. Chavaz and Elliott (2020) find that groups affected by ring-fencing substantially reduce their investment banking activities prior to the implementation of ring-fencing. Moreover, RFBs are able to offer lower interest rates on deposits than prior to ring-fencing due to the change in their funding mix. In contrast, while our model captures the change in liabilities due to the implementation of ring-fencing, it does not capture any difference in banks' funding mix.

A larger literature explores the broader implications of separating retail and investment banking. Caprio et al. (2007) find that banks in countries that impose greater restrictions on bank activities tend to have lower valuations than in countries that impose fewer restrictions. Laeven and Levine (2007) find that valuations of groups that engage both in lending and non-lending activities are lower than if the groups were broken down into specialised entities. Indeed, our model predicts that, when all banking groups implement ring-fencing so that the external leverage (and therefore the riskiness) of RFBs decreases,

the equity valuation of banking groups decreases. Cornett et al. (2002) find that commercial banks with an investment subsidiary have larger cash returns on their assets, without being riskier. A number of studies (Kroszner and Rajan, 1994; Puri, 1994, 1996; Gande et al., 1997; Drucker and Puri, 2005) focuses on whether bundling retail and investment banking leads to synergies or conflicts of interest, and on the implications for their clients (Neuhann and Saidi, 2018; Akiyoshi, 2019). Theoretical studies suggest that separating retail and investment banking could reduce moral hazard and risk-taking (Boyd et al., 1998; Freixas et al., 2007; Farhi and Tirole, 2021).

We model solvency contagion due to the re-evaluation of interbank assets as in Bardoscia et al. (2019) and Barucca et al. (2020).⁴ This means that in contrast with models of contagion on default (Eisenberg and Noe, 2001; Rogers and Veraart, 2013), shocks propagate to counterparties even in the absence of defaults. Risks stemming from this channel appear to have peaked during the GFC and sharply decreased since (Bardoscia et al., 2019), but to be concentrated (Fink et al., 2016). Several studies have investigated how structural features of the financial network impact its stability and resilience to shocks (Allen and Gale, 2000; Freixas et al., 2007; Nier et al., 2007; Gai and Kapadia, 2010; Battiston et al., 2012a,b; Elliott et al., 2014; Acemoglu et al., 2015; Bardoscia et al., 2017). Here, even though the implementation of ring-fencing changes affects banks' balance sheets, it does not change the underlying structure of the financial network. In fact, RFBs are fully isolated from the rest of the network and the network of nRFBs is identical to the network of banking groups prior to ring-fencing.

This chapter is organised as follows. In Section 5.2 we discuss the institutional details of ring-fencing in the UK and briefly compare it to some other jurisdictions, in Section 5.3 we introduce a simple model of ring-fencing for one bank, whereas in Section 5.4 we extend the model to the case of multiple banks interconnected in a financial network and derive our main results. We draw our conclusions in Section 5.5.

5.2 Institutional details

The UK ring-fencing regime has required banks with more than £25 billion in retail deposits to separate their retail and investment activities by the beginning of 2019. In practice, this means that such banks must create a new legal entity, the ring-fenced bank (RFB). The legislation specifies “core activities”, which can be provided only by RFBs, and “prohibited activities”, which cannot be provided by RFBs. The following lists closely follow Britton et al. (2016). Core activities include taking deposits from retail and SMEs in the UK. whereas prohibited activities include: Trading and selling securities, commodities and derivatives; having exposures to financial institutions other

⁴For alternative valuation frameworks, see Elsinger et al. (2006); Fischer (2014); Veraart (2020). For earlier work on pre-default contagion, see Bardoscia et al. (2015, 2016); Fink et al. (2016).

than other RFBs; having operations outside the EEA; underwriting securities; buying securitisations of other financial institutions. Prohibited activities can be provided by other entities within the same banking group. For convenience, we collectively refer to those entities as the non-ring-fenced bank (nRFB). Some other activities can be provided both by RFBs and by nRFBs: deposit-taking activities for large corporates and other RFBs; lending to individuals and corporates; transactions with central banks; holding own securitisations; trade finance; payment services; hedging liquidity, interest rate, currency, commodity and credit risks; selling simple derivatives to corporates and other RFBs.

Importantly, the RFB is required to be independent of the nRFB within the same banking group. This means, for example, that the RFB governance and management should allow the RFB to make decisions in its own interest, independently of the rest of the group. It also means that the RFB is subject to capital and liquidity requirements separately from other entities within the banking group. Finally, the financial relationships between the RFB and the nRFB within the same group, if any, should not be privileged when compared to those between the RFB and other financial institutions.

An independent review of the ring-fencing regime in the UK has been recently published (Ring-fencing and Proprietary Trading Independent Review, 2022). The final report acknowledges that the regime has made the UK banking system safer because RFBs are easier to supervise. However, it also recognises that the definition of critical functions provided by banks has broadened since the original recommendation by the ICB to include activities that fall within nRFBs (see PRA (2014)). Moreover, it suggests that the resolution regime might be sufficient for implicit government guarantees to too-big-to-fail banks and that ring-fencing might be redundant in this respect. The report includes several recommendations, on which the UK government has announced the intention to consult (HMT, 2022; HMT, 2023).

A similar structural separation was initially proposed (Liikanen, 2012) and then rejected in the EU. In the US the 1933 Glass-Steagall Act prohibited banks that took insured deposits from providing investment banking activities. This separation was stronger than the current UK ring-fencing regime, as the deposit-taker and the entity providing investment banking activities could not be part of the same banking group. The provisions of the 1933 Glass-Steagall Act were gradually relaxed over time, eventually allowing those entities to be part of the same group (for more details, see Appendix A in Chavaz and Elliott (2020)). This remains the case after the GFC when the Dodd-Frank Act imposed further restrictions on the relationships between the two entities.

5.3 Ring-fencing one bank

We start by discussing the mechanics of ring-fencing one bank. We consider one bank that, prior to ring-fencing, has assets A and liabilities (debt) L .⁵ After ring-fencing, the bank is split into two separate entities: the ring-fenced bank (RFB) with assets A^{RF} and liabilities L^{RF} , and the non-ring-fenced bank (nRFB) with assets A^{nRF} and liabilities L^{nRF} . Total assets and liabilities of the bank prior to ring-fencing are simply $A = A^{\text{RF}} + A^{\text{nRF}}$ and $L = L^{\text{RF}} + L^{\text{nRF}}$. A and L can be also interpreted as the total assets and liabilities of the banking group that consolidates the balance sheets of the RFB and nRFB after the implementation of ring-fencing.

Let $\psi^A \in [0, 1]$ and $\psi^L \in [0, 1]$ be respectively the fraction of total assets and liabilities of the RFB. Therefore, $1 - \psi^A$ and $1 - \psi^L$ are the fraction of the total assets and liabilities of the nRFB:

$$A^{\text{RF}} = \psi^A A, \quad A^{\text{nRF}} = (1 - \psi^A)A, \quad (5.1a)$$

$$L^{\text{RF}} = \psi^L L, \quad L^{\text{nRF}} = (1 - \psi^L)L. \quad (5.1b)$$

For all entities, equities are defined as the difference between assets and liabilities:

$$E = A - L, \quad (5.2a)$$

$$E^{\text{RF}} = A^{\text{RF}} - L^{\text{RF}} = \psi^A A - \psi^L L, \quad (5.2b)$$

$$E^{\text{nRF}} = A^{\text{nRF}} - L^{\text{nRF}} = (1 - \psi^A)A - (1 - \psi^L)L. \quad (5.2c)$$

Therefore, we have that the equity of the bank prior to ring-fencing (or of the consolidated group) is equal to the sum of the equities of the RFB and of the nRFB:

$$E = E^{\text{RF}} + E^{\text{nRF}}. \quad (5.3)$$

Eq. (5.3) may seem very intuitive, but we anticipate that this identity will not necessarily hold for banks embedded in a financial network.

The corner cases $\psi^A = 0$ and $\psi^A = 1$ correspond to transferring all assets to the RFB or to the nRFB. $\psi^L = 0$ means that the RFB is fully funded by equity ($E^{\text{RF}} = \psi^A A$), whereas $\psi^L = 1$ means that the nRFB is fully funded by equity ($E^{\text{nRF}} = (1 - \psi^A)A$). Starting from a solvent bank ($E > 0$) it is certainly possible to implement ring-fencing, i.e. to pick ψ^A and ψ^L so that either the RFB or the nRFB are not solvent. We rule out those cases as there would be no point in implementing ring-fencing if one of the two entities were not solvent. More precisely, we say that ring-fencing with the pair (ψ^A, ψ^L) is *feasible* or that the bank *implements ring-fencing feasibly* if $E^{\text{RF}} > 0$ and $E^{\text{nRF}} > 0$.

⁵We refer to the entity prior to the implementation of ring-fencing as to the “bank” or to the “banking group” interchangeably.

In the following, we will assume that (ψ^A, ψ^L) is feasible. We note that if (ψ^A, ψ^L) is feasible, also the bank prior to ring-fencing is solvent ($E > 0$).

We now introduce the *leverage* of the bank prior to ring-fencing and of the RFB and nRFB. Provided that they are solvent (i.e. that their equities are strictly positive), the leverages of the bank prior to ring-fencing, the RFB, and the nRFB are the ratios between their assets and equity:

$$\lambda = \frac{A}{E} \quad (5.4a)$$

$$\lambda^{\text{RF}} = \frac{A^{\text{RF}}}{E^{\text{RF}}} = \frac{\psi^A A}{E^{\text{RF}}} \quad (5.4b)$$

$$\lambda^{\text{nRF}} = \frac{A^{\text{nRF}}}{E^{\text{nRF}}} = \frac{(1 - \psi^A)A}{E^{\text{nRF}}}. \quad (5.4c)$$

The relationship between the leverages of the RFB and the nRFB depends on ψ^A and ψ^L . We have the following result.

Proposition 5.3.1. *Let the bank implement ring-fencing feasibly, i.e. let the RFB and nRFB be solvent. The following statements are equivalent:*

- A larger proportion of assets than liabilities is allocated to the RFB:

$$\psi^A \geq \psi^L,$$

- The leverage of the RFB is smaller than the leverage of the bank prior to ring-fencing:

$$\lambda^{\text{RF}} \leq \lambda,$$

- The leverage of the nRFB bank is larger than the leverage of the bank prior to ring-fencing:

$$\lambda \leq \lambda^{\text{nRF}}.$$

Similar equivalences hold with reversed inequalities.

One immediate implication of Proposition 5.3.1 is that there are three possibilities. First, $\psi^A > \psi^L$, in which case we have that $\lambda^{\text{RF}} < \lambda < \lambda^{\text{nRF}}$. Second, $\psi^A < \psi^L$, in which case we have that $\lambda^{\text{RF}} > \lambda > \lambda^{\text{nRF}}$. Third, $\psi^A = \psi^L$, in which case we have that $\lambda^{\text{RF}} = \lambda = \lambda^{\text{nRF}}$. As a consequence, if the RFB has a smaller leverage than the bank prior to ring-fencing, the nRFB must necessarily have a larger leverage.

So far we have made no explicit assumptions on the intrinsic riskiness of the assets. Let us assume that assets A follow a geometric Brownian motion: $dA(t) = \mu A(t)dt + \sigma A(t)dW(t)$, where μ is the drift and σ the volatility. In order to introduce probabilities of default, we assume that investors are risk-neutral. In this context, the probability

of default in the interval $[t, T]$ is defined as the probability that the equity of the bank is negative at time T , conditional on the information available at time t . When there are no arbitrage opportunities and the market is complete, it can be computed as the conditional risk-neutral expectation $p_{[t,T]} = \mathbb{E}^{\mathbb{Q}} [\mathbb{1}_{E(T) < 0} | A(t)]$, where $A(t)$ is the value of assets observed at time t . By further assuming that no dividends are distributed and that the risk-free rate is equal to zero, we have (Merton, 1974):

$$p_{[t,T]} = 1 - \mathcal{N} \left[\frac{\log \frac{A(t)}{A(t) - E(t)} - \frac{\sigma^2(T-t)}{2}}{\sigma \sqrt{T-t}} \right], \quad (5.5)$$

where \mathcal{N} is the cumulative distribution function of the normal distribution. For convenience, in the following, we drop the dependence on time, as we consider all quantities to be observed at time t . Eq. (5.5) can be re-written as:

$$p_{[t,T]} = 1 - \mathcal{N} \left[\frac{\log \frac{\lambda}{\lambda-1} - \frac{\sigma^2(T-t)}{2}}{\sigma \sqrt{T-t}} \right],$$

which is a function only of the leverage λ and the volatility σ . More precisely, $p_{[t,T]}$ is an increasing function of both λ and σ . This property is shared also by other credit structural models, such as Black and Cox (1976), in which banks default as soon as their equity becomes negative.

By multiplying both sides of $dA(t)$ by ψ^A and $1 - \psi^A$, we have that: $dA^{\text{RF}}(t) = \mu A^{\text{RF}}(t)dt + \sigma A^{\text{RF}}(t)dW(t)$ and that $dA^{\text{nRF}}(t) = \mu A^{\text{nRF}}(t)dt + \sigma A^{\text{nRF}}(t)dW(t)$, meaning that both A^{RF} and A^{nRF} follow the same geometric Brownian motion as A . By combining Proposition 5.3.1 with the fact that $p_{[t,T]}$ is increasing with λ we have the following result.

Corollary 5.3.2. *Let the bank implement ring-fencing feasibly, i.e. let the RFB and nRFB be solvent, and let probabilities of default be increasing functions of leverage.*

If a larger proportion of external assets than external liabilities is allocated to the RFB:

$$\psi^A \geq \psi^L,$$

then the probability of default of the RFB is smaller than or equal to the probability of default of the bank prior to ring-fencing, which is, in turn, smaller than or equal to the probability of default of the nRFB:

$$p_{[t,T]}^{\text{RF}} \leq p_{[t,T]} \leq p_{[t,T]}^{\text{nRF}}.$$

Vice versa, if a smaller proportion of external assets than external liabilities is allocated

to the RFB:

$$\psi^A \leq \psi^L,$$

then the probability of default of the RFB is larger than or equal to the probability of default of the bank prior to ring-fencing, which is, in turn, larger than or equal to the probability of default of the nRFB:

$$p_{[t,T]}^{RF} \geq p_{[t,T]} \geq p_{[t,T]}^{nRF}.$$

This result is intuitive: if $\psi^A \geq \psi^L$ the RFB is *less* leveraged than the bank prior to ring-fencing, which is less leveraged than the nRFB. Therefore, the probability of default of the RFB is smaller than the probability of default of the bank prior to ring-fencing, which is, in turn, smaller than the probability of default of the nRFB. Corollary 5.3.2 will serve as the blueprint of similar results in the case in which banks are embedded in a financial network.

5.4 Ring-fencing banks in a financial network

Now we consider a set of N banks, prior to the implementation of ring-fencing, denoted with $\mathcal{N} = \{1, \dots, N\}$. In this framework, we assume banks are able to lend to each other. When bank i lends to bank j , bank i holds an interbank asset A_{ij} and bank j holds a matching interbank liability $L_{ji} = A_{ij}$. We denote the total interbank assets and liabilities of bank i with $\bar{A}_i = \sum_{j=1}^N A_{ij}$ and $\bar{L}_i = \sum_{j=1}^N L_{ij}$ respectively. The matrices of interbank assets \mathbf{A} (or equivalently of interbank liabilities \mathbf{L}) can be thought of as the weighted adjacency matrix of the interbank network. It will be useful to denote with \mathcal{G}^A and \mathcal{G}^L respectively the graphs defined by the weighted adjacency matrices \mathbf{A} and \mathbf{L} . In addition to interbank assets and liabilities, each bank i also holds external assets A_i^e and external liabilities L_i^e . In order to avoid corner cases we assume that $A_i^e > 0$ for all i , that is that all banks prior to ring-fencing hold some (possibly very small amount of) external assets.

Ring-fencing is implemented similarly to Section 5.3, with the additional assumption that RFBs can only hold external assets and liabilities, or equivalently that only nRFBs can hold interbank assets and liabilities. Indeed, interbank assets and liabilities appear to constitute a negligible proportion of RFBs balance sheets at the end of 2020 (see Figures 3.3 and 3.4 in RFPT, 2022). External assets are investments in entities outside the financial network, such as mortgages or corporate lending. External liabilities correspond to funding provided by entities outside the financial network, such as deposits or bonds. In practice, deposit-taking from households and SMEs must be carried out by RFBs, but deposit-taking from large corporates and lending to households and corporates can be carried out either by RFBs or by nRFBs. Therefore, external assets and liabilities can

be held both by RFBs and nRFBs.⁶

Let Ψ^A and Ψ^L , with $\psi_i^A \in [0, 1]$ and $\psi_i^L \in [0, 1]$, for $i = 1, \dots, N$ be respectively the vectors of the fractions of *external* assets and liabilities of the RFB. External assets and liabilities of the RFB i are equal to $\psi_i^A A_i^e$ and $\psi_i^L L_i^e$, whereas external assets and liabilities of the nRFB i are equal to $(1 - \psi_i^A) A_i^e$ and $(1 - \psi_i^L) L_i^e$. If $\psi_i^A = 0 = \psi_i^L$ no assets or liabilities are transferred to the RFB i , meaning that in practice no ring-fenced entity is created from bank i . Formally, in our model, this corresponds to the nRFB i being equal to bank i prior to the implementation of ring-fencing. For this reason, we also refer to banks that after the implementation of ring-fencing have not actually created any ring-fenced entity as nRFBs. As a consequence, we can split banks into two sets. Let:

$$\overline{\mathcal{R}} = \{i \in \mathcal{N} : \psi_i^A = 0 \quad \text{and} \quad \psi_i^L = 0\}, \quad (5.6)$$

be the set of banks that do not implement ring-fencing i.e. that do not transfer any assets or liabilities to a RFB. Let:

$$\mathcal{R} = \mathcal{N} \setminus \overline{\mathcal{R}} \quad (5.7)$$

be a set of banks that implement ring-fencing, i.e. that transfer some assets or liabilities to a RFB. Clearly, $\mathcal{R} \cup \overline{\mathcal{R}} = \mathcal{N}$. In order to avoid corner cases, we assume that $\psi_i^A < 1$ for all i , that is all nRFBs hold some (possibly very small amount of) external assets.

As already mentioned, in reality, ψ_i^A and ψ_i^L are partly determined by law and regulation and partly by banks' choices. For example, banks that are not required to implement ring-fencing are unlikely to implement it purely by choice and will therefore be part of $\overline{\mathcal{R}}$. Banks that are required to implement ring-fencing must allocate assets and liabilities corresponding to core activities to their RFB and assets and liabilities corresponding to prohibited activities to their nRFB but can choose where to allocate assets and liabilities corresponding to neither core nor prohibited activities. Therefore, banks that implement ring-fencing can choose, to a certain extent, both ψ_i^A and ψ_i^L .

5.4.1 Naive equity and external leverage

Banks that hold interbank assets (i.e. banks prior to ring-fencing and nRFBs) perform a valuation of their interbank assets based on the creditworthiness of their counterparties. As explained in Section 5.4.2, these valuations will impact their equity. For the moment, we introduce *naive equities*, which do *not* incorporate valuations of interbank assets. Therefore, they are defined as the difference between total assets and liabilities computed

⁶Because we assume RFBs cannot hold interbank assets or liabilities, they are completely disconnected from the financial network, including from the nRFB within their own group. In reality, while RFBs cannot be exposed to nRFBs, they could still be exposed to other RFBs, and they could be funded by nRFBs. In other words, RFBs could still hold interbank assets (towards other RFBs) and interbank liabilities (from other RFBs and nRFBs). Accounting for this possibility would, however, considerably complicate the analysis.

by taking interbank assets at their face value and are denoted with the superscript 0. For banks prior to ring-fencing and nRFBs, we have, for all i :

$$E_i^0 = A_i^e + \bar{A}_i - L_i^e - \bar{L}_i \quad (5.8a)$$

$$= A_i^e + \sum_{j=1}^N A_{ij} - L_i^e - \sum_{j=1}^N L_{ij} \quad (5.8b)$$

$$E_i^{\text{nRF},0} = (1 - \psi_i^A)A_i^e + \bar{A}_i - (1 - \psi_i^L)L_i^e - \bar{L}_i, \quad (5.8c)$$

$$= (1 - \psi_i^A)A_i^e + \sum_{j=1}^N A_{ij} - (1 - \psi_i^L)L_i^e - \sum_{j=1}^N L_{ij}. \quad (5.8d)$$

RFBs do not hold interbank assets, and therefore we do not distinguish between their naive equities ($E_i^{\text{RF},0}$) and the equities that incorporate the valuation of interbank assets (E_i^{RF}). For all i :

$$E_i^{\text{RF},0} = E_i^{\text{RF}} = \psi_i^A A_i^e - \psi_i^L L_i^e. \quad (5.8e)$$

Analogously to Section 5.3, we have that the naive equity of the bank i prior to ring-fencing (or of the consolidated group) is equal to the sum of the equity of the RFB and of the naive equity of the nRFB:

$$E_i^0 = E_i^{\text{RF}} + E_i^{\text{nRF},0}. \quad (5.9)$$

Similarly to Section 5.3, we rule out cases in which either at least one RFB is not solvent (there exists i such that $E_i^{\text{RF}} \leq 0$) or in which at least one nRFB is not *naively* solvent (there exists i such that $E_i^{\text{nRF},0} \leq 0$). We define the pair (Ψ^A, Ψ^L) to be *feasible* if all pairs (ψ_i^A, ψ_i^L) are feasible, i.e. if $E_i^{\text{RF}} > 0$ and $E_i^{\text{nRF},0} > 0$, for all i . When the pair (ψ_i^A, ψ_i^L) is feasible we also say that bank i implements ring-fencing feasibly and when the pair (Ψ^A, Ψ^L) is feasible that all banks implement ring-fencing feasibly. In the following we will assume that (Ψ^A, Ψ^L) is always feasible. If (Ψ^A, Ψ^L) is feasible, also all banks prior to ring-fencing are naively solvent ($E_i^0 > 0$, for all i).

When banks are embedded in a financial network an important role is played by the external leverage, that is the leverage restricted to external assets. More precisely, we introduce the *naive external leverage*, which is computed with naive equities. Provided that they are naively solvent (i.e. that their naive equities alter strictly positive), the naive external leverages of bank i prior to ring-fencing and of RFB i and nRFB i are the

ratios between their external assets and naive equity:

$$B_i^0 = \frac{A_i^e}{E_i^0} \quad (5.10a)$$

$$B_i^{\text{RF},0} = \frac{\psi_i^A A_i^e}{E_i^{\text{RF},0}} \quad (5.10b)$$

$$B_i^{\text{nRF},0} = \frac{(1 - \psi_i^A) A_i^e}{E_i^{\text{nRF},0}}. \quad (5.10c)$$

As RFBs do not hold interbank assets, their assets are only external and their equities are equal to their naive equities. Hence, the naive external leverage of a RFB is equal to its leverage, i.e. for all i :

$$B_i^{\text{RF},0} = \frac{\psi_i^A A_i^e}{E_i^{\text{RF},0}} = \frac{\psi_i^A A_i^e}{E_i^{\text{RF}}} = \lambda_i^{\text{RF}}.$$

It is possible to extend Proposition 5.3.1 to the case in which banks are embedded in a financial network.

Proposition 5.4.1. *Let bank i implement ring-fencing feasibly, i.e. let RFB i and nRFB i be naively solvent. The following statements are equivalent:*

- *The allocation of assets and liabilities to the RFB is such that:*

$$\psi_i^A (L_i^e - (\bar{A}_i - \bar{L}_i)) \geq \psi_i^L L_i^e.$$

- *The leverage of the RFB is smaller than the naive external leverage of the bank prior to ring-fencing:*

$$\lambda_i^{\text{RF}} \leq B_i^0.$$

- *The naive external leverage of the nRFB bank is larger than the naive external leverage of the bank prior to ring-fencing:*

$$B_i^0 \leq B_i^{\text{nRF},0}.$$

Similar equivalences hold with reversed inequalities.

Proposition 5.3.1 means that, in the case of one bank, the knowledge ψ^A and ψ^L is sufficient to determine whether implementing ring-fencing decreases the leverage of the RFB and increases the leverage of the nRFB with respect to the bank prior to ring-fencing. Instead, when bank i is embedded in a financial network, the knowledge ψ_i^A and ψ_i^L is not sufficient anymore, and one needs to know also *net* interbank assets $\bar{A}_i - \bar{L}_i$ and external liabilities L_i^e . In particular, we have that:

Corollary 5.4.2. *Let bank i implement ring-fencing feasibly, i.e. let RFB i and nRFB i be naively solvent. If:*

$$\bar{A}_i - \bar{L}_i \geq L_i^e,$$

then:

$$\lambda_i^{RF} \geq B_i^0 \geq B_i^{nRF,0}.$$

If *net* interbank assets of bank i are larger than (or equal to) its external liabilities, then implementing ring-fencing increases the leverage of the RFB i and decreases the naive external leverage of the nRFB i with respect to bank i prior to ring-fencing.

By comparing Proposition 5.4.1 with Proposition 5.3.1 we can assess the impact of interbank lending and borrowing on naive external leverage. Let us recall from Proposition 5.3.1 that, when a bank is not embedded in a financial network, that is when that bank does not lend or borrow from other banks, then allocating a larger proportion of assets than liabilities to the RFB ($\psi^A > \psi^L$) has the effect of lowering the leverage of the RFB ($\lambda^{RF} < \lambda$). When the net interbank lending of bank i is equal to zero ($\bar{A}_i = \bar{L}_i$), then the condition to lower the naive external leverage of the RFB is the same as when bank i does not lend to and borrow from other banks ($\psi_i^A > \psi_i^L$).

However, when bank i is a net lender to other banks ($\bar{A}_i > \bar{L}_i$), in order to lower the leverage of its RFB ($\lambda_i^{RF} < B_i^0$), bank i needs to allocate proportionally more assets (or fewer liabilities) to the RFB with respect to the case in which its net interbank lending is zero. Similarly, when bank i is a net borrower from other banks ($\bar{A}_i < \bar{L}_i$) in order to lower the leverage of its RFB ($\lambda_i^{RF} < B_i^0$), bank i needs to allocate proportionally fewer assets (or more liabilities) to the RFB with respect to the case in which its net interbank lending is zero.

5.4.2 Valuation framework

Banks that hold interbank assets perform the valuation of their interbank assets by applying a discount factor known as *valuation function*.⁷ Intuitively, valuation functions quantify banks' creditworthiness. When the valuation function of bank i is equal to one, other banks that have invested in it expect to recover their investment fully and therefore take their investment at face value. Conversely, when the valuation function of bank i is equal to zero, other banks expect to recover nothing, and therefore fully write off the corresponding asset.

Following Barucca et al. (2020), it is convenient to introduce valuation functions by isolating their dependence on equity (E) from their dependence on additional quantities (\mathcal{C}).⁸

⁷Clearly such valuation is performed only by banks that hold interbank assets, that is by banks prior to ring-fencing or by nRFBs.

⁸In Barucca et al. (2020) the valuation function of bank i can in principle depend on the vector

Definition 5.4.3 (Valuation function, Barucca et al. (2020)). *A function $\mathbb{V} : \mathbb{R} \rightarrow [0, 1]$ is called a feasible valuation function if and only if:*

- *It is non-decreasing $E \leq E' \implies \mathbb{V}(E|\mathcal{C}) \leq \mathbb{V}(E'|\mathcal{C}) \quad \forall E, E' \in \mathbb{R}$*
- *It is continuous from above.*

Valuation functions decrease with the equity because all other things being equal, a smaller equity indicates a deterioration of the creditworthiness and therefore a smaller discount factor. Continuity from above is a technical requirement and its usefulness will be clarified later.

The valuation of interbank assets feeds into equity valuations. The equity valuation of bank i will depend on the valuation of bank i 's interbank assets and, via valuation functions, on the equity valuations of bank i 's counterparties. In equilibrium, equity valuations \mathbf{E}^* of all banks are self-consistent and, for all i , satisfy:

$$E_i^* = A_i^e + \sum_{j=1}^N A_{ij} \mathbb{V}(E_j^* | \mathcal{C}_j) - L_i^e - \sum_{j=1}^N L_{ij}, \quad (5.11a)$$

$$E_i^{\text{nRF},*} = (1 - \psi_i^A) A_i^e + \sum_{j=1}^N A_{ij} \mathbb{V}(E_j^{\text{nRF},*} | \mathcal{C}_j^{\text{nRF}}) - (1 - \psi_i^L) L_i^e - \sum_{j=1}^N L_{ij}, \quad (5.11b)$$

which is analogous to (5.8), but with valuation functions. As anticipated, with \mathcal{C}_j and $\mathcal{C}_j^{\text{nRF}}$ we denote quantities on which valuation functions depend, in addition to equity. We note that \mathbf{E}^* can be negative. Therefore, those should be interpreted as valuations of banks' net worth and the valuations of shares held by investors that enjoy limited liability.

In general, the set of equations (5.11a) and (5.11b) admit more than one solution, but in Barucca et al. (2020) it is shown that they always admit one *greatest solution*, i.e. one solution in which the equity of each bank is not smaller than its equity in any other solution. In other words, there are no solutions in which any bank is better off than the greatest solution. Moreover, the greatest solution can be easily computed iteratively by starting from naive equities \mathbf{E}^0 and $\mathbf{E}^{\text{nRF},0}$ and by iterating (5.11a) and (5.11b) until convergence. Further details on the existence and convergence of the greatest solution is provided in Appendix 8.F. From this point onwards we will focus on equities corresponding to the greatest solution, which we will denote with \mathbf{E}^* for banks prior to ring-fencing and with $\mathbf{E}^{\text{nRF},*}$ for nRFBs.

We define the (non-naive) *external leverage* of each bank prior to ring-fencing and nRFB as the ratio between their external assets and their equity valuations. Since the greatest

of equities of all banks. Here we simplify the exposition by focusing on the case in which it depends explicitly only on the quantities relative to bank i .

solution for equities is smaller than or equal to naive equities (both for banks prior to ring-fencing and for nRFBs), assuming that (ψ_i^A, ψ_i^L) is feasible does not ensure that $E_i^* > 0$ or that $E_i^{\text{nRF}*} > 0$. Therefore, in order to introduce the external leverage, we need to explicitly assume that the equity valuations banks prior to ring-fencing and of nRFBs are strictly positive. Provided that they are solvent (i.e. that their equity valuations are strictly positive), the external leverages of bank i prior to ring-fencing and of nRFB i are the ratios between their external assets and equity valuations:

$$B_i^* = \frac{A_i^e}{E_i^*} \quad (5.12a)$$

$$B_i^{\text{nRF},*} = \frac{(1 - \psi_i^A)A_i^e}{E_i^{\text{nRF},*}}. \quad (5.12b)$$

In the following, we will consider valuation functions that depend explicitly only on external leverage and on the volatility of external assets. Before introducing formally such a class of valuation functions, we motivate this choice by following the approach in Bardoscia et al. (2019). In order to keep the notation light, let us focus for a moment on banks prior to ring-fencing. The same line of reasoning applies to nRFBs.

Bardoscia et al. (2019) derive the functional form for valuation functions under the following assumptions: (i) the recovery rate on defaulted interbank assets is equal to zero⁹; (ii) the external assets of banks follow independent geometric Brownian motions with drifts $\boldsymbol{\mu}$ and volatilities $\boldsymbol{\sigma}$; (iii) banks perform a risk-neutral valuation of interbank assets; (iv) there are no arbitrage opportunities and the market is complete; (v) banks do not distribute dividends; (vi) the risk-free rate is equal to zero. Bardoscia et al. (2019) consider, two different definitions of banks' default. If banks default when their equities are smaller than or equal to zero at time T (as in Merton (1974)), then the valuation functions at time $t \leq T$ are:

$$\mathbb{V}(E(t)|\mathcal{C}(t)) = \begin{cases} 1 & \text{if } E(t) \geq A^e(t), \\ \mathcal{N}\left[\frac{\log \frac{A^e(t)}{A^e(t)-E(t)} - \frac{\sigma^2(T-t)}{2}}{\sigma\sqrt{T-t}}\right] & \text{if } E(t) < A^e(t). \end{cases} \quad (5.13a)$$

If banks default as soon as their equities become smaller than or equal to zero between times t and T (as in Black and Cox (1976)), then the valuation functions at time $t \leq T$

⁹Valuation functions can still be larger than zero because there is uncertainty on whether defaults will occur or not in the future.

are:

$$\mathbb{V}(E(t)|\mathcal{C}(t)) = \begin{cases} 1 & \text{if } E(t) \geq A^e(t), \\ \mathcal{N}\left[\frac{\log \frac{A^e(t)}{A^e(t)-E(t)} - \frac{\sigma^2(T-t)}{2}}{\sigma\sqrt{T-t}}\right] - \frac{A^e(t)}{A^e(t)-E(t)} \mathcal{N}\left[\frac{-\log \frac{A^e(t)}{A^e(t)-E(t)} - \frac{\sigma^2(T-t)}{2}}{\sigma\sqrt{T-t}}\right] & \text{if } 0 \leq E(t) < A^e(t), \\ 0 & \text{if } E(t) < 0. \end{cases} \quad (5.13b)$$

In both cases, Bardoscia et al. (2019) show that probabilities of default at time t are:

$$p_{[t,T]} = 1 - \mathbb{V}(E(t)|\mathcal{C}(t)). \quad (5.14)$$

We note that valuation functions (5.13) depend explicitly only on $A^e(t)/E(t)$, which is the external leverage at time t , and on $\sigma\sqrt{T-t}$, which is the volatility of external assets over a period $T-t$. As one would expect, those are decreasing functions of the external leverage and of the volatility of external assets. Intuitively, if one bank has a smaller external leverage or if the volatility of its external assets is smaller, its counterparties will deem it to be safer. Therefore, they will expect to recover a larger proposition of their investments in that bank, which corresponds to a larger valuation function for that bank. We can use (5.13) and (5.14) also to compute valuation functions and probabilities of default for nRFBs, simply by plugging in the appropriate quantities: $\mathcal{C}_i^{\text{nRF}}(t) = \{(1 - \psi_i^A)A_i^e(t), \sigma_i\sqrt{T-t}\}$. We point out that it makes sense to compute (5.13) and (5.14) also in the case in which banks do not hold any interbank assets or interbank liabilities. In this case, external assets are equal to total assets and the volatility of external assets is equal to the volatility of total assets, and indeed one recovers the original results in Merton (1974) and Black and Cox (1976). In particular, this means that one can use (5.13) and (5.14) to compute the probability of default of RFBs, again by plugging in the appropriate quantities: $\mathcal{C}_i^{\text{RF}}(t) = \{\psi_i^A A_i^e(t), \sigma_i\sqrt{T-t}\}$.

For the sake of brevity, and with a slight abuse of notation, in the following, we drop the dependence of all quantities on t and denote the volatility of external assets over a period $T-t$ simply with σ . Let us now introduce the following class of valuation functions.

Definition 5.4.4 (Simple ex-ante valuation functions). *A function $\mathbb{V}(E|\mathcal{C})$ with $\mathcal{C} = \{A^e, \sigma\}$, $A^e > 0$, $\sigma > 0$ is a simple ex-ante valuation function if it depends explicitly only on the inverse of external leverage $\tilde{B} = E/A^e$ and on the volatility of external assets σ :*

$$\mathbb{V}(E|\mathcal{C}) = f(\tilde{B}, \sigma),$$

where $f : \mathbb{R} \times \mathbb{R}^+ \rightarrow [0, 1]$ satisfies the following properties:

- it is non-decreasing in \tilde{B} ,
- it is right-continuous in \tilde{B} .

One can check that simple ex-ante valuation functions satisfy the hypotheses of Definition 5.4.3, and therefore are also feasible valuation functions. Moreover, it is easy to see that both valuation functions in (5.13) are simple ex-ante valuation functions and are also non-increasing in σ .¹⁰ Having assumed that $A_i^e > 0$ and $\psi_i^A < 1$ for all i ensures that simple ex-ante valuation functions are well-defined for all banks prior to ring-fencing and for all nRFBs.

All our results apply to simple ex-ante valuation functions, to the extent that one interprets valuation functions to be equal to one minus probabilities of default, as in equilibrium — that is at the greatest solution — for banks prior to ring-fencing and for nRFBs:

$$p_{i,[t,T]}^* = 1 - \mathbb{V}(E_i^* | \mathcal{C}_i), \quad (5.15a)$$

$$p_{i,[t,T]}^{\text{nRF},*} = 1 - \mathbb{V}(E_i^{\text{nRF},*} | \mathcal{C}_i^{\text{nRF}}), \quad (5.15b)$$

whereas for RFBs:

$$p_{i,[t,T]}^{\text{RF}} = 1 - \mathbb{V}(E_i^{\text{RF}} | \mathcal{C}_i^{\text{RF}}). \quad (5.15c)$$

5.4.3 Results on RFBs

In Proposition 5.4.1 we derive necessary and sufficient conditions so that leverage of RFBs and naive external leverage of nRFBs decrease or increase when compared with the bank prior to ring-fencing. The situation is less clear-cut for external leverages (i.e. for external leverages compute with fixed-point equities rather than with book-value equities).

We start by deriving sufficient conditions so that the leverage of RFBs decreases when compared with the external leverage of the bank prior to ring-fencing. For valuation functions that are non-decreasing with the external leverage (as in (5.15)), this naturally implies that the RFB is safer than the bank prior to ring-fencing.

Corollary 5.4.5. *Let bank i implement ring-fencing feasibly, i.e. let RFB i and nRFB i be naively solvent. If the allocation of assets and liabilities to the RFB is such that:*

$$\psi_i^A (L_i^e - (\bar{A}_i - \bar{L}_i)) \geq \psi_i^L L_i^e,$$

then the leverage of RFB i is smaller than the external leverage of bank i prior to ring-fencing:

$$\lambda_i^{\text{RF}} \leq B_i^*.$$

¹⁰Simple ex-ante valuation functions are non-increasing in the external leverage $1/\tilde{B} = A^e/E$, but are defined as functions of \tilde{B} to avoid the discontinuity at $E = 0$.

Moreover, if probabilities of default are computed with simple ex-ante valuation functions (as in (5.15)), then the probability of RFB i is smaller than or equal to the probability of default of bank i prior to ring-fencing:

$$p_{i,[t,T]}^{RF} \leq p_{i,[t,T]}^*.$$

By comparing Corollary 5.4.5 with Proposition 5.3.1, we can now assess the impact of interbank lending and borrowing on (non-naive) external leverage. Corollary 5.4.5 implies that, when the net interbank lending of bank i is equal to zero ($\bar{A}_i = \bar{L}_i$), then the condition to make the leverage of RFB i smaller than the external leverage of bank i prior to ring-fencing is the same as when bank i does not lend to and borrow from other banks ($\psi_i^A > \psi_i^L$, under the mild assumption that $L_i^e > 0$). When bank i is a net lender to other banks ($\bar{A}_i > \bar{L}_i$), in order to lower the leverage of its RFB ($\lambda_i^{RF} \leq B_i^*$), bank i needs to allocate proportionally more assets (or fewer liabilities) to the RFB with respect to the case in which its net interbank lending is zero. When bank i is a net borrower to other banks ($\bar{A}_i < \bar{L}_i$), in order to lower the leverage of its RFB ($\lambda_i^{RF} \leq B_i^*$), bank i needs to allocate proportionally fewer assets (or more liabilities) to the RFB with respect to the case in which its net interbank lending is zero.

The reason why the condition $\psi_i^A (L_i^e - (\bar{A}_i - \bar{L}_i)) \geq \psi_i^L L_i^e$ is only sufficient, but not necessary, for $\lambda_i^{RF} \leq B_i^*$ is that B_i^* depends on the greatest solution E_i^* , which accounts for the valuation of interbank assets. In fact, B_i^* can be larger than λ_i^{RF} if the valuation of the interbank assets of bank i , and therefore E_i^* , is sufficiently small. This cannot happen if B_i^* is smaller than λ_i^{RF} regardless of the valuation of the interbank assets of bank i , that is if B_i^* is smaller than λ_i^{RF} even when the interbank assets of bank i are worth nothing. This intuition is formalised in the following proposition.

Proposition 5.4.6. *If the allocation of assets than liabilities to the RFB is such that:*

$$\psi_i^A (L_i^e + \bar{L}_i) \leq \psi_i^L L_i^e,$$

then the leverage of RFB i is greater than the external leverage of bank i prior to ring-fencing:

$$\lambda_i^{RF} \geq B_i^*.$$

Moreover, if probabilities of default are computed with simple ex-ante valuation functions (as in (5.15)), then the probability of RFB i is larger than or equal to the probability of default of bank i prior to ring-fencing:

$$p_{i,[t,T]}^{RF} \geq p_{i,[t,T]}^*.$$

We can now put together the results in Proposition 5.4.1, Corollary 5.4.5, and Proposition

5.4.6 and classify banks that implement ring-fencing in three groups. If bank i implements ring-fencing so that $\psi_i^L L_i^e \leq \psi_i^A (L_i^e - (\bar{A}_i - \bar{L}_i))$, we have that $\lambda_i^{\text{RF}} \leq B_i^0 \leq B_i^*$, i.e. the RFB has smaller leverage than the external leverage of the bank prior to ring-fencing. As a consequence, the probability of default of the RFB is smaller than the probability of default of the bank prior to ring-fencing. If bank i implements ring-fencing so that $\psi_i^A (L_i^e + \bar{L}_i) \leq \psi_i^L L_i^e$, we have that $\lambda_i^{\text{RF}} \geq B_i^* \geq B_i^0$, i.e. the RFB has larger leverage than the external leverage of the bank prior to ring-fencing. As a consequence, the probability of default of the RFB is larger than the probability of default of the bank prior to ring-fencing. However, if bank i implements ring-fencing so that $\psi_i^A (L_i^e - (\bar{A}_i - \bar{L}_i)) < \psi_i^L L_i^e < \psi_i^A (L_i^e + \bar{L}_i)$, we can still say that $\lambda_i^{\text{RF}} \geq B_i^0$, but we cannot make any statement on the relationship between the leverage of RFB and the external leverage of the bank prior to ring-fencing.

Importantly, Corollary 5.4.5 and Proposition 5.4.6 allow us to make statements about whether the probability of default of the RFB has decreased or increased with respect to the bank prior to ring-fencing using only on quantities $(\psi_i^A, \psi_i^L, \bar{A}_i, \bar{L}_i, L_i^e)$ that refer to those two banks. Even if the bank prior to ring-fencing is embedded in a financial network, and therefore its equity depends on other banks, Corollary 5.4.5 and Proposition 5.4.6 do not require the knowledge of any of these quantities, not even of the detailed breakdown of interbank assets $(A_{ij}, \text{ for all banks } j \text{ to which } i \text{ is exposed})$ and liabilities $(L_{ij}, \text{ for all banks } j \text{ that are exposed to } i)$ of bank i .

By comparing Corollaries 5.3.2 and 5.4.5 we can assess the impact of interbank lending and borrowing on the probability of default of the RFB. As long as the RFB has a smaller leverage than the external leverage of the bank prior to ring-fencing, it has also a smaller probability of default. From Corollary 5.4.5 we know that when bank i is a net lender (borrower) to other banks, in order to make the leverage of the RFB smaller than the external leverage of the bank prior to ring-fencing, bank i needs to allocate proportionally more (fewer) assets or fewer (more) liabilities to the RFB with respect to the case in which its net interbank lending is zero.

5.4.4 Results on nRFBs and banking groups

In contrast, we will see that in order to make statements about the probability of default of a nRFB, at least some knowledge of the topology of the financial network is required. We start by introducing the concept of asset risk orbit. Let $i \in \mathcal{N}$ and let \mathbf{A} be a matrix of interbank assets. The asset risk orbit of i is¹¹:

$$\mathcal{O}^A(i) = \{j \in \mathcal{N} : \text{there exists a directed path from } i \text{ to } j \text{ in } \mathcal{G}^A\} .$$

¹¹The liability risk orbit has an analogous definition, but it is based on the matrix of interbank liabilities \mathbf{L} : $\mathcal{O}^L(i) = \{j \in \mathcal{N} : \text{there exists a directed path from } i \text{ to } j \text{ in } \mathcal{G}^L\}$. It has been introduced in Eisenberg and Noe (2001) simply as *risk orbit*.

For example, if i has invested in j , then $A_{ij} > 0$, i.e. i has an interbank asset towards j . This means that in \mathcal{G}^A there is a directed path (consisting only of the edge $i \rightarrow j$) from i to j , and therefore that j is in the asset risk orbit of i . In fact, i holds an interbank asset corresponding to the investment made in j , and therefore it is exposed to changes in the creditworthiness of j . Now let us imagine that j has invested in k , i.e. that $A_{jk} > 0$. Also in this case there is a directed path from i to k ($i \rightarrow j \rightarrow k$), and therefore k is in the asset risk orbit of i . Indeed, j is exposed directly to changes in the creditworthiness of k , but, since i is exposed directly to changes in the creditworthiness of j , also i is exposed to changes in the creditworthiness of k , but *indirectly*.

Similarly to the case of one bank, $E_i^{\text{RF}} + E_i^{\text{nRF},*}$ can be interpreted as the equity of the banking group that consolidates the RFB i and the nRFB i . When banks are embedded in a financial network (5.3) does not necessarily hold, i.e. in general it is not true that the equity of the banking group is equal to E_i^* the equity of the bank prior to ring-fencing. However, as long as a bank is not exposed (either directly or indirectly) to any bank that has implemented ring-fencing, then the equity of the consolidated group is still equal to the equity of the bank prior to ring-fencing.

Proposition 5.4.7. *Let equity valuations of banks prior to ring-fencing and of nRFBs be the greatest solutions in a network valuation framework with simple ex-ante valuation functions.*

If no bank in the asset risk orbit of bank i implements ring-fencing:

$$\mathcal{O}^A(i) \cap \mathcal{R} = \emptyset,$$

then the sum of the equities of RFB i and nRFB i are equal to the equity of the bank prior to ring-fencing:

$$E_i^{\text{RF}} + E_i^{\text{nRF},*} = E_i^*.$$

Intuitively, this happens because, after the implementation of ring-fencing, nothing has changed for any of the banks that could have a downstream impact on the nRFB bank i . What happens in the more general case in which banks that implement ring-fencing have a downstream impact on other banks? In the case in which *all banks in one asset risk orbit* implement ring-fencing consistently, i.e. when the leverage of all their RFBs is smaller than the naive external leverage (or larger than the external leverage) of their banks prior to ring-fencing, it is possible to prove the following result.

Theorem 5.4.8. *Let equity valuations of banks prior to ring-fencing and of nRFBs be the greatest solutions in a network valuation framework with simple ex-ante valuation functions.*

If all banks in the asset risk orbit of bank i either do not ring-fence or implement ring-fencing feasibly so that the leverage of their RFB is smaller than the naive external

leverage of their bank prior to ring-fencing:

$$\forall j \in \mathcal{O}^A(i) \cap \mathcal{R} : \quad \lambda_j^{RF} \leq B_j^0,$$

then the sum of the equities of RFB i and nRFB i is smaller than or equal to the equity of the bank prior to ring-fencing:

$$E_i^{RF} + E_i^{nRF,*} \leq E_i^*.$$

Vice versa, if all banks in the asset risk orbit of bank i either do not ring-fence or ring-fence feasibly so that the leverage of their RFB is larger than the external leverage of their bank prior to ring-fencing:

$$\forall j \in \mathcal{O}^A(i) \cap \mathcal{R} : \quad \lambda_j^{RF} \geq B_j^*,$$

then the sum of the equities of RFB i and nRFB i is larger than or equal to the equity of the bank prior to ring-fencing:

$$E_i^{RF} + E_i^{nRF,*} \geq E_i^*.$$

An important implication of Theorem 5.4.8 is that there cases in which $E_i^{RF} + E_i^{nRF,*} \neq E_i^*$ i.e. in which the equity of the group that consolidates RFB and nRFB is different from the equity of the bank prior to ring-fencing. In other words, the implementation of ring-fencing can either decrease or increase the equity of a banking group. This happens because, when banks are embedded in a financial network, equities are the product of a collective (self-consistent) valuation, and allocating assets and liabilities to RFBs and nRFBs can alter the valuation process. More precisely, equity valuations of nRFBs and of banks prior to ring-fencing depend on how much their interbank assets are worth, and therefore on how risky their counterparties are.

Intuitively, if enough assets are allocated to a RFB to lower its leverage and make it safer, fewer assets will be available to the corresponding nRFB. Everything else equal, this will make the nRFB riskier. A riskier nRFB will have a downstream impact on the other nRFBs exposed to it, lowering the valuation of the corresponding interbank assets. This will ultimately lead to smaller equities for those nRFBs exposed to the riskier nRFB and for their groups. According to Theorem 5.4.8, this happens when banks in the asset risk orbit of bank i implement ring-fencing by decreasing the leverage of their RFBs with respect to their *naive* external leverage prior to ring-fencing. Since the naive external leverage is always smaller than the external leverage, we have that those RFBs are safer than their banks prior to ring-fencing. However, the converse is not true. In fact, one bank in the asset risk orbit of bank i can make its RFB safer than its bank prior to

ring-fencing (by making the leverage of its RFB smaller than the external leverage of its bank prior to ring-fencing), but the leverage of its RFB can be still larger than its *naive* external leverage prior to ring-fencing, making Theorem 5.4.8 not applicable.

Theorem 5.4.8 also tells us that, when banks in the asset risk orbit of bank i implement ring-fencing by increasing the leverage of their RFBs with respect to their external leverage prior to ring-fencing, thereby making them less safe, the equity of the group that consolidates RFB and nRFB is larger than or equal to the equity of the bank prior to ring-fencing.

We also observe that the hypotheses of Theorem 5.4.8 are only about banks in the asset risk orbit of bank i , not about bank i itself. In fact, it is irrelevant whether bank i implements ring-fencing at all. How bank i implements ring-fencing is relevant only if bank i is in its own asset risk orbit, i.e. if $i \in \mathcal{O}^A(i)$. At the same time, we stress that Theorem 5.4.8 applies only if *all* banks in the asset risk orbit of bank i either do not implement ring-fencing, or implement ring-fencing consistently. For example, if all banks in the asset risk orbit of bank i implement ring-fencing by making the leverage of their RFBs smaller than the naive external leverage of their banks prior to ring-fencing, except for one bank that makes the leverage of their RFB larger, then Theorem 5.4.8 does not apply.

An immediate consequence of Theorem 5.4.8 is that, if *all* banks implement ring-fencing consistently, the inequalities of Theorem 5.4.8 hold also for the aggregate equity. For example, if all RFBs have a smaller leverage than the naive external leverage of their banks prior to ring-fencing, then the aggregate equity after ring-fencing has been implemented is smaller than or equal to the aggregate equity prior to ring-fencing. Vice versa, if all RFBs have a larger leverage than the external leverage of their banks prior to ring-fencing, then the aggregate equity after ring-fencing has been implemented is larger than or equal to the aggregate equity prior to ring-fencing.

Corollary 5.4.9. *Let equity valuations of banks prior to ring-fencing and of nRFBs be the greatest solutions in a network valuation framework with simple ex-ante valuation functions.*

If all banks either do not ring-fence or implement ring-fencing feasibly so that the leverage of their RFB is smaller than the naive external leverage of their bank prior to ring-fencing:

$$\forall j \in \mathcal{N} \cap \mathcal{R} : \quad \lambda_j^{RF} \leq B_j^0,$$

then the sum of the equities of RFB i and nRFB i is smaller than or equal to the equity of the bank prior to ring-fencing:

$$\sum_i E_i^{RF} + \sum_i E_i^{nRF,*} \leq \sum_i E_i^*.$$

Vice versa, if all banks either do not ring-fence or ring-fence feasibly so that the leverage of their RFB is larger than the external leverage of their bank prior to ring-fencing:

$$\forall j \in \mathcal{N} \cap \mathcal{R} : \quad \lambda_j^{RF} \geq B_j^*,$$

then the sum of the equities of RFB i and nRFB i is larger than or equal to the equity of the bank prior to ring-fencing:

$$\sum_i E_i^{RF} + \sum_i E_i^{nRF,*} \geq \sum_i E_i^*.$$

We have already pointed out that Theorem 5.4.8 requires only banks in the asset risk orbit of bank i to ring-fence in a certain way, and not bank i itself. However, if *also* bank i implements ring-fencing consistently with the banks in its asset risk orbit, then the external leverage of its nRFB increases (decreases) with respect to the bank prior to ring-fencing. More specifically, when the leverage of RFB i decreases with respect to the naive external leverage of bank i prior to ring-fencing, then the external leverage of nRFB i increases with respect to the external leverage of bank i prior to ring-fencing. Therefore, the probability of default of RFB i will be smaller than (or equal to) the probability of default of bank i prior to ring-fencing, which in turn will be smaller than (or equal to) the probability of default of the nRFB i . Similarly, when the leverage of RFB i increases with respect to the external leverage of bank i prior to ring-fencing, then the external leverage of nRFB i decreases with respect to the external leverage of bank i prior to ring-fencing. Therefore, the probability of default of RFB i will be larger than (or equal to) the probability of default of bank i prior to ring-fencing, which in turn will be larger than (or equal to) the probability of default of the nRFB i .

Proposition 5.4.10. *Let external leverages of banks prior to ring-fencing and of nRFBs be computed with equity valuations corresponding to the greatest solutions in a network valuation framework with simple ex-ante valuation functions.*

If:

- *all banks in the asset risk orbit of bank i either do not ring-fence or implement ring-fencing feasibly so that the leverage of their RFB is smaller than the naive external leverage of their bank prior to ring-fencing:*

$$\forall j \in \mathcal{O}^A(i) \cap \mathcal{R} : \quad \lambda_j^{RF} \leq B_j^0,$$

- *bank i implements ring-fencing feasibly so that the leverage of its RFB is smaller than the naive external leverage of its bank prior to ring-fencing:*

$$\lambda_i^{RF} \leq B_i^0,$$

then the external leverage of bank i prior to ring-fencing is smaller than or equal to the external leverage of $nRFB$ i :

$$B_i^* \leq B_i^{nRF,*}.$$

Moreover, if probabilities of default are computed with simple ex-ante valuation functions (as in (5.15)), then the probability of default of RFB i is smaller than or equal to that of bank i prior to ring-fencing, which in turn is smaller than or equal to that of $nRFB$ i :

$$p_{i,[t,T]}^{RF} \leq p_{i,[t,T]}^* \leq p_{i,[t,T]}^{nRF,*}.$$

Vice versa if:

- all banks in the asset risk orbit of bank i either do not ring-fence or implement ring-fencing feasibly so that the leverage of their RFB is larger than the external leverage of their bank prior to ring-fencing:

$$\forall j \in \mathcal{O}^A(i) \cap \mathcal{R} : \quad \lambda_j^{RF} \geq B_j^*,$$

- bank i implements ring-fencing feasibly so that the leverage of its RFB is smaller than the naive external leverage of its bank prior to ring-fencing:

$$\lambda_i^{RF} \geq B_i^*,$$

then the external leverage of bank i prior to ring-fencing is larger than or equal to the external leverage of $nRFB$ i :

$$B_i^* \geq B_i^{nRF,*}.$$

Moreover, if probabilities of default are computed with simple ex-ante valuation functions (as in (5.15)), then the probability of default of RFB i is larger than or equal to that of bank i prior to ring-fencing, which in turn is larger than or equal to that of $nRFB$ i :

$$p_{i,[t,T]}^{RF} \geq p_{i,[t,T]}^* \geq p_{i,[t,T]}^{nRF,*}.$$

5.5 Conclusion

We build a simple framework to think about the impact of ring-fencing on banks interconnected in a financial network of mutual investments. To summarise, we find that, making RFBs safer with respect to their banking group prior to ring-fencing can make nRFBs riskier and reduce the overall equity valuation of banking groups exposed to those riskier nRFB. In particular, this happens when all groups to which one group is directly or indirectly exposed implement ring-fencing so that the leverage of their RFBs is sufficiently below the external leverage of their groups prior to ring-fencing.

In our model risks for banks' balance sheets come from two sources. First, from external assets, that is from investments in the real economy. The larger the external leverage, the larger the risk. Second, from interbank assets, that is from investments in other banks. The larger the exposures to other banks or their probability of default, the larger this risk. While nRFBs and banks prior to ring-fencing are subject to both risks, implementing ring-fencing insulates RFBs from risks arising from interbank assets, leaving them exposed only to risks from external assets. In order to make those risks sufficiently small, one can allocate a sufficiently large amount of external assets to RFBs to make their leverage sufficiently small. By doing so, fewer or riskier assets will be allocated to nRFBs, exposing them more to risks from external assets. However, because nRFB also holds interbank assets, this increased riskiness has a downstream impact on other nRFBs. If a nRFB is exposed to other riskier nRFBs, its interbank assets will be worth less. This will make the equity of that nRFB and of the group to which it belongs smaller.

nRFBs can react in several ways. First, they can reduce their interbank assets, and therefore their exposure to other nRFBs. Second, they can reduce their exposure to risks from external assets. This can be achieved either by deleveraging — selling some external assets to repay liabilities — or by rebalancing their portfolio, by divesting from riskier assets and investing in safer assets. Third, they could improve their resilience by raising additional capital that would act as an additional buffer to withstand shocks to assets and therefore to equity. Finally, reallocating some external assets from RFBs to nRFBs would reduce the external leverage of nRFBs, but it would do so at the expense of RFBs, whose leverage and therefore their probability of default would increase.

Some current limitations of our model naturally outline possible directions for future research. First, our results descend purely from allocating assets and liabilities of the banking group into two different entities. Even though we can suggest actions that individual banking groups could implement to counter some adverse effects of ring-fencing, we do not approach this point quantitatively. For example, how much does a nRFB need to deleverage to become as risky as the banking group prior to ring-fencing? Second, we assume that RFBs are fully insulated from the financial network, on the asset side — they can only invest in the real economy — and on the liability side — they cannot be

funded by other banks. In practice, RFBs could still invest and be funded by other RFBs. This means that also RFBs could hold interbank assets and liabilities, albeit safer than those held by nRFBs, and therefore they would be part of a parallel financial network. Third, we assume that the intrinsic riskiness (i.e. the volatility) of assets held by RFBs and nRFBs is the same. In reality, it is reasonable to expect that RFBs would hold safer assets than nRFBs. We leave the case in which RFBs and nRFBs hold different assets to future extensions of this work, as it would considerably complicate the analysis.

Chapter 6

An analysis of network filtering methods to sovereign bond yields during COVID-19

6.1 Introduction

The novel coronavirus disease 2019 (COVID-19) epidemic caused by SARS-CoV-2 began in China in December 2019 and rapidly spread around the world. The confirmed cases increased in different cities in China, Japan, and South Korea in a few days of early January 2020, but spread globally with new cases in Iran, Spain, and Italy within the middle of February.

We focus on sovereign bonds during the COVID-19 period to highlight the extent to which the pandemic has influenced the financial markets. A sovereign bond is a bond that is issued by sovereign entities or administrative regions. The yield of these bonds is the interest rate which is paid to the buyer of the bond by the issuer. Each issued sovereign bond has an associated maturity date and is considered risk-free. However, the yields of sovereign bonds can depend highly on factors such as inflation, political stability, and the debt of the issuing country.

In the last few years, bond yields across the Euro-zone were decreasing under a range of European Central Bank (ECB) interventions and overall remained stable compared with the German Bund, a benchmark used for European sovereign bonds. These movements were disrupted during the COVID-19 pandemic, which has affected the future trajectory of bond yields from highly impacted countries, e.g., Spain and Italy. However, in the last months, the European central banks intervened in financial and monetary markets to consolidate stability through an adequate supply of liquidity countering the possible margin calls and the risks of different markets and payment systems. These interventions played a specific role in sovereign bonds because, on the one side, supported the stability

of financial markets and, on the other side, supported the governments' financial stability and developed a global reference interest rate scheme. Understanding how correlations now differ and similarities observed in previous financial events is important in dealing with the future economic effects of COVID-19.

We consider an analysis of sovereign bonds by using network filtering methods, which is part of a growing literature within the area of Econophysics Li et al. (2019); Stavroglou et al. (2016); Maeng et al. (2012); Leon et al. (2014); Gilmore et al. (2010). The advantage of using filtering methods is the extraction of a network-type structure from the financial correlations between sovereign bonds. Hence, the correlation-based networks and hierarchical clustering methodologies allow us to understand the nature of financial markets and some sovereign bond features. It is not clear which approach should be used in analysing sovereign bond yields, so we implement various filtering methods to the sovereign bond yield data and compare the resulting structure of different networks. Through this analysis, we can evaluate the impact which the topological structure of filtered networks has on the economic and health relations between nodes.

We consider different network filtering methods because there are connections between assets which may be missed by only using one method. A commonly used method is the Minimum Spanning Tree method by Kruskal (1956), which is widely used in areas of social science, computer science and mathematics. A key property of a Minimum Spanning Tree is that only the minimum number of edges are included such that all nodes are connected.

The Triangular Maximal Filtering Graph by Massara et al. (2016) is an alternative method, which assumes more information about the filtered network by increasing the number of included edges. In comparison to the Minimum Spanning Tree, the construction of a connected planar graph adds additional information, while still maintaining a level of sparsity between nodes. The construction of a planar graph is also considered by Tumminello et al. (2005), but the difference in this method compared with Massara et al. (2016) is that the computational time to construct the network is longer. Including this method along with the Minimum Spanning Tree provides a more extensive analysis, where we can then compare various financial aspects during the COVID-19 period using different filtered networks. In addition, we also include Asset Graphs by Onnela et al. (2003b) and Maximum Spanning Trees by Qian et al. (2010), and how these networks compare to the Minimum Spanning Tree.

Our results show that the mean correlation peaks in October 2019 and then decreases during the 2020 period, when COVID-19 is most active in Europe. These dynamics are reflected across all network filtering methods and represent the wide impact of COVID-19 on the spectrum of correlations, compared to previous financial events. We also find a clustering of Euro-area countries and a disintegration with non-Euro countries during the COVID-19 period. These network structures reflect the financial state of sovereign bonds

observed within previous financial events but are also related by exogenous variables, e.g., death rates of countries, which we can analyse under an exponential random graph model.

Previous studies have used different methods to analyse historic correlations as random matrix theory to identify the distribution of eigenvalues concerning financial correlations Laloux et al. (2000); Plerou et al. (2002); Junior and Franca (2012), the partial transfer entropy to quantify the indirect influence that stock indices have on one another Sandoval Junior et al. (2015), the approaches from information theory in exploring the uncertainty within the financial system Huang et al. (2012); Darbellay and Wuertz (2000), community structure analysis Vodenska et al. (2016), multilayer network methods Aldasoro and Alves (2018); Bargigli et al. (2016); Tonzer (2015); Montagna and Kok (2016); Guleva et al. (2015); Poledna et al. (2015), and filtering methods.

Several authors have used network filtering methods to explain financial structures Mantegna (1999); Onnela et al. (2003b), hierarchy and networks in financial markets Tumminello et al. (2010), relations between financial markets and real economy Musmeci et al. (2015), volatility Verma et al. (2019), interest rates Di Matteo et al. (2005), stock markets Isogai (2017); Wang et al. (2017); Wu et al. (2018); Alqaryouti et al. (2019), future markets Bartolozzi et al. (2007) or topological dynamics Tang et al. (2018) to list a few. Also, the comparison of filtering methods to market data has been used for financial instruments. Birch et al. (2016) consider a comparison of filtering methods of the DAX30 stocks. Musmeci et al. (2017) propose a multiplex visual network approach and consider data of multiple stock indexes. Kukreti et al. (2020) use the S&P500 market data and incorporate entropy measures with a range of network filtering methods. Aste et al. (2010) apply a comparison of network filtering methods on the US equity market data and assess the dynamics using network measures, Schwendner et al. (2015) applied a correlation influence approach and constructed noise-filtered influence networks to understand the collective yield dynamics of the Euro area sovereign bonds.

To evaluate the European sovereign bonds based on filtering methods, this work is organised as follows. In Section 6.2, we describe the network filtering methods and present the data sets with some preliminary empirical analyses. We apply in Section 6.3 the filtering methods to sovereign bond yields analyse the trend of financial correlations over the last decade and consider aspects of the network topology. We construct plots in Section 6.4 representing the COVID-19 period and consider an analysis using the exponential random graph model for each filtering method. In Section 6.5, we discuss the results and future directions.

6.2 Materials and methods

We introduce a range of network filtering methods and consider a framework as in Mantegna (1999) for sovereign bond yields. We define $n \in \mathbb{N}$ to be the number of sovereign bonds and bond yields $Y_i(t)$ of the i th sovereign bond at time- t , where $i \in \{1, \dots, n\}$. The correlation coefficients $r_{ij}(t) \in [-1, 1]$ are defined using Pearson correlation as

$$r_{ij} = \frac{\langle Y_i Y_j \rangle - \langle Y_i \rangle \langle Y_j \rangle}{\sqrt{(\langle Y_i^2 \rangle - \langle Y_i \rangle^2) (\langle Y_j^2 \rangle - \langle Y_j \rangle^2)}}, \quad (6.1)$$

with $\langle \cdot \rangle$ denoting the average yield values. The classical approach in using the Pearson correlation is well established, but it does not take into account the increases in correlation from market volatility. We can account for these changes by considering the conditional Pearson correlation approach as in Forbes and Rigobon (2002). We define an adjustment factor $\beta_{ij}(t) \in [0, \infty)$ and the conditional correlation r_{ij}^* at time- t as follows:

$$r_{ij}^* = r_{ij} \sqrt{\frac{1 + \beta_{ij}}{1 + \beta_{ij} r_{ij}^2}}, \quad \text{where } \beta_{ij} = \frac{\sigma_{ij}^h}{\sigma_{ij}^l} - 1. \quad (6.2)$$

This adjustment factor is represented by the relative difference between two subgroups of high covariance $\sigma_{ij}^h(t) \in [0, \infty)$ and low covariance $\sigma_{ij}^l(t) \in [0, \infty)$ of bond yields at time- t . As the relative difference in covariance increases, this increases the adjustment factor $\beta_{ij}(t)$ and the magnitude of the conditional Pearson correlation. This adjustment preserves the symmetry of correlation values between sovereign bonds i and j while taking into account market conditions. We form both subgroups by equally dividing yield values, where the high variance σ_{ij}^h group consists of the 25% lowest and highest yield values, with the remaining values allocated within the low variance σ_{ij}^l group. This allocation is applied individually to each sovereign bond in which the covariance is computed.

Under the conditional Pearson correlation, we establish the notion of distance $d_{ij} \in [0, 2]$. We consider the values of the entries r_{ij}^* on the conditional correlation matrix $R^* \in [-1, 1]^{n \times n}$, with $d_{ij} = \sqrt{2(1 - r_{ij}^*)}$. A distance of $d_{ij} = 0$ represents perfectly positive correlations and $d_{ij} = 2$ represents bonds with negative correlations. The network filtering methods are then applied to the distance matrix $D \in [0, 2]^{n \times n}$, where a subset of links (or edges) are chosen under each filtering method. The set of edges is indicated by $\{(i, j) \in E(t) : \text{nodes } i \text{ and } j \text{ are connected}\}$ at time- t , defined for each filtering method. We define the time frames of financial correlations as X for the set of observations, with n different columns and T rows. From the set of observations X , we consider windows of length 120, which is equal to six months of data values. We then displace δ windows by 10 data points, which is equal to two weeks of data values, and discard previous observations until all data points are used. By displacing the data in this way, we can examine a time series trend between each window X .

6.2.1 Network filtering methods

We consider multiple network filtering methods to analyse the dynamics from multiple perspectives. We introduce the commonly used minimum spanning tree (MST) method, which has been used within currency markets Jang et al. (2011), stock market Sandoval Jr (2012); Situngkir and Surya (2005) and sovereign bond yields Dias (2012). The MST from Table 6.1 considers the smallest edges and prioritises connections of high correlation to form a connected and undirected tree network. These networks can be constructed from a greedy type algorithm e.g. Kruskal’s and Prim’s algorithm and satisfies the properties of subdominant ultrametric distance e.g. $d_{ij} \leq \max\{d_{ik}, d_{kj}\} \forall i, j, k \in \{1, \dots, n\}$.

This approach is used as it establishes three key properties within a subset of correlations. We argue these properties are relevant within filtering methods but can also be individually constrained when applied in conjunction (as within the MST) for topological and economic reasons. By considering four methods, we can analyse the influence of each feature on the properties of the network:

- **Connectivity:** Under the MST, all nodes are connected within the network. As there has been a broad impact from COVID-19, many sovereign bonds have experienced a comovement in yield trends under market conditions. This criterion in which the network structure is connected also excludes some highly positive links and decreases the information between positively correlated sovereign bonds. Therefore, we consider the Asset Graph (AG), which includes all positive correlations of interest while maintaining the network density.
- **Sparsity:** The key motivation in filtering methods is the decrease in links, in which we can establish network properties of interest, e.g., network centrality. As observed in the 2012 Euro debt crisis, specific sovereign bonds are large contributors to the spillover effects observed in other bond yield trends. The fixed number of links within the MST can be also argued to oversimplify the network and reduce connectivity. Hence, we consider the Triangulated Maximal Filtering Graph (TMFG), which establishes a planar graph and increases the total number of links compared with the MST.
- **Positivity:** From an economic perspective, positive correlations are relevant in identifying the trends in different financial instruments and periods of high volatility. However, focusing on this subset of correlations may exclude sovereign bonds that act differently, i.e., although the majority of bond yields increased within the COVID-19 period, several bond yields like Germany and Switzerland decreased. To account for these dynamics, we consider a Maximum Spanning Tree (MaST), which prioritises negative correlations within the network.

Network Filtering Methods	Number of links (edges)	Reference	Description
Minimum Spanning Tree (MST)	$n - 1$	Kruskal (1956)	A connected and undirected network for n nodes which minimises the total edge weight.
Maximum Spanning Tree (MaST)	$n - 1$	Qian et al. (2010)	A connected and undirected network for n nodes which maximises the total edge weight.
Asset Graph (AG)	$n - 1$	Onnela et al. (2003a)	Choose the smallest $n - 1$ edges from the distance matrix.
Triangulated Maximal Filtering Graph (TMFG)	$3(n - 2)$	Massara et al. (2016)	A planar filtered graph under an assigned objective function.

Table 6.1: List of network filtering methods.

We provide further descriptions of the methods described above. An AG considers positive correlations between nodes of a given threshold. All $n - 1$ highest correlations are considered in an AG, allowing for the formation of cliques not observed within an MST network. The use of AG has been considered by Onnela et al. (2004), which identifies clustering within stock market data. As the method only considers $n - 1$ links, some nodes within the AG may not be connected for the given threshold. Therefore, the connection of unconnected nodes is unknown, relative to connected components.

The TMFG constructs a network of $3(n - 2)$ fixed edges for n nodes, similar to the planar maximal filtered graph (PMFG) Tumminello et al. (2005), which has been used to analyse US stock trends Musmeci et al. (2017). The algorithm initially chooses a clique of 4 nodes, where edges are then added sequentially, to optimise the objective function e.g., the total edge weight of the network, until all nodes are connected. This approach is non-greedy in choosing edges and incorporates the formation of cliques within the network structure. A TMFG is also an approximate solution to the weighted planar maximal graph problem and is computationally faster than the PMFG. The resulting network includes more information about the correlation matrix compared with spanning tree approaches.

The MaST constructs a connected and undirected tree network with $n - 1$ edges in maximising the total edge weight. Analyses involving MaST have been used as comparisons to results observed within MST approaches Dias (2013); Heimo et al. (2009). A MaST approach is informative for connections of perfectly anti-correlation between nodes, which are not displayed within the MST.

6.2.2 Sovereign bond data

The European sovereign debt has evolved in the last ten years, with some situations affecting the convergence between bond yields. After the 2008 crisis, European countries experienced a financial stress situation starting in 2010 that affected bond yields. Thus, the investors saw an excessive amount of sovereign debt and demanded higher interest rates in low economic growth situations and high fiscal deficit levels. During 2010-2012, several European countries suffered downgrades in their bond ratings to junk status that affected investors' trust and fears of sovereign risk contagion resulting, in some cases, a differential of over 1,000 basis points in several sovereign bonds. After the introduction of austerity measures in GIIPS (Greece, Ireland, Italy, Portugal, and Spain) countries, the bond markets returned to normality in 2015.

The 2012 European debt crisis revealed spillover effects between different sovereign bonds, which have been studied using various time series models, e.g., VAR by Claeys and Vašíček (2014); Antonakakis and Vergos (2013) and GARCH by Balli (2009). The results showed that Portugal, Greece, and Ireland have a greater domestic effect, with Italy and Spain contributing to the spillover effects in other European bond markets. A core group of ABFN (Austria, Belgium, France, and the Netherlands) countries had a lower contribution to the spillover effects, with some of the least impacted countries residing outside of the Eurozone.

Country	Min	Max	Mean	Variance	Skewness	Kurtosis	AC(1)	AC ² (1)
Austria	-0.47	3.90	1.30	1.45	0.55	2.11	0.05	0.14
Belgium	-0.43	5.83	1.58	2.01	0.61	2.13	0.17	0.41
Czech	0.24	4.55	1.88	1.32	0.61	2.33	-0.07	0.11
France	-0.44	3.79	1.40	1.37	0.40	1.91	0.06	0.18
Germany	-0.85	3.50	0.95	1.13	0.57	2.42	-0.01	0.21
Greece	0.56	39.85	9.16	51.02	1.74	6.31	0.07	0.01
Hungary	1.55	10.73	4.67	4.62	0.55	1.90	0.01	0.22
Iceland	2.19	8.15	5.72	1.73	-0.88	3.14	0.04	0.17
Ireland	-0.32	14.45	2.82	9.17	1.23	3.65	-0.36	0.50
Italy	0.48	7.31	2.96	2.40	0.55	2.28	0.07	0.08
Netherlands	-0.64	3.78	1.16	1.28	0.50	2.16	0.01	0.20
Poland	1.15	6.40	3.68	1.87	0.34	2.23	0.05	0.16
Portugal	-0.05	17.36	4.30	11.94	1.10	3.54	-0.28	0.32
Romania	2.56	10.80	4.91	2.20	0.73	2.60	-0.37	0.30
Spain	-0.01	7.56	2.70	3.60	0.52	1.91	0.13	0.14
Switzerland	-1.11	2.14	0.33	0.57	0.64	2.42	0.02	0.08
UK	0.07	4.28	1.81	0.91	0.42	2.61	-0.04	0.17

Table 6.2: Summary statistics of the 10Y sovereign bond yield data of 17 European countries from January 2010 to December 2020. AC(1) represents the first-order autocorrelation of the difference between yield values and AC²(1) represents the first-order autocorrelation of the squared series.

During the sovereign debt crisis, public indebtedness increased after Greece had to correct

the public finance falsified data, and other countries created schemes to solve their public finance problems, especially, bank bailouts. In consequence, the average debt-to-GDP ratio across the Euro-zone countries rose from 72% in 2006 to 119.5% in 2014, as well as the increase in sovereign credit risk Alter and Beyer (2014); Beck et al. (2016).

After the Fiscal Compact Treaty went into effect at the start of 2013, the yield of sovereign bonds started a correction. This treaty defined that fiscal principles had to be embedded in the national legislation of each country that signed the treaty. Although some investors and institutions pushed for financial and monetary authorities to introduce an additional decision, that permitted them to include sovereign bonds in their portfolios. The interest rate policy of the European Central Bank helped to consolidate the trust in this kind of asset; the bonds confirmed their adjustment especially in Germany, France and Spain, during the fourth quarter of 2013, while countries like Greece and Italy started in 2014 with variations of over 500 basis points during the following months. By 2015, all European bonds increased their yields as a result of an adjustment of the market rally of 2014.

We analyse the sovereign bond yield data for the following countries Austria (AUT), Belgium (BEL), Czech Republic (CZE), France (FRA), Germany (DEU), Greece (GRC), Hungary (HUN), Iceland (ISL), Ireland (IRL), Italy (ITA), Netherlands (NLD), Poland (POL), Portugal (PRT), Romania (ROU), Spain (ESP), Switzerland (CHE), and the UK (GBR). We consider sovereign bond yields with a 10-year maturity between January 2010 and Dec 2020. This data is taken from the financial news platform Investing ¹. In total, there are 2,615 data values for each country with an average of 238 data points within 1 year.

Table 6.2 provides summary statistics of the 10Y bond yield data. The data shows that the lowest recorded yields for many countries were within 2020, during the COVID-19 period and highest in 2011, before the 2012 European debt crisis. The lowest yield values are Germany and Switzerland, which both record yield values lower than -0.80 . In contrast, Greece has the highest yield value of 39.85 and a variance of 51.02. The left skewed yield distributions (except for Iceland) represent an average decrease in yield values and are high for GIIPS countries compared with the UK, France, and Germany, with flattening yield trends. If we examine the autocorrelation, we find this to be small overall but high for some countries e.g., Belgium, Ireland and Portugal within the squared series.

¹Investing.com, World Government Bonds, <https://www.investing.com/rates-bonds/world-government-bonds>

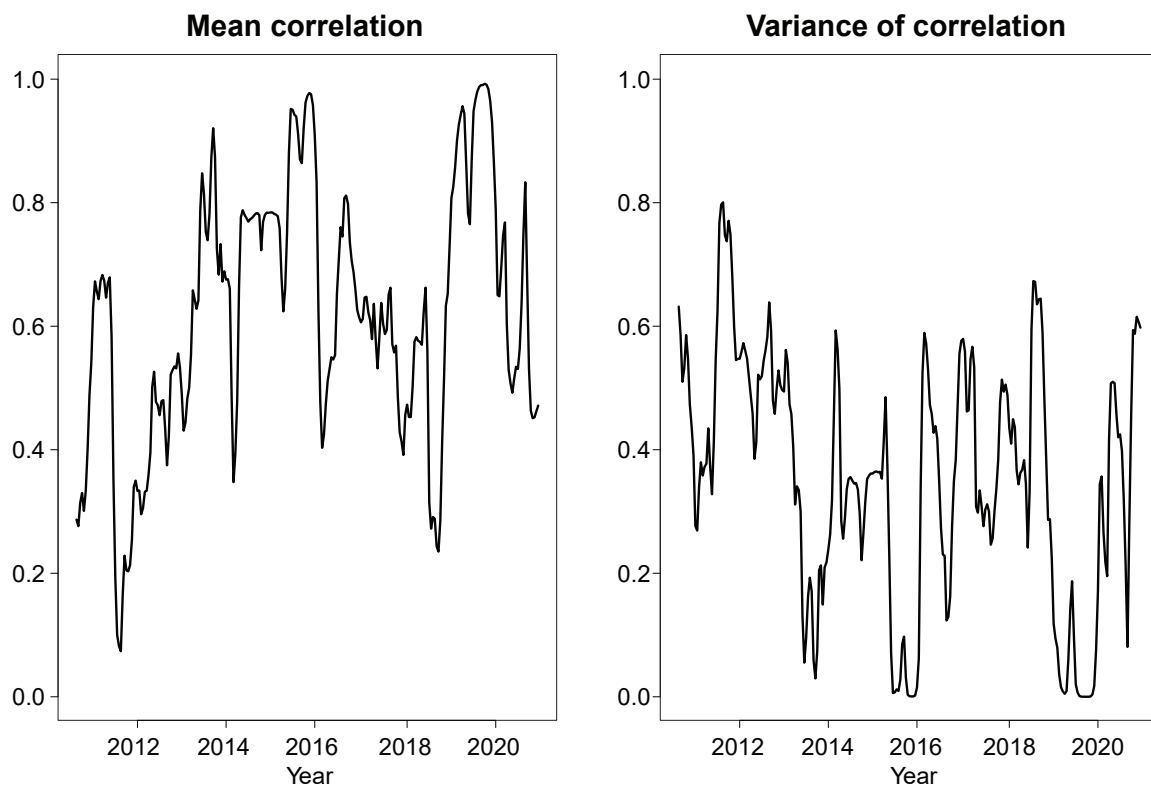


Figure 6.1: The plots represent the mean and variance of the conditional Pearson correlation matrix. The length of windows is 120 with a displacement value of $\delta = 10$ days.

6.3 Network measures

We compute the correlation matrix for each window X with a displacement of δ between windows and consider the mean and variance for the correlation matrix. We define the mean correlation $\bar{r}(t)$ given the conditional correlation values r_{ij}^* for n sovereign bonds

$$\bar{r}(t) = \frac{2}{n(n-1)} \sum_{i < j} r_{ij}^*(t), \quad (6.3)$$

and the variance of correlations $u(t)$ at time- t

$$u(t) = \frac{2}{n(n-1)} \sum_{i < j} (r_{ij}^*(t) - \bar{r}(t))^2. \quad (6.4)$$

From Figure 6.1, we find that the mean correlation $\bar{r}(t)$ is highest at 0.99 in Oct 2019. This suggests that a COVID-19 impact was a continuation of the decrease of the mean correlation and throughout the punitive lockdown measures introduced by the majority of European countries in Feb-Mar 2020. The decreases in mean correlation are observed within the 2012 period during the European debt crisis, in which several European countries received EU-IMF bailouts to cope with government debt. Within 2016, there was a combination of political uncertainty which followed from the UK and the increased

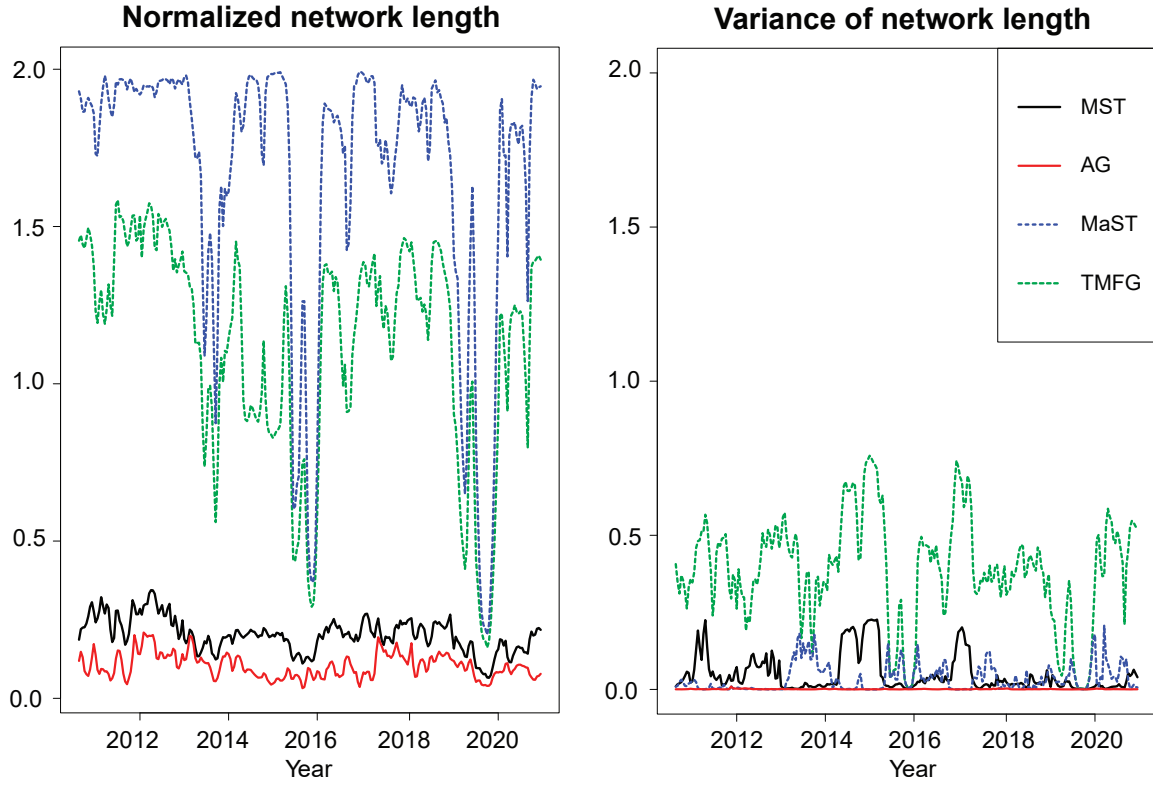


Figure 6.2: The plots represent the normalised and variance of the network length for MST, TMFG, MaST, and AG networks, with windows of length 120 and $\delta = 10$ days.

debt accumulation by Italian banks. The variance $u(t)$ also follows a trend similar to the mean correlation, with the smallest variance of 4.48×10^{-5} in October 2019. Within 2020, the variance increases between sovereign bonds and reflects the differences between the correlations of low and high yield.

6.3.1 Network length

We consider the normalised network length $L(t)$, which is introduced in Onnela et al. (2003a) as the normalised tree length. We define the measure as the normalised network length, as this measure is considered for AG and TMFG non-tree networks. The network length is a measure of the mean link weights on the subset of links $E(t)$, which are present within the filtered network on the distance matrix at time- t

$$L(t) = \frac{1}{\#\{(i, j) \in E(t)\}} \sum_{(i, j) \in E(t)} d_{ij}(t), \quad (6.5)$$

with the variance $V(t)$ defined on network links

$$V(t) = \frac{1}{\#\{(i, j) \in E(t)\}} \sum_{(i, j) \in E(t)} (d_{ij}(t) - L(t))^2. \quad (6.6)$$

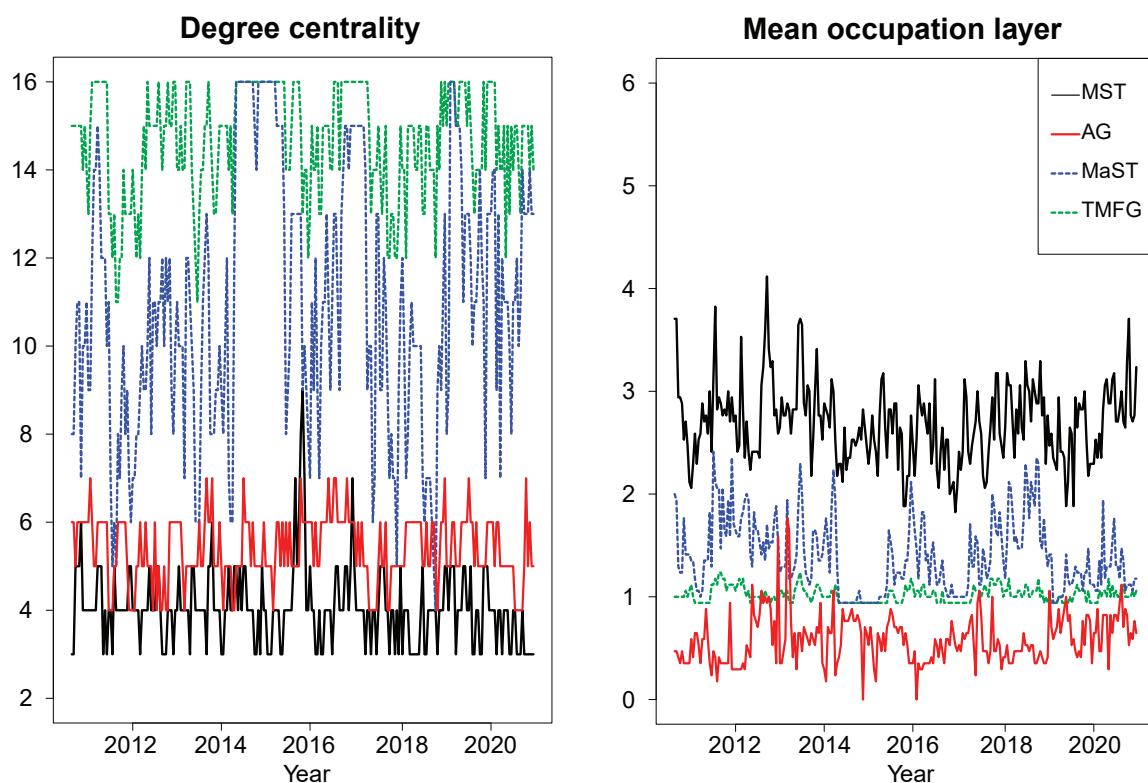


Figure 6.3: The plots represent the degree centrality and mean occupation layer for MST, TMFG, MaST and AG networks, with windows of length 120 and $\delta = 10$ days.

The plots in Figure 6.2 represent the mean and variance of the network length. As each filtering method considers a subset of weighted links, the normalised length $L(t)$ is monotonic between all methods and decreases with the increased proportion of positively correlated links within the network. We highlight movements in the normalised network length during the COVID-19 period, which is reflected across all filtering methods. This movement was also observed within 2016, but only towards a subset of correlations within the MaST and TMFG compared with the MST and AG. The relative difference between the normalised network lengths is least evident in periods of low variance; this is observed in the 2019-2020 period, where the difference between all methods decreases.

We find the variance is highest within the TMFG and lowest with the AG approach. Compared with the mean and variance of the correlation values in Figure 6.1, the difference between values within the equivalent network measures is overall higher, particularly within the MaST. There appears to be an overall reciprocal relation between the variance trends of spanning-tree approaches, where both values are small for some periods. When we consider the variance of the AG, the concentration of links, and the adjustment in the conditional correlation result in a flattened trend.

6.3.2 Network centrality

We define the degree centrality for the node of maximum degree $C(t)$ at time- t . This measure considers the number of direct links

$$C(t) = \max_{i \in \{1, \dots, n\}} \sum_{j \in E(t)} 1(d_{ij} > 0). \quad (6.7)$$

The mean occupation layer $\eta(t)$ (MOL) introduced in Onnela et al. (2003a) is a measure of the centrality of the network, relative to the central node $v(t)$. We define $lev_i(t)$ as the level of the node, which is the distance of the node relative to $v(t)$, where the central node and nodes unconnected relative to the central node have a level value of 0,

$$\eta(t) = \frac{1}{n} \sum_{i=1}^n lev_i(v(t)). \quad (6.8)$$

We use the betweenness centrality to define the central node $v(t)$ for the MOL. Introduced in Freeman (1977), the betweenness $B(t)$ considers the number of shortest paths $s_{ij}(k)$ between i and j which pass through the node k , relative to the total number of shortest paths s_{ij} between i and j , where $i \neq j \neq k$

$$B_k(t) = \sum_{i \neq k} \sum_{j \neq k, j \neq i} \frac{s_{ij}(k)}{s_{ij}}. \quad (6.9)$$

Within the MST, the majority of degree centrality ranges between 3 to 5 but can be as high as 9 for some periods. The trend within the MST remains stable, where the central node under degree centrality is associated with multiple sovereign bonds, e.g., Netherlands 11%, Portugal 10%, and Italy 10% across all periods. The MaST has the highest variation, with a centralised network structure in some periods, e.g., $C(t)$ of 16, forming a star-shaped network structure. This is usually associated with Greece 27%, Iceland 25%, and Romania 18%, which are identified as the central node 70% of the time. The degree centrality on average is naturally highest with the TMFG, under a higher network density, where the central nodes are identified as Iceland and Romania, similar to the MaST. The AG identifies the Netherlands and France within the degree centrality, under a higher proportion of 30% and 13% compared with the MST.

Within Figure 6.3, the MOL on average is smallest for the AG because of the 0 level values from unconnected nodes, in which an unconnected node is present within all considered windows. We find that all nodes within the TMFG have a maximum path length of 3 between any two nodes, across all periods. Between the MST and MaST, the MOL is higher within the MaST, where the degree centrality of nodes within the network is higher.

6.4 COVID-19 networks

We analyse the temporal changes in sovereign bond yields between Jan 2020 and Dec 2020. This interval establishes a period in which COVID-19 was highly active across multiple European countries.

We first construct networks under each of the filtering methods and relate the network topology to economic trends. Then, we implement an exponential random graph model (ERGM) to verify the significance of these explanatory variables within each constructed network. We consider analysis as in Deev and Lyócsa (2020), in which they use an ERGM to analyse the interconnectedness of financial institutions across Europe under different node variables.

6.4.1 Network plots

Under the MST for the COVID-19 period, we find France has the highest degree centrality of 3. The network also exhibits clusters between a subset of southern European countries, as observed within the connected component of Italy, Portugal and Spain. Within the network, there is a connection between all ABFN countries, but countries within this group also facilitate the connecting component within GIIPS countries, where Belgium is connected with Greek sovereign bonds. The UK and Eastern European countries remain on the periphery, with ABFN countries occupying the core of the network structure. For the MaST in Figure 6.4, there exists a high degree centrality for Icelandic bond yields. This contrasts with the observed regional hub structure within the MST, where the degree centrality is similar between all nodes. The UK remains within the periphery of the MaST structure when considering anti-correlations, and shows UK bond yields fluctuate less with movements of other European bonds, compared with previous years. This is also observed for sovereign bonds for other countries with non-Euro currencies e.g., the Czech Republic and Hungary.

We find nodes within the TMFG to have the highest degree in Iceland at 13 and the Czech Republic at 11. This resembles the links within the MaST, where 75% of links are present within both networks. There is also the associated degree centrality of the MaST, which is observed within the TMFG-connected nodes. Under the TMFG, nodes have a higher degree of connectivity when considering an increased number of links. This is the case for the UK, which has a degree value of 10 compared with other filtered networks. We find the AG exhibits one large component which consists of ABFN and GIIPS countries, where the majority of remaining nodes are non-Euro countries and are unconnected within the network. By solely considering the most positive correlations, we include the formation of cliques between countries, which is prevalent within the Western European group of 6 nodes. This level of disintegration which is observed during COVID-19 is supported by previous studies of the 2012 Eurozone debt crisis Baur (2020).

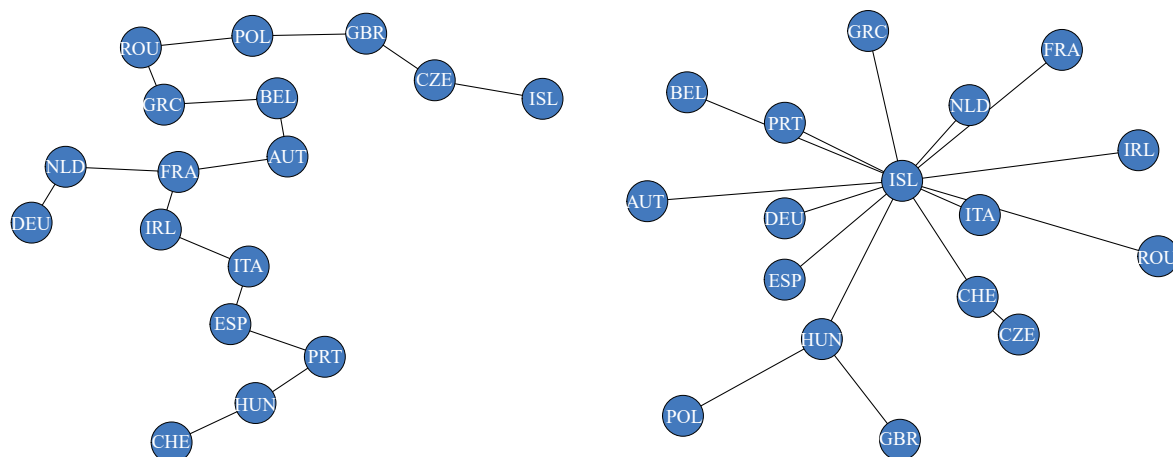


Figure 6.4: The plots represent the minimum spanning tree (left) and maximum spanning tree (right) for the Jan 2020 - Dec 2020 period.

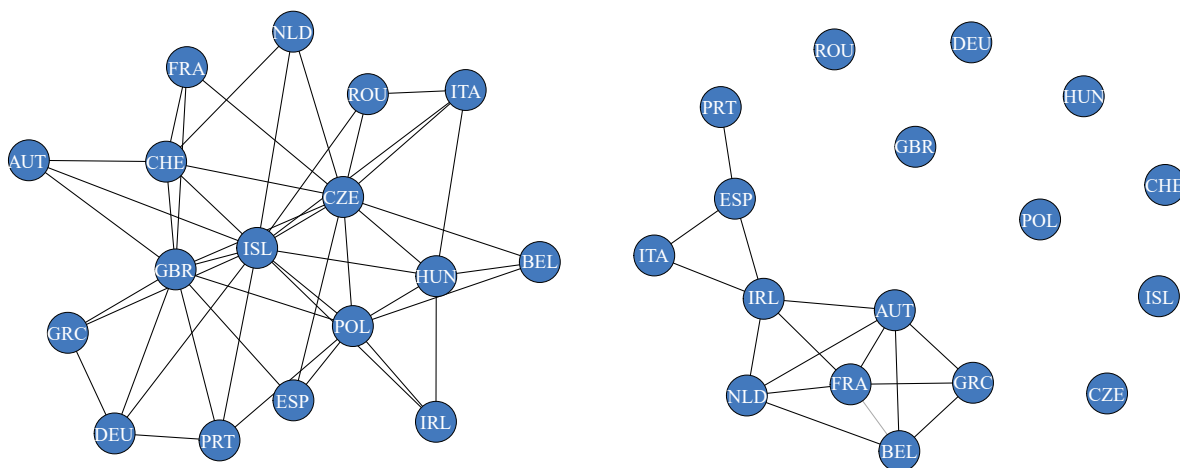


Figure 6.5: The plots represent the triangulated filtering maximal graph (left) and asset graph (right) for the Jan 2020 - Dec 2020 period.

Under various constraints, there is a commonality between sovereign bonds across network filtering methods. We find for positive correlations, that Euro-zone countries have a high degree centrality, with non-Euro countries predominately located within the periphery of the network. This is distinctive within the AG, where cliques are only formed between GIIPS and ABFN countries. The anti-correlations within the MaST inform the trends between non-Euro countries and the remaining Euro-area countries. This structure is supported within the TMFG, with the planar graph presenting similarities with the MaST on the degree centrality of nodes i.e., particularly for Iceland.

6.4.2 Exponential Random Graph Model for COVID-19 networks

We analyse the filtered networks as in Section 6.4 under an ERGM. In this approach, we consider a family of random unweighted networks W on the observed network w . We define the function of network statistics $z(w)$ and can computationally use the Maximum Likelihood Estimator (MLE) to consider this space of networks. We define the general model for p number of parameters with coefficient values θ as follows:

$$\mathbb{P}(W = w) = \frac{\exp\{\theta^T z(w)\}}{\kappa(\theta)}, \quad (6.10)$$

$$\log(\exp\{\theta^T z(w)\}) = \theta_1 z_1(w) + \theta_2 z_2(w) + \dots + \theta_p z_p(w) \quad (6.11)$$

and $\kappa(\theta)$ as the normalising constant. Although these computations can be expensive for a large number of nodes n , we can address these issues by using Markov Chain Monte Carlo (MCMC) methods. We analyse the local interactions between nodes and generate 10,000 random networks for each filtering method.

For the ERGM, we define the "intercept" of the model as the number of links observed within each filtered network. We then consider node-level variables under a discrete classification for different economic groups. If the node is within the economic group, we assign a value of "1", otherwise the node has a "0" value. We also incorporate continuous variables which are represented by economic and health data for all nodes. The data is provided by the International Monetary Fund (IMF) ² and the European Centre for Disease Prevention and Control (ECDC) ³ within the 2020 year. As we consider the coefficient values for different parameters, we further discuss the global model adequacy and fit under the ERGM. We consider the Akaike information criterion (AIC) and Bayesian information criterion (BIC) for the model adequacy, which are measures of the goodness of fit compared with the number of parameters used. We then use the log-likelihood value $LL(\theta)$, and consider the relative difference between the log-likelihood of the ERGM and null model as a measure of the model fit.

Within Table 6.3, we define two economic groups of GIIPS and ABFN countries. All of these countries have adopted the Euro and represent the core of connected nodes within the different filtering methods. We use the country's debt relative to the GDP, inflation rate, and account balance for 2020 as known economic indicators within the ERGM. As a health indicator of COVID-19, we consider the total number of COVID-19 deaths relative to the size of the country's population recorded within the 2020 year. If we compare the relative number of COVID-19 deaths with the debt of countries within Table 6.3, we find

²IMF.org, IMF World Economic Outlook, <https://www.imf.org/external/datamapper/datasets/WEO>

³ecdc.europa.eu, COVID-19 Death Statistics, <https://www.ecdc.europa.eu/en/geographical-distribution-2019-ncov-cases>

Country	GIIPS	ABFN	Euro	COVID-19 Deaths (%)	Debt to GDP	Inflation Rate	Account Balance
Austria		✓	✓	0.07	84.30	1.80	2.50
Belgium		✓	✓	0.17	117.10	1.20	-0.80
Czech				0.11	41.40	2.40	-0.50
France		✓	✓	0.10	118.60	0.60	-1.80
Germany			✓	0.04	72.20	1.10	6.80
Greece	✓		✓	0.05	200.50	0.70	-4.50
Hungary				0.10	75.90	3.40	-0.90
Iceland				0.01	52.50	2.80	0.20
Ireland	✓		✓	0.05	61.30	0.60	5.50
Italy	✓		✓	0.12	158.30	0.60	3.00
Netherlands		✓	✓	0.07	61.10	1.50	9.00
Poland				0.08	60.20	2.30	1.80
Portugal	✓		✓	0.07	130.00	1.10	-3.50
Romania				0.08	49.60	2.50	-4.50
Spain	✓		✓	0.11	121.30	0.80	0.90
Switzerland				0.08	48.50	0.00	9.00
UK				0.11	111.50	1.20	-3.80

Table 6.3: The following table represents health and economic attributes for countries within the ERGM. The debt is defined as the gross amount relative to the GDP, the inflation rate is recorded for the average consumer prices and the current account balance is the volume of recorded transactions relative to the country’s GDP within 2020. We consider the total number of COVID-19 deaths which occurred in 2020 relative to the population size of each country.

several countries have high levels of COVID-19 deaths and debt to GDP, e.g., Belgium, Italy, and the UK. For other economic indicators, we find an overall negative relationship between inflation and debt, however, some countries, i.e., both Switzerland and Ireland have low inflation and debt value. The account balance of countries is highest with the Netherlands and Switzerland, with Greece and Romania having the most negative values. We find the AG to have the highest model fit under the ERGM and the MST with the lowest fit (see Table 6.4). We observe that the GIIPS and ABFN coefficient values are high within the AG, which mainly describes the large component of Euro countries. Under the MST, nodes within the Euro establish links with other Euro countries because of positive correlations and non-Euro countries to satisfy the topological constraints. As the interpreted co-movement is concentrated within Euro countries, the MST removes the representative cliques between nodes, which decreases the coefficient values of GIIPS and ABFN.

The coefficient of COVID-19 deaths is highly significant within the MaST. Because of the centralised structure around Iceland COVID-19 deaths in Iceland are low compared with all other nodes (the death rate of the next lowest value is four times higher than in Iceland). As there is a centralised structure when considering negative correlations, we find compatibility of the topological requirement with the ERGM, which is not observed

Panel A	Parameters	MST	TMFG	MaST	AG
	Edges	-2.36	0.82	0.43	-36.14
	GIIPS	0.60	-0.23	1.22	20.59
	ABFN	0.70	-0.19	1.76	22.17
	Euro	-0.27	-1.75*	-3.50*	-0.62
	COVID-19 Deaths	1.77	-4.93	-39.20***	-6.95
	Debt to GDP	-0.00	0.01	0.02	-0.01
	Inflation	0.01	0.12	0.71	-1.14
	Account Balance	-0.04	0.02	0.11	0.00
Panel B	Diagnostics				
	Goodness of Fit Test: AIC	112.92	155.20	69.38	58.41
	Goodness of Fit Test: BIC	136.22	178.50	92.69	81.71
	Log Likelihood ($LL^M(\theta)$)	-48.46	-69.60	-26.69	-21.21
	Log Likelihood ($LL^0(\theta)$)	-49.26	-86.33	-49.26	-49.26
	Model Fit	1.62%	19.38%	45.82%	56.94%

*** $p < 0.001$; ** $p < 0.01$; * $p < 0.05$

Table 6.4: The table represents filtered networks under the ERGM. The goodness of fit is defined under the AIC and BIC, a smaller value represents higher model adequacy. We define the model fit as $100 \times [1 - (LL^M(\theta)/LL^0(\theta))]$, where $LL^M(\theta)$ is the log-likelihood of ERGM and $LL^0(\theta)$ is the log-likelihood of the null model. The $LL^M(\theta)$ includes the link and node level parameters, whereas the null model $LL^0(\theta)$ only includes the link parameter.

under positive correlations. When the density of the network increases within the TMFG, the network structure decreases the model fit and the model adequacy of the ERGM. We still observe a coefficient value where there is a formation of links between non-Euro countries, i.e., the Czech Republic and Iceland with Euro area countries.

If we consider economic indicators, there is a smaller coefficient value across all parameters compared with COVID-19 deaths. The inflation rate under the MaST is positive between the two nodes and represents the links with other countries with high inflation rates. This contrasts with the coefficient value within the AG, which has a negative coefficient between locally connected nodes. Overall, we find altering any one of the conditions within the MST increases the model fitness to the ERGM. This also results in a decrease in the model adequacy in some networks compared with the MST. For negative correlations, we find higher compatibility between the topological structure and model fit under the MaST compared with the MST for positive correlations. Through these approaches, we can capture the core interactions observed between Euro countries and their links with non-Euro countries. We can also factor in economic and health node variables, in which we find COVID-19 deaths to be highly significant.

6.5 Conclusion

As a response to the COVID-19 pandemic, most countries implemented various socio-economic policies and business restrictions almost simultaneously. An immediate consequence was an increase in yield rates for these nations. The resulting upward co-movement and upward movements in other yield rates explain the decrease in the mean correlation in bond dynamics, coinciding with the pandemic outbreak. Thus, understanding the dynamics of financial instruments in the Euro area is relevant to assessing the increased economic strain from events seen in the last decade.

We consider the movements of European sovereign bond yields for network filtering methods, where we focus on the COVID-19 period. We find that the impact of COVID-19 decreased the mean correlation, which was reflected within the normalised network length of all filtering methods. The network topology remained consistent with previous years, in which the trends between approaches were distinctive. The degree centrality was highest for GIIPS and ABFN countries when considering positive correlations and non-Euro countries within negatively correlated type networks. We identified the network structures of filtering methods within the COVID-19 period, which showed one large component consisting of GIIPS and ABFN countries for positive correlations. We were able to verify several of these relationships under an ERGM, in which we find COVID-19 deaths to be significant within negatively correlated networks.

However, depending on the terms of each bond, the European bond market reacted positively after central banks (e.g., Bank of England, European Central Bank, Swiss National Bank) increased their financial programs directed at alleviating the financial pressure on markets and providing financial liquidity to issuers. Namely, the bond purchase programs had aimed to consolidate market recovery and help displace investors toward other financial assets. As a result, prices recovered and remain close to the high levels of the 2020 second quarter, but not at the same level before March's stress situation, especially in 10Y bonds. Additionally, if liquidity provided by central banks starts to drop off, the market dynamics could adjust to economic performance and not its financial performance. In other words, the resulting dynamics could explain an increase in mean correlation in bond dynamics coinciding with the economic dynamics after the pandemic and the increment in yield rates.

Although we consider the sovereign bond yields with a 10Y maturity as a benchmark, this research can be extended to sovereign bonds with different maturities (e.g., short-term 1Y, 2Y or 5Y, and long-term 20Y or 30Y) because these bonds could reveal interesting effects and confirm that sovereign bonds are a good indicator to identify the economic impact of COVID-19. As each sovereign bond has different yield and volatility trends, we considered using the zero-coupon curve to evaluate the full extent of COVID-19 on sovereign bonds.

Chapter 7

Conclusion and Discussion

In this thesis, we contribute to the understanding of fire sales and policy interventions using tools in financial networks and complex systems. Fire sales are a larger contributor to systemic risk, which we empirically show using regulatory data and theoretically show using new valuation models. Allowing these losses to spread can have a lingering impact on the financial system, and therefore different policy interventions are explored. As the implementation of the policy can change its effectiveness, we use financial networks to consider how policies reduce losses, by accounting for all the individual characteristics of banks. The use of networks has been the underlying theme of this thesis, where we explore financial networks for assessing fire sales and in the design of policy interventions. We introduce the main messages of the thesis, provide conclusions of thesis chapters and discuss future research directions.

Fire sales and financial networks: One of the key themes of this thesis was the connections between fire sales and financial networks. We explored the application of financial networks through the incorporation of data in the contagion of fire sales. We considered situations where the full information cannot be fully obtained and cases where there is uncertainty on the severity of fire sale losses.

We explored the application of financial networks through the use of matrix reconstruction methods for partial information and the introduction of a new reverse stress testing approach for fire sales risk. In both cases, we made assumptions on the construction of the financial network and how the financial network can be used to derive scenarios that maximised the total assets losses of banks in a fire sale. The context of financial networks was important because this showed the extent to which banks' losses come from fire sales. We made contributions to the area of fire sales and financial networks in both the application of fire sales under partial information and in the consideration of a new reverse stress testing approach. In the area of fire sales under partial information, there have been no previous empirical studies to our knowledge where policy interventions have been considered under partial information for the fully observed data in fire sales. Secondly,

we formulate a new reverse stress testing approach that has not been considered for the fire sales measures by Greenwood et al. (2015), and show how these results compare to other benchmark scenarios.

Using financial network-motivated tools, it was clear multiple methods could be used to assess or mitigate the scale of fire sales. This was shown in the similarity of fire sales losses and the closeness of policy interventions from matrix reconstruction methods under partial information, compared with the full observed data. This was also shown in deriving several scenarios from reverse stress tests, where losses from each of these scenarios were larger than other benchmark scenarios. Therefore, other benchmarks could be considered to further evaluate the performance of each method for modelling fire sales.

While there can be several methods to address the absence or uncertainty in the data, methods that accounted for the features in the data, in general, showed a better performance for modelling fire sales. This was observed in the use of policy interventions which were informed by sampling-based matrix reconstruction methods under partial information. This consideration is also one of the main reasons why we introduced a new reverse stress testing approach for fire sales. As the financial network is reflected in the data, this data can then be used in the consideration of policy interventions and the formulation of scenarios.

Policy interventions and financial networks: The second theme of the thesis was focused on policy interventions towards financial networks. We explored policy interventions which had structural changes in the financial network. One policy focused on assets used as collateral as part of the bank's initial margin requirements, and how this could amplify the losses of fire sales for banks' external asset holdings and counterparty losses for banks with interbank assets and liabilities. We also explored the influence of the financial network from the policy of ring-fencing, representing a separation of the bank's balance sheet into two separate entities.

We provide contributions in both areas regarding the interaction of policy interventions and financial networks. With the addition of two channels of fire sales in a collateral-based model, we formulated a new extended collateral-based clearing model and showed the extent to which fire sales amplify losses. For ring-fencing, we provide the first framework to our knowledge of how the direction of ring-fencing can be fully evaluated, with consideration of the financial network.

From both works, we find unintended consequences of how the policy can negatively impact banks. While initially, these policies decrease systemic risk, with the consideration of the contagion mechanism, these policies can increase losses. This is because the consideration of assets as collateral and the ring-fencing policy represent structural changes to the network. A decrease in losses for one bank can increase the losses which other banks are

exposed to. The increase in losses for these banks can amplify losses to their associated counterparties, causing larger losses than the initial decrease from the intended policy. In this respect, there is an associated trade-off in these types of policies. Because we are re-allocating and rewiring the network, we are increasing and decreasing the exposure of banks to systemic risks. This is not the case for policy interventions explored in Chapter 2, as additional capital provided in any form always decreases losses. The questions in these types of policies are not about its benefits, but how to optimise the effectiveness of this policy in the reduction of fire sales. Hence, we show how financial networks can be used to inform a range of policy interventions and model the consequences towards the system.

In Chapter 2, we considered fire sales under partial information and how this can inform policy interventions. We find that for different matrix reconstruction methods, the magnitude of losses under a fire sale from partial information is similar to the fully observed data. Across all matrix reconstruction methods, there was a mixed performance in the similarity of matrix reconstruction methods to fire sale losses, which was dependent on the fire sale scenario and data used.

For policy interventions, there is a similarity in the decrease in losses from capital injections informed by matrix reconstruction methods under partial information compared with the fully observed data. The decrease in losses from capital injections is larger compared with a leverage cap (assuming the same quantity of additional capital), as the reduction in losses from capital injections accounts for the financial network and initial losses of banks. The similarity in the reduction of fire sales for capital injections was closest to Bayesian methods under the GIIPS shock. In other cases, the use of matrix reconstruction methods resulted in fire sales losses which were further away than capital injections which do not use matrix reconstruction methods i.e., using the MinDen matrix reconstruction method compared with an allocation based on the total asset holdings of banks. Hence, the suitability of the reconstruction method for both the overall fit of the data and the type of policy implemented is important for modelling fire sales under partial information.

In Chapter 3, we considered a reverse stress testing approach to fire sales. This assumed the total losses of banks and derived a scenario that corresponds to these losses. Under the multi-stage fire sales mechanism by Greenwood et al. (2015), we formulated an optimisation-based approach to reverse stress testing.

Our results show the total losses and the number of stressed banks were the largest from a reverse stress test, compared to other benchmark scenarios. Even when banks can maintain their target leverages, some scenarios from reverse stress tests resulted in 90% losses of the banks' total asset holdings. This shows the extent to which banks can be affected by a fire sales scenario.

When we considered the distribution of the scenario in the initial stages of fire sales, we showed the allocation of shocks in fire sales resembled a fractional knapsack problem. In these scenarios, shocks were allocated to assets that were held by banks of high target leverage. This reflects the nature of the fire sales mechanism, in which the assets of banks of high leverage are targeted because losses incurred by these banks would sell a larger volume of assets.

In Chapter 4, we extended the collateral model by Ghamami et al. (2022), where banks with an interbank obligation also post assets used as collateral. We incorporated banks' external illiquid asset holdings into the clearing mechanism by Feinstein (2017) and formulated a new collateral-based clearing model with two channels of fire sales. We analysed the total payments of banks using this extended collateral clearing model, and how this was affected by different financial factors.

Using networks generated from a random graph model, we find that illiquid assets that were used as collateral and held by banks' external asset holdings can increase total losses. This is because the assets sold have a high price impact, which further decreases the value of the asset from the fire sales. This affects the ability of the bank to meet its obligations, triggering further losses and an increase in defaults. The losses from illiquid assets in a fire sale can be higher than banks which hold no external assets, as there is no overlap in assets and no increase in assets sold from a fire sale.

We also considered bank payments under different network densities, and how this impacts the clearing scenario. We find the losses to banks were smaller from the clearing mechanism as the network density increased. The increase in the number of links decreases the losses that any one bank incurs from the clearing scenario, where losses are dispersed to other banks in the network.

In Chapter 5, we focus on the UK policy of ring-fencing. This involved separating the bank's retail and investment assets into two separate entities: a RFB and nRFB. This policy aims to protect the assets of the RFB associated with the real economy from the riskier investment assets of the nRFB.

From ring-fencing, we compared the change in external leverage which we associated with a probability of default for banks before and after ring-fencing. We find the change from ring-fencing for banks in the network can result in an increase or decrease in the total equity of the bank. In the case of ring-fencing where the RFB is safer (riskier), there is a decrease (increase) in the total re-evaluated equity, because there was an increase (decrease) in the external leverage of the nRFB. The change in equity only occurs if there is a bank which is exposed to bank ring-fencing. For the bank ring-fencing, it is only affected by ring-fencing if it is indirectly exposed to itself or to another bank which performs ring-fencing. In this regard, the operation of ring-fencing does not cause a change

in equity, but only when the bank ring-fencing has liabilities with other banks in the network.

In Chapter 6, we analyse the period of COVID-19 and the trends of sovereign bond yields using network filtering methods. Different network filtering methods were used to reflect different subgroups of correlations between assets, which were represented as part of a network structure. We can then analyse these filtered networks using network measures to consider the centrality and community of sovereign bond yields, across various years. We find the average correlations were highest during the COVID-19 period. This was reflected in the average of the correlation matrix, and the correlations of filtered networks. This showed the extent of COVID-19, which had an impact across a range of sovereign bond yields. During the COVID-19 period, two distinct communities from network filtering methods represented Euro and non-Euro-denominated assets. Within the group of Euro assets, there were two sub-communities of GIIPS and ABFN countries, where these groups represented Euro countries that were both highly and less impacted by previous systemic events. These network structures showed a level of fragmentation that has not been observed since the 2008 financial crisis and the 2012 Euro debt crisis.

There are several extensions which can be considered from the work presented in this thesis. From the data aspect, there can be further investigations into the inclusion of information to form a reconstructed matrix. This was explored to some degree in Chapter 2 in the appendix, where a subset of the information from the fully observed data was included in the Entropy method. Only when the information from the fully observed data which included the asset holdings of shocked assets was there an increase in the similarity of fire sales losses to the fully observed data. Further work can explore how to include other financial variables into the reconstructed matrix i.e., volatility of assets and different maturities of the bank's asset holdings, while not decreasing the accuracy of fire sales from matrix reconstruction methods.

Another direction is an economic approach to how ring-fencing should be conducted. In Chapter 5, we considered all types of feasible ring-fencing and how this affected the RFB and nRFB. But from the context of the policy in the UK, there are some types of ring-fencing which are more favourable i.e., decreasing the probability of default for the RFB (making the RFB safer) to decrease the riskiness of banks holding retail assets. Therefore, obtaining the optimal allocations of external assets and liabilities for banks ring-fencing that minimises the probability of default while factoring in the decrease in equity for nRFBs could be another direction of interest.

Bibliography

- Acemoglu, D., Ozdaglar, A., and Tahbaz-Salehi, A. (2015). Systemic Risk and Stability in Financial Networks. *American Economic Review*, 105(2):564–608. doi: 10.1257/aer.20130456.
- Adrian, T. and Shin, H. S. (2010). Liquidity and leverage. *Journal of Financial Intermediation*, 19(3):418–437. <https://doi.org/10.1016/j.jfi.2008.12.002>.
- Akiyoshi, F. (2019). Effects of separating commercial and investment banking: Evidence from the dissolution of a joint venture investment bank. *Journal of Financial Economics*, 134(3):703–714. <https://doi.org/10.1016/j.jfineco.2019.05.004>.
- Aldasoro, I. and Alves, I. (2018). Multiplex interbank networks and systemic importance: An application to European data. *Journal of Financial Stability*, 35:17–37. <https://doi.org/10.1016/j.jfs.2016.12.008>.
- Allen, F. and Gale, D. (2000). Financial Contagion. *Journal of Political Economy*, 108(1):1–33. <https://doi.org/10.1086/262109>.
- Alqaryouti, O., Farouk, T., and Siyam, N. (2019). Clustering Stock Markets for Balanced Portfolio Construction. In *Proceedings of the International Conference on Advanced Intelligent Systems and Informatics 2018 4*, pages 577–587. Springer. https://doi.org/10.1007/978-3-319-99010-1_53.
- Alter, A. and Beyer, A. (2014). The dynamics of spillover effects during the european sovereign debt turmoil. *Journal of Banking & Finance*, 42:134–153. <https://doi.org/10.1016/j.jbankfin.2014.01.030>.
- Amini, H., Filipović, D., and Minca, A. (2016). Uniqueness of equilibrium in a payment system with liquidation costs. *Operations Research Letters*, 44(1):1–5. <https://doi.org/10.1016/j.orl.2015.10.005>.
- Anand, K., Craig, B., and Von Peter, G. (2015). Filling in the blanks: network structure and interbank contagion. *Quantitative Finance*, 15(4):625–636. <https://doi.org/10.1080/14697688.2014.968195>.

- Anand, K., Van Lelyveld, I., Banai, Á., Friedrich, S., Garratt, R., Halaj, G., Figue, J., Hansen, I., Jaramillo, S. M., Lee, H., et al. (2018). The missing links: A global study on uncovering financial network structures from partial data. *Journal of Financial Stability*, 35:107–119. <https://doi.org/10.1016/j.jfs.2017.05.012>.
- Anderson, R. W. (2016). Stress testing and macroprudential regulation: A transatlantic assessment. *Stress Testing and Macroprudential Regulation*, page 1.
- Antonakakis, N. and Vergos, K. (2013). Sovereign bond yield spillovers in the Euro zone during the financial and debt crisis. *Journal of International Financial Markets, Institutions and Money*, 26:258–272. <https://doi.org/10.1016/j.intfin.2013.06.004>.
- Aste, T., Shaw, W., and Di Matteo, T. (2010). Correlation structure and dynamics in volatile markets. *New Journal of Physics*, 12(8):085009. <https://doi.org/10.1088/1367-2630/12/8/085009>.
- Baes, M. and Schaanning, E. (2023). Reverse stress testing: Scenario design for macroprudential stress tests. *Mathematical Finance*, 33(2):209–256. <https://doi.org/10.1111/mafi.12373>.
- Balli, F. (2009). Spillover effects on government bond yields in euro zone. Does full financial integration exist in European government bond markets? *Journal of Economics and Finance*, 33(4):331. <https://doi.org/10.1007/s12197-008-9029-3>.
- Banerjee, T. and Feinstein, Z. (2021). Price mediated contagion through capital ratio requirements with VWAP liquidation prices. *European Journal of Operational Research*, 295(3):1147–1160. <https://doi.org/10.1016/j.ejor.2021.03.053>.
- Bank of England (2022). Banks in scope of ring-fencing as of 1 January 2022. <https://bit.ly/3I0yty7>.
- Bardoscia, M., Barucca, P., Codd, A. B., and Hill, J. (2019). Forward-looking solvency contagion. *Journal of Economic Dynamics and Control*, 108:103755. <https://doi.org/10.1016/j.jedc.2019.103755>.
- Bardoscia, M., Battiston, S., Caccioli, F., and Caldarelli, G. (2015). DebtRank: A Microscopic Foundation for Shock Propagation. *PloS One*, 10(6):e0130406. <https://doi.org/10.1371/journal.pone.0134888>.
- Bardoscia, M., Battiston, S., Caccioli, F., and Caldarelli, G. (2017). Pathways towards instability in financial networks. *Nature Communications*, 8(1):1–7. <https://doi.org/10.1038/ncomms14416>.

- Bardoscia, M., Caccioli, F., Perotti, J. I., Vivaldo, G., and Caldarelli, G. (2016). Distress Propagation in Complex Networks: The Case of Non-Linear DebtRank. *PloS One*, 11(10):e0163825. <https://doi.org/10.1371/journal.pone.0163825>.
- Bardoscia, M. and Pang, R. K.-K. (2023). Ring-fencing in financial networks. *Bank of England Staff Working Papers*, 1046. <https://www.bankofengland.co.uk/working-paper/2023/ring-fencing-in-financial-networks>.
- Bargigli, L., di Iasio, G., Infante, L., Lillo, F., and Pierobon, F. (2016). Interbank Markets and Multiplex Networks: Centrality Measures and Statistical Null Models. *Interconnected Networks*, pages 179–194. https://doi.org/10.1007/978-3-319-23947-7_11.
- Bartolozzi, M., Mellen, C., Di Matteo, T., and Aste, T. (2007). Multi-scale correlations in different futures markets. *The European Physical Journal B*, 58:207–220. <https://doi.org/10.1140/epjb/e2007-00216-2>.
- Barucca, P., Bardoscia, M., Caccioli, F., D’Errico, M., Visentin, G., Caldarelli, G., and Battiston, S. (2020). Network valuation in financial systems. *Mathematical Finance*, 30(4):1181–1204. <https://doi.org/10.1111/mafi.12272>.
- Battiston, S., Gatti, D. D., Gallegati, M., Greenwald, B., and Stiglitz, J. E. (2012a). Default cascades: When does risk diversification increase stability? *Journal of Financial Stability*, 8(3):138–149. <https://doi.org/10.1016/j.jfs.2012.01.002>.
- Battiston, S., Gatti, D. D., Gallegati, M., Greenwald, B., and Stiglitz, J. E. (2012b). Liaisons dangereuses: Increasing connectivity, risk sharing, and systemic risk. *Journal of Economic Dynamics and Control*, 36(8):1121–1141. <https://doi.org/10.1016/j.jedc.2012.04.001>.
- Battiston, S., Puliga, M., Kaushik, R., Tasca, P., and Caldarelli, G. (2012c). DebtRank: Too Central to Fail? Financial Networks, the FED and Systemic Risk. *Scientific Reports*, 2(1):1–6. <https://doi.org/10.1038/srep00541>.
- Baur, D. G. (2020). Decoupling and Contagion: The Special Case of the Eurozone Sovereign Debt Crisis. *International Review of Finance*, 20(1):133–154. <https://doi.org/10.1111/irfi.12220>.
- Beck, R., Georgiadis, G., and Gräßl, J. (2016). The geography of the great rebalancing in euro area bond markets during the sovereign debt crisis. *Journal of Empirical Finance*, 38:449–460. <https://doi.org/10.1016/j.jempfin.2016.01.003>.
- Bertsekas, D., Nedic, A., and Ozdaglar, A. (2003). *Convex Analysis and Optimization*, volume 1. Athena Scientific.

- Bichuch, M. and Feinstein, Z. (2019). Optimization of Fire Sales and Borrowing in Systemic Risk. *SIAM Journal on Financial Mathematics*, 10(1):68–88. <https://doi.org/10.1137/18M1195425>.
- Bichuch, M. and Feinstein, Z. (2022). Endogenous Inverse Demand Functions. *Operations Research*, 70(5):2702–2714. <https://doi.org/10.1287/opre.2022.2325>.
- Birch, J., Pantelous, A. A., and Soramäki, K. (2016). Analysis of Correlation Based Networks Representing DAX 30 Stock Price Returns. *Computational Economics*, 47(4):501–525. <https://doi.org/10.1007/s10614-015-9481-z>.
- BIS (2011). Capital treatment for bilateral counterparty credit risk finalised by the Basel Committee. <https://www.bis.org/press/p110601.htm>.
- Black, F. and Cox, J. C. (1976). Valuing Corporate Securities: Some Effects Of Bond Indenture Provisions. *The Journal of Finance*, 31(2):351–367. <https://doi.org/10.1111/j.1540-6261.1976.tb01891.x>.
- Board, F. S. (2017). Review of OTC derivatives market reforms: Effectiveness and broader effects of the reforms. *Financial Stability Board Report*.
- Boyd, J. H., Chang, C., and Smith, B. D. (1998). Moral Hazard under Commercial and Universal Banking. *Journal of Money, Credit and Banking*, pages 426–468. <https://doi.org/10.2307/2601249>.
- Braouezec, Y. and Wagalath, L. (2019). Strategic fire-sales and price-mediated contagion in the banking system. *European Journal of Operational Research*, 274(3):1180–1197. <https://doi.org/10.1016/j.ejor.2018.11.012>.
- Brazier, A. (2017). How to: Macropru. 5 principles for macroprudential policy. Speech given by Alex Brazier, Executive Director for Financial Stability Strategy and Risk Member of the Financial Policy Committee, Bank of England, at the London School of Economics, Financial Regulation Seminar Monday 13 February 2017. Available at <https://www.bankofengland.co.uk/speech/2017/how-to-macropru-5-principles-for-macroprudential-policy>.
- Breuer, T. and Summer, M. (2020). Systematic stress tests on public data. *Journal of Banking & Finance*, 118:105886. <https://doi.org/10.1016/j.jbankfin.2020.105886>.
- Britton, K., Dawkes, L., Debbage, S., and Idris, T. (2016). Ring-Fencing: What is It and How Will It Affect Banks and Their Customers? *Bank of England Quarterly Bulletin*, page Q4.

- Byrd, R. H., Nocedal, J., and Waltz, R. A. (2006). KNITRO: An Integrated Package for Nonlinear Optimization. *Large-scale nonlinear optimization*, pages 35–59. https://doi.org/10.1007/0-387-30065-1_4.
- Caballero, R. J. and Simsek, A. (2013). Fire Sales in a Model of Complexity. *The Journal of Finance*, 68(6):2549–2587. <https://doi.org/10.1111/jofi.12087>.
- Caccioli, F., Catanach, T. A., and Farmer, J. D. (2012). Heterogeneity, Correlations And Financial Contagion. *Advances in Complex Systems*, 15(2):1250058. <https://doi.org/10.1142/S0219525912500580>.
- Capponi, A., Glasserman, P., and Weber, M. (2020). Swing Pricing for Mutual Funds: Breaking the Feedback Loop Between Fire Sales and Fund Redemptions. *Management Science*, 66(8):3581–3602. <https://doi.org/10.1287/mnsc.2019.3353>.
- Capponi, A. and Larsson, M. (2015). Price Contagion through Balance Sheet Linkages. *The Review of Asset Pricing Studies*, 5(2):227–253. <https://doi.org/10.1093/raps/tu/rav006>.
- Capponi, A. and Weber, M. (2022). Systemic Portfolio Diversification. *Available at SSRN 3345399*. <https://dx.doi.org/10.2139/ssrn.3345399>.
- Caprio, G., Laeven, L., and Levine, R. (2007). Governance and bank valuation. *Journal of Financial Intermediation*, 16(4):584–617. <https://doi.org/10.1016/j.jfi.2006.10.003>.
- Chang, J.-W. (2019). Collateralized Debt Networks with Lender Default. *Available at SSRN 3468267*. <https://dx.doi.org/10.2139/ssrn.3468267>.
- Chang, J.-W. and Chuan, G. (2023). Contagion in Debt and Collateral Markets. *FEDS Working Paper*. <https://dx.doi.org/10.17016/FEDS.2023.016>.
- Chari, V., Lacoste-Julien, S., Laptev, I., and Sivic, J. (2015). On Pairwise Costs for Network Flow Multi-Object Tracking. In *Proceedings of the IEEE Conference on Computer Vision and Pattern Recognition*, pages 5537–5545.
- Chavaz, M. and Elliott, D. (2020). Separating retail and investment banking: Evidence from the UK. <https://www.bankofengland.co.uk/-/media/boe/files/working-paper/2020/separating-retail-and-investment-banking-evidence-from-the-uk.pdf>.
- Cifuentes, R., Ferrucci, G., and Shin, H. S. (2005). Liquidity Risk and Contagion. *Journal of the European Economic Association*, 3(2-3):556–566. <https://doi.org/10.1162/jeea.2005.3.2-3.556>.

- Cimini, G., Squartini, T., Garlaschelli, D., and Gabrielli, A. (2015). Systemic Risk Analysis on Reconstructed Economic and Financial Networks. *Scientific reports*, 5(1):15758. <https://doi.org/10.1038/srep15758>.
- Claeys, P. and Vašíček, B. (2014). Measuring bilateral spillover and testing contagion on sovereign bond markets in Europe. *Journal of Banking & Finance*, 46:151–165. <https://doi.org/10.1016/j.jbankfin.2014.05.011>.
- Cont, R. (2018). Margin Requirements for Non-Cleared Derivatives. *Available at SSRN 3168751*. <https://dx.doi.org/10.2139/ssrn.3168751>.
- Cont, R., Kotlicki, A., and Valderrama, L. (2020). Liquidity at risk: Joint stress testing of solvency and liquidity. *Journal of Banking & Finance*, 118:105871. <https://doi.org/10.1016/j.jbankfin.2020.105871>.
- Cont, R. and Schaanning, E. (2017). Fire Sales, Indirect Contagion and Systemic Stress Testing. *Indirect Contagion and Systemic Stress Testing (June 13, 2017)*. <https://dx.doi.org/10.2139/ssrn.2541114>.
- Cont, R. and Schaanning, E. (2019). Monitoring indirect contagion. *Journal of Banking & Finance*, 104:85–102. <https://doi.org/10.1016/j.jbankfin.2019.04.007>.
- Cont, R. and Wagalath, L. (2013). Running For The Exist: Distressed Selling And Endogenous Correlation In Financial Markets. *Mathematical Finance: An International Journal of Mathematics, Statistics and Financial Economics*, 23(4):718–741. <https://doi.org/10.1111/j.1467-9965.2011.00510.x>.
- Cornett, M. M., Ors, E., and Tehranian, H. (2002). Bank Performance around the Introduction of a Section 20 Subsidiary. *The Journal of Finance*, 57(1):501–521. <https://doi.org/10.1111/1540-6261.00430>.
- Dantzig, G. B. (1957). Discrete-Variable Extremum Problems. *Operations Research*, 5(2):266–288. <https://doi.org/10.1287/opre.5.2.266>.
- Darbellay, G. A. and Wuertz, D. (2000). The entropy as a tool for analysing statistical dependences in financial time series. *Physica A: Statistical Mechanics and its Applications*, 287(3-4):429–439. [https://doi.org/10.1016/S0378-4371\(00\)00382-4](https://doi.org/10.1016/S0378-4371(00)00382-4).
- Deev, O. and Lyócsa, Š. (2020). Connectedness of financial institutions in Europe: A network approach across quantiles. *Physica A: Statistical Mechanics and its Applications*, 550:124035. <https://doi.org/10.1016/j.physa.2019.124035>.
- Detering, N., Meyer-Brandis, T., Panagiotou, K., and Ritter, D. (2022). Suffocating Fire Sales. *SIAM Journal on Financial Mathematics*, 13(1):70–108. <https://doi.org/10.1137/20M1379800>.

- Di Gangi, D., Lillo, F., and Pirino, D. (2018). Assessing systemic risk due to fire sales spillover through maximum entropy network reconstruction. *Journal of Economic Dynamics and Control*, 94:117–141. <https://doi.org/10.1016/j.jedc.2018.07.001>.
- Di Matteo, T., Aste, T., Hyde, S., and Ramsden, S. (2005). Interest rates hierarchical structure. *Physica A: Statistical Mechanics and its Applications*, 355(1):21–33. <https://doi.org/10.1016/j.physa.2005.02.063>.
- Dias, J. (2012). Sovereign debt crisis in the European Union: A minimum spanning tree approach. *Physica A: Statistical Mechanics and its Applications*, 391(5):2046–2055. <https://doi.org/10.1016/j.physa.2011.11.004>.
- Dias, J. (2013). Spanning trees and the Eurozone crisis. *Physica A: Statistical Mechanics and its Applications*, 392(23):5974–5984. <https://doi.org/10.1016/j.physa.2013.08.001>.
- Diem, C., Pichler, A., and Thurner, S. (2020). What is the minimal systemic risk in financial exposure networks? *Journal of Economic Dynamics and Control*, 116:103900. <https://doi.org/10.1016/j.jedc.2020.103900>.
- Drucker, S. and Puri, M. (2005). On the Benefits of Concurrent Lending and Underwriting. *The Journal of Finance*, 60(6):2763–2799. <https://doi.org/10.1111/j.1540-6261.2005.00816.x>.
- Duarte, F. and Eisenbach, T. M. (2021). Fire-Sale Spillovers and Systemic Risk. *The Journal of Finance*, 76(3):1251–1294. <https://doi.org/10.1111/jofi.13010>.
- Duffie, D. (2018). Financial Regulatory Reform After the Crisis: An Assessment. *Management Science*, 64(10):4835–4857. <https://doi.org/10.1287/mnsc.2017.2768>.
- Eisenberg, L. and Noe, T. H. (2001). Systemic Risk in Financial Systems. *Management Science*, 47(2):236–249. <https://doi.org/10.1287/mnsc.47.2.236.9835>.
- Elliott, M., Golub, B., and Jackson, M. O. (2014). Financial Networks and Contagion. *American Economic Review*, 104(10):3115–3153. doi: 10.1257/aer.104.10.3115.
- Elsinger, H. (2011). Financial Networks, Cross Holdings, and Limited Liability. *Wien: Oesterreichische Nationalbank. Working Paper*, 156:37.
- Elsinger, H., Lehar, A., and Summer, M. (2006). Risk Assessment for Banking Systems. *Management Science*, 52(9):1301–1314. <https://doi.org/10.1287/mnsc.1060.0531>.
- Erdős, P. and Rényi, A. (1959). On random graphs, I. *Publicationes Mathematicae (Debrecen)*, 6:290–297.

- Erten, I., Neamțu, I., Thanassoulis, J. E., et al. (2022). The ring-fencing bonus. <https://www.bankofengland.co.uk/working-paper/2022/the-ring-fencing-bonus>.
- Farhi, E. and Tirole, J. (2021). Shadow Banking and the Four Pillars of Traditional Financial Intermediation. *The Review of Economic Studies*, 88(6):2622–2653. <https://doi.org/10.1093/restud/rdaa059>.
- Feinstein, Z. (2017). Financial contagion and asset liquidation strategies. *Operations Research Letters*, 45(2):109–114. <https://doi.org/10.1016/j.orl.2017.01.004>.
- Feinstein, Z. (2020). Capital regulation under price impacts and dynamic financial contagion. *European Journal of Operational Research*, 281(2):449–463. <https://doi.org/10.1016/j.ejor.2019.08.044>.
- Feinstein, Z. and El-Masri, F. (2017). The effects of leverage requirements and fire sales on financial contagion via asset liquidation strategies in financial networks. *Statistics & Risk Modeling*, 34(3-4):113–139. <https://doi.org/10.1515/strm-2015-0030>.
- Fink, K., Krüger, U., Meller, B., and Wong, L.-H. (2016). The credit quality channel: Modeling contagion in the interbank market. *Journal of Financial Stability*, 25:83–97. <https://doi.org/10.1016/j.jfs.2016.06.002>.
- Fischer, T. (2014). No-Arbitrage Pricing Under Systemic Risk: Accounting For Cross-Ownership. *Mathematical Finance: An International Journal of Mathematics, Statistics and Financial Economics*, 24(1):97–124. <https://doi.org/10.1111/j.1467-9965.2012.00526.x>.
- Flood, M. D. and Korenko, G. G. (2015). Systematic scenario selection: stress testing and the nature of uncertainty. *Quantitative Finance*, 15(1):43–59. <https://doi.org/10.1080/14697688.2014.926018>.
- Forbes, K. J. and Rigobon, R. (2002). No Contagion, Only Interdependence: Measuring Stock Market Comovements. *The Journal of Finance*, 57(5):2223–2261. <https://doi.org/10.1111/0022-1082.00494>.
- Frank, M. and Wolfe, P. (1956). An algorithm for quadratic programming. *Naval Research Logistics Quarterly*, 3(1-2):95–110.
- Freeman, L. C. (1977). A Set of Measures of Centrality Based on Betweenness. *Sociometry*, 40(1):35–41. <https://doi.org/10.2307/3033543>.
- Freixas, X., Lóránth, G., and Morrison, A. D. (2007). Regulating financial conglomerates. *Journal of Financial Intermediation*, 16(4):479–514. <https://doi.org/10.1016/j.jfi.2007.03.004>.

- Gai, P., Haldane, A., and Kapadia, S. (2011). Complexity, concentration and contagion. *Journal of Monetary Economics*, 58(5):453–470. <https://doi.org/10.1016/j.jmoneco.2011.05.005>.
- Gai, P. and Kapadia, S. (2010). Contagion in financial networks. *Proceedings of the Royal Society A: Mathematical, Physical and Engineering Sciences*, 466(2120):2401–2423. <https://doi.org/10.1098/rspa.2009.0410>.
- Gande, A., Puri, M., Saunders, A., and Walter, I. (1997). Bank Underwriting of Debt Securities: Modern Evidence. *The Review of Financial Studies*, 10(4):1175–1202. <https://doi.org/10.1093/rfs/10.4.1175>.
- Gandy, A. and Veraart, L. A. M. (2017). A Bayesian Methodology for Systemic Risk Assessment in Financial Networks. *Management Science*, 63(12):4428–4446. <https://doi.org/10.1287/mnsc.2016.2546>.
- Gandy, A. and Veraart, L. A. M. (2019). Adjustable network reconstruction with applications to CDS exposures. *Journal of Multivariate Analysis*, 172:193–209. <https://doi.org/10.1016/j.jmva.2018.08.011>.
- Ghamami, S., Glasserman, P., and Young, H. P. (2022). Collateralized Networks. *Management Science*, 68(3):2202–2225. <https://doi.org/10.1287/mnsc.2020.3938>.
- Gilmore, C. G., Lucey, B. M., and Boscia, M. W. (2010). Comovements in government bond markets: A minimum spanning tree analysis. *Physica A: Statistical Mechanics and its Applications*, 389:4875–4886. <https://doi.org/10.1016/j.physa.2010.06.057>.
- Glasserman, P., Kang, C., and Kang, W. (2015). Stress scenario selection by empirical likelihood. *Quantitative Finance*, 15(1):25–41. <https://doi.org/10.1080/14697688.2014.926019>.
- Glasserman, P. and Young, H. P. (2015). How likely is contagion in financial networks? *Journal of Banking & Finance*, 50:383–399. <https://doi.org/10.1016/j.jbankfin.2014.02.006>.
- Gorton, G. and Metrick, A. (2012). Securitized banking and the run on repo. *Journal of Financial Economics*, 104(3):425–451. <https://doi.org/10.1016/j.jfineco.2011.03.016>.
- Greenwood, R., Landier, A., and Thesmar, D. (2015). Vulnerable banks. *Journal of Financial Economics*, 115(3):471–485. <https://doi.org/10.1016/j.jfineco.2014.11.006>.

- Grigat, D. and Caccioli, F. (2017). Reverse stress testing interbank networks. *Scientific Reports*, 7(1):1–11. <https://doi.org/10.1038/s41598-017-14470-1>.
- Guleva, V. Y., Skvorcova, M. V., and Boukhanovsky, A. V. (2015). Using Multiplex Networks for Banking Systems Dynamics Modelling. *Procedia Computer Science*, 66:257–266. <https://doi.org/10.1016/j.procs.2015.11.031>.
- Hazan, E. and Luo, H. (2016). Variance-Reduced and Projection-Free Stochastic Optimization. *Proceedings of Machine Learning Research*, 48:1263–1271. <http://proceedings.mlr.press/v48/hazana16.pdf>.
- Heimo, T., Kaski, K., and Saramäki, J. (2009). Maximal spanning trees, asset graphs and random matrix denoising in the analysis of dynamics of financial networks. *Physica A: Statistical Mechanics and its Applications*, 388(2-3):145–156. <https://doi.org/10.1016/j.physa.2008.10.007>.
- HM Treasury (2022). Government response to the independent review on ring-fencing and proprietary trading. <https://www.gov.uk/government/publications/ring-fencing-reforms/government-response-to-the-independent-review-on-ring-fencing-and-proprietary-trading>.
- HM Treasury (2023). Aligning the ring-fencing and resolution regimes. <https://www.gov.uk/government/consultations/aligning-the-ring-fencing-and-resolution-regimes-call-for-evidence>.
- Huang, J., Shang, P., and Zhao, X. (2012). Multifractal diffusion entropy analysis on stock volatility in financial markets. *Physica A: Statistical Mechanics and its Applications*, 391(22):5739–5745. <https://doi.org/10.1016/j.physa.2012.06.039>.
- Huang, X., Vodenska, I., Havlin, S., and Stanley, H. E. (2013). Cascading Failures in Bi-partite Graphs: Model for Systemic Risk Propagation. *Scientific reports*, 3(1):1219. <https://doi.org/10.1038/srep01219>.
- Independent Commission on Banking (2011). Final report. <https://webarchive.nationalarchives.gov.uk/ukgwa/20120827143059/http://bankingcommission.independent.gov.uk//>.
- Isogai, T. (2017). Dynamic correlation network analysis of financial asset returns with network clustering. *Applied Network Science*, 2(1):8. <https://doi.org/10.1007/s41109-017-0031-6>.
- Jang, W., Lee, J., and Chang, W. (2011). Currency crises and the evolution of foreign exchange market: Evidence from minimum spanning tree. *Physica A: Statistical Me-*

- chanics and its Applications*, 390(4):707–718. <https://doi.org/10.1016/j.physa.2010.10.028>.
- Junior, L. S. and Franca, I. D. P. (2012). Correlation of financial markets in times of crisis. *Physica A: Statistical Mechanics and its Applications*, 391(1-2):187–208. <https://doi.org/10.1016/j.physa.2011.07.023>.
- Korte, B. H., Vygen, J., Korte, B., and Vygen, J. (2011). *Combinatorial Optimization*, volume 1. Springer.
- Krishnamurthy, A., Nagel, S., and Orlov, D. (2014). Sizing Up Repo. *The Journal of Finance*, 69(6):2381–2417. <https://doi.org/10.1111/jofi.12168>.
- Kroszner, R. S. and Rajan, R. G. (1994). Is the Glass-Steagall Act Justified? A Study of the U.S. Experience with Universal Banking Before 1933. *American Economic Review*, pages 810–832.
- Kruskal, J. B. (1956). On the shortest spanning subtree of a graph and the travelling salesman problem. *Proceedings of the American Mathematical Society*, 7(1):48–50. <https://doi.org/10.2307/2033241>.
- Kukreti, V., Pharasi, H. K., Gupta, P., and Kumar, S. (2020). A Perspective on Correlation-Based Financial Networks and Entropy Measures. *Frontiers in Physics*, 8:323. <https://doi.org/10.3389/fphy.2020.00323>.
- Laeven, L. and Levine, R. (2007). Is there a diversification discount in financial conglomerates? *Journal of Financial Economics*, 85(2):331–367. <https://doi.org/10.1016/j.jfineco.2005.06.001>.
- Laloux, L., Cizeau, P., Potters, M., and Bouchaud, J.-P. (2000). Random Matrix Theory And Financial Correlations. *International Journal of Theoretical and Applied Finance*, 3(03):391–397. <https://doi.org/10.1142/S0219024900000255>.
- Lan, G. (2020). *First-order and Stochastic Optimization Methods for Machine Learning*, volume 1. Springer.
- Lebacher, M., Cook, S., Klein, N., and Kauermann, G. (2019). In Search of Lost Edges: A Case Study on Reconstructing Financial Networks. *arXiv preprint arXiv:1909.01274*. <https://doi.org/10.48550/arXiv.1909.01274>.
- Leon, C., Leiton, K., and Perez, J. (2014). Extracting the sovereigns’ CDS market hierarchy: A correlation-filtering approach. *Physica A: Statistical Mechanics and its Applications*, 415:407–420. <https://doi.org/10.1016/j.physa.2014.08.020>.

- Li, Y., Jiang, X.-F., Tian, Y., Li, S.-P., and Zheng, B. (2019). Portfolio optimization based on network topology. *Physica A: Statistical Mechanics and its Applications*, 515:671–681. <https://doi.org/10.1016/j.physa.2018.10.014>.
- Liikanen, E. (2012). Reforming the structure of the EU banking sector: Final report. https://finance.ec.europa.eu/publications/liikanen-report_en.
- Maeng, S. E., Choi, H. W., and Lee, J. W. (2012). Complex Networks And Minimal Spanning Trees In International Trade Network. *International Journal of Modern Physics: Conference Series*, 16:50–60. <https://doi.org/10.1142/S2010194512007775>.
- Mantegna, R. N. (1999). Hierarchical structure in financial markets. *The European Physical Journal B-Condensed Matter and Complex Systems*, 11(1):193–197. <https://doi.org/10.1007/s100510050929>.
- Massara, G. P., Di Matteo, T., and Aste, T. (2016). Network Filtering for Big Data: Triangulated Maximally Filtered Graph. *Journal of Complex Networks*, 5(2):161–178. <https://doi.org/10.1093/comnet/cnw015>.
- McNeil, A. J. and Smith, A. D. (2012). Multivariate stress scenarios and solvency. *Insurance: Mathematics and Economics*, 50(3):299–308. <https://doi.org/10.1016/j.insmatheco.2011.12.005>.
- Merton, R. C. (1974). On the Pricing of Corporate Debt: The Risk Structure of Interest Rates. *The Journal of Finance*, 29(2):449–470. <https://doi.org/10.2307/2978814>.
- Montagna, M. and Kok, C. (2016). Multi-Layered Interbank Model For Assessing Systemic Risk. *ECB Working Paper*. <https://dx.doi.org/10.2139/ssrn.2830546>.
- Musmeci, N., Aste, T., and Di Matteo, T. (2015). Relation between Financial Market Structure and the Real Economy: Comparison between Clustering Methods. *PloS one*, 10(3):e0116201. <https://doi.org/10.1371/journal.pone.0116201>.
- Musmeci, N., Nicosia, V., Aste, T., Di Matteo, T., Latora, V., et al. (2017). The Multiplex Dependency Structure of Financial Markets. *Complexity*, 2017:13. <https://doi.org/10.1155/2017/9586064>.
- Neuhann, D. and Saidi, F. (2018). Do universal banks finance riskier but more productive firms? *Journal of Financial Economics*, 128(1):66–85. <https://doi.org/10.1016/j.jfineco.2018.01.011>.
- Nier, E., Yang, J., Yorulmazer, T., and Alentorn, A. (2007). Network models and financial stability. *Journal of Economic Dynamics and Control*, 31(6):2033–2060. <https://doi.org/10.1016/j.jedc.2007.01.014>.

- Onnela, J.-P., Chakraborti, A., Kaski, K., and Kertesz, J. (2003a). Dynamic asset trees and Black Monday. *Physica A: Statistical Mechanics and its Applications*, 324(1-2):247–252. [https://doi.org/10.1016/S0378-4371\(02\)01882-4](https://doi.org/10.1016/S0378-4371(02)01882-4).
- Onnela, J.-P., Chakraborti, A., Kaski, K., Kertesz, J., and Kanto, A. (2003b). Asset Trees and Asset Graphs in Financial Markets. *Physica Scripta*, 2003(T106):48. <https://doi.org/10.1238/Physica.Topical.106a00048>.
- Onnela, J.-P., Kaski, K., and Kertész, J. (2004). Clustering and information in correlation based financial networks. *The European Physical Journal B*, 38(2):353–362. <https://doi.org/10.1140/epjb/e2004-00128-7>.
- Pang, R. K.-K., Granados, O. M., Chhajter, H., and Legara, E. F. T. (2021). An analysis of network filtering methods to sovereign bond yields during COVID-19. *Physica A: Statistical Mechanics and its Applications*, 574:125995. <https://doi.org/10.1016/j.physa.2021.125995>.
- Pang, R. K.-K. and Veraart, L. A. M. (2023). Assessing and mitigating fire sales risk under partial information. *Journal of Banking & Finance*, 155:106989. <https://doi.org/10.1016/j.jbankfin.2023.106989>.
- Pichler, A., Poledna, S., and Thurner, S. (2021). Systemic risk-efficient asset allocations: Minimization of systemic risk as a network optimization problem. *Journal of Financial Stability*, 52:100809. <https://doi.org/10.1016/j.jfs.2020.100809>.
- Plerou, V., Gopikrishnan, P., Rosenow, B., Amaral, L. A. N., Guhr, T., and Stanley, H. E. (2002). Random matrix approach to cross correlations in financial data. *Physical Review E*, 65(6):066126. <https://doi.org/10.1103/PhysRevE.65.066126>.
- Poledna, S., Molina-Borboa, J. L., Martínez-Jaramillo, S., Van Der Leij, M., and Thurner, S. (2015). The multi-layer network nature of systemic risk and its implications for the costs of financial crises. *Journal of Financial Stability*, 20:70–81. <https://doi.org/10.1016/j.jfs.2015.08.001>.
- PRA (2014). The Prudential Regulation Authority’s approach to banking supervision. <https://www.bankofengland.co.uk/-/media/boe/files/prudential-regulation/approach/banking-approach-2014.pdf>.
- Puri, M. (1994). The long-term default performance of bank underwritten security issues. *Journal of Banking & Finance*, 18(2):397–418. [https://doi.org/10.1016/0378-4266\(94\)00040-9](https://doi.org/10.1016/0378-4266(94)00040-9).

- Puri, M. (1996). Commercial banks in investment banking conflict of interest or certification role? *Journal of Financial Economics*, 40(3):373–401. [https://doi.org/10.1016/0304-405X\(95\)00855-9](https://doi.org/10.1016/0304-405X(95)00855-9).
- Qian, M.-C., Jiang, Z.-Q., and Zhou, W.-X. (2010). Universal and nonuniversal allometric scaling behaviours in the visibility graphs of world stock market indices. *Journal of Physics A: Mathematical and Theoretical*, 43(33):335002. doi: 10.1088/1751-8113/43/33/335002.
- Ramadijah, A., Caccioli, F., and Fricke, D. (2020). Reconstructing and stress testing credit networks. *Journal of Economic Dynamics and Control*, 111:103817. <https://doi.org/10.1016/j.jedc.2019.103817>.
- Ramadijah, A., Fricke, D., and Caccioli, F. (2022). Backtesting macroprudential stress tests. *Journal of Economic Dynamics and Control*, 137:104333. <https://doi.org/10.1016/j.jedc.2022.104333>.
- Ring-fencing and Proprietary Trading Independent Review (2022). Final report. https://rfpt.independent-review.uk/uploads/CCS0821108226-006_RFPT_Web%20Accessible.pdf.
- Rogers, L. C. G. and Veraart, L. A. M. (2013). Failure and Rescue in an Interbank Network. *Management Science*, 59(4):882–898. <https://doi.org/10.1287/mnsc.1120.1569>.
- Rosen, J. B. (1961). The Gradient Projection Method for Nonlinear Programming. Part II. Nonlinear Constraints. *Journal of the Society for Industrial and Applied Mathematics*, 9(4):514–532.
- Sahinidis, N. V. (1996). BARON: A general purpose global optimization software package. *Journal of Global Optimization*, 8:201–205. <https://doi.org/10.1007/BF00138693>.
- Sandoval Jr, L. (2012). Pruning a minimum spanning tree. *Physica A: Statistical Mechanics and its Applications*, 391(8):2678–2711. <https://doi.org/10.1016/j.physa.2011.12.052>.
- Sandoval Junior, L., Mullokandov, A., and Kenett, D. Y. (2015). Dependency Relations among International Stock Market Indices. *Journal of Risk and Financial Management*, 8(2):227–265. <https://doi.org/10.3390/jrfm8020227>.
- Schwendner, P., Schuele, M., Ott, T., and Hillebrand, M. (2015). European Government Bond Dynamics and Stability Policies: Taming Contagion Risks. *European Stability Mechanism Working Paper*. <https://dx.doi.org/10.2139/ssrn.3144053>.

- Sharpe, W. F. (1964). Capital Asset Prices: A Theory Of Market Equilibrium Under Conditions Of Risk. *The Journal of Finance*, 19(3):425–442. <https://doi.org/10.1111/j.1540-6261.1964.tb02865.x>.
- Shleifer, A. and Vishny, R. W. (2010). Asset Fire Sales and Credit Easing. *American Economic Review*, 100(2):46–50. doi: 10.1257/aer.100.2.46.
- Situngkir, H. and Surya, Y. (2005). On stock market dynamics through ultrametricity of minimum spanning tree. Technical report, Bandung Fe Institute.
- Squartini, T., Almog, A., Caldarelli, G., Van Lelyveld, I., Garlaschelli, D., and Cimini, G. (2017). Enhanced capital-asset pricing model for the reconstruction of bipartite financial networks. *Physical Review E*, 96(3):032315. <https://doi.org/10.1103/PhysRevE.96.032315>.
- Stavroglou, S. K., Pantelous, A. A., Soramaki, K., and Zuev, K. (2016). Causality Networks of Financial Assets. *Journal of Network Theory in Finance*, 3:17–67.
- Tang, Y., Xiong, J. J., Jia, Z.-Y., Zhang, Y.-C., et al. (2018). Complexities in Financial Network Topological Dynamics: Modeling of Emerging and Developed Stock Markets. *Complexity*, 2018. <https://doi.org/10.1155/2018/4680140>.
- Tarski, A. (1955). A lattice-theoretical fixpoint theorem and its applications. *Pacific Journal of Mathematics*, 5(2):285–309.
- Tonzer, L. (2015). Cross-border interbank networks, banking risk and contagion. *Journal of Financial Stability*, 18:19–32. <https://doi.org/10.1016/j.jfs.2015.02.002>.
- Tumminello, M., Aste, T., Di Matteo, T., and Mantegna, R. N. (2005). A tool for filtering information in complex systems. *Proceedings of the National Academy of Sciences*, 102(30):10421–10426. <https://doi.org/10.1073/pnas.0500298102>.
- Tumminello, M., Lillo, F., and Mantegna, R. N. (2010). Correlation, hierarchies, and networks in financial markets. *Journal of Economic Behavior & Organization*, 75(1):40–58. <https://doi.org/10.1016/j.jebo.2010.01.004>.
- Upper, C. and Worms, A. (2004). Estimating bilateral exposures in the German interbank market: Is there a danger of contagion? *European Economic Review*, 48(4):827–849. <https://doi.org/10.1016/j.euroecorev.2003.12.009>.
- Veraart, L. A. M. (2020). Distress and default contagion in financial networks. *Mathematical Finance*, 30(3):705–737. <https://doi.org/10.1111/mafi.12247>.
- Veraart, L. A. M. (2022). When does portfolio compression reduce systemic risk? *Mathematical Finance*, 32(3):727–778. <https://doi.org/10.1111/mafi.12346>.

- Veraart, L. A. M. and Aldasoro, I. (2022). Systemic Risk in Markets with Multiple Central Counterparties. *Available at SSRN 4105186*. <https://dx.doi.org/10.2139/ssrn.4105186>.
- Verma, A., Buonocore, R. J., and Di Matteo, T. (2019). A cluster driven log-volatility factor model: a deepening on the source of the volatility clustering. *Quantitative Finance*, 19(6):981–996. <https://doi.org/10.1080/14697688.2018.1535183>.
- Vodenska, I., Becker, A. P., Zhou, D., Kenett, D. Y., Stanley, H. E., and Havlin, S. (2016). Community Analysis of Global Financial Markets. *Risks*, 4(2):13. <https://doi.org/10.3390/risks4020013>.
- Wang, G.-J., Xie, C., and Chen, S. (2017). Multiscale correlation networks analysis of the US stock market: a wavelet analysis. *Journal of Economic Interaction and Coordination*, 12(3):561–594. <https://doi.org/10.1007/s11403-016-0176-x>.
- Weber, S. and Weske, K. (2017). The joint impact of bankruptcy costs, fire sales and cross-holdings on systemic risk in financial networks. *Probability, Uncertainty and Quantitative Risk*, 2(1):1–38. <https://doi.org/10.1186/s41546-017-0020-9>.
- Wu, S., He, J., Li, S., and Wang, C. (2018). Network formation in a multi-asset artificial stock market. *The European Physical Journal B*, 91:1–10. <https://doi.org/10.1140/epjb/e2018-80384-6>.

Chapter 8

Appendix

8.A Chapter 2: Background information on matrix reconstruction methods

The matrix reconstruction methods considered can be classified into optimisation-based reconstruction methods, i.e., they determine a matrix that is consistent with given row and column sums by solving a deterministic optimisation problem, and sampling-based reconstruction methods, which assume that the matrix of interest is random and they develop tools to generate a sample from the distribution of the matrix.

8.A.1 Optimisation-based reconstruction methods

We consider two matrix reconstruction methods, the Entropy method and the MinDen method. Both solve suitable optimisation problems to identify a matrix that is consistent with given row and column sums.

Entropy method

The method that we refer to as the Entropy method in this paper, is also known under several other names, such as iterative proportional fitting procedure, or RAS algorithm, to name a few and has been used in several fields, e.g., in mathematics, economics, computer science etc. To the best of our knowledge it has first been applied to financial networks by Upper and Worms (2004) who used the method to reconstruct a network of interbank liabilities from row and column sums. It has also been considered in the context of reconstructing networks of asset holding matrices in Di Gangi et al. (2018). The Entropy method is an optimisation-based method that minimises the Kullback-Leibler (KL) divergence between a matrix X and a target matrix X^{Entropy} . Applied to our setting it consists of solving the following optimisation problem

$$\begin{aligned}
& \min_X \sum_{n=1}^N \sum_{k=1}^K X_{nk} \log \left(\frac{X_{nk}}{X_{nk}^{\text{Entropy}}} \right), \\
& \text{subject to: } \alpha_{n1} = \sum_{k=1}^K X_{nk} \quad \forall n \in \{1, \dots, N\}, \\
& c_k = \sum_{n=1}^N X_{nk} \quad \forall k \in \{1, \dots, K\}, \\
& X_{nk} \geq 0 \quad \forall n \in \{1, \dots, N\}, \forall k \in \{1, \dots, K\},
\end{aligned} \tag{8.1}$$

where the initial matrix is defined as

$$X_{nk}^{\text{Entropy}} = \frac{\alpha_{n1} c_k}{A} \quad \forall n \in \{1, \dots, N\}, \forall k \in \{1, \dots, K\}, \tag{8.2}$$

where $A = \sum_{n=1}^N \alpha_{n1} = \sum_{k=1}^K c_k$.

One can easily check that X^{Entropy} solves this optimisation problem. The reason why this reconstruction problem simplifies so significantly in our situation is that since we consider an asset holdings matrix we only need to require the non-negativity of the matrix and that it satisfies the given row and column sums. We are not in a situation in which the diagonal entries of the matrix that solves the optimisation problem are required to be zero. This additional constraint occurs, for example, in Upper and Worms (2004), in which the network represents interbank lending. Since a bank does not borrow from itself the additional constraint, that the entries on the diagonal are zero, is necessary there.

As one can see from the definition of X^{Entropy} , the reconstructed matrix usually contains only non-zero entries (an entry X_{nk}^{Entropy} in the matrix can only be zero if the corresponding row α_{n1} or column c_k aggregate is zero).

It has been discussed in Di Gangi et al. (2018) how the specific form of X^{Entropy} here can be interpreted as reflecting investors' preference in line with the capital asset pricing model (CAPM) (Sharpe, 1964).

Since the Entropy method provides a closed-form expression for the reconstructed asset holding matrix, all fire sale measures by Greenwood et al. (2015) applied to this reconstructed matrix can be expressed in closed form. Therefore, one immediately obtains the following results.

Proposition 8.A.1. *Suppose the asset holding matrix is estimated using X^{Entropy} given in (8.2). Let $n \in \mathcal{N}$ and $k \in \mathcal{S}$. Then,*

1. *the elements of the portfolio weights matrix are given by $m_{nk}(X^{\text{Entropy}}) = \frac{X_{nk}^{\text{Entropy}}}{\alpha_{n1}} = \frac{c_k}{A}$,*

2. *the unlevered return is $R^{\text{Entropy}} = R_{n1}(X^{\text{Entropy}}) = \frac{\sum_{k=1}^K c_k f_{k1}}{A}$;*

3. the connectivity is $\gamma^{Entropy} = \gamma_{n1}(X^{Entropy}) = \sum_{k=1}^K c_k l_k \frac{X_{nk}^{Entropy}}{\alpha_{n1}} = \frac{\sum_{k=1}^K c_k^2 l_k}{A}$;
4. the direct vulnerability is $\mathcal{DV}^{X^{Entropy}}(n) = -\frac{\alpha_{n1}}{e_{n1}} R^{Entropy}$;
5. the systemicness is $\mathcal{SYS}^{X^{Entropy}}(n) = \frac{-\gamma^{Entropy} R^{Entropy}}{\sum_{\nu=1}^N e_{\nu 1}} \alpha_{n1} b_{n1}$;
6. the aggregate vulnerability is $\mathcal{AV}^{X^{Entropy}} = \sum_{n=1}^N \mathcal{SYS}^{X^{Entropy}}(n) = \frac{-\gamma^{Entropy} R^{Entropy}}{\sum_{\nu=1}^N e_{\nu 1}} \sum_{n=1}^N \alpha_{n1} b_{n1}$;
7. the indirect vulnerability is $\mathcal{IV}^{X^{Entropy}}(n) = -\gamma^{Entropy} R^{Entropy} \frac{\sum_{\nu=1}^N \alpha_{\nu 1} b_{\nu 1}}{A} \frac{\alpha_{n1}}{e_{n1}}$.

Proof of Proposition 8.A.1. 1. The statement follows directly from the definition of

$$X^{Entropy}, \text{ since } m_{nk}(X^{Entropy}) = \frac{X_{nk}^{Entropy}}{\alpha_{n1}} = \frac{\alpha_{n1} c_k}{\alpha_{n1} A} = \frac{c_k}{A}.$$

2.-7. The statements follow directly from part 1. and the definitions of the risk measures. \square

Hence, we find that for the Entropy reconstruction method, the two quantities that depend on the network $R_{n1}(X^{Entropy})$ and $\gamma_{n1}(X^{Entropy})$ do not depend on n , which means they are not specific to a given institution. For an all asset shock $f_{k1} = f$ for all $k \in \mathcal{S}$, $R^{Entropy} = f$ in line with Proposition 2.3.1.

Remark 8.A.2 (Comparison of systemicness and indirect vulnerability using the Entropy method). These results show that under the Entropy method, the systemicness is a product of an institution-specific factor $\alpha_{n1} b_{n1}$ (representing total assets times leverage) and a common factor $\frac{-\gamma^{Entropy} R^{Entropy}}{\sum_{\nu=1}^N e_{\nu 1}}$. The indirect vulnerability also consists of an institution-specific factor $\frac{\alpha_{n1}}{e_{n1}}$ (representing total asset holdings divided by equity) and a common factor $-\gamma^{Entropy} R^{Entropy} \frac{\sum_{\nu=1}^N \alpha_{\nu 1} b_{\nu 1}}{A}$. Hence, we see that institutions with high total asset holdings times leverage will have a high systemicness, i.e., will play a major role in causing fire sale losses, whereas institutions with large total asset holdings divided by their equity will have a large indirect vulnerability, i.e., they will be susceptible to fire sale losses. So leverage influences systemicness, whereas equity influences indirect vulnerability.

Proposition 8.A.1 also allows us to provide an analytical expression for the proportional capital injection strategy.

Corollary 8.A.3. *Suppose the asset holding matrix is estimated using $X^{Entropy}$ given in (8.2). Let $n \in \mathcal{N}$ and $k \in \mathcal{S}$. Then, the proportional capital injection defined in Definition 2.4.5, reduces to*

$$i_n^{Prop}(X^{Entropy}) = I \frac{\mathcal{SYS}^{X^{Entropy}}(n)}{\mathcal{AV}^{X^{Entropy}}} = I \frac{\alpha_{n1} b_{n1}}{\sum_{\nu=1}^N \alpha_{\nu 1} b_{\nu 1}}.$$

This means that capital is injected relative to a measure in which the total assets are weighted by leverage. Therefore, $i_n^{\text{Prop}}(X^{\text{Entropy}})$ differs from the naive capital injection strategy $i_n^{\text{Naive}} = I \frac{\alpha_{n1}}{\sum_{\nu=1}^N \alpha_{\nu 1}}$ in which only the total asset holdings are considered.

Minimum density method

The minimum density method for network reconstruction was introduced in Anand et al. (2015) in the context of a matrix representing interbank lending. We apply it here to a matrix with a different economic interpretation, namely asset holdings between different banks. It solves an optimisation problem with the objective of finding a matrix with the minimum number of edges that is consistent with given row and column sums. The resulting network is therefore usually very sparse. Formally, the optimisation problem in our setting is as follows.

$$\begin{aligned} & \min_X \sum_{n=1}^N \sum_{k=1}^K \mathbb{I}_{\{X_{nk} > 0\}}, \\ \text{subject to: } & \alpha_{n1} = \sum_{k=1}^K X_{nk} \quad \forall n \in \{1, \dots, N\}, \\ & c_k = \sum_{n=1}^N X_{nk} \quad \forall k \in \{1, \dots, K\}, \\ & X_{nk} \geq 0 \quad \forall n \in \{1, \dots, N\}, \forall k \in \{1, \dots, K\}. \end{aligned}$$

Anand et al. (2015) provide an algorithm to solve this optimisation problem and also consider generalisations that result in less sparse matrices. We will mainly consider one matrix in our analysis that represents the sparsest solution. As part of our sensitivity analysis, we also consider the generalisation by Anand et al. (2015) that constructs less sparse matrices.

8.A.2 Sampling-based reconstruction methods

We also consider two matrix reconstruction methods that assume that the matrix itself is random and provide methodologies to sample from the appropriate distribution.

Statistical physics method

The method that we refer to as the Statistical Physics method, due to its modelling ideas coming from this area, was developed by Cimini et al. (2015). It was originally proposed to reconstruct a network of interbank lending. It has then been applied to the case of bipartite networks of asset holding networks by Squartini et al. (2017) which is what we do here. Applied to our setting, it is characterised by an $N \times K$ -dimensional random

matrix X^{StatPhys} , whose individual entries X_{nk} , $n \in \mathcal{N}, k \in \mathcal{S}$ are independent random variables from the following discrete distributions.

$$\mathbb{P}\left(X_{nk}^{\text{StatPhys}} = \frac{\alpha_{n1}c_k}{p_{nk}A}\right) = p_{nk},$$

$$\mathbb{P}(X_{nk}^{\text{StatPhys}} = 0) = 1 - p_{nk},$$

where again $A = \sum_{\nu=1}^N \alpha_{\nu 1}$. Furthermore, $p_{nk} = \frac{\phi \alpha_{n1} c_k}{1 + \phi \alpha_{n1} c_k} \quad \forall n \in \mathcal{N}, \forall k \in \mathcal{S}$, and $\alpha_{n1} > 0 \forall n \in \mathcal{N}$, $c_k > 0 \forall k \in \mathcal{S}$, are the given row and column sums, respectively and $\phi > 0$ is a parameter that can be used to calibrate the model¹. One can check that $p_{nk} \in [0, 1] \forall n \in \mathcal{N}, \forall k \in \mathcal{S}$. Hence, we see that each entry in the random matrix can only take two possible values - zero or another non-negative value.

It follows directly from the definition that

$$\mathbb{E}\left[\sum_{n=1}^N X_{nk}^{\text{StatPhys}}\right] = c_k, \quad \forall k \in \mathcal{S} \quad \text{and} \quad \mathbb{E}\left[\sum_{k=1}^K X_{nk}^{\text{StatPhys}}\right] = \alpha_{n1}, \quad \forall n \in \mathcal{N}.$$

This means, that the random matrix X^{StatPhys} satisfies the row and column sums in expectation. If one generates a sample of matrices from this probability distribution, then the individual matrices in the sample will usually not satisfy the row and column sums.

To calibrate the model to a given target density $\delta^{\text{target}} \in (0, 1)$ of a network one can use the fact that the expected density of X^{StatPhys} is given by

$$f(\theta) = \frac{1}{NK} \mathbb{E}\left[\sum_{n=1}^N \sum_{k=1}^K \mathbb{I}_{\{X_{nk}^{\text{StatPhys}} > 0\}}\right] = \frac{1}{NK} \sum_{n=1}^N \sum_{k=1}^K p_{nk} = \frac{1}{NK} \sum_{n=1}^N \sum_{k=1}^K \frac{\phi \alpha_{n1} c_k}{1 + \phi \alpha_{n1} c_k}$$

and solve $f(\theta) = \delta^{\text{target}}$ for θ . Note that f is a continuous and non-decreasing function satisfying $f(0) = 0$. Furthermore, $\lim_{\theta \rightarrow \infty} f(\theta) = 1$ if $\alpha_{n1}c_k > 0$ for all $n \in \mathcal{N}$ and for all $k \in \mathcal{S}$. Hence, we see that if all row and column sums are non-zero, the model can be calibrated to any target density $\delta^{\text{target}} \in (0, 1)$. If some row or column sums are zero, then the underlying network cannot have a density of 1 or a similarly large value and this is indeed reflected by the function f .

Some fire sales measures evaluated using the StatPhys method are related to those evaluated under the Entropy method.

For example, the expected portfolio weights matrix using the StatPhys method satisfies

$$\mathbb{E}[m_{nk}(X^{\text{StatPhys}})] = \frac{1}{\alpha_{n1}} \mathbb{E}[X_{nk}^{\text{StatPhys}}] = \frac{1}{\alpha_{n1}} \frac{\alpha_{n1}c_k}{p_{nk}A} p_{nk} = \frac{c_k}{A} = m_{nk}(X^{\text{Entropy}}) \quad \forall n \in \mathcal{N}, \forall k \in \mathcal{S}$$

¹This has also already been discussed in Gandy and Veraart (2019)

and hence coincide with the portfolio weights using the Entropy method. This implies that the quantities that depend on the network are given by

$$\begin{aligned}\mathbb{E}[R_{n1}(X^{\text{StatPhys}})] &= \sum_{k=1}^K \mathbb{E}[m_{nk}(X^{\text{StatPhys}})] f_{k1} = R_{n1}(X^{\text{Entropy}}) = R^{\text{Entropy}}, \\ \mathbb{E}[\gamma_{n1}(X^{\text{StatPhys}})] &= \sum_{k=1}^K c_k l_k \mathbb{E}[m_{nk}(X^{\text{StatPhys}})] = \gamma_{n1}(X^{\text{Entropy}}) = \gamma^{\text{Entropy}},\end{aligned}$$

for all $n \in \mathcal{N}$.

It follows directly that the expected direct vulnerability using the StatPhys method coincides with the direct vulnerability using the Entropy method, formally

$$\mathbb{E}[\mathcal{DV}^{X^{\text{StatPhys}}}(n)] = -\frac{\alpha_{n1}}{e_{n1}} \mathbb{E}[R_{n1}(X^{\text{StatPhys}})] = -\frac{\alpha_{n1}}{e_{n1}} R^{\text{Entropy}} = \mathcal{DV}^{X^{\text{Entropy}}}(n).$$

For the other fire sale measure, however, the expectation of the measure applied to the random matrix X^{StatPhys} does not generally coincide with the measure applied to the deterministic matrix X^{Entropy} . For example, systemicness, follows from direct calculations that

$$\mathbb{E}[\mathcal{SYS}^{X^{\text{StatPhys}}}(n)] = \frac{-\alpha_{n1} b_{n1}}{\sum_{\nu=1}^N e_{\nu 1}} \mathbb{E}[\gamma_{n1}(X^{\text{StatPhys}}) R_{n1}(X^{\text{StatPhys}})],$$

where

$$\mathbb{E}[\gamma_{n1}(X^{\text{StatPhys}}) R_{n1}(X^{\text{StatPhys}})] = \gamma^{\text{Entropy}} R^{\text{Entropy}} + \frac{1}{\alpha_{n1}} \frac{\sum_{k=1}^K c_k^2 l_k f_{k1}}{\phi A^2}.$$

Since, $\frac{1}{\alpha_{n1}} \frac{\sum_{k=1}^K c_k^2 l_k f_{k1}}{\phi A^2} \leq 0$, this implies that the expected systemicness and the expected aggregate vulnerability under the StatPhys method is greater or equal than the corresponding quantities derived using the Entropy method. This is indeed what we find in Table 2.4.

Bayesian methods

The reconstruction method developed in Gandy and Veraart (2017) takes a Bayesian perspective. Gandy and Veraart (2017) specify a generative model for the network matrix and then condition on the observations, i.e., the row and column sums (and possibly additional known entries of the matrix). Hence, the network reconstruction is achieved through the posterior distribution in the Bayesian setting.

For the generative model several a-priori distributions have been considered in Gandy and Veraart (2017, 2019). We consider two special choices developed in these papers.

The model assumes a generalisation of the Erdős-Rényi random graph model, see Erdős

and Rényi (1959), by assuming that directed edges from n to k are generated using independent Bernoulli trials with success probability p_{nk} and weights from an exponential distribution are assigned to existing edges. Formally, the a-priori model assumes that for all $n \in \mathcal{N}$ and for all $k \in \mathcal{S}$

$$\begin{aligned} P(X_{nk} > 0) &= p_{nk}, \\ X_{nk} \mid X_{nk} > 0 &\sim \text{Exp}(\lambda_{nk}), \end{aligned}$$

where $p = (p_{nk}) \in [0, 1]^{N \times K}$, $\lambda = (\lambda_{nk}) \in [0, \infty)^{N \times K}$.

We are then interested in the distribution of the random matrix X conditional on the given row and column sums. Since this distribution is not available in closed form, Gandy and Veraart (2017) have developed an MCMC sampler to generate samples from this distribution.

In the following, we will assume that all parameters of the exponential distributions governing the weights are identical, i.e., $\lambda_{nk} = \tilde{\lambda} \in [0, \infty)$ for all $n \in \mathcal{N}$, $k \in \mathcal{S}$.

We will now consider two different choices for $p = (p_{nk})$. First, we assume that all a-priori link existence probabilities are identical, i.e., we set $p_{nk} = \tilde{p} \in [0, 1]$ for all $n \in \mathcal{N}$, $k \in \mathcal{S}$. We will refer to the Bayesian model with this a-priori assumption as the BayeER model (where ER stands for Erdős-Rényi). As discussed in Gandy and Veraart (2019), this model can be calibrated to a given network density by choosing appropriate values for \tilde{p} and $\tilde{\lambda}$ and this is what we do in this paper.

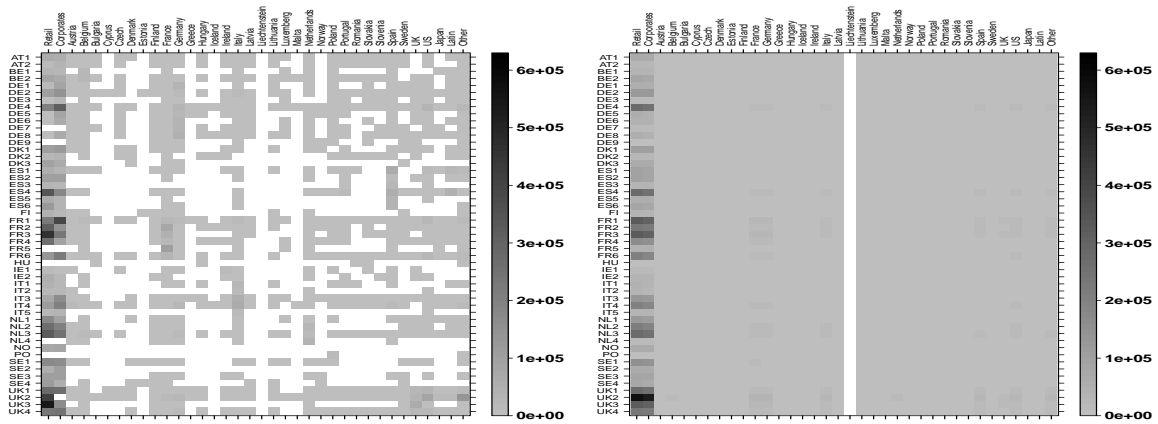
Second, we assume that the a-priori link existence probabilities have the same structure as in the StatPhys model. In particular, they are given by $p_{nk} = \frac{\phi \alpha_{n1} c_k}{1 + \phi \alpha_{n1} c_k}$ for all $n \in \mathcal{N}$, $k \in \mathcal{S}$. Here again α_{n1} and c_k represent the row and column sums and $\phi > 0$ is a constant used to calibrate the model. We refer to this Bayesian model as the BayeEF model (where EF stands for Empirical Fitness). This is (as the StatPhys model) a fitness model for the underlying network. Fitness network models assume that the link existence probability between a pair of nodes is a function of characteristics of the nodes, so-called fitnesses. In our setting, the row and column sums can be interpreted as fitnesses and the link existence probabilities are indeed functions of the row and column sums. Note, however, that the p_{nk} in the BayeEF model are a-priori link existence probabilities. They do usually not correspond to the posterior link existence probabilities. The StatPhys and the BayeEF are fundamentally different models despite having some similarities in the choice of model inputs. As shown in Gandy and Veraart (2019) the BayeEF can be calibrated to a given network density and this is what we will do for this second type of Bayesian model as well. The calibration is described in detail in Gandy and Veraart (2019).

8.B Chapter 2: Additional empirical results and sensitivity analysis

8.B.1 Observed and reconstructed asset holding matrices

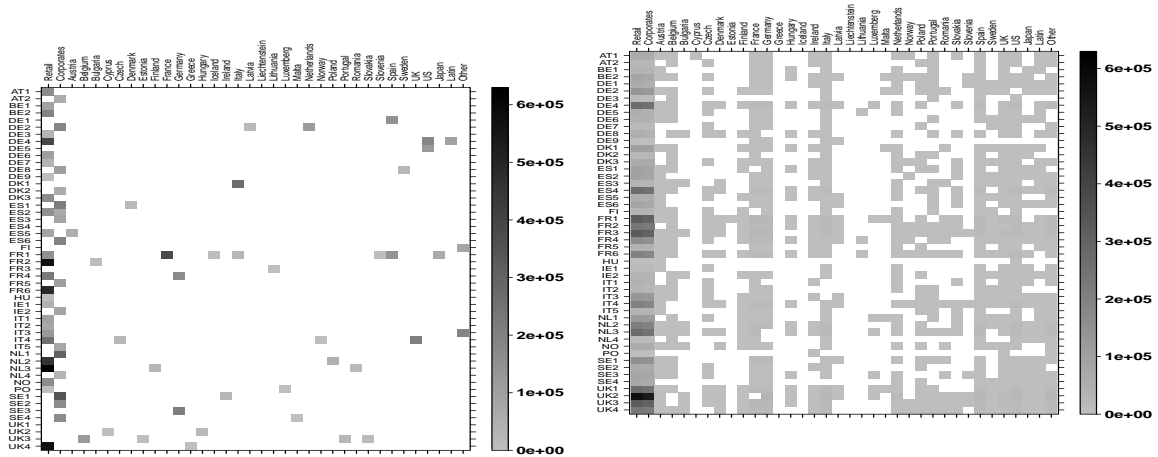
To provide some intuition on the empirical asset holding matrix and the performance of different reconstruction methods, we illustrate their performance when applied to the EBA data from 2016. Figure 8.1 shows a heatmap of the true asset holdings matrix X (top left) and five heatmaps corresponding to reconstructed asset holding matrices that only used partial information. For methods that generate a sample of matrices, i.e., the StatPhys method and the Bayesian methods we only show one realisation of a reconstructed asset holding matrix.

Figure 8.1 shows that the matrix obtained using the Entropy method corresponds to a network in which all institutions hold positions in all but one asset. This one asset has a market capitalisation of 0 and corresponds to Liechtenstein sovereign loans.



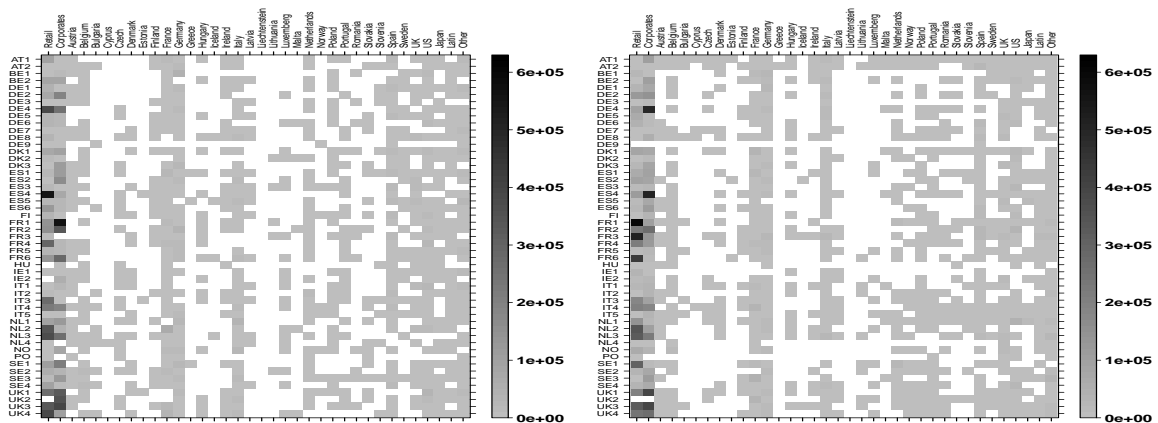
(a) Observed asset holdings matrix.

(b) Reconstruction based on Entropy method.



(c) Reconstruction based on MinDen method.

(d) One reconstruction based on StatPhys method.



(e) One reconstruction based on BayeER method.

(f) One reconstruction based on BayeEF method.

Figure 8.1: Asset holdings matrix for the true matrix (top left) and five reconstructed networks based on different methods for the EBA 2016 data.

For the reconstructed matrix based on the MinDen method, the asset holdings appear scattered where the largest assets holdings are in corporate, retail, German, US, and other sovereign assets. The MinDen matrix does assign zero weights to some of the largest positions observed in the true network i.e., several UK banks hold large positions in retail assets in 2016, but the corresponding entries in the reconstructed matrix based on the MinDen methods are zero.

The sample matrix generated by the StatPhys method shows that according to this reconstruction, all banks invest in the two asset classes corporate and retail (the lower two rows). The weights are consistent with the corresponding two rows in the matrix obtained from using the Entropy method. According to the reconstruction based on the Entropy method and this one sample from the StatPhys method, the bank with label UK1 has the largest holdings in the two asset classes corporate and retail. In contrast, to the Entropy method, the reconstructed matrix based on the StatPhys method is much sparser - it has been calibrated to match the density of the true network. When looking at the samples generated by the Bayesian method we observe that the overall density of the network matches the density of the true network, as was the case for the StatPhys method, since these methods are flexible enough that they can easily be calibrated to a given density. Throughout our empirical analysis, we calibrate the StatPhys and the Bayesian methods to the true density of the network unless stated otherwise. The density remains almost the same in both years (0.44 in 2011 and 0.48 in 2016), so our sampling-based methods are calibrated such that almost half the entries of the asset holding matrices are filled. Furthermore, we see that the reconstructed samples from the Bayesian methods assign weights that are very different from weights obtained by the Entropy or the StatPhys method. In particular, we do observe several high weights and also some zero weights within the lower two rows that represent the holdings in corporate and retail assets. This is not surprising given the greater flexibility of the Bayesian method when it comes to modelling the weight and not just the existence of edges compared to the StatPhys method.

8.B.2 Computing the maximum and minimum aggregate vulnerability for given row and column sums

In our partial information setting, we assume that only the row and column sums of the asset holding matrix are given. Throughout the paper, we study various network reconstruction methods that reconstruct the asset holding matrix from this partial information. These reconstructed networks can then be plugged into any measure of fire sale risk of interest, such as the aggregate vulnerability, the systemicness, the direct and the indirect vulnerability.

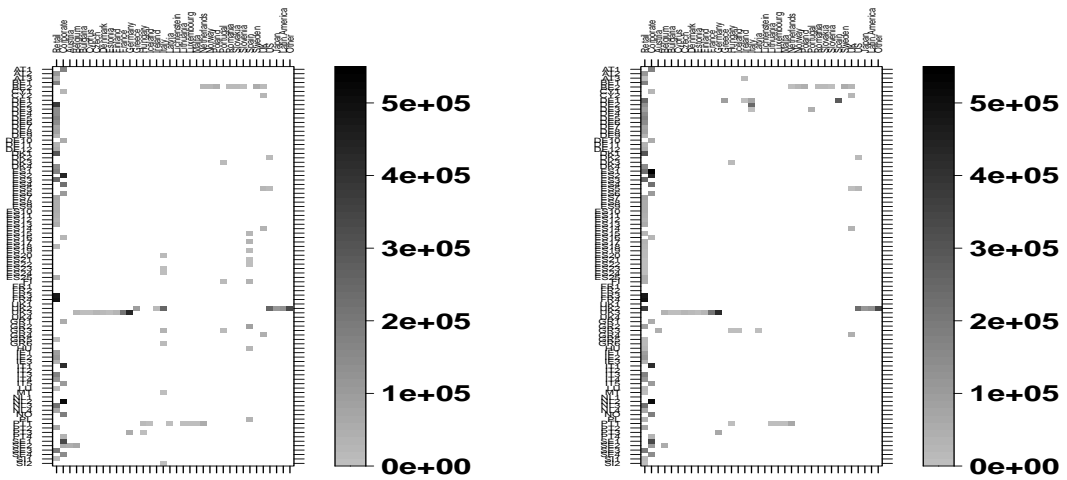
For a fixed measure of fire sale risk, however, one can also try to find an asset holding matrix that maximises (or minimises) this measure over all matrices that satisfy the given constraints on the row and column sums. This is what we do next for the aggregate vulnerability. This optimisation approach will be useful as a benchmark.

We consider the following optimisation problem for finding the maximum aggregate vulnerability:

$$\begin{aligned}
 & \max_X \quad \mathcal{AV}(X), \\
 & \text{subject to: } \alpha_{n1} = \sum_{k=1}^K X_{nk} \quad \forall n \in \{1, \dots, N\}, \\
 & \quad \quad \quad c_k = \sum_{n=1}^N X_{nk} \quad \forall k \in \{1, \dots, K\}, \\
 & \quad \quad \quad X_{nk} \geq 0 \quad \forall n \in \{1, \dots, N\}, \quad \forall k \in \{1, \dots, K\}.
 \end{aligned} \tag{8.3}$$

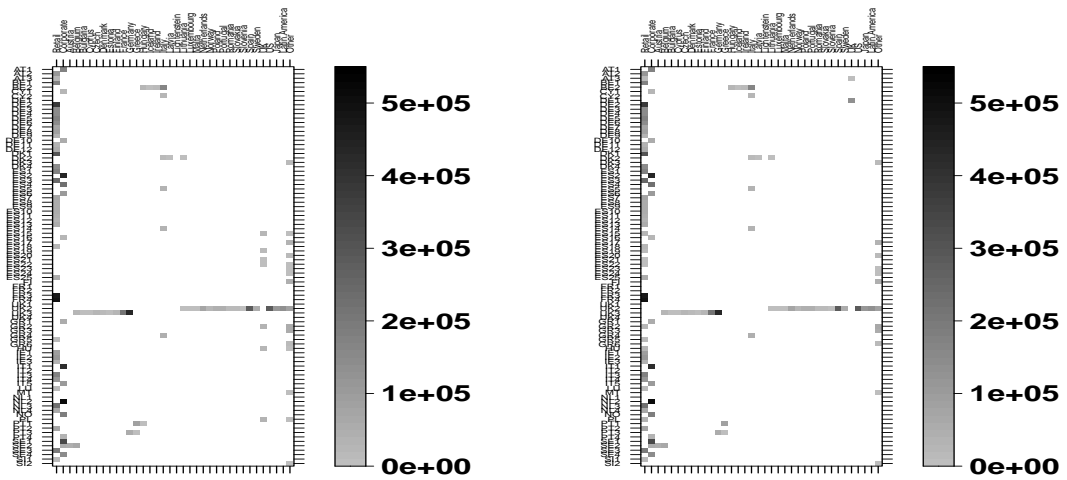
The corresponding optimisation problem that determines the minimum aggregate vulnerability can be defined in the same way by minimising the aggregate vulnerability rather than maximising it.

Figure 8.2 shows examples of asset holding matrices that correspond to the minimum or maximum aggregate vulnerability for different shocks. We find that the matrices are generally very sparse. We observe large positions in corporate and retail assets, which correspond to 80% of the total value of asset holdings across all banks. It is striking to see how similar the two matrices are that correspond to the minimum and the maximum aggregate vulnerability for a given stress scenario. This shows the large influence of a small number of positions on aggregate vulnerability. There may be other matrices with different levels of sparsity that result in similarly small or large aggregate vulnerabilities.



(a) Min AV under the GIIPS scenario.

(b) Max AV under the GIIPS scenario.



(c) Min AV under the Bad Brexit scenario.

(d) Max AV under the Bad Brexit scenario.

Figure 8.2: Examples of asset holdings matrices that maximise or minimise the aggregate vulnerability while respecting the non-negativity and marginal sums of the true matrix. We use the 2011 EBA data for the GIIPS and Bad Brexit scenarios. The aggregate vulnerability are as follows a) 172%, b) 373%, c) 49%, and d) 144%.

8.B.3 Additional sensitivity analysis

Network reconstruction for different densities

In the following, we provide further details on the sensitivity of different network reconstruction methods concerning the assumed density of the network.

In Section 2.3.5 we have already discussed how the aggregate vulnerability computed using the StatPhys, BayeER, and BayeEF network reconstruction methods depends on the choice of the target density of the network for the 2011 data and a capitalisation-dependent price impact, see Figure 2.1. In particular, we find that the aggregate vulnerability can be estimated reasonably precisely even if the true density of the network is not available. Further analysis of these sensitivities for constant price impact and the data from 2016 confirm these conclusions. We do not report the details here.

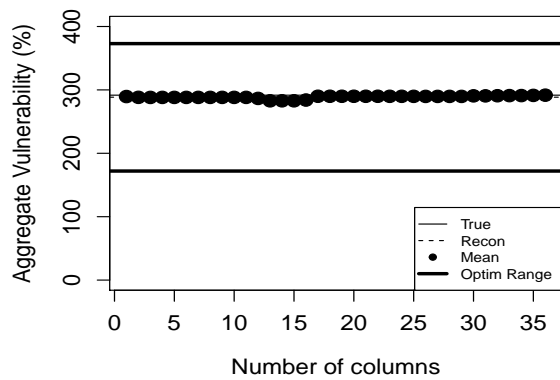
Next, we analyse how additional information can be included in the Entropy and MinDen methods.

For the Entropy method, we cannot just assume a target density but we will need to provide a suitable target matrix \tilde{X} instead. We do this by replacing some columns in the target matrix with the true asset holding matrix. In particular, first, we assume that the first column of the target matrix consists of the true asset holdings and the remaining entries correspond to those in the Entropy method matrix i.e., $\tilde{X}_{n1} = X_{n1} \quad \forall n \in \mathcal{N}$ and $\tilde{X}_{nk} = X_{nk}^{\text{Entropy}}, \quad k \in [2, \dots, K]$. The column sums remain the same but the row sums are no longer consistent with the partial information. We, therefore, re-balance the matrix such that marginal sums are equal to the true matrix. We repeat this process for each column sequentially until the target matrix consists only of the true entries. We do this column by column.

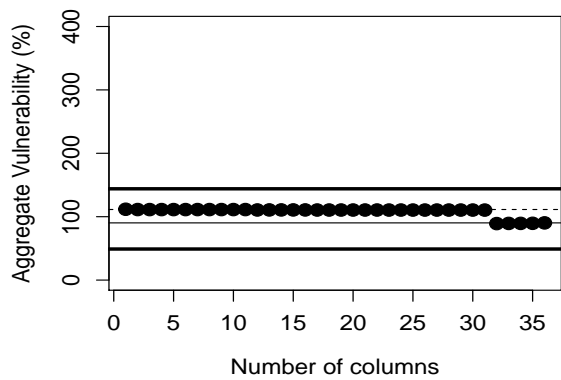
Our results in Figure 8.3 show that the aggregate vulnerabilities are similar under the additional information for the Entropy method. For several points, incorporating additional information can result in a worse performance of the aggregate vulnerability. Although more information is known about the true matrix, the proportional scaling from the re-balancing method alters other entries. This leads to changes in other assets with high influence, for example, changes in position in UK assets within the Bad Brexit scenario. Only when the information about the shocked asset is included, we observe that the estimated aggregate vulnerability becomes closer to the true one.

For the MinDen method, it is possible to consider a generalisation, see Anand et al. (2015) for details, that can be calibrated to a target density. We find that the aggregate vulnerabilities, computed from the MinDen method that have been calibrated to different densities, can vary and different densities can lead to similar aggregate vulnerabilities.

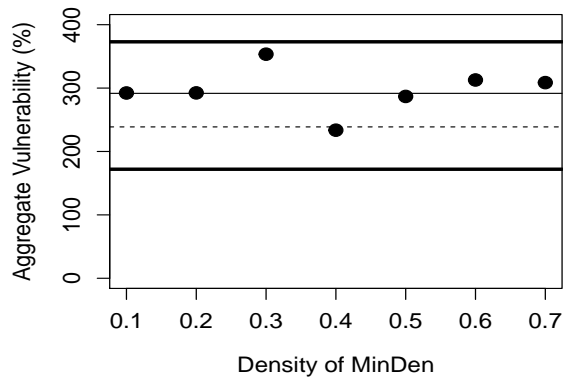
We have also conducted the same sensitivity checks for a constant price impact and also for the 2016 data and come to the same conclusions, therefore we do not report them here.



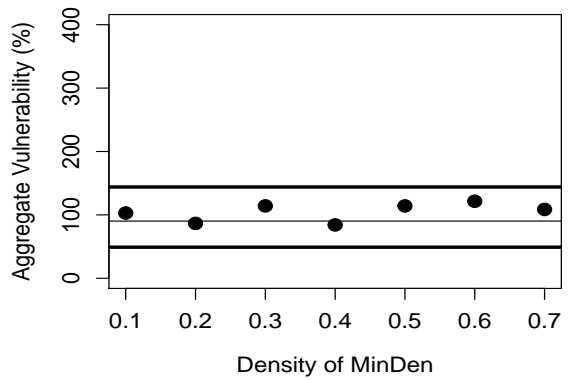
(a) Entropy under GIIPS 2011.



(b) Entropy under Bad Brexit 2011.



(c) MinDen under GIIPS 2011.



(d) MinDen under Bad Brexit 2011.

Figure 8.3: Aggregate vulnerabilities as a function of the number of known columns in the target matrix of the Entropy method (top), and aggregate vulnerabilities as a function of the network density for the MinDen method (bottom). This is for the 2011 data and a capitalisation-dependent price impact.

Network reconstruction for noisy observations

Finally, we investigate how sensitive our results are, if the row and column sums of the asset holding matrix are not observed directly but with noise. To do so we add a noise term to the row and column sums of the true asset holding matrix, i.e., we consider the new row and column sums

$$\begin{aligned}\alpha_{n1}^{\text{noise}} &= \alpha_{n1} + \epsilon_n^{(\alpha)}, \quad \forall n \in \mathcal{N}, \\ c_k^{\text{noise}} &= c_k + \epsilon_k^{(c)}, \quad \forall k \in \mathcal{S},\end{aligned}$$

where $\epsilon_1^{(\alpha)}, \dots, \epsilon_N^{(\alpha)}$ and $\epsilon_1^{(c)}, \dots, \epsilon_K^{(c)}$ are i.i.d. normally distributed random variables with mean 0 and variance σ^2 . We chose a realisation of the noise in which all new row and column sums are non-negative. We consider two different choices of the parameter $\sigma \in \{100, 1000\}$ (million EUR). Finally, we normalise row and column sums of the data with noise such that the new row sums $\tilde{\alpha}_{n1}^{\text{noise}}$ and column sums $\tilde{c}_k^{\text{noise}}$ with noise satisfy

$$\sum_{n=1}^N \tilde{\alpha}_{n1}^{\text{noise}} = \sum_{k=1}^K \tilde{c}_k^{\text{noise}} = \sum_{n=1}^N \sum_{k=1}^K X_{nk}.$$

For the network reconstruction with noise, we use the normalised row and column sums with noise as the available partial information.

Table 8.1 reports the results. Overall, we observe only a small or no deviation from the results without noise for all reconstruction methods except the MinDen method. The results of the MinDen method are sensitive to noisy observation. The mean equity losses for reconstructed matrices under 1bn standard deviation of the noise are further away than for 100mn but with a similar standard deviation for the sampling methods. This shows that our results are robust under noise and across different fire-sales measures. Overall we find that the addition of noise does not lead to any different conclusion in terms of the relative ranking of the different network reconstruction methods, see Table 2.4 for comparison.

Capitalisation-dependent price impact ($l_k = \rho/c_k \forall k$)											
Matrix	True	MinDen		Entropy		StatPhy		BayeER		BayeEF	
σ	0	100	1000	100	1000	100	1000	100	1000	100	1000
GIIPS(%)											
$\mathcal{DV}11$	15.58	32.74	2.60	7.81	7.80	7.80	7.81	20.20	20.17	17.69	17.53
	-	-	-	-	-	(0.54)	(0.53)	(3.09)	(3.05)	(3.01)	(3.01)
$\mathcal{TV}11$	460.79	1075.10	293.85	416.77	416.17	417.42	416.99	611.87	610.83	544.72	542.05
	-	-	-	-	-	(10.66)	(10.71)	(38.63)	(38.49)	(30.36)	(30.46)
$\mathcal{AV}11$	291.70	289.01	316.26	288.21	287.85	288.98	288.42	292.41	291.48	294.22	293.44
	-	-	-	-	-	(6.02)	(6.15)	(5.27)	(5.28)	(5.01)	(5.03)
Bad Brexit(%)											
$\mathcal{DV}11$	1.47	0.85	4.03	3.01	3.01	3.02	3.01	8.37	8.36	6.47	8.36
	-	-	-	-	-	(0.47)	(0.46)	(02.50)	(2.54)	(2.43)	(2.39)
$\mathcal{TV}11$	120.19	175.99	225.61	160.90	160.71	161.18	160.91	239.96	239.41	207.53	206.42
	-	-	-	-	-	(7.31)	(7.37)	(22.66)	(22.96)	(17.30)	(17.04)
$\mathcal{AV}11$	90.23	144.05	119.90	111.27	111.16	111.59	111.30	112.14	111.91	113.67	113.47
	-	-	-	-	-	(4.77)	(4.83)	(3.95)	(4.04)	(3.90)	(3.92)
Constant price Impact ($l_k = 5 \times 10^{-13} \forall k$)											
GIIPS(%)											
$\mathcal{DV}11$	Same results as for capitalisation-dependent price impact										
$\mathcal{TV}11$	506.76	312.90	321.79	523.55	522.83	523.48	522.85	275.16	274.39	325.14	325.60
	-	-	-	-	-	(13.51)	(13.50)	(16.68)	(16.81)	(17.83)	(17.85)
$\mathcal{AV}11$	357.49	226.56	204.36	362.05	361.62	362.43	361.73	275.50	274.60	293.51	293.20
	-	-	-	-	-	(7.24)	(7.41)	(11.35)	(11.42)	(10.11)	(10.21)
Bad Brexit(%)											
$\mathcal{DV}11$	Same results as for capitalisation-dependent price impact										
$\mathcal{TV}11$	155.05	251.16	119.47	202.13	201.90	202.13	201.76	103.91	103.81	126.40	126.83
	-	-	-	-	-	(9.24)	(9.30)	(8.87)	(8.98)	(9.53)	(9.59)
$\mathcal{AV}11$	109.02	165.48	67.01	139.78	139.65	139.94	139.59	104.08	103.99	114.60	114.72
	-	-	-	-	-	(5.95)	(6.03)	(8.09)	(8.19)	(7.38)	(7.39)
Bold	-	1	0	3	4	2	2	2	2	2	2

Table 8.1: The table presents average fire sale risk measures (averaged over the banks and additionally averaged over the reconstructed samples) for the 2011 EBA data for two different shock scenarios for the true matrix and for reconstructed matrices that were reconstructed from noisy observations of the row and column sums.

8.C Chapter 3: Target leverage condition

We consider a subset of scenarios in which all banks can meet their target leverages in each stage of fire sales. Under the target leverage condition, we obtain a differentiable objective function of the bank's total asset holdings.

Definition 8.C.1 (Target leverage condition). *A bank $n \in \mathcal{N}$ satisfies the target leverage condition if it can sell a proportion of its asset holdings to meet its target leverage in each round of fire sales i.e.,*

$$\delta(R_{nt}) = -b_n R_{nt} \quad \forall t \geq 1.$$

The equality of the selling function to the leveraged net returns represents one of the two terms in the selling function.

Let us consider the inputs of the selling function. The bank can meet its target leverage if its leveraged net returns are smaller than the value of its remaining asset holdings for all periods. Hence, a condition which satisfies the target leverage condition is if the net returns are bounded above by the bank's target leverage component.

Lemma 8.C.2. *The bank $n \in \mathcal{N}$ satisfies the target leverage condition if its net returns at each stage of fire sales are bounded by its target leverage component i.e.,*

$$-R_{nt} \leq \frac{1}{1 + b_n} \quad \forall t \geq 1.$$

Proof of Lemma 8.C.2. The bound on the net returns on the leverage component is equivalent to the leveraged net returns being smaller than the remaining value of the bank's asset holdings. This inequality implies the selling function is equal to the leveraged net returns, where the selling function is positive because the leveraged net returns are negative:

$$-R_{nt} \leq \frac{1}{1 + b_n} \iff -b_n R_{nt} \leq 1 + R_{nt} \implies \delta(R_{nt}) = -b_n R_{nt}.$$

□

We require the bank to be able to meet its target leverage in all rounds of fire sales.² We show for conditions on the initial net returns and the connectivity of banks, all banks can meet their target leverages in all rounds of fire sales.

Proposition 8.C.3. *If the initial net returns and connectivity component of all banks are bounded above by the target leverage i.e.,*

$$-R_{n1} \leq \frac{1}{1 + b_n} \quad \text{and} \quad \gamma_{n1} \leq \frac{1}{1 + b_n} \quad \forall n \in \mathcal{N}$$

²With the inequality in Lemma 8.C.2, the selling function $\delta(R_n) \leq 1$ represents the bank is always able to sell a proportion of its total assets to meet its target leverage.

then all banks are able to meet their target leverage in each round of fire sales i.e.,

$$\delta(R_{nt}) = -b_n R_{nt} \quad \forall n \in \mathcal{N}, \quad \forall t \geq 1.$$

Proof of Proposition 8.C.3. We use proof by induction to show the net returns are bounded by the leverage of the bank. We show the base case in which $t = 1$ and the inductive step in which t implies $t + 1$.

From the assumption of the initial net returns and connectivity, this holds for the base case. For the inductive step, we assume $(-R_{nt}) \leq \frac{1}{1+b_n}$ and $\gamma_{n1} \leq \frac{1}{1+b_n} \quad \forall n \in \mathcal{N} \quad t \geq 1$ holds, then

$$\begin{aligned} (-R_{n(t+1)}) &= \sum_{k=1}^K m_{nk} (-f_{k(t+1)}) \\ &= \sum_{k=1}^K m_{nk} l_k \left(\sum_{p=1}^N m_{pk} \alpha_{pt} \delta(R_{pt}) \right) \\ &= \sum_{k=1}^K m_{nk} l_k \left(\sum_{p=1}^N m_{pk} \alpha_{pt} b_p (-R_{pt}) \right) \\ &\leq \sum_{k=1}^K m_{nk} l_k \left(\sum_{p=1}^N m_{pk} \alpha_{pt} \frac{b_p}{1+b_p} \right) \quad (*) \\ &< \sum_{k=1}^K m_{nk} l_k \left(\sum_{p=1}^N m_{pk} \alpha_{pt} \right) \\ &= \gamma_{nt} \\ &\leq \gamma_{n1} \leq \frac{1}{1+b_n}. \quad (**) \end{aligned}$$

The (*) comes from the inductive assumption on the net returns for all banks. The (**) is from the non-decreasing property of the total assets of the bank. From Lemma 8.C.2, all banks satisfy the target leverage condition. \square

The bound on the initial net returns and connectivity only depends on the target leverage of the bank. These two quantities form part of the fire sales measures introduced by Greenwood et al. (2015).

For one bank to meet its target leverage, it must hold for all banks. If only one bank is initially able to meet its target leverage, then the bank could still be affected by the losses of other banks which were not able to maintain their target leverages. Also, only considering a bound on the net returns is not sufficient, as the fire sales losses from the indirect shock can be larger than the initial shock assumed for assets.

Under the capitalisation-dependent assumption on the price impact, the connectivity of all banks is represented by the connectivity constant. As the maximum leverage of the

bank is bounded by the regulatory constraint, then the connectivity is bounded above by the maximum leverage component:

$$\rho \leq \frac{1}{1 + b^{\max}}. \quad (8.4)$$

For this choice of price impact, if the connectivity constant is bounded by the maximum leverage, then the target leverage condition only depends on a bound for the initial net returns. In general, Proposition 8.C.3 holds for different choices of the price impact.³ The bound on the initial net returns and connectivity of banks also leads to a bound on the cumulative net returns, across all rounds of fire sales.

Corollary 8.C.4. *If the initial net returns and connectivity component of all banks are bounded above by the target leverage i.e.,*

$$-R_{n1} \leq \frac{1}{1 + b_n} \quad \text{and} \quad \gamma_{n1} \leq \frac{1}{1 + b_n} \quad \forall n \in \mathcal{N}$$

then the cumulative net returns are bounded above by the connectivity of the bank i.e.,

$$\sum_{t=1}^{T-1} -R_{n(t+1)} \leq \gamma_{n1} \quad \forall n \in \mathcal{N} \quad \text{and} \quad T \geq 2.$$

Proof of Corollary 8.C.4. Assuming the initial conditions from Proposition 8.C.3, we can substitute the total assets of the bank into the multi-period asset shock,

$$f_{kt+1} = l_k \sum_{p=1}^N m_{pk} (\alpha_{p(t+1)} - \alpha_{pt}).$$

By summing over $t \geq 2$, the right-hand side becomes a telescoping sum

$$\sum_{t=2}^T f_{kt} = l_k \sum_{p=1}^N m_{pk} (\alpha_{pT+1} - \alpha_{p1}) \geq -l_k \sum_{p=1}^N m_{pk} \alpha_{p1}.$$

Using the definition of the connectivity component and $\sum_{k=1}^K m_{nk} = 1 \quad \forall n \in \mathcal{N}$ for the RHS, we arrive at the inequality. \square

The inequality shows that the losses to other banks are higher than the losses on itself. This represents the interconnections from other banks and the restriction on the net returns from the target leverage condition. From the assumptions on the initial input from Proposition 8.C.3 on the target leverage condition, the total assets of banks are always non-negative without the positive indicator.

³For a constant price, an equivalent constraint as in (8.4) for the capitalisation-dependent price impact is given by $l \leq \frac{1}{\max_n ((1+b_n) \sum_{k=1}^K m_{nk} (\sum_{p=1}^N m_{pk} \alpha_{p1}))}$.

Corollary 8.C.5. *If the initial net returns and connectivity component of all banks are bounded above by the target leverage i.e.,*

$$-R_{n1} \leq \frac{1}{1+b_n} \quad \text{and} \quad \gamma_{n1} \leq \frac{1}{1+b_n} \quad \forall n \in \mathcal{N}$$

then the total asset holdings with the leveraged net returns component are non-negative for all banks:

$$\alpha_{n(t+1)} = \alpha_{nt} \left(1 + b_n \sum_{k=1}^K m_{nk} f_{kt} \right) \geq 0 \quad \forall n \in \mathcal{N} \text{ and } \forall t \geq 1.$$

Proof of Corollary 8.C.5. The total assets of the bank at time-t can be represented by the bank's initial asset holdings and the leveraged net returns at each round of fire sales:

$$\alpha_{n(t+1)} = \alpha_{n1} \prod_{j=1}^t \left(1 + b_n \sum_{k=1}^K m_{nk} f_{kj} \right) \quad \forall t \geq 1.$$

The initial total assets holdings of banks are non-negative and each component of the leveraged net returns is positive from Proposition 8.C.3. Hence, the total asset holdings of all banks at time-t without the positive indicator are non-negative. \square

The bank always has non-negative total assets without a positive indicator from Corollary 8.C.5. The objective function representing the total assets of all banks is differentiable w.r.t to the fire sales scenario. From the target leverage condition, the fire sales mechanism with Lemma 8.C.2 and Corollary 8.C.5 is defined as follows:

$$\begin{aligned} \alpha_{n(t+1)} &= \alpha_{nt} \left(1 + b_n \sum_{k=1}^K m_{nk} f_{kt} \right) \quad \forall n \in \mathcal{N}, \\ f_{k(t+1)} &= l_k \sum_{p=1}^N m_{pk} \alpha_{pt} b_p R_{pt} \quad \forall k \in \mathcal{S} \quad \forall t \geq 1, \end{aligned} \tag{8.5}$$

$$\text{where} \quad -R_{n1} \leq \frac{1}{1+b_n} \quad \forall n \in \mathcal{N} \quad \text{and} \quad \rho \leq \frac{1}{1+b^{\max}}.$$

As all banks can meet their target leverages, the indirect shocks depend on the leveraged net returns of the bank. The constraint on the net returns and the connectivity constant in (8.5) is the same condition for the optimisation problem (3.4).

8.D Chapter 3: Multi-period fire sales measures

The change in the total assets of the bank and shocks representing the fire sales contagion can be represented relative to the equity holdings. This captures the leverage targeting

behaviour from the fire sales measures, in which banks maintain their target leverage. From Greenwood et al. (2015), two measures were introduced for evaluating the fire sales risk. The first was systemicness $\mathcal{SYS}_t \in [0, \infty) \quad \forall t \geq 0$, which represents the equity loss a bank contributes at time- t . We define the fire sales measures for multiple rounds:

$$\mathcal{SYS}_t(n) = \mathcal{SYS}_{t-1}(n) + \gamma_{nt} \frac{\alpha_{nt}}{\sum_{n=1}^N e_{n1}} (-\delta(R_{nt}))$$

where

$$\gamma_{nt} = \sum_{k=1}^K m_{nk} l_k \left(\sum_{p=1}^N \alpha_{pt} m_{pk} \right), \quad \forall t \geq 1$$

and

$$\delta(x_p) = (\min(-b_p x_p, 1 + x_p))^+,$$

and

$$\mathcal{SYS}_0(n) = 0.$$

The γ_{nt} is defined as a time-dependent connectivity component. As the above is a recursive formula, we can rewrite the expression as follows:

$$\mathcal{SYS}_t(n) = \sum_{t=1}^T \gamma_{nt} \frac{\alpha_{nt}}{\sum_{n=1}^N e_{n1}} (-\delta(R_{nt})).$$

The total equity contribution of equity losses at time- t is defined as $\mathcal{AV}_t \in [0, \infty)$, which is the sum of systemicness values of all banks:

$$\mathcal{AV}_t = \sum_{n=1}^N \mathcal{SYS}_t(n) \quad \forall t \geq 0.$$

The second measure represents the equity losses incurred by the bank. This aspect can be considered in two parts: the direct and indirect losses of the fire sales. The direct vulnerability is denoted as $\mathcal{DV}(n) \in [0, \infty)$. This is a measure of the initial losses and so remains unchanged in the multi-period case,

$$\mathcal{DV}(n) = \frac{\alpha_{n1}}{e_{n1}} (-R_{n1}) \quad \forall n \in \mathcal{N}.$$

The indirect measure which accounts for losses at multiple periods is defined as $\mathcal{IV}_t(n) \in [0, \infty)$ for all banks. The indirect losses can be represented by the recursive formula of losses at each fire sales round:

$$\mathcal{IV}_t(n) = \mathcal{IV}_{t-1}(n) + \frac{\alpha_{nt}}{e_{n1}} \sum_{k=1}^K m_{nk} l_k \left(\sum_{p=1}^N m_{pk} \alpha_{pt} (-\delta(R_{pt})) \right) \quad \forall t \geq 1,$$

with

$$\mathcal{IV}_0(n) = 0 \quad \forall n \in \mathcal{N}.$$

The above formula can be rewritten as follows

$$\mathcal{IV}_t(n) = \sum_{t=1}^T \frac{\alpha_{nt}}{e_{n1}} \sum_{k=1}^K m_{nk} l_k \left(\sum_{p=1}^N m_{pk} \alpha_{pt} (-\delta(R_{pt})) \right).$$

One of the properties to denote both measures is that the total losses are conserved. The only difference between both measures is the perspective of equity losses in the system. We define this identity for time t and for the direct losses in the fire sale:

Lemma 8.D.1. *For the initial equity of banks $e_{n1} \geq 0$, the initial losses of the bank $\mathcal{DV}(n)$ are equal to the initial shock of the asset capitalisation:*

$$\sum_{n=1}^N e_{n1} \mathcal{DV}(n) = \sum_{k=1}^K c_{k1} (-f_{k1}).$$

For all time periods $t \geq 1$, the aggregate vulnerability of the total equity is equal to the total indirect vulnerability of the bank's equity:

$$\mathcal{AV}_t \sum_{n=1}^N e_{n1} = \sum_{n=1}^N e_{n1} \mathcal{IV}_t(n) \quad \forall t \geq 1.$$

Proof of Lemma 8.D.1: For the direct vulnerability, we rewrite the returns on the assets w.r.t to the shock on the asset capitalisation:

$$\begin{aligned} \sum_{n=1}^N e_{n1} \mathcal{DV}(n) &= \sum_{n=1}^N e_{n1} \left(\frac{\alpha_{n1} (-R_{n1})}{e_{n1}} \right) \\ &= \sum_{n=1}^N \alpha_{n1} (-R_{n1}) \\ &= \sum_{n=1}^N \alpha_{n1} \left(\sum_{k=1}^K m_{nk} (-f_{k1}) \right) \\ &= \sum_{k=1}^K \sum_{n=1}^N \alpha_{n1} m_{nk} (-f_k) = \sum_{k=1}^K c_{k1} (-f_{k1}). \end{aligned}$$

Using the recursive relation of the aggregate and indirect vulnerability. We can equivalently show:

$$\left(\sum_{n=1}^N e_{n1} \right) \sum_{n=1}^N \mathcal{SV}_t(n) = \sum_{n=1}^N e_{n1} \mathcal{IV}_t(n) \quad \forall t \geq 1.$$

Then,

$$\begin{aligned}
 \left(\sum_{n=1}^N e_{n1} \right) \sum_{n=1}^N \mathcal{S}\mathcal{V}\mathcal{S}_t(n) &= \sum_{n=1}^N \left[\sum_{k=1}^K \left(\sum_{p=1}^N \alpha_{pt} m_{pk} \right) l_k m_{nk} \right] \alpha_{nt} (-\delta(R_{n(t-1)})) \\
 &= \left[\sum_{k=1}^K \left(\sum_{p=1}^N \alpha_{pt} m_{pk} \right) l_k \right] \sum_{n=1}^N m_{nk} \alpha_{nt} (-\delta(R_{n(t-1)})) \\
 &= \sum_{p=1}^N \alpha_{pt} \sum_{k=1}^K l_k m_{pk} \left[\sum_{n=1}^N m_{nk} \alpha_{nt} (-\delta(R_{n(t-1)})) \right] \\
 &= \sum_{p=1}^N e_{p1} \left(\frac{\alpha_{pt}}{e_{p1}} \sum_{k=1}^K l_k m_{pk} \left[\sum_{n=1}^N m_{nk} \alpha_{nt} (-\delta(R_{n(t-1)})) \right] \right) \\
 &= \sum_{p=1}^N e_{p1} \mathcal{I}\mathcal{V}_t(p).
 \end{aligned}$$

□

These identities above show that the total direct losses are independent of the network topology. This would hold for all asset holdings matrices which respect the column sums. Secondly, the identity of the fire sales measures is a two-way perspective on the asset losses of banks, relative to the equity.

8.E Chapter 4: Collateral clearing model: Existence of and convergence to the greatest solution

To prove the existence and convergence of the collateral clearing model to the greatest solution, in the first round of clearing, we show the monotonicity of the first round clearing function with Lemma 8.E.1. The proofs for Lemma 8.E.1 follow in the same way as in Veraart and Aldasoro (2022), where we additionally account for the bank's external illiquid asset holdings.

Lemma 8.E.1. *For the first round function $\Phi^{R1} : [0, 1] \times [0, \bar{p}^{R1}] \rightarrow [0, 1] \times [0, \bar{p}^{R1}]$. The first round clearing function is order-preserving i.e., for the price impact of collateral and illiquid assets $\pi, \tilde{\pi} \in [0, \infty)$ where $\pi \leq \tilde{\pi}$ and the obligations matrix $p, \tilde{p} \in [0, \bar{p}]$ where $p \leq \tilde{p}$, then*

$$\begin{aligned}
 \Phi_{1,(k)}^{R1}(\pi, p) &\leq \Phi_{1,(k)}^{R1}(\tilde{\pi}, \tilde{p}) \quad \forall k \in \mathcal{S}, \\
 \Phi_{2,(ij)}^{R1}(\pi, p) &\leq \Phi_{2,(ij)}^{R1}(\tilde{\pi}, \tilde{p}) \quad \forall i, j \in \mathcal{N}.
 \end{aligned}$$

Proof. We assume that $\pi \leq \tilde{\pi}$ and $p \leq \tilde{p}$. Let $\pi, \tilde{\pi} \in [0, 1]$ and $p, \tilde{p} \in [0, \bar{p}^{R1}]$, we show

that Φ^{R1} is an order-preserving function. If the term for the collateral sold is such that

$$\Upsilon_{ij}(\pi, p) \geq \Upsilon_{ij}(\tilde{\pi}, \tilde{p}).$$

Then, for all assets sold and as $\Omega(\pi, p)$ is non-increasing in both components by definition,

$$\begin{aligned} \Delta_k(\pi, p) &= \sum_{i=1}^N \min \{S_{ik}, \Omega_{ik}(\pi, p)\} + \sum_{i=1}^N \sum_{j=1}^N \Upsilon_{ij}(\pi, p) \mathbf{1}(T_{ij} = k) \\ &\geq \sum_{i=1}^N \min \{S_{ik}, \Omega_{ik}(\tilde{\pi}, \tilde{p})\} + \sum_{i=1}^N \sum_{j=1}^N \Upsilon_{ij}(\tilde{\pi}, \tilde{p}) \mathbf{1}(T_{ij} = k) \\ &= \Delta_k(\tilde{\pi}, \tilde{p}) \quad \forall k \in \mathcal{S}. \end{aligned}$$

Hence,

$$\Phi_{1,(k)}^{R1}(\pi, p) = \exp(-l_k \Delta_k(\pi, p)) \leq \exp(-l_k \Delta_k(\tilde{\pi}, \tilde{p})) = \Phi_{1,(k)}^{R1}(\tilde{\pi}, \tilde{p}).$$

Under the ordering of $(\tilde{\pi}, \tilde{p})$ and (π, p) , the total assets in the first round of clearing are such that

$$A_i^{R1}(\pi, p) = b_i + \sum_{k=1}^K S_{ik} \pi_k + \sum_{j=1}^N p_{ji} \leq b_i + \sum_{k=1}^K S_{ik} \tilde{\pi}_k + \sum_{j=1}^N \tilde{p}_{ji} = A_i^{R1}(\tilde{\pi}, \tilde{p}).$$

From the definition of the set of defaults,

$$\mathcal{D}^{R1}(\tilde{\pi}, \tilde{p}) \subseteq \mathcal{D}^{R1}(\pi, p).$$

For the order-preservation of the collateral sold $\Upsilon(\pi, p)$ under the matrix T , we consider the following cases:

1. If $i \in \mathcal{N} \setminus \mathcal{D}^{R1}(\tilde{\pi}, \tilde{p})$, then

$$\Upsilon_{ij}(\pi, p) \geq 0 = \Upsilon_{ij}(\tilde{\pi}, \tilde{p}).$$

2. If $i \in \mathcal{D}^{R1}(\tilde{\pi}, \tilde{p})$, then $i \in \mathcal{D}^{R1}(\pi, p)$. Then we define the terms of the collateral sold as follows:

- If $\pi > 0$, then $\tilde{\pi} > 0$. This implies on the second term $\frac{\bar{p}_{ij}^{R1}}{\pi_{T_{ij}}} \geq \frac{\bar{p}_{ij}^{R1}}{\tilde{\pi}_{T_{ij}}}$. Hence

$$\Upsilon_{ij}(\tilde{\pi}, \tilde{p}) = \min \left\{ \zeta_{ij}, \frac{\bar{p}_{ij}^{R1}}{\tilde{\pi}_{T_{ij}}} \right\} \leq \min \left\{ \zeta_{ij}, \frac{\bar{p}_{ij}^{R1}}{\pi_{T_{ij}}} \right\} = \Upsilon_{ij}(\pi, p).$$

– If $\tilde{\pi} > \pi = 0$ and $\bar{p}^{R1} > 0$, then $\Upsilon_k(\pi, p) = \zeta_{ij}$ and $\Upsilon_k(\tilde{\pi}, \tilde{p}) = \min \left\{ \zeta_{ij}, \frac{\bar{p}_{ij}^{R1}}{\tilde{\pi}_{T_{ij}}} \right\}$.

Hence

$$\Upsilon_{ij}(\tilde{\pi}, \tilde{p}) = \min \left\{ \zeta_{ij}, \frac{\bar{p}_{ij}^{R1}}{\tilde{\pi}_{T_{ij}}} \right\} \leq \zeta_{ij} = \Upsilon_{ij}(\pi, p).$$

If $\bar{p}^{R1} = 0$, then $\Upsilon_k(\pi, p) = 0$ and $\Upsilon_k(\tilde{\pi}, \tilde{p}) = \min \left\{ \zeta_{ij}, \frac{\bar{p}_{ij}^{R1}}{\tilde{\pi}_{T_{ij}}} \right\}$. Hence

$$\Upsilon_k(\tilde{\pi}, \tilde{p}) = \min \left\{ \zeta_{ij}, \frac{\bar{p}_{ij}^{R1}}{\tilde{\pi}_{T_{ij}}} \right\} = 0 = \Upsilon_k(\pi, p).$$

– If $\tilde{\pi} = 0$ and $\pi = 0$, and $\bar{p}^{R1} > 0$ then

$$\Upsilon_{ij}(\tilde{\pi}, \tilde{p}) = \zeta_{ij} = \Upsilon_{ij}(\pi, p)$$

else, if $\bar{p}^{R1} = 0$

$$\Upsilon_{ij}(\tilde{\pi}, \tilde{p}) = 0 = \Upsilon_{ij}(\pi, p).$$

In all cases, the assets used as collateral sold in the first round are order-preserving in both components. Hence, the ordering of the total assets and collateral assets sold under both components is preserved.

We consider the order-preservation of the second component Φ_2^{R1} of the fixed point function. We show Φ_2^{R1} is an order-preserving function for π and p . We consider the order preservation for p . We consider two cases for the bank:

1. $i \in \mathcal{N} \setminus \mathcal{D}^{R1}(\tilde{\pi}, \tilde{p})$, then

$$\Phi_{2,(ij)}^{R1}(\tilde{\pi}, \tilde{p}) = \bar{p}_{ij}^{R1} \geq \Phi_{2,(ij)}^{R1}(\pi, p).$$

2. $i \in \mathcal{D}^{R1}(\tilde{\pi}, \tilde{p})$ then $i \in \mathcal{D}^{R1}(\pi, p)$ and

$$\begin{aligned} \Phi_{2,(ij)}^{R1}(\pi, p) &= \min \left\{ \bar{p}_{ij}^{R1}, \pi_{T_{ij}} \zeta_{ij} + a_{ij}^{R1}(\pi) \left(\gamma_i^1 \left(b_i + \sum_{k=1}^K S_{ik} \pi_k \right) + \gamma_i^2 \sum_{j=1}^N p_{ji} \right) \right\}, \\ \Phi_{2,(ij)}^{R1}(\tilde{\pi}, \tilde{p}) &= \min \left\{ \bar{p}_{ij}^{R1}, \tilde{\pi}_{T_{ij}} \zeta_{ij} + a_{ij}^{R1}(\tilde{\pi}) \left(\gamma_i^1 \left(b_i + \sum_{k=1}^K S_{ik} \tilde{\pi}_k \right) + \gamma_i^2 \sum_{j=1}^N \tilde{p}_{ji} \right) \right\}. \end{aligned}$$

First, if $\Phi_{2,(ij)}^{R1}(\tilde{\pi}, \tilde{p}) = \bar{p}_{ij}^{R1}$, then

$$\Phi_{2,(ij)}^{R1}(\tilde{\pi}, \tilde{p}) = \bar{p}_{ij}^{R1} \geq \Phi_{2,(ij)}^{R1}(\pi, p).$$

If $\Phi_{2,(ij)}^{R1}(\tilde{\pi}, \tilde{p}) < \bar{p}_{ij}^{R1}$, then

$$\bar{p}_{ij}^{R1} > \tilde{\pi}_{T_{ij}} \zeta_{ij} + a_{ij}^{R1}(\tilde{\pi}) \left(\gamma_i^1 \left(b_i + \sum_{k=1}^K S_{ik} \tilde{\pi}_k \right) + \gamma_i^2 \sum_{j=1}^N \tilde{p}_{ji} \right).$$

Using the definition of the relative payment matrix a^{R1} and rearranging the terms, then

$$1 > \frac{\gamma_i^1 \left(b_i + \sum_{k=1}^K S_{ik} \tilde{\pi}_k \right) + \gamma_i^2 \sum_{j=1}^N \tilde{p}_{ji}}{\sum_{l=1}^N \max \{0, \bar{p}_{il}^{R1} - \tilde{\pi}_{T_{il}} \zeta_{il}\}}. \quad (8.6)$$

If $\Phi_{2,(ij)}^{R1}(\pi, p) < \bar{p}_{ij}^{R1}$, we show

$$\Phi_{2,(ij)}^{R1}(\pi, p) = \pi_{T_{ij}} \zeta_{ij} + a_{ij}^{R1}(\pi) \left(\gamma_i^1 \left(b_i + \sum_{k=1}^K S_{ik} \pi_k \right) + \gamma_i^2 \sum_{j=1}^N p_{ji} \right).$$

From the second component of the clearing function, for a bank in default

$$\begin{aligned} & \pi_{T_{ij}} \zeta_{ij} + a_{ij}^{R1}(\pi) \left(\gamma_i^1 \left(b_i + \sum_{k=1}^K S_{ik} \pi_k \right) + \gamma_i^2 \sum_{j=1}^N p_{ji} \right) \\ &= \pi_{T_{ij}} \zeta_{ij} + \max \{0, \bar{p}_{ij}^{R1} - \pi_{T_{ij}} \zeta_{ij}\} \left(\frac{\gamma_i^1 \left(b_i + \sum_{k=1}^K S_{ik} \pi_k \right) + \gamma_i^2 \sum_{j=1}^N p_{ji}}{\sum_{l=1}^N \max \{0, \bar{p}_{il}^{R1} - \pi_{T_{il}} \zeta_{il}\}} \right) \\ &\leq \pi_{T_{ij}} \zeta_{ij} + \max \{0, \bar{p}_{ij}^{R1} - \pi_{T_{ij}} \zeta_{ij}\} \underbrace{\left(\frac{\gamma_i^1 \left(b_i + \sum_{k=1}^K S_{ik} \tilde{\pi}_k \right) + \gamma_i^2 \sum_{j=1}^N \tilde{p}_{ji}}{\sum_{l=1}^N \max \{0, \bar{p}_{il}^{R1} - \tilde{\pi}_{T_{il}} \zeta_{il}\}} \right)}_{<1} \\ &< \pi_{T_{ij}} \zeta_{ij} + \max \{0, \bar{p}_{ij}^{R1} - \pi_{T_{ij}} \zeta_{ij}\}, \end{aligned}$$

We consider two cases of the relative payment matrix if $a^{R1}(\pi) = 0$, then $0 = a^{R1}(\pi) \leq a^{R1}(\tilde{\pi})$ and

$$\begin{aligned} & \pi_{T_{ij}} \zeta_{ij} + a_{ij}^{R1}(\pi) \left(\gamma_i^1 \left(b_i + \sum_{k=1}^K S_{ik} \pi_k \right) + \gamma_i^2 \sum_{j=1}^N p_{ji} \right) \\ &\leq \tilde{\pi}_{T_{ij}} \zeta_{ij} + a_{ij}^{R1}(\tilde{\pi}) \left(\gamma_i^1 \left(b_i + \sum_{k=1}^K S_{ik} \tilde{\pi}_k \right) + \gamma_i^2 \sum_{j=1}^N \tilde{p}_{ji} \right) \\ &= \Phi^{R1}(\tilde{\pi}, \tilde{p}) < \bar{p}^{R1}. \end{aligned}$$

In the second case in which $a^{R1}(\pi) > 0$, then $\bar{p}_{ij}^{R1} > \pi_{T_{ij}}\zeta_{ij}$ and

$$\begin{aligned} & \pi_{T_{ij}}\zeta_{ij} + a_{ij}^{R1}(\pi) \left(\gamma_i^1 \left(b_i + \sum_{k=1}^K S_{ik}\pi_k \right) + \gamma_i^2 \sum_{j=1}^N p_{ji} \right) \\ & \leq \pi_{T_{ij}}\zeta_{ij} + \max \{0, \bar{p}_{ij}^{R1} - \pi_{T_{ij}}\zeta_{ij}\} = \bar{p}_{ij}^{R1}, \end{aligned}$$

and therefore

$$\Phi_{2,(ij)}^{R1}(\pi, p) = \pi_{T_{ij}}\zeta_{ij} + a_{ij}^{R1}(\pi) \left(\gamma_i^1 \left(b_i + \sum_{k=1}^K S_{ik}\pi_k \right) + \gamma_i^2 \sum_{j=1}^N p_{ji} \right). \quad (8.7)$$

We show that the function (8.7) is order-preserving under both components. We observe in the case for p , this holds. We show $\Phi_{2,(ij)}^{R1}$ is order-preserving in π . We define the function $f : [0, 1] \rightarrow [0, \infty)$, where

$$f(\pi) = \pi_{T_{ij}}\zeta_{ij} + a_{ij}^{R1}(\pi) \underbrace{\left(\gamma_i^1 \left(b_i + \sum_{k=1}^K S_{ik}\pi_k \right) + \gamma_i^2 \sum_{j=1}^N p_{ji} \right)}_{B(\pi, p; \gamma^1, \gamma^2)}.$$

Similarly to the arguments by Ghamami et al. (2022) and Veraart and Aldasoro (2022), then:

$$\frac{\partial f}{\partial \pi} = \zeta_{ij} + \frac{\partial a_{ij}^{R1}(\pi)}{\partial \pi} B(\pi, p; \gamma^1, \gamma^2) + a_{ij}^{R1}(\pi) \frac{\partial B(\pi, p; \gamma^1, \gamma^2)}{\partial \pi},$$

where

$$\frac{\partial a_{ij}^{R1}(\pi)}{\partial \pi} = \frac{\sum_{l=1}^N \max \{0, \bar{p}_{il}^{R1} - \pi_{T_{il}}\zeta_{il}\} (-\zeta_{ij}) + (\bar{p}_{ij}^{R1} - \pi_{T_{ij}}\zeta_{ij})^+ \sum_{l=1}^N \zeta_{il} \mathbf{1}(\bar{p}_{il}^{R1} > \pi_{T_{il}}\zeta_{il})}{\left(\sum_{l=1}^N \max \{0, \bar{p}_{il}^{R1} - \pi_{T_{il}}\zeta_{il}\} \right)^2},$$

and

$$\frac{\partial B(\pi, p; \gamma^1, \gamma^2)}{\partial \pi} = \gamma_i^1 S_{ik}.$$

Substituting the derivative of the relative asset holdings to the derivative of the function,

$$\begin{aligned} \frac{\partial f}{\partial \pi} &= \zeta_{ij} \underbrace{\left(1 - \frac{B_i(\pi, p; \gamma^1, \gamma^2)}{\sum_{l=1}^N \max \{0, \bar{p}_{il}^{R1} - \pi_{T_{il}}\zeta_{il}\}} \right)}_{\geq 0} \\ &+ B_i(\pi, p; \gamma^1, \gamma^2) (\bar{p}_{ij}^{R1} - \pi_{T_{ij}}\zeta_{ij})^+ \frac{\sum_{l=1}^N \zeta_{il} \mathbf{1}(\bar{p}_{il}^{R1} > \pi_{T_{il}}\zeta_{il})}{\left(\sum_{l=1}^N \max \{0, \bar{p}_{il}^{R1} - \pi_{T_{il}}\zeta_{il}\} \right)^2} + a_{ij}^{R1}(\pi) (\gamma_i^1 S_{ik}). \end{aligned}$$

The first term is positive from the inequality (8.6), with the second and last terms only

comprising positive terms. Therefore, the function $\Phi_{2,(ij)}^{R1}$ is order-preserving in π . Hence, Φ^{R1} is an order-preserving function. \square

We present the existence of and convergence to the greatest solution, in the first round of clearing under Theorem 8.E.2. The proof follows in the same way as in Veraart and Aldasoro (2022), where we additionally account for the bank's external illiquid asset holdings.

Theorem 8.E.2 (Existence of the greatest fixed point in the first round of clearing). *For $\Phi^{R1} : [0, 1] \times [0, \bar{p}^{R1}] \rightarrow [0, 1] \times [0, \bar{p}^{R1}]$ is the function for the first round of clearing. If $\Omega(\pi, p)$ is non-increasing in (π, p) , then the following holds:*

- The set of fixed points Φ^{R1} is a complete lattice, with a least and greatest fixed point.
- For $(\pi^0, p^0) = (1, \bar{p})$ and under the recursive relation $\kappa \in \mathbb{N}_0$, where

$$(\pi^{\kappa+1}, p^{\kappa+1}) = \Phi^{R1}(\pi^\kappa, p^\kappa)$$

it holds that

1. (π^κ, p^κ) is a monotonically decreasing sequence for $\kappa \in \mathbb{N}_0$.
2. The limit $\lim_{\kappa \rightarrow \infty} (\pi^\kappa, p^\kappa)$ exists and admits the greatest solution of the function Φ^{R1} .

Proof of Theorem 8.E.2. 1. Firstly, the mapping Φ^{R1} is a complete lattice for $[0, 1] \times [0, \bar{p}^{R1}]$. From the definition, the function is a mapping from $[0, 1] \times [0, \bar{p}^{R1}] \rightarrow [0, 1] \times [0, \bar{p}^{R1}]$ and from Lemma 8.E.1, the function is order-preserving in both components. By Tarski's fixed point theorem Tarski (1955), the set of fixed points is a complete lattice, for which there exists a least and greatest fixed point.

2. We show (π^κ, p^κ) is a monotonically decreasing sequence. We use induction to show the following statement. For $\kappa = 0$, from the definitions of each component in the mapping then

- $\pi_k^1 = \Phi_{1,(k)}^{R1}(\pi^0, p^0) = \exp(-l_k \Delta_k(\pi^0, p^0)) \leq 1 = \pi_k^0 \quad \forall k \in \mathcal{S}$.
- $p_{ij}^1 = \Phi_{2,(ij)}^{R1}(\pi^0, p^0) \leq \bar{p}_{ij}^{R1} = p_{ij}^0 \quad \forall i, j \in \mathcal{N}$.

We assume for the induction step, $(\pi^\kappa, p^\kappa) \leq (\pi^{\kappa+1}, p^{\kappa+1})$ is true for $\kappa \in \mathbb{N}_0$. Then,

$$(\pi^{\kappa+1}, p^{\kappa+1}) = \Phi^{R1}(\pi^\kappa, p^\kappa) \leq \Phi^{R1}(\pi^{\kappa+1}, p^{\kappa+1}) = (\pi^{\kappa+2}, p^{\kappa+2}).$$

This follows from the induction step and the order-preservation of the mapping Φ^{R1} . As the clearing function is bounded $(0, 0)$ below in each component (0 represents

a $K + 1$ dimensional vector and 0 a $N \times N$ matrix, with zero in all entries), there exists a monotone limit $(\hat{\pi}, \hat{p}) = \lim_{\kappa \rightarrow \infty} (\pi^\kappa, p^\kappa)$, which is also a fixed point,

$$\begin{aligned} \Phi^{R1}(\hat{\pi}, \hat{p}) &= \Phi^{R1}\left(\lim_{\kappa \rightarrow \infty} (\pi^\kappa, p^\kappa)\right) \\ &= \lim_{\kappa \rightarrow \infty} \Phi^{R1}(\pi^\kappa, p^\kappa) \\ &= \lim_{\kappa \rightarrow \infty} (\pi^{\kappa+1}, p^{\kappa+1}) \\ &= (\hat{\pi}, \hat{p}). \end{aligned} \tag{*}$$

The (*) comes from the fact the function is continuous from above. We show the greatest fixed point is the monotone limit of Φ^{R1} . We use a proof by induction to show that $(\pi^\kappa, p^\kappa) \geq (\pi^*, p^*) \quad \forall \kappa \in \mathbb{N}_0$. For $\kappa = 0$,

$$(\pi^0, p^0) = (1, \bar{p}^{R1}) \geq (\pi^*, p^*).$$

For the induction step, where we assume $(\pi^\kappa, p^\kappa) \geq (\pi^*, p^*)$ to be true, then

$$(\pi^{\kappa+1}, p^{\kappa+1}) = \Phi^{R1}(\pi^\kappa, p^\kappa) \geq \Phi^{R1}(\pi^*, p^*) = (\pi^*, p^*).$$

We use the fact that the mapping is order-preserving as in Lemma 8.E.1 and the properties of the fixed point. Taking the limit of the sequence, then

$$(\hat{\pi}, \hat{p}) = \lim_{\kappa \rightarrow \infty} (\pi^\kappa, p^\kappa) \geq (\pi^*, p^*).$$

As $(\hat{\pi}, \hat{p}) = \Phi^{R1}(\hat{\pi}, \hat{p})$, then $(\hat{\pi}, \hat{p}) = (\pi^*, p^*)$. □

The iterative method in which the greatest fixed point is computed economically reflects that banks fulfil their obligations to other banks when possible.

8.F Chapter 5: Valuation framework: Existence of and convergence to the greatest solution

We adapt Theorems 3.1 and 3.2 in Barucca et al. (2020) to banks prior to ring-fencing and to nRFBs.

Theorem 8.F.1 (Existence of and convergence to the greatest solution). *If all valuation functions are feasible, the set of equations (5.11a) and (5.11b) admit the greatest solutions*

\mathbf{E}^+ and $\mathbf{E}^{nRF,+}$. Moreover, the sequences $\{\mathbf{E}^\kappa\}$ and $\{\mathbf{E}^{nRF,\kappa}\}$, defined, for all i , as follows:

$$\begin{aligned} E_i^0 &= A_i^e + \sum_{j=1}^N A_{ij} - L_i^e - \sum_{j=1}^N L_{ij} \\ E_i^{nRF,0} &= (1 - \psi_i^A)A_i^e + \sum_{j=1}^N A_{ij} - (1 - \psi_i^L)L_i^e - \sum_{j=1}^N L_{ij}, \end{aligned}$$

and for $\kappa \geq 1$:

$$\begin{aligned} E_i^{\kappa+1} &= A_i^e + \sum_{j=1}^N A_{ij} \mathbb{V}(E_j^\kappa | \mathcal{C}_j) - L_i^e - \sum_{j=1}^N L_{ij} \\ E_i^{nRF,\kappa+1} &= (1 - \psi_i^A)A_i^e + \sum_{j=1}^N A_{ij} \mathbb{V}(E_j^{nRF,\kappa} | \mathcal{C}_j^{nRF}) - (1 - \psi_i^L)L_i^e - \sum_{j=1}^N L_{ij}, \end{aligned}$$

are monotonically non-increasing and convergent to the greatest solutions:

$$\begin{aligned} \lim_{\kappa \rightarrow \infty} \mathbf{E}^\kappa &= \mathbf{E}^+ \\ \lim_{\kappa \rightarrow \infty} \mathbf{E}^{nRF,\kappa} &= \mathbf{E}^{nRF,+}. \end{aligned}$$

One consequence of Theorem 8.F.1 is that we can interpret the sequences $\{\mathbf{E}^\kappa\}$ and $\{\mathbf{E}^{nRF,\kappa}\}$ as incremental adjustments to equity valuations. In the beginning, equities are naive, in the sense that they incorporate a naive valuation of interbank assets, which are taken at face value. In the first iteration, $\{\mathbf{E}^1\}$ and $\{\mathbf{E}^{nRF,1}\}$ incorporate the valuation of interbank assets only of their direct counterparties. In the second iteration, $\{\mathbf{E}^2\}$ and $\{\mathbf{E}^{nRF,2}\}$ incorporate the valuation of interbank assets of their direct counterparties and of the direct counterparties of their counterparties, and so on, until convergence. Since the $\{\mathbf{E}^\kappa\}$ and $\{\mathbf{E}^{nRF,\kappa}\}$ are non-increasing, all incremental adjustments to equity valuations are downwards, i.e. $\mathbf{E}^+ \leq \mathbf{E}^0$ and $\mathbf{E}^{nRF,+} \leq \mathbf{E}^{nRF,0}$.

8.G Proofs

8.G.1 Chapter 2 proofs

Proof of Proposition 2.3.1. 1.-3. From the definition of the systemicness of bank $n \in \mathcal{N}$ in (2.4), it is clear that $\mathcal{SYS}(n) = \gamma_{n1} \frac{\alpha_{n1}}{\sum_{\nu=1}^N e_{\nu 1}} b_{n1}(-R_{n1})$ depends on the network matrix X only via the two factors γ_{n1} and R_{n1} , since all other factors appearing in the formula are aggregate information that is available from the balance sheets of the banks.

This implies that the aggregate vulnerability, as the sum of all individual systemic-

nesses, depends on the network matrix X only via γ_{n1} and R_{n1} , where $n \in \mathcal{N}$. We also see directly from the definition, that the direct vulnerability of a bank $n \in \mathcal{N}$ depends on the network matrix X only via the factor R_{n1} .

4. To see that γ_{n1} depends on the individual entries of X only via its n th row, we rewrite γ_{n1} given in (2.5) as follows

$$\gamma_{n1} = \sum_{k=1}^K \left(\sum_{p=1}^N \alpha_{p1} m_{pk} \right) l_k m_{nk} = \sum_{k=1}^K \left(\sum_{p=1}^N \alpha_{p1} \frac{X_{pk}}{\alpha_{p1}} \right) l_k \frac{X_{nk}}{\alpha_{n1}} = \sum_{k=1}^K c_k l_k \frac{X_{nk}}{\alpha_{n1}}. \quad (8.8)$$

Hence, we see that γ_{n1} only depends on X_{n1}, \dots, X_{nK} . To make the dependence of γ_{n1} on X explicit, we will sometimes write $\gamma_{n1}(X)$.

First, if one assumes a constant price impact, then formula (8.8) reduces to

$$\gamma_{n1} = \frac{l}{\alpha_{n1}} \sum_{k=1}^K c_k X_{nk}. \quad (8.9)$$

Indeed, γ_{n1} depends on the individual entries in the n th row of the matrix X since it is proportional to a capitalisation-weighted aggregate of the positions of node n in the K assets. If additionally their market capitalisation was identical, i.e., if $c_1 = \dots = c_K = c$ (which would be unlikely in practice), then (8.9) would simplify even further to $\gamma_{n1} = \frac{l}{\alpha_{n1}} c \sum_{k=1}^K X_{nk} = lc$, which then no longer depends on the individual entries of X .

Second, if one assumes a capitalisation-dependent price impact, then $c_k l_k = \rho$ for all $k \in \mathcal{S}$ and hence $\gamma_{n1} = \frac{\rho}{\alpha_{n1}} \sum_{k=1}^K X_{nk} = \rho \quad \forall n \in \mathcal{N}$, which does not depend on X .

5. We find that

$$R_{n1} = \sum_{k=1}^K m_{nk} f_k = \sum_{k=1}^K \frac{X_{nk}}{\alpha_{n1}} f_k = \frac{1}{\alpha_{n1}} \sum_{k=1}^K X_{nk} f_k, \quad (8.10)$$

which again only depends on the matrix X via its n th row. To make the dependence of R_{n1} on X explicit, we will sometimes write $R_{n1}(X)$.

First, if we consider an all asset shock with $f_1 = \dots = f_K = f$, expression (8.10) simplifies to $R_{n1} = \frac{f}{\alpha_{n1}} \sum_{k=1}^K X_{nk} = f$ and hence does not depend on the matrix X .

Second, we consider a shock that only affects $\tilde{K} < K$ assets with indices in $\mathcal{I}^{\tilde{K}}$.

Then,

$$R_{n1} = \sum_{k=1}^K m_{nk} f_k = \sum_{k=1}^K \frac{X_{nk}}{\alpha_{n1}} f_k = \frac{1}{\alpha_{n1}} \sum_{k=1}^K X_{nk} f_k = \frac{1}{\alpha_{n1}} \sum_{k \in \mathcal{I}^{\tilde{K}}} X_{nk} f_k.$$

Hence, R_{n1} only depends on the columns with indices in $\mathcal{I}^{\tilde{K}}$ within the n th row, but not the full n th row of X .

Since $\mathcal{DV}(n)$ depends on X only via R_{n1} the results for $\mathcal{DV}(n)$ follow directly from the results on R_{n1} . □

Proof of Corollary 2.3.2. 1. Under an all asset shock and a capitalisation-dependent price impact, we know from the proof of Proposition 2.3.1 that $R_{n1} = f$ and $\gamma_{n1} = \rho$. Hence,

$$\begin{aligned} \mathcal{SY}\mathcal{S}(n) &= -f\rho \frac{\alpha_{n1}}{\sum_{\nu=1}^N e_{\nu 1}} b_{n1}, \\ \mathcal{AV} &= \sum_{n=1}^N \mathcal{SY}\mathcal{S}(n) = \frac{-f\rho}{\sum_{\nu=1}^N e_{\nu 1}} \sum_{n=1}^N \alpha_{n1} b_{n1}, \\ \mathcal{DV}(n) &= \frac{-f\alpha_{n1}}{e_{n1}}, \end{aligned}$$

which do not depend on the individual entries of X .

2. This statement follows directly from Proposition 2.3.1 and the analytical formulae of γ_{n1} and R_{n1} provided in its proof. □

8.G.2 Chapter 4 proofs

To show Theorem 4.3.1 and Theorem 4.3.2, we first state Lemma 8.G.1 which is Lemma 2.1 in Ghamami et al. (2022). This lemma still holds in our setting where banks can hold multiple external asset holdings. We then introduce Proposition 8.G.2, where Proposition 8.G.2 is an extension of Proposition 3.2 in Ghamami et al. (2022), where banks can hold multiple external asset holdings.

Lemma 8.G.1. *If $a_{ij}^{R2} \neq 0$, then $a_{ij}^{R2} = a_{ij}^{R1} \quad \forall i, j \in \mathcal{N}$.*

Proposition 8.G.2. *Under the fixed point values in the first round of clearing $(\pi^{*,R1}, p^{*,R1})$. For the bank payments and market value of assets under the second round of clearing (π^{R2}, p^{R2}) , then:*

$$p_{ij}^{*,R1} + \Phi_{2,(ij)}^{R2}(\pi^{R2}, p^{R2}) = \min \left\{ \bar{p}_{ij}^{R1}, \zeta_{ij} \pi_{T_{ij}}^{*,R1} + a_{ij}^{R1}(\pi^{*,R1}) C_i(\pi^{R2}, p^{R2}) \right\}, \quad (8.11)$$

where $\forall i \in \mathcal{N}$:

$$C_i(\pi, p) = \gamma_i^1 \left(b_i + \sum_{k=1}^K S_{ik} \pi_k^{*,R1} \right) + c_i^{*,R1} + \sum_{k=1}^K r_{ik}(\pi^{*,R1}, p^{*,R1}) \pi_k + \gamma_i^2 \sum_{j=1}^N p_{ji}^{*,R1} + \sum_{j=1}^N p_{ji}.$$

Proof of Proposition 8.G.2. The proof follows in a similar way as in Ghamami et al. (2022), where we account for the bank's illiquid asset holdings and bankruptcy costs. We show the total payment expression for all bank payments and the market price of assets, in the second round of clearing. We consider the different states of default for the bank, and how this corresponds to the total clearing payment:

1. If $i \in \mathcal{N} \setminus \mathcal{D}^{R1}(\pi^{*,R1}, p^{*,R1})$, then the bank can meet its obligations in full $p^{*,R1} = \bar{p}^{R1}$. Hence

$$\bar{p}_{ij}^{R2} = 0 \implies i \in \mathcal{N} \setminus \mathcal{D}^{R2}(\pi^{R2}, p^{R2}).$$

2. If $i \in \mathcal{D}^{R1}(\pi^{*,R1}, p^{*,R1})$, the fixed point of the first round is defined as follows

$$p_{ij}^{*,R1} = \min \left\{ \bar{p}_{ij}^{R1}, \pi_{T_{ij}}^{*,R1} \zeta_{ij} + a_{ij}^{R1}(\pi^{*,R1}) \left(\gamma_i^1 \left(b_i + \sum_{k=1}^K S_{ik} \pi_k^{*,R1} \right) + \gamma_i^2 \sum_{j=1}^N p_{ji}^{*,R1} \right) \right\}.$$

We consider two cases of the fixed point, for which $i \in \mathcal{D}^{R1}(\pi^{*,R1}, p^{*,R1})$.

- If $p^{*,R1} = \bar{p}^{R1}$, then the bank is able to meet its obligations. Hence

$$\bar{p}_{ij}^{R2} = 0 \implies i \in \mathcal{N} \setminus \mathcal{D}^{R2}(\pi^{R2}, p^{R2}).$$

- If $p^{*,R1} < \bar{p}^{R1}$, then

$$\bar{p}_{ij}^{R2} = \bar{p}_{ij}^{R1} - p_{ij}^{*,R1}$$

and

$$\Phi_{2,(ij)}^{R2}(\pi^{R2}, p^{R2}) = \min \left\{ \bar{p}_{ij}^{R2}, a_{ij}^{R2} \left(c_i^{*,R1} + \sum_{k=1}^K r_{ik}(\pi^{*,R1}, p^{*,R1}) \pi_k^{R2} + \sum_{j=1}^N p_{ji}^{R2} \right) \right\}.$$

We consider two cases of the clearing payment in the second round. In the case $p^{R2} = \bar{p}^{R2}$, then

$$p_{ij}^{*,R1} + \Phi_{2,(ij)}^{R2}(\pi^{R2}, p^{R2}) = p_{ij}^{*,R1} + (\bar{p}_{ij}^{R1} - p_{ij}^{*,R1}) = \bar{p}_{ij}^{R1},$$

and $i \in \mathcal{N} \setminus \mathcal{D}^{R2}(\pi^{R2}, p^{R2})$. For the case $p^{R2} < \bar{p}^{R2}$, then

$$\begin{aligned}
 & p_{ij}^{*,R1} + \Phi_{2,(ij)}^{R2}(\pi^{R2}, p^{R2}) \\
 &= \pi_{T_{ij}}^{*,R1} \zeta_{ij} + a_{ij}^{R1}(\pi^{*,R1}) \left(\gamma_i^1 \left(b_i + \sum_{k=1}^K S_{ik} \pi_k^{*,R1} \right) + \gamma_i^2 \sum_{j=1}^N p_{ji}^{*,R1} \right) \\
 &+ a_{ij}^{R2} \left(c_i^{*,R1} + \sum_{k=1}^K r_{ik}(\pi^{*,R1}, p^{*,R1}) \pi_k^{R2} + \sum_{j=1}^N p_{ji}^{R2} \right) \quad (*) \\
 &= \pi_{T_{ij}}^{*,R1} \zeta_{ij} + a_{ij}^{R1}(\pi^{*,R1}) C_i(\pi^{R2}, p^{R2}),
 \end{aligned}$$

where

$$\begin{aligned}
 & C_i(\pi, p) \\
 &= \gamma_i^1 \left(b_i + \sum_{k=1}^K S_{ik} \pi_k^{*,R1} \right) + c_i^{*,R1} + \sum_{k=1}^K r_{ik}(\pi^{*,R1}, p^{*,R1}) \pi_k + \gamma_i^2 \sum_{j=1}^N p_{ji}^{*,R1} + \sum_{j=1}^N p_{ji}.
 \end{aligned}$$

The change in the relative proportion obligations matrix (*) comes from Lemma 8.G.1, for which the bank is in default in the first round of clearing. As $p^{R2} < \bar{p}^{R2}$ then $p^{*,R1} + p^{R2} < \bar{p}^{R1}$ and hence $i \in \mathcal{D}^{R2}(\pi^{R2}, p^{R2})$.

In all cases, the value of the total payments after both rounds takes the following values:

$$\begin{aligned}
 & p_{ij}^{*,R1} + \Phi_{2,(ij)}^{R2}(\pi^{R2}, p^{R2}) \\
 &= \begin{cases} \bar{p}_{ij}^{R1} & \text{if } i \in \mathcal{N} \setminus \mathcal{D}^{R2}(\pi^{R2}, p^{R2}), \\ \pi_{T_{ij}}^{*,R1} \zeta_{ij} + a_{ij}^{R1}(\pi^{*,R1}) C_i(\pi^{R2}, p^{R2}) & \text{if } i \in \mathcal{D}^{R2}(\pi^{R2}, p^{R2}). \end{cases}
 \end{aligned}$$

The only case for which $i \in \mathcal{D}^{R2}(\pi^{R2}, p^{R2})$ is if

$$\pi_{T_{ij}}^{*,R1} \zeta_{ij} + a_{ij}^{R1}(\pi^{*,R1}) C_i(\pi^{R2}, p^{R2}) < \bar{p}_{ij}^{R1}.$$

The conditional statement is equivalent to the statement in the proposition. \square

Proof of Theorem 4.3.1. We define the clearing function $\Phi^{\nu, R1}$ under the different selling

strategies $\nu = \{A, B\}$ as follows:

$$\begin{aligned} & \Phi_{1,(k)}^{R1,\nu}(\pi, p) = \exp(-l_k^\nu \Delta_k^\nu(\pi, p)), \\ & \Phi_{2,(ij)}^{R1,\nu}(\pi, p) \\ = & \begin{cases} \min \left\{ \bar{p}_{ij}^{R1}, \pi_{T_{ij}} \zeta_{ij} \right. \\ \left. + a_{ij}^{R1}(\pi) \left(\gamma_i^{1,\nu} \left(b_i^\nu + \sum_{k=1}^K S_{ik} \pi_k \right) + \gamma_i^{2,\nu} \sum_{j=1}^N p_{ji} \right) \right\} & \text{if } i \in \mathcal{D}^{R1,\nu}(\pi, p), \\ \bar{p}_{ij}^{R1} & \text{if } i \in \mathcal{N} \setminus \mathcal{D}^{R1,\nu}(\pi, p). \end{cases} \end{aligned}$$

where

$$\mathcal{D}^{R1,\nu}(\pi, p) = \{i \in \mathcal{N} \mid e_i^{R1,\nu}(\pi, p) < 0\}$$

and

$$e_i^{R1,\nu}(\pi, p) = b_i^\nu + \sum_{k=1}^K S_{ik} \pi_k + \sum_{j=1}^N p_{ji} - \bar{p}_i^{R1} \quad \forall i \in \mathcal{N}.$$

By the previous Theorem 4.3.1, the greatest solution can be considered under a recursive relation of the fixed point, for $\kappa \in \mathbb{N}_0$:

$$(\pi^{\kappa+1, R1,\nu}, p^{\kappa+1, R1,\nu}) = \Phi^{R1,\nu}(\pi^{\kappa, R1,\nu}, p^{\kappa, R1,\nu}),$$

for which there exists the greatest fixed point $\lim_{\kappa \rightarrow \infty} (\pi^{\kappa, R1,\nu}, p^{\kappa, R1,\nu}) = (\pi^{*, R1,\nu}, p^{*, R1,\nu})$.

We show the following statement for the first round of clearing by proof by induction.

For $\kappa = 0$, then

$$\pi_k^{0, R1, A} = 1 = \pi_k^{0, R1, B} \quad \forall k \in \mathcal{S}$$

and

$$p_{ij}^{0, R1, A} = \bar{p}_{ij}^{R1} = p_{ij}^{0, R1, B}.$$

For the induction step, we assume $\pi^{\kappa, R1, B} \geq \pi^{\kappa, R1, A}$ and $p^{\kappa, R1, B} \geq p^{\kappa, R1, A}$. We define the total assets sold under each system as:

$$\Delta_k^\nu(\pi, p) = \sum_{k=1}^K \min \{S_{ik}, \Omega_{ik}^\nu(\pi, p)\} + \sum_{i=1}^N \sum_{j=1}^N \Upsilon_{ij}^\nu(\pi, p)$$

where

$$\Omega_{ik}^\nu(\pi, p) = \frac{S_{ik}}{\sum_{k=1}^K S_{ik} \pi_k} \left(\bar{p}_i^{R1} - b_i^\nu - \sum_{j=1}^N p_{ji} \right)^+$$

and

$$\Upsilon_{ij}^\nu(\pi, p) = \begin{cases} \min \left\{ \zeta_{ij}, \frac{\bar{p}_{ij}^{R1}}{\pi_{T_{ij}}} \right\} & \text{if } i \in \mathcal{D}^{R1, \nu}(\pi, p), \\ 0 & \text{if } i \in \mathcal{N} \setminus \mathcal{D}^{R1, \nu}(\pi, p), \end{cases}$$

for $\pi_k > 0 \quad \forall k \in \mathcal{S}$. In the other case in which $\pi_k = 0$:

$$\Upsilon_{ij}^\nu(\pi, p) = \begin{cases} \zeta_{ij} & \text{if } i \in \mathcal{D}^{R1, \nu}(\pi, p) \quad \text{and} \quad \bar{p}_{ij}^{R1} > 0, \\ 0 & \text{if } i \in \mathcal{N} \setminus \mathcal{D}^{R1, \nu}(\pi, p). \end{cases}$$

From the non-increasing property of collateral sold, as the ordering preserves the ordering on bank defaults, where

$$\mathcal{D}^{R1, B}(\pi, p) \subseteq \mathcal{D}^{R1, A}(\pi, p)$$

then using the non-increasing property of collateral sold in both (π, p) :

$$\Upsilon_{ij}^A(\pi^{\kappa, R1, A}, p^{\kappa, R1, A}) \geq \Upsilon_{ij}^B(\pi^{\kappa, R1, A}, p^{\kappa, R1, A}) \geq \Upsilon_{ij}^B(\pi^{\kappa, R1, B}, p^{\kappa, R1, B}).$$

As the proportion selling function is non-increasing in both the liquidity buffer and (π, p) :

$$\Omega_{ik}^A(\pi^{\kappa, R1, A}, p^{\kappa, R1, A}) \geq \Omega_{ik}^B(\pi^{\kappa, R1, A}, p^{\kappa, R1, A}) \geq \Omega_{ik}^B(\pi^{\kappa, R1, B}, p^{\kappa, R1, B})$$

and

$$\begin{aligned} \Delta_k^A(\pi^{\kappa, R1, A}, p^{\kappa, R1, A}) &= \sum_{k=1}^K \min \{ S_{ik}, \Omega_{ik}^A(\pi^{\kappa, R1, A}, p^{\kappa, R1, A}) \} + \sum_{i=1}^N \sum_{j=1}^N \Upsilon_{ij}^A(\pi^{\kappa, R1, A}, p^{\kappa, R1, A}) \\ &\geq \sum_{k=1}^K \min \{ S_{ik}, \Omega_{ik}^B(\pi^{\kappa, R1, B}, p^{\kappa, R1, B}) \} + \sum_{i=1}^N \sum_{j=1}^N \Upsilon_{ij}^B(\pi^{\kappa, R1, B}, p^{\kappa, R1, B}) \\ &= \Delta_k^B(\pi^{\kappa, R1, B}, p^{\kappa, R1, B}). \end{aligned}$$

Hence,

$$\begin{aligned} \pi_k^{\kappa+1, R1, A} &= \exp(-l_k^A \Delta_k^A(\pi^{\kappa, R1, A}, p^{\kappa, R1, A})) \leq \exp(-l_k^A \Delta_k^B(\pi^{\kappa, R1, B}, p^{\kappa, R1, B})) \\ &\leq \exp(-l_k^B \Delta_k^B(\pi^{\kappa, R1, B}, p^{\kappa, R1, B})) \\ &= \pi_k^{\kappa+1, R1, B} \quad \forall k \in \mathcal{S}. \end{aligned}$$

We secondly show the induction step for the first round clearing function $\Phi_2^{R1, \nu}$. We assume $p^{\kappa, R1, A} \leq p^{\kappa, R1, B}$ and $\pi^{\kappa, R1, A} \leq \pi^{\kappa, R1, B}$ hold. Establishing the monotonic relation of the second component in the first round clearing function follows similarly as in Lemma 8.E.1. As the ordering is preserved from the assumptions on the ordering of $(l^\nu, b^\nu, \gamma^{1, \nu}, \gamma^{2, \nu})$, then:

$$p_{ij}^{\kappa+1, R1, B} \geq p_{ij}^{\kappa+1, R1, A}.$$

Hence, taking the limit of both points:

$$\pi^{*,1,A} = \lim_{\kappa \rightarrow \infty} \pi^{\kappa,1,A} \leq \lim_{\kappa \rightarrow \infty} \pi^{\kappa,1,B} = \pi^{*,1,B}$$

and

$$p^{*,1,A} = \lim_{\kappa \rightarrow \infty} p^{\kappa,1,A} \leq \lim_{\kappa \rightarrow \infty} p^{\kappa,1,B} = p^{*,1,B}.$$

□

We introduce Lemma 8.G.3 which is needed to show Theorem 4.3.2.

Lemma 8.G.3. *For $i \in \mathcal{D}^{R1}(\pi^{*,R1}, p^{*,R1})$, if the collateral assets and corresponding obligations for all banks are such that*

$$\bar{p}_{ij}^{R1} \geq \zeta_{ij} \quad \forall i, j \in \mathcal{N}$$

then

$$\sum_{j=1}^N \Upsilon_{ij}(\pi^{*,R1}, p^{*,R1}) \mathbf{1}(T_{ij} = k) + \Gamma_{ik}(\pi, p) = \sum_{j=1}^N \zeta_{ij} \mathbf{1}(T_{ij} = k) \quad \forall i \in \mathcal{N}, \quad \forall k \in \mathcal{S}.$$

Proof. As the bank is in default in the first round and $\bar{p}_{ij}^{R1} \geq \zeta_{ij} \geq \pi_{T_{ij}}^{*,R1} \zeta_{ij} \quad \forall i, j \in \mathcal{N}$:

$$\Upsilon_{ij}(\pi^{*,R1}, p^{*,R1}) = \zeta_{ij}.$$

For the remaining collateral, as the bank is in default in the first round:

$$r_{ik}(\pi^{*,R1}, p^{*,R1}) = \sum_{j=1}^N (\zeta_{ij} - \Upsilon_{ij}(\pi^{*,R1}, p^{*,R1})) \mathbf{1}(T_{ij} = k) = 0.$$

From the definition of the remaining collateral in the second round clearing function, this implies $\Gamma_{ik}(\pi, p) = 0$. □

Proof of Theorem 4.3.2. From Theorem 4.3.1, for an ordering of different parameterisations $(l^\nu, b^\nu, \gamma^{1,\nu}, \gamma^{2,\nu})$ then

$$\pi^{*,R1,A} \leq \pi^{*,R1,B}$$

and

$$p^{*,R1,A} \leq p^{*,R1,B}.$$

From the combined payment obligations in Proposition 8.G.2, and assuming the absence of interbank bankruptcy costs $\gamma_i^{2,A} = \gamma_i^{2,B} = 1 \quad \forall i \in \mathcal{N}$ then

$$p_{ij}^{*,R1,\nu} + \Phi_{2,(ij)}^{R2,\nu}(\pi, p) = \min \left\{ \bar{p}_{ij}^{R1}, \pi_{T_{ij}}^{*,R1,\nu} \zeta_{ij} + a_{ij}^{R1}(\pi^{*,R1,\nu}) C_i^\nu(\pi, p) \right\} \quad (8.12)$$

where

$$C_i^\nu(\pi, p) = \gamma_i^{1,\nu} \left(b_i^\nu + \sum_{k=1}^K S_{ik} \pi_k^{*,R1,\nu} \right) + c_i^{*,R1,\nu} + \sum_{k=1}^K r_{ik}^\nu(\pi^{*,R1,\nu}, p^{*,R1,\nu}) \pi_k + \sum_{j=1}^N \left(p_{ji}^{*,R1,\nu} + p_{ji} \right),$$

and

$$c_i^{*,R1,\nu} = r_{i(K+1)}^\nu(\pi^{*,R1,\nu}, p^{*,R1,\nu})$$

and

$$r_{ik}^\nu(\pi^{*,R1,\nu}, p^{*,R1,\nu}) = \begin{cases} \sum_{j=1}^N (\zeta_{ij} - \Upsilon_{ij}^\nu(\pi^{*,R1,\nu}, p^{*,R1,\nu})) \mathbf{1}(T_{ij} = k) & \text{if } i \in \mathcal{D}^{R1,\nu}(\pi^{*,R1,\nu}, p^{*,R1,\nu}), \\ \sum_{j \in \mathcal{D}^{R1,\nu}(\pi^{*,R1,\nu}, p^{*,R1,\nu})} \zeta_{ij} \mathbf{1}(T_{ij} = k) & \text{if } i \in \mathcal{N} \setminus \mathcal{D}^{R1,\nu}(\pi^{*,R1,\nu}, p^{*,R1,\nu}). \end{cases}$$

The total collateral assets sold in R2 for different systems $\nu = \{A, B\}$ is denoted as

$$\Gamma_k^\nu(\pi, p) = \sum_{i=1}^N \Gamma_{ik}^\nu(\pi, p)$$

where

$$\Gamma_{ik}^\nu(\pi, p) = \min \left\{ \frac{r_{ik}^\nu(\pi^{*,R1,\nu}, p^{*,R1,\nu})}{\sum_{k=1}^K r_{ik}^\nu(\pi^{*,R1,\nu}, p^{*,R1,\nu}) \pi_k} \left(\sum_{j=1}^N \bar{p}_{ij}^{R2,\nu} - c_i^{*,R1,\nu} - \sum_{j=1}^N p_{ji} \right)^+, r_{ik}^\nu(\pi^{*,R1,\nu}, p^{*,R1,\nu}) \right\}.$$

We consider the different cases for which collateral assets are sold as follows:

- If $i \in \mathcal{D}^{R1,\nu}(\pi^{*,R1,\nu}, p^{*,R1,\nu})$, then by assumption on the collateral posted $r_{ik}^\nu(\pi^{*,R1,\nu}, p^{*,R1,\nu}) = 0$ and $\Gamma_{ik}^\nu(\pi, p) = 0$.
- If $i \in \mathcal{N} \setminus \mathcal{D}^{R1,\nu}(\pi^{*,R1,\nu}, p^{*,R1,\nu})$, then the bank has no outstanding obligations $\bar{p}_{ij}^{R2,\nu} = \bar{p}_{ij}^{R1} - p_{ij}^{*,R1,\nu} = 0 \quad \forall j \in \mathcal{N}$. Hence, the bank has no outstanding obligations and $\Gamma_{ik}^\nu(\pi, p) = 0$.

For all banks, there is no change in the reallocated collateral sold in the second round, under the assumptions on collateral posted. Then,

$$\pi_k^{*,R2,A} = \pi_k^{*,R1,A} \leq \pi_k^{*,R1,B} = \pi_k^{*,R2,B} \quad \forall k \in \mathcal{S}.$$

This leads to a simplification of the payment in the clearing process:

$$\begin{aligned}
 & p_{ij}^{*,R1,\nu} + \Phi_{2,(ij)}^{R2,\nu}(\pi, p) \\
 = & \min \left\{ \bar{p}_{ij}^{R1}, \zeta_{ij} \pi_{T_{ij}}^{*,R1,\nu} \right. \\
 & \left. + a_{ij}^{R1,\nu}(\pi^{*,R1,\nu}) \left(\gamma_i^{1,\nu} \left(b_i^\nu + \sum_{k=1}^K S_{ik} \pi_k^{*,R1,\nu} \right) + \sum_{j=1}^N \left(p_{ji}^{*,R1,\nu} + p_{ji} \right) \right) \right\}.
 \end{aligned}$$

Under the ordering of the given parameters, the ordering at each iteration can be shown using proof by induction, similar to Lemma 8.E.1.

The limit of the inductive points exists from Theorem 8.E.2, hence showing the inequality for the greatest fixed point. \square

Proof of Proposition 4.3.3. We show the ordering on the fixed point on outstanding payments using proof by induction. We consider the second round clearing function. We define the clearing function for $\nu \in \{A, B\}$ as follows:

$$\begin{aligned}
 \Phi_{1,(k)}^{R2,\nu}(\pi, p) &= \pi_k^{*,R1,\nu} \exp(-l_k^\nu \Gamma_k^\nu(\pi, p)) \\
 \Phi_{2,(ij)}^{R2,\nu}(\pi, p) &= \min \left\{ \bar{p}_{ij}^{R2,\nu}, a_{ij}^{R2,\nu} \left(c_i^{*,R1,\nu} + \sum_{k=1}^K r_{ik}^\nu(\pi^{*,R1,\nu}, p^{*,R1,\nu}) \pi_k + \sum_{j=1}^N p_{ji} \right) \right\}
 \end{aligned}$$

where

$$a_{ij}^{R2,\nu} = \frac{\bar{p}_{ij}^{R2,\nu}}{\sum_{l=1}^N \bar{p}_{il}^{R2,\nu}}.$$

As in arguments in the proof of Theorem 4.3.2, the assumptions of collateral lead to no change in market price, between the first and second rounds. Hence,

$$\pi^{*,R2,A} \leq \pi^{*,R2,B}.$$

For bank payments, if the bank has no outstanding obligations, then $p^{*,R2,\nu} = \bar{p}^{R2,\nu}$ and the inequality holds. If the bank has outstanding obligations in the first round, in the absence of fire sales in R2 this leads to the simplified clearing function for R2:

$$\Phi_{2,(ij)}^{R2,\nu}(p) = \min \left\{ \bar{p}_{ij}^{R2,\nu}, a_{ij}^{R2,\nu} \sum_{j=1}^N p_{ji} \right\}.$$

We show the ordering of the R2 using proof by induction. For the base case, from the outstanding obligations and the inequality on R1 fixed point payments under Theorem

4.3.1, then

$$\bar{p}^{R2,A} = \bar{p}^{R1} - p^{*,R1,A} \geq \bar{p}^{R1} - p^{*,R1,B} = \bar{p}^{R2,B}.$$

Next, we assume $p^{\kappa,R2,A} \geq p^{\kappa,R2,B}$. We compare the following cases between the fixed point outstanding payments in R2, between both financial systems:

- If $p_i^{\kappa+1,R2,A} = \bar{p}_i^{R2,A}$, then

$$p^{\kappa+1,R2,A} = \bar{p}^{R2,A} \geq \bar{p}^{R2,B} \geq p^{\kappa+1,R2,B}.$$

- If $p^{\kappa+1,R2,A} < \bar{p}^{R2,A}$, we show that $p^{\kappa+1,R2,B} < \bar{p}^{R2,B}$. From the inequality on the outstanding obligations for $\nu = A$, then:

$$\bar{p}_{ij}^{R2,A} > a_{ij}^{R2,A} \sum_{j=1}^N p_{ji}^{\kappa,R2,A}.$$

Using the definition of the relative outstanding obligations matrix, then

$$\sum_{j=1}^N p_{ji}^{\kappa,R2,A} < \sum_{l=1}^N \bar{p}_{il}^{R2,A}. \quad (8.13)$$

Hence,

$$a_{ij}^{R2,B} \sum_{j=1}^N p_{ji}^{\kappa,R2,B} \leq a_{ij}^{R2,B} \sum_{j=1}^N p_{ji}^{\kappa,R2,A} \stackrel{(*)}{<} a_{ij}^{R2,B} \sum_{l=1}^N \bar{p}_{il}^{R2,A} = \bar{p}_{ij}^{R2,B} \left(\frac{\sum_{l=1}^N \bar{p}_{il}^{R2,A}}{\sum_{l=1}^N \bar{p}_{il}^{R2,B}} \right).$$

The (*) comes from (8.13). As the total relative remaining obligations in the system A is higher than B , then:

$$p^{\kappa+1,R2,B} = \min \left\{ \bar{p}_{ij}^{R2,B}, a_{ij}^{R2,B} \sum_{j=1}^N p_{ji}^{\kappa,R2,B} \right\} < \bar{p}_{ij}^{R2,B} \min \left\{ 1, \frac{\sum_{l=1}^N \bar{p}_{il}^{R2,A}}{\sum_{l=1}^N \bar{p}_{il}^{R2,B}} \right\} = \bar{p}_{ij}^{R2,B}.$$

For the case in which $p^{\kappa+1,R2,A} < \bar{p}^{R2,A}$, we show that the clearing function is non-decreasing in the second round.

For the second round component of interbank assets, the function is non-decreasing. As the relative outstanding obligations matrix relies only on R1, we show that the function is non-increasing in $p^{*,R1}$. We define the function $J : [0, \bar{p}^{R1}] \rightarrow [0, 1]$ as follows:

$$J(p) = \frac{\bar{p}_{ij}^{R1} - p_{ij}}{\sum_{l=1}^N (\bar{p}_{il}^{R1} - p_{il})}.$$

Then, taking the derivative of the function:

$$\frac{\partial J}{\partial p} = \frac{(\bar{p}_{ij}^{R1} - p_{ij}) - \sum_{l=1}^N (\bar{p}_{il}^{R1} - p_{il})}{\left(\sum_{l=1}^N (\bar{p}_{il}^{R1} - p_{il})\right)^2}.$$

As the derivative is negative, then the function is non-increasing in the R1 fixed point payment. Hence,

$$p^{\kappa+1,R2,A} = a_{ij}^{R2,A} \sum_{j=1}^N p_{ji}^{\kappa,R2,A} \geq a_{ij}^{R2,B} \sum_{j=1}^N p_{ji}^{\kappa,R2,A} \geq a_{ij}^{R2,B} \sum_{j=1}^N p_{ji}^{\kappa,R2,B} = p^{\kappa+1,R2,B}$$

and function is ordered under the different systems. Taking the limit of the inductive components then

$$p^{*,R2,A} = \lim_{\kappa \rightarrow \infty} p^{\kappa,R2,A} \geq \lim_{\kappa \rightarrow \infty} p^{\kappa,R2,B} = p^{*,R2,B}.$$

□

Proof of Theorem 4.3.4. From the fixed point relation in Theorem 4.3.1, where

$$e_i^{*,R1,\nu} = e_i^{R1,\nu} (\pi^{*,R1,\nu}, p^{*,R1,\nu}) \quad \nu \in \{A, B\} \text{ and } \forall i \in \mathcal{N},$$

then

$$\begin{aligned} e_i^{*,R1,A} &= b_i^A + \sum_{k=1}^K S_{ik} \pi_k^{*,R1,A} + \sum_{j=1}^N p_{ji}^{*,R1,A} - \bar{p}_i^{R1} \\ &\leq b_i^B + \sum_{k=1}^K S_{ik} \pi_k^{*,R1,B} + \sum_{j=1}^N p_{ji}^{*,R1,B} - \bar{p}_i^{R1} \\ &= e_i^{*,R1,B}. \end{aligned}$$

For the total number of defaults in the first round:

$$\Lambda^{R1,A} = \sum_{i=1}^N \mathbf{1} \left(e_i^{*,R1,A} < 0 \right) \geq \sum_{i=1}^N \mathbf{1} \left(e_i^{*,R1,B} < 0 \right) = \Lambda^{R1,B}.$$

For the relative obligations in the first round obligations measure, under the assumptions of collateral posted in Theorem 4.3.1 and Proposition 4.3.3, then:

$$\mathcal{P}^A = \frac{\sum_{j=1}^N p_{ij}^{*,R1,A}}{\sum_{j=1}^N p_{ij}^{*,R1,A} + \sum_{j=1}^N p_{ij}^{*,R2,A}} = \frac{1}{1 + \frac{\sum_{j=1}^N p_{ij}^{*,R2,A}}{\sum_{j=1}^N p_{ij}^{*,R1,A}}} \leq \frac{1}{1 + \frac{\sum_{j=1}^N p_{ij}^{*,R2,B}}{\sum_{j=1}^N p_{ij}^{*,R1,B}}} = \mathcal{P}^B.$$

For the relative shortfall of banks and relative total shortfall, then under the assumptions

of collateral posted and interbank bankruptcy costs in Theorem 4.3.2,

$$\begin{aligned} h_i^A &= \frac{\sum_{j=1}^N \max \left\{ \bar{p}_{ij}^{R1} - p_{ij}^{*,R1,A} - p_{ij}^{*,R2,A}, 0 \right\}}{\sum_{i=1}^N \sum_{j=1}^N \bar{p}_{ij}^{R1}} \\ &\geq \frac{\sum_{j=1}^N \max \left\{ \bar{p}_{ij}^{R1} - p_{ij}^{*,R1,B} - p_{ij}^{*,R2,B}, 0 \right\}}{\sum_{i=1}^N \sum_{j=1}^N \bar{p}_{ij}^{R1}} = h_i^B \end{aligned}$$

and

$$H^A = \sum_{i=1}^N h_i^A \geq \sum_{i=1}^N h_i^B = H^B.$$

For the number of banks with outstanding obligations in R2, then for the R2 equity

$$\begin{aligned} e_i^{*,R2,\nu} &= e_i^{R2,\nu} (\pi^{*,R2,\nu}, p^{*,R2,\nu}) \\ &= c_i^{*,R1,\nu} + \sum_{k=1}^K r_{ik}^\nu (\pi^{*,R1,\nu}, p^{*,R1,\nu}) \pi_k^{*,R2,\nu} + \sum_{j=1}^N p_{ji}^{*,R2,\nu} - \bar{p}_i^{R2,\nu} \end{aligned}$$

for $\nu = \{A, B\}$, we show that if $i \in \mathcal{D}^{R2} (\pi^{*,R2,A}, p^{*,R2,A})$, then

$$e_i^{*,R2,A} \leq e_i^{*,R2,B}. \quad (8.14)$$

Using the inequality from Theorem 4.3.2, then

$$p_{ij}^{*,R2,B} + p_{ij}^{*,R1,B} \geq p_{ij}^{*,R2,A} + p_{ij}^{*,R1,A}.$$

From the definition of the fixed points in R2,

$$\begin{aligned} &\min \left\{ \bar{p}_{ij}^{R2,B}, a_{ij}^{R2,B} \left(c_i^{*,R1,B} + \sum_{k=1}^K r_{ik}^B (\pi^{*,R1,B}, p^{*,R1,B}) \pi_k^{*,R2,B} + \sum_{j=1}^N p_{ji}^{*,R2,B} \right) \right\} + p_{ij}^{*,R1,B} \\ &\geq \min \left\{ \bar{p}_{ij}^{R2,A}, a_{ij}^{R2,A} \left(c_i^{*,R1,A} + \sum_{k=1}^K r_{ik}^A (\pi^{*,R1,A}, p^{*,R1,A}) \pi_k^{*,R2,A} + \sum_{j=1}^N p_{ji}^{*,R2,A} \right) \right\} + p_{ij}^{*,R1,A}. \end{aligned}$$

As we only consider banks for which $i \in \mathcal{D}^{R2} (\pi^{*,R2,A}, p^{*,R2,A})$, we take the second component of the fixed term on the RHS. For the LHS, we take the second component as an upper bound of total payments, then:

$$\begin{aligned} &a_{ij}^{R2,B} \left(c_i^{*,R1,B} + \sum_{k=1}^K r_{ik}^B (\pi^{*,R1,B}, p^{*,R1,B}) \pi_k^{*,R2,B} + \sum_{j=1}^N p_{ji}^{*,R2,B} \right) + p_{ij}^{*,R1,B} \\ &\geq a_{ij}^{R2,A} \left(c_i^{*,R1,A} + \sum_{k=1}^K r_{ik}^A (\pi^{*,R1,A}, p^{*,R1,A}) \pi_k^{*,R2,A} + \sum_{j=1}^N p_{ji}^{*,R2,A} \right) + p_{ij}^{*,R1,A}. \end{aligned}$$

Taking the summation over $\forall j \in \mathcal{N}$ and the definition of the equity at the fixed point, then

$$e_i^{*,R2,B} + \bar{p}_i^{R2,B} + p_i^{*,R1,B} \geq e_i^{*,R2,A} + \bar{p}_i^{R2,A} + p_i^{*,R1,A}.$$

From the definition of the outstanding obligations in R2 under both systems, we have the inequality for the equity as in (8.14). Hence, for the number of banks with outstanding obligations across two rounds of clearing:

$$\Lambda^{R2,A} = \sum_{j=1}^N \mathbf{1} \left(e_i^{*,R2,A} < 0 \right) \geq \sum_{j=1}^N \mathbf{1} \left(e_i^{*,R2,B} < 0 \right) = \Lambda^{R2,B}.$$

□

8.G.3 Chapter 5 proofs

Proof of Proposition 5.3.1. We also prove that $\psi^A \geq \psi^L$ is equivalent to the following two statements:

- The equity of the RFB is bounded from below by:

$$\psi^A E \leq E^{\text{RF}}$$

- The equity of the nRFB bank is bounded from above by:

$$E^{\text{nRF}} \leq (1 - \psi^A)E.$$

Analogous inequalities hold when $\psi^A < \psi^L$.

We have that:

$$\begin{aligned} \psi^A E \leq E^{\text{RF}} &\iff \psi^A A - \psi^A L \leq \psi^A A - \psi^L L \\ &\iff -\psi^A L \leq -\psi^L L \\ &\iff \psi^A \geq \psi^L, \end{aligned}$$

and analogously for $E^{\text{nRF}} \leq (1 - \psi^A)E$. Moreover, since (ψ^A, ψ^L) is feasible:

$$\begin{aligned} \psi^A E \leq E^{\text{RF}} &\iff \frac{\psi^A}{E^{\text{RF}}} \leq \frac{1}{E} \\ &\iff \frac{\psi^A A}{E^{\text{RF}}} \leq \frac{A}{E} \\ &\iff \lambda^{\text{RF}} \leq \lambda, \end{aligned}$$

and analogously for $E^{\text{nRF}} \leq (1 - \psi^A)E \iff \lambda \leq \lambda^{\text{nRF}}$.

□

Proof of Corollary 5.3.2. The proof follows immediately from Proposition 5.3.1 and from the fact that the probability of default is a non-increasing function of the leverage. \square

Proof of Proposition 5.4.1. We also prove that $\psi_i^A (L_i^e - (\bar{A}_i - \bar{L}_i)) \geq \psi_i^L L_i^e$ is equivalent to the following two statements:

- The equity of the RFB is bounded from below by:

$$\psi_i^A E_i^0 \leq E_i^{\text{RF}}.$$

- The naive equity of the nRFB bank is bounded from above by:

$$E_i^{\text{nRF},0} \leq (1 - \psi_i^A) E_i^0.$$

Analogous inequalities hold when $\psi_i^A (L_i^e - (\bar{A}_i - \bar{L}_i)) < \psi_i^L L_i^e$.

The proof is analogous to the proof of Proposition 5.3.1. We have that:

$$\begin{aligned} \psi_i^A E_i^0 \leq E_i^{\text{RF}} &\iff \psi_i^A (A_i^e - L_i^e + \bar{A}_i - \bar{L}_i) \leq \psi_i^A A_i^e - \psi_i^L L_i^e \\ &\iff \psi_i^A (-L_i^e + \bar{A}_i - \bar{L}_i) \leq -\psi_i^L L_i^e \\ &\iff \psi_i^A (L_i^e - (\bar{A}_i - \bar{L}_i)) \geq \psi_i^L L_i^e. \end{aligned}$$

Moreover, by using (5.9):

$$\begin{aligned} \psi_i^A E_i^0 \leq E_i^{\text{RF}} &\iff -\psi_i^A E_i^0 \geq -E_i^{\text{RF}} \\ &\iff E_i^0 - \psi_i^A E_i^0 \geq E_i^0 - E_i^{\text{RF}} \\ &\iff (1 - \psi_i^A) E_i^0 \geq E_i^{\text{nRF},0}. \end{aligned}$$

Since (ψ_i^A, ψ_i^L) is feasible:

$$\begin{aligned} \psi_i^A E_i^0 \leq E_i^{\text{RF}} &\iff \frac{\psi_i^A}{E_i^{\text{RF}}} \leq \frac{1}{E_i^0} \\ &\iff \frac{\psi_i^A A_i^e}{E_i^{\text{RF}}} \leq \frac{A_i^e}{E_i^0} \\ &\iff \lambda_i^{\text{RF}} \leq B_i^0, \end{aligned}$$

and analogously for $E_i^{\text{nRF},0} \leq (1 - \psi_i^A) E_i^0 \iff B_i^0 \leq B_i^{\text{nRF},0}$. \square

Proof of Corollary 5.4.2. This is a straightforward consequence of Proposition 5.4.1. \square

Proof of Corollary 5.4.5. From Proposition 5.4.1 and from the fact that the greatest solution is smaller than or equal to the naive equity ($\mathbf{E}^* \leq \mathbf{E}^0$) it follows that:

$$\psi_i^A E_i^* \leq E_i^{\text{RF}}.$$

Therefore, we immediately have also that: $\lambda_i^{\text{RF}} \leq B_i^*$. The result on probabilities of default comes from the fact that simple ex-ante valuation functions are non-decreasing with external leverage (see Definition 5.4.4) and therefore the probability of default computed as in (5.15) are non-increasing with external leverage. \square

Proof of Proposition 5.4.6. Under the hypotheses, we also prove that:

$$E_i^{\text{RF}} \leq \psi_i^A E_i^* .$$

We have that:

$$\begin{aligned} \psi_i^A (L_i^e + \bar{L}_i) \leq \psi_i^L L_i^e &\iff -\psi_i^A (L_i^e + \bar{L}_i) \geq -\psi_i^L L_i^e \\ &\iff \psi_i^A (A_i^e - L_i^e - \bar{L}_i) \geq \psi_i^A A_i^e - \psi_i^L L_i^e \\ &\iff \psi_i^A (A_i^e - L_i^e - \bar{L}_i) \geq E_i^{\text{RF}} . \end{aligned}$$

At the same time:

$$\begin{aligned} E_i^* = A_i^e + \sum_{j=1}^N A_{ij} \mathbb{V}(E_j^* | \mathcal{C}_j) - L_i^e - \bar{L}_i &\implies E_i^* \geq A_i^e - L_i^e - \bar{L}_i \\ &\iff \psi_i^A E_i^* \geq \psi_i^A (A_i^e - L_i^e - \bar{L}_i) , \end{aligned}$$

therefore, if $\psi_i^A (L_i^e + \bar{L}_i) \leq \psi_i^L L_i^e$:

$$\psi_i^A E_i^* \geq \psi_i^A (A_i^e - L_i^e - \bar{L}_i) \geq E_i^{\text{RF}} .$$

If $E_i^* > 0$ and since (ψ_i^A, ψ_i^L) is feasible we have:

$$\begin{aligned} \psi_i^A E_i^* \geq E_i^{\text{RF}} &\iff \frac{\psi_i^A}{E_i^{\text{RF}}} \geq \frac{1}{E_i^*} \\ &\iff \frac{\psi_i^A A_i^e}{E_i^{\text{RF}}} \geq \frac{A_i^e}{E_i^*} \\ &\iff \lambda_i^{\text{RF}} \geq B_i^* . \end{aligned}$$

The result on probabilities of default comes from the fact that simple ex-ante valuation functions are non-decreasing with external leverage (see Definition 5.4.4) and therefore the probability of default computed as in (5.15) are non-increasing with external leverage. \square

Proof of Proposition 5.4.7. To prove that:

$$E_i^{\text{nRF},*} + E_i^{\text{RF}} = E_i^* , \tag{8.15}$$

it is sufficient to prove that:

$$\sum_{j \in \mathcal{N}(i)} A_{ij} \left[\mathbb{V}(E_j^{\text{nRF},*} | \mathcal{C}_j^{\text{nRF}}) - \mathbb{V}(E_j^* | \mathcal{C}_j) \right] = 0, \quad (8.16)$$

where we denote with $\mathcal{N}(i)$ the neighbours of i .

Let us prove that:

$$E_p^{\text{nRF},\kappa} = E_p^\kappa \quad \forall p \in \mathcal{O}^A(i), \forall \kappa. \quad (8.17)$$

We proceed by induction. Eq. (8.17) holds for $\kappa = 0$ because:

$$\mathbf{E}^{\text{nRF},0} + \mathbf{E}^{\text{RF}} = \mathbf{E}^0$$

and $E_p^{\text{RF}} = 0$, for all $\forall p \in \mathcal{O}^A(i)$. Let us now assume that (8.17) holds for $\kappa > 0$, proving that holds (8.17) for $\kappa + 1$ is equivalent to proving that:

$$\sum_{s \in \mathcal{N}(p)} A_{ps} \left[\mathbb{V}(E_s^{\text{nRF},\kappa} | \mathcal{C}_s^{\text{nRF}}) - \mathbb{V}(E_s^\kappa | \mathcal{C}_s) \right] = 0. \quad (8.18)$$

Our induction hypothesis holds for all nodes in the asset risk orbit of i , and therefore also for all the nodes in the asset risk orbit of one of the nodes in the asset risk orbit of i : $E_s^{\text{nRF},\kappa} = E_s^\kappa$, for all $s \in \mathcal{N}(p)$, for all $p \in \mathcal{O}^A(i)$. Moreover, since all banks in the asset risk orbit of i do not ring-fence, then $\mathcal{C}_s = \mathcal{C}_s^{\text{nRF}}$, for all $s \in \mathcal{N}(p)$, for all $p \in \mathcal{O}^A(i)$. As a consequence, (8.18) holds and therefore also (8.17). By plugging (8.17) into (8.16) and since $\mathcal{C}_j = \mathcal{C}_j^{\text{nRF}}$ also for all $j \in \mathcal{N}(i)$, we have that (8.16), and therefore (8.15) holds. \square

The following result relates valuation functions for nRFBs to valuation functions for banks prior to ring-fencing, and it is needed to prove Theorem 5.4.8.

Lemma 8.G.4. *Let \mathbb{V} be a simple ex-ante valuation function and let $\mathcal{C} = \{A^e, \sigma\}$ and $\mathcal{C}^{\text{nRF}} = \{(1 - \psi^A)A^e, \sigma\}$, with $A^e > 0$, $\sigma > 0$, and $\psi^A \in [0, 1]$. Then:*

$$\mathbb{V}(E | \mathcal{C}^{\text{nRF}}) = \mathbb{V}\left(\frac{E}{1 - \psi^A} \middle| \mathcal{C}\right).$$

Proof. We have:

$$\begin{aligned} \mathbb{V}(E | \mathcal{C}^{\text{nRF}}) &= f\left(\frac{E}{(1 - \psi^A)A^e}, \sigma\right) \\ &= \mathbb{V}\left(\frac{E}{1 - \psi^A} \middle| \mathcal{C}\right). \end{aligned}$$

\square

Proof of Theorem 5.4.8. We start with the first statement. To prove that:

$$E_i^{\text{nRF},*} + E_i^{\text{RF}} \leq E_i^*, \quad (8.19)$$

it is sufficient to prove that a similar inequality holds for every iteration κ :

$$E_i^{\text{nRF},\kappa} + E_i^{\text{RF}} \leq E_i^\kappa, \quad (8.20)$$

which in turn is equivalent to:

$$\sum_{j \in \mathcal{N}(i)} A_{ij} \left[\mathbb{V}(E_j^{\text{nRF},\kappa} | \mathcal{C}_j^{\text{nRF}}) - \mathbb{V}(E_j^\kappa | \mathcal{C}_j) \right] \leq 0, \quad (8.21)$$

where we denote with $\mathcal{N}(i)$ the neighbours of i .

Let us prove that:

$$E_p^{\text{nRF},\kappa} + E_p^{\text{RF}} \leq E_p^\kappa \quad \forall p \in \mathcal{O}^A(i), \forall \kappa. \quad (8.22)$$

We proceed by induction. Eq. (8.22) obviously holds for $\kappa = 0$, simply because:

$$\mathbf{E}^{\text{nRF},0} + \mathbf{E}^{\text{RF}} = \mathbf{E}^0.$$

Let us now assume that (8.22) holds for $\kappa > 0$, proving that holds (8.22) for $\kappa + 1$ is equivalent to proving that:

$$\sum_{s \in \mathcal{N}(p)} A_{ps} \left[\mathbb{V}(E_s^{\text{nRF},\kappa} | \mathcal{C}_s^{\text{nRF}}) - \mathbb{V}(E_s^\kappa | \mathcal{C}_s) \right] \leq 0. \quad (8.23)$$

For all banks s that are neighbours of a node p in the asset risk orbit of i that do not ring-fence we have that:

$$\begin{aligned} \mathbb{V}(E_s^{\text{nRF},\kappa} | \mathcal{C}_s^{\text{nRF}}) &\leq \mathbb{V}(E_s^\kappa - E_s^{\text{RF}} | \mathcal{C}_s^{\text{nRF}}) \\ &\leq \mathbb{V}(E_s^\kappa | \mathcal{C}_s), \end{aligned}$$

where the second line comes from the fact that for banks that do not ring-fence $E_s^{\text{RF}} = 0$ and $\mathcal{C}_s^{\text{nRF}} = \mathcal{C}_s$. Instead, for all other banks s that are neighbours of a node p in the asset risk orbit of i we have that:

$$\begin{aligned} \mathbb{V}(E_s^{\text{nRF},\kappa} | \mathcal{C}_s^{\text{nRF}}) &\leq \mathbb{V}(E_s^\kappa - E_s^{\text{RF}} | \mathcal{C}_s^{\text{nRF}}) \\ &= \mathbb{V}\left(\frac{E_s^\kappa - E_s^{\text{RF}}}{1 - \psi_s^A} | \mathcal{C}_s\right) \\ &\leq \mathbb{V}(E_s^\kappa | \mathcal{C}_s) \end{aligned}$$

where the first line comes from our induction hypothesis (8.22), which holds for all nodes

in the asset risk orbit of i , and therefore for all neighbours of all nodes in the asset risk orbit of i (which are also part of the asset risk orbit of i), and the second step from Lemma 8.G.4. The third step comes from the fact that for all nodes in the asset risk orbit of i that do ring-fence, we have that $\lambda_s^{\text{RF}} \leq B_s^0$. In fact:

$$\begin{aligned} \frac{E_s^\kappa - E_s^{\text{RF}}}{1 - \psi_s^A} &\leq E_s^\kappa \iff \\ E_s^\kappa - E_s^{\text{RF}} &\leq E_s^\kappa - \psi_s^A E_s^\kappa \iff \\ E_s^{\text{RF}} &\geq \psi_s^A E_s^\kappa, \end{aligned}$$

but Proposition 5.4.1 implies that $E_s^{\text{RF}} \geq \psi_s^A E_s^0 \geq \psi_s^A E_s^\kappa$. We have proved (8.23), and thus also (8.22). In particular, (8.22) holds for all neighbours of i . Therefore, one can easily prove (8.21) by reproducing the same steps used to prove (8.23).

The proof proceeds analogously in the second case. In this case, instead of Proposition 5.4.1 one uses Proposition 5.4.6, according to which, for all banks s for which $\lambda_s^{\text{RF}} \geq B_s^*$, we have that $E_s^{\text{RF}} \leq \psi_s^A E_s^* \leq \psi_s^A E_s^\kappa$. \square

Proof of Corollary 5.4.9. For the first statement, all banks satisfy the conditions of the first case of Theorem 5.4.8, and therefore $E_i^{\text{nRF},*} + E_i^{\text{RF}} \leq E_i^*$, for all i . The proof follows by summing on both sides of the equation overall i . Analogously for the second case. \square

Proof of Proposition 5.4.10. Let us start with the first statement. Since $\lambda_i^{\text{RF}} \leq B_i^0$, using Proposition 5.4.1 and Corollary 5.4.5 we have that: $\psi_i^A E_i^* \leq E_i^{\text{RF}}$. At the same time the first statement of Theorem 5.4.8 is applicable: $E_i^{\text{nRF},*} + E_i^{\text{RF}} \leq E_i^*$. Combining the two we have:

$$E_i^{\text{nRF},*} + E_i^{\text{RF}} \leq E_i^* \leq \frac{E_i^{\text{RF}}}{\psi_i^A}.$$

We note that assuming that $E_i^{\text{RF}} > 0$ implies that some external assets must have been allocated to the RFB, i.e. $\psi_i^A > 0$. Combining the two inequalities above also yields:

$$\begin{aligned} \psi_i^A \left(E_i^{\text{nRF},*} + E_i^{\text{RF}} \right) &\leq E_i^{\text{RF}} \iff \\ -\psi_i^A \left(E_i^{\text{nRF},*} + E_i^{\text{RF}} \right) &\geq -E_i^{\text{RF}} \iff \\ E_i^{\text{nRF},*} + E_i^{\text{RF}} - \psi_i^A \left(E_i^{\text{nRF},*} + E_i^{\text{RF}} \right) &\geq E_i^{\text{nRF},*} + E_i^{\text{RF}} - E_i^{\text{RF}} \iff \\ (1 - \psi_i^A) \left(E_i^{\text{nRF},*} + E_i^{\text{RF}} \right) &\geq E_i^{\text{nRF},*} \iff \\ E_i^{\text{nRF},*} + E_i^{\text{RF}} &\geq \frac{E_i^{\text{nRF},*}}{1 - \psi_i^A}. \end{aligned}$$

Putting all inequalities together we have:

$$\frac{E_i^{\text{nRF},*}}{1 - \psi_i^A} \leq E_i^{\text{nRF},*} + E_i^{\text{RF}} \leq E_i^* \leq \frac{E_i^{\text{RF}}}{\psi_i^A},$$

from which the inequality of external leverages easily follows.

The second statement is analogous when noting that, since $\lambda_i^{\text{RF}} \geq B_i^*$, by using Proposition 5.4.6 we have that $\psi_i^A E_i^* \geq E_i^{\text{RF}}$. In this case, we have:

$$\frac{E_i^{\text{nRF},*}}{1 - \psi_i^A} \geq E_i^{\text{nRF},*} + E_i^{\text{RF}} \geq E_i^* \geq \frac{E_i^{\text{RF}}}{\psi_i^A}.$$

The results on probabilities of default come from the fact that simple ex-ante valuation functions are non-decreasing with external leverage (see Definition 5.4.4) and therefore the probability of default computed as in (5.15) are non-increasing with external leverage. \square